The Role of Specific MHV-68 Genes in Persistent Infection in the Lung and Virus Pathogenesis

Kerra Marianne Templeton

September 2006

Submitted for the degree of Doctor of Philosophy

The programme of research was carried out as part of a BBSRC-funded PhD entitled "Pathogenesis of MHV-68" at the Laboratory for Clinical & Molecular Virology, Royal (Dick) School of Veterinary Studies, University of Edinburgh, Summerhall, Edinburgh, UK

Declaration

I declare that all work included in this thesis is my own except where otherwise stated. No part of this work has been, or will be, submitted for any other degree of professional qualification.

Kerra Templeton

2006

Laboratory for Clinical & Molecular Virology
University of Edinburgh
Summerhall
Edinburgh
EH9 1QH

Acknowledgements

I would like to thank my supervisors Professor Tony Nash and Dr Bernadette Dutia. Tony has inspired the project and supported me throughout my four years in the department. Bernadette has provided endless help and support in all aspects of my work, from developing my ideas to technical advice and many hours spent perfusing mice! Other technical help came from Ian Bennet, whose assistance with cloning was invaluable; Clive McKimmie and Lucy Breakwell for help and discussions about real time PCR; and Stuart Reid who helped with the growth curves. The rest of the MHV-68 group have also helped throughout my time in the lab and deserve a big thank you. Dr Susan Rhind assisted greatly with histology analysis.

My PhD could not have been completed without support from my friends and family. Lucy and Anna went through it all with me, distracting me in the bad times and celebrating in the good. Matt has frequently provided an escape from the lab, as well as chocolate, diet coke, and all the help and encouragement I could need. The members of George Watson's, Edinburgh University and Clydesdale Boat Clubs have at various points put up with me, and are among the only people who can make me get out of bed at 6 am! Finally, the biggest thank you to my family, in particular my parents and my Aunt Marian. I couldn't have done it without you.

Abstract

The gammaherpesvirus subfamily has long been the study of intensive investigation owing to the association between infection and development of lymphoproliferative disease. Well-known members of the *Gammaherpesvirinae* include Epstein-Barr virus (EBV) and Kaposi's Sarcoma-associated herpesvirus (KSHV). Common properties of gammaherpesviruses include a narrow host range of infection and limited productive growth *in vitro*, and these factors make the study of acute infection problematic. Murine gammaherpesvirus-68 (MHV-68) is able to undergo lytic replication in a range of cell types *in vitro* and can infect inbred strains of mice. These properties make MHV-68 an excellent model for the study of gammaherpesvirus pathogenesis.

Herpesviruses have been indicated in development of diseases in the lung, including pneumonia and idiopathic pulmonary fibrosis. MHV-68 allows investigation of gammaherpesvirus infection of and persistence in the lung – following intranasal inoculation the virus establishes a life-long infection in this organ, with virus persisting in epithelial cells and/or B cells. Identification of key viral genes required for persistence may allow for development of vaccination and/or treatment strategies. Using real-time PCR the long-term viral load in the lungs was reduced following the deletion of key genes from the viral genome. Genes identified are the thymidine kinase gene, previously shown to play a role during acute infection of the lung and ORF73, a homologue of the KSHV LANA-1 gene. Initial data also suggests that the ORF72 and M11 genes, both involved in reactivation from latency, may play a role in maintaining viral load at late time points post-infection.

In vivo investigation of the M1 gene of MHV-68 has demonstrated a potential role in control of viral reactivation from latency in the spleen. A novel MHV-68 mutant, M1Δ, lacking 1171 bp of the M1 ORF, was used to study the role of M1 in pathogenesis. Initial data suggests that *in vivo* infection with M1Δ results in increased viral titres during acute infection of the lung, indicating a potential role in control of initial infection. The major role of M1 appears to be during acute phase latency in the spleen, with the M1Δ virus failing to drive splenomegaly and establishing latency at lower levels. Despite the presence of fewer latently infected splenocytes, M1Δ

reactivates at significantly higher levels, indicating that a function of M1 is to control viral reactivation from latency.

A viral mutant (M4In1) was created that carries a stop codon inserted at genome co-ordinate 8386 in the region between the M3 and M4 genes. The mutation is thought to be in an untranscribed region of the genome, potentially in the promoter region of the M3 or M4 genes. Studies demonstrated that the virus is attenuated following infection of both wild-type and IFNγR$^{-/-}$ mice with respect to lung pathology scores. The lethality of M4In1 in juvenile IFNγR$^{-/-}$ mice is reduced compared with wild-type MHV-68 infection. Despite the location of the mutation within potential promoter regions, M4In1 transcribes both M3 and M4 at wild type levels *in vitro*, and *in vivo* in the spleen. This evidence suggests an apparently untranscribed region of the MHV-68 genome is able to influence pathogenesis in the lung independent of the neighbouring genes.

Contents

List of Figures

List of Tables

Abbreviations

AIDS	Acquired Immune Deficiency Syndrome
AlHV	Alcelaphine Herpesvirus
ATP	Adenosine triphosphate
BAC	Bacterial Artificial Chromosome
BART	*Bam*HI Rightward Transcript
bp	Base pair
Bcl-2	B-cell lymphoma-2
BHK	Baby hamster kidney
BL	Burkitt's Lymphoma
BoHV	Bovine Herpesvirus
CDK	Cyclin-dependent kinase
cDNA	Complementary DNA
CNS	Central nervous system
CTL	Cytotoxic T lymphocyte
CTP	Cytidine triphosphate
DMEM	Dulbecco's modified Eagle's medium
DNA	Deoxyribonucleic acid
ds	Double stranded
DTT	Dithiothreitol
E	Early
EBER	Epstein Barr virus-encoded small RNA
EBNA	Epstein Barr nuclear antigen
E. coli	*Escherichia Coli*
EBV	Epstein Barr virus
EDTA	Ethylenediaminetetraacetic acid
EHV	Equine Herpesvirus
FADD	Fas associated death domain
FCS	Fetal calf serum
FLICE	FADD-like interleukin 1β-converting enzyme
FLIP	FLICE inhibitory protein
GAPDH	Glyceraldehyde-3-phosphate dehydrogenase
GFP	Green fluorescent protein
gp	Glycoprotein

GTP	Guanine triphosphate
GPCR	G protein coupled receptor
HCl	Hydrochloric acid
HCMV	Human Cytomegalovirus
HHV	Human Herpesvirus
HIV	Human Immunodeficiency Virus
HLA	Human leukocyte antigen
HSV	Herpes Simplex Virus
HVS	Herpesvirus Saimiri
ICAM	Intracellular adhesion molecule
ICP	Infected cell protein
Ig	Immunoglobulin
IE	Immediate early
IFN	Interferon
IL	Interleukin
IM	Infectious mononucleosis
IR	Inverted repeat
IRF	Interferon regulatory factor
Kb	Kilobase
KS	Kaposi's Sarcoma
KSHV	Kaposi's Sarcoma-associated Herpesvirus
L	Late
LANA	Latency associated nuclear antigen
LAT	Latency associated transcript
LB	Luria-Bertani
LCV	Lymphocryptovirus
LMP	Latent membrane protein
MCD	Multicentric Castleman's Disease
MDV	Marek's Disease Virus
miRNA	Micro RNA
mRNA	Messenger RNA
MHC	Major histocompatibility complex
MHV	Murine herpesvirus
MOI	Multiplicity of infection

ND	Nuclear domain
NPC	Nasopharyngeal carcinoma
dNTP	Deoxy nucleotide triphosphate
ORF	Open reading frame
OvHV	Ovine Herpesvirus
PBS	Phosphate buffered saline
PCR	Polymerase chain reaction
PEC	Peritoneal exudate cell
PEL	Primary effusion lymphoma
PFU	Plaque forming units
P.I.	Post infection
PKR	Protein kinase R
PTLD	Post transplantation lymphoproliferative disease
pRB	Retinoblastoma protein
RNA	Ribonucleic acid
RPMI	Roswell Park Memorial Institute
RT	Reverse transcriptase
RTA	Replication and transcription activator
SDS	Sodium dodecyl sulphate
SIV	Simian Immunodeficiency Virus
ss	Single stranded
SPBS	Sterile phosphate buffered saline
SSC	Saline sodium citrate
STP	Simian transforming protein
TAE	Tris acetate EDTA
Taq	*Thermus Acquaticus*
TBE	Tris borate EDTA
TE	Tris EDTA
TK	Thymidine kinase
TNF	Tumour necrosis factor
tRNA	Transfer RNA
UTP	Uracil triphosphate
UTR	Untranslated region
UV	Ultraviolet

v	Viral prefix
vtRNA	Viral tRNA-like molecule
v/v	Volume per volume
VZV	Varicella Zoster Virus
w/v	Weight per volume
XLP	X-linked lymphoproliferative syndrome

Chapter 1: Introduction

1.1 Herpesviruses

The large and ever-increasing herpesvirus family consists of at least 130 viruses, the hosts of which cover a range from oysters to elephants. Between these two extremes lie the herpesviruses that infect humans, fish, birds and many other species. The long co-evolution of herpesviruses with their hosts has produced a family of viruses well adapted to persist in their natural host for a lifetime without (in the majority of cases) overt signs of disease.

Members of the herpesvirus family have four important properties in common:

1. The genome encodes a large range of enzymes involved in nucleic acid metabolism (e.g. dUTPase), DNA synthesis (e.g. DNA polymerase) and processing of proteins (e.g. protein kinase).
2. Viral DNA synthesis and capsid assembly occurs in the nucleus.
3. Production of infectious progeny is accompanied by the destruction of the infected cell.
4. They are able to undergo a latent infection in their natural host, a process that requires the formation of closed circular viral genomes and the expression of only a small subset of viral genes (Roizman & Pellet, 2001).

It is this last characteristic that allows the persistence of herpesviruses for the lifetime of a host. The ability of the virus to remain in a quiescent state allows avoidance of the host immune system, and periodic reactivation from latency allows production of infectious virions for transmission to new hosts.

1.1.1 Classification of Herpesviruses

Current classification has the herpesviruses defined as the family *Herpesviridae*, with three subfamilies contained within this group: the *Alphaherpesvirinae*, the *Betaherpesvirinae*, and the *Gammaherpesvirinae*. Historically, membership of the herpesvirus family was assigned based on virion morphology; subfamilies were designated according to biological characteristics. The onset of genome sequencing has allowed refinement of subfamily classification, and is now the primary approach for phylogenetic studies (McGeoch *et al.*, 2006).

The *Herpesviridae* Study Group of the International Committee on Taxonomy of Viruses is currently considering revision of the above classifications; investigations of a number of piscine and amphibian herpesviruses have suggested these would be better characterised by assignment to a new family, the *Alloherpesviridae*. The single invertebrate herpesvirus will be given its own family, the *Malacoherpesviridae*, and all herpesvirus families will further fall into the order *Herpesvirales* (McGeoch *et al.*, 2006). However, as these proposals have yet to be accepted, discussions will be limited to the traditional three herpesvirus subfamilies, the alpha-, beta- and gammaherpesviruses.

1.1.1.1 Alphaherpesviruses

The members of the *Alphaherpesvirinae* are characterised by their ability to establish latency predominantly in sensory ganglia. Other properties include a variable host range, relatively short reproductive cycle and rapid spread in culture. This subfamily includes the genera *Simplexvirus* (e.g. herpes simplex virus [HSV]-1 and –2); *Varicellovirus* (e.g. varicella zoster virus [VZV]), *Mardivirus* (e.g. Marek's disease virus, which unusually is latent in T cells), and *Infectious laryngeotracheitis-like virus*.

1.1.1.2 Betaherpesviruses

The site of latency for the betaherpesviruses is predominantly the mononuclear cells (Mocarski & Courcelle, 2001), but infection can persist in secretory glands, lymphoreticular cells, kidneys and other tissues. Infection is further characterised by the enlargement of infected cells, a process known as cytomegalia. In culture the reproductive cycle is long, and the time to produce cytopathic effects is long. This is not the case *in vivo*, where viral load can double in less than 2 days (Emery *et al.*, 1999). This subfamily contains the genera *Cytomegalovirus* (e.g. human cytomegalovirus, HCMV), *Muromegalovirus* (MCMV) and *Roseolovirus* (human herpesvirus-7, HHV-7).

1.1.1.3 Gammaherpesviruses

The gammaherpesvirus subfamily shows an extremely narrow host range, with infection often limited to the family or order of the natural host. *In vitro* viruses replicate in lymphoblastoid cells, and some can undergo lytic replication in epithelial

and fibroblast cell lines. Latency usually (but not exclusively) occurs in B and T cells, and *in vivo* virus is frequently detected in lymphoid tissue. This subfamily is further divided into the *Lymphocryptoviruses* (e.g. EBV) and *Rhadinoviruses* (e.g. Kaposi's sarcoma associated herpesvirus [KSHV], herpesvirus saimiri [HVS] and murine gammaherpesvirus [MHV-68]).

1.1.2 Herpesvirus Structure

The herpesvirus virion consists of several different layers. The virion core is covered by the capsid, which in turn is covered by the tegument, which is finally covered by the envelope.

The core consists of the viral double stranded DNA. This is surrounded by the capsid, an icosadeltahedral structure made up of 162 capsomeres. The capsid is linked to the envelope by the tegument. This is an amorphous layer of varying thickness containing a number of viral proteins – in the case of HSV-1 more than 15 proteins are associated with this structure (Metteleiter *et al.*, 2002a). The viral envelope appears to be derived from patches of altered cellular membranes containing viral proteins and glycoproteins. The overall size of the herpesvirions varies from 120 to 300 nm, with the variation due to variability in tegument thickness and the state of the envelope – damaged envelopes appear much larger than intact virions (Roizman & Pellet, 2001).

1.1.3 Herpesvirus Genomes

The herpesvirus genomes range in size from approximately 120 kb for VZV to 250 kb for HCMV. Individual herpesviruses also show up to 10 kb variation within the species owing to polymorphisms in terminal and internal repeat copy numbers. Total G+C composition of herpesviruses varies from as little as 32% for canine herpesvirus-1 to 75% for cercopithecine herpesvirus-1 (HV simiae). G+C composition can be homogeneous across the genome, as seen for HSV-1; or largely localised to reiterated sequences of high G+C content at the ends of the genome, with unique regions of low G+C content (e.g. the genome of ateline herpesvirus-2).

The sequence arrangements of the herpesviruses can be categorised into one of 6 groups depending on the presence and localisation of repeat regions (see figure 1.1). These genomes contain between 70 and 200 open reading frames (ORFs), with overlapping genes common – these include genes embedded within other genes, the

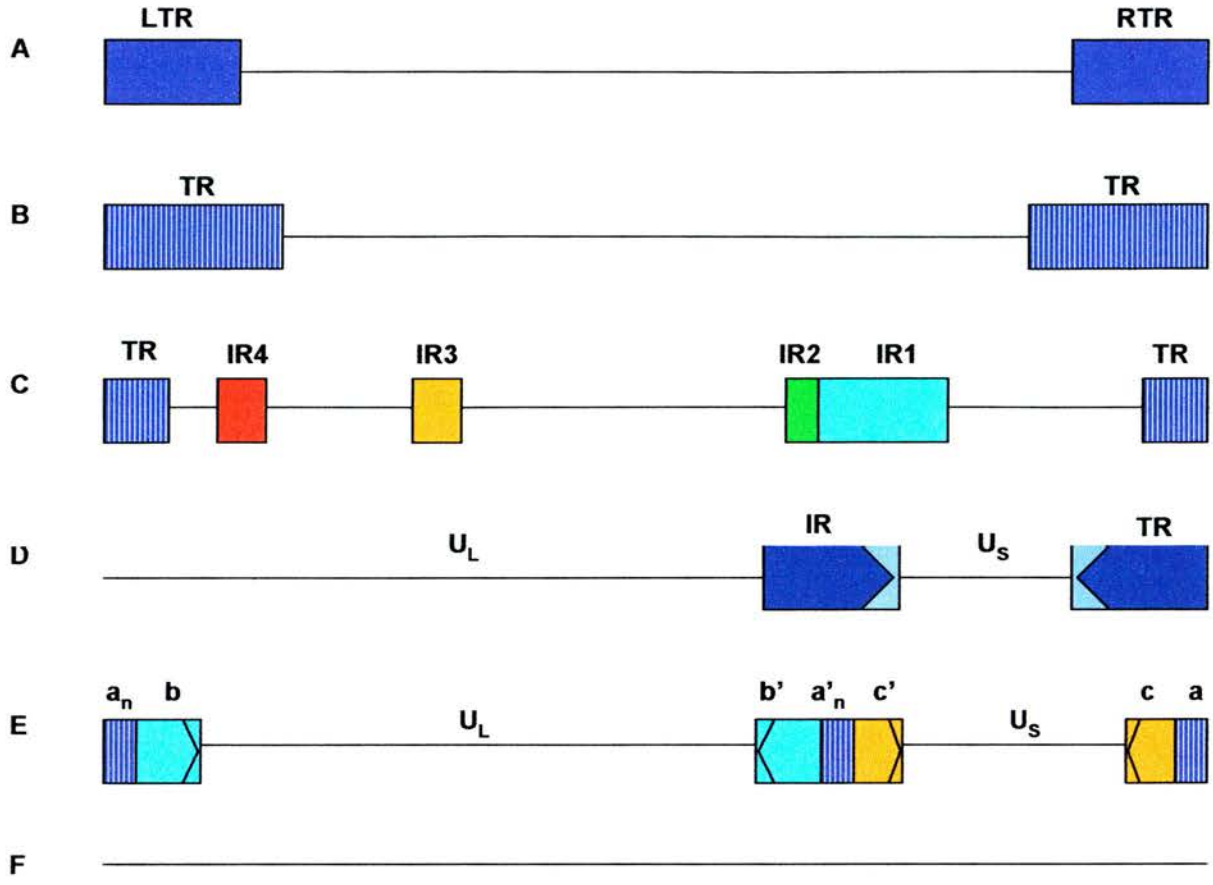

Figure 1.1 Herpesvirus genome arrangements. Herpesvirus genome arrangements fall into one of the 6 categories (A-F) shown above. Class A (e.g. channel catfish virus) has both left and right long terminal repeats (LTRs). Class B (e.g. Herpesvirus Saimiri) have reiterated terminal repeat sequences (TRs). Class C (e.g. EBV) have four internal repeat sequences (IR1-IR4) within the unique region of the genome, as well as reiterated terminal repeat sequences. Class D (e.g. VZV) have a single LTR which is found in an inverted orientation within the unique region of the genome. Class E (e.g. HSV) consist of two elements: one terminus contains *n* copies of sequence *a* next to sequence *b*. The other terminus has one directly repeated *a* sequence next to sequence *c*. The terminal *ab* and *ac* sequences are inserted in an inverted orientation (b'a'$_n$c') separating the unique regions into U_L and U_S domains. Class F (e.g. tuapia herpesvirus) has no identified repeat regions. Adapted from Roizman & Pellet, 2001.

product of which is a truncated version of the larger gene (e.g. HSV U_L26 and $U_L26.5$), and genes expressed from entirely antisense sequence (e.g. HSV-1 $\gamma_1 34.5$ and ORFs P and O). Introns are relatively infrequent in herpesvirus genes, although most will contain a limited number of spliced genes. Most genes contain a promoter region of between 50 and 200 bp lying upstream of a TATA box. Transcription initiation sites are normally 20-25 bp downstream of the TATA box, and this is followed by a 5' non-translated leader sequence of 30-300 bp. At the start of the ORF is a translation initiation codon, followed by 10-30 bp of 3' non-translated sequence, and finally a polyA signal. Transcription is carried out by the host RNA polymerase II.

In addition many herpesvirus genomes contain non-coding RNA molecules, such as the EBERs of EBV and the vtRNAs of MHV-68. The recent discovery of microRNAs (Pfeffer *et al.*, 2004; Pfeffer *et al.*, 2005) increases the number of identified non-coding RNAs.

Herpesvirus genes can be broadly divided into two classes: those essential for growth in culture (including genes encoding the proteins of DNA replication and the virion structural proteins), and non-essential genes which may have a more significant effect on replication *in vivo*. These non-essential genes may be involved in evasion of the host immune response, establishment of latency, or alteration of the cellular environment to improve conditions for replication or latency.

Approximately 26 "core" genes are conserved across the alpha-, beta- and gammaherpesvirus subfamilies. These genes are contained within seven core gene blocks, with between 2 and 12 genes in a block. Within the blocks gene order and polarity are conserved, and within the subfamilies block arrangement is usually conserved. The core genes include virion structural genes, nucleotide metabolism genes, DNA replication genes, and genes with regulatory roles. Within the subfamilies there are further conserved genes. The alphaherpesviruses share latency-associated genes and glycoprotein D, while betaherpesviruses all have a block of 14 genes not found in the other subfamilies. Gammaherpesviruses have shared homologues of cellular genes, along with ORFs encoding proteins required to maintain latent genomes in cycling cells (Roizman & Pellet, 2001).

1.1.4 Herpesvirus Life Cycle

The majority of research has focused on the replication of herpes simplex virus, and as such most of the mechanisms of replication discussed below relate to this virus. Where possible examples are given from other members of the herpesvirus family.

1.1.4.1 Attachment

Virion glycoproteins are involved in the initial attachment of the virus to the target cell. In the case of HSV these glycoproteins target glycosaminoglycan (GAG) chains of cell surface proteoglycans. The virion glycoproteins gB and gC are involved in this binding process, targeting the host heparan sulfate proteoglycan. Loss of gC reduces HSV infectivity but does not abolish it completely, indicating the attachment step is not an absolute requirement for infection (Herold *et al.*, 1991). Loss of both gB and gC substantially reduces binding and also prevents infectivity, due to the role of gB in viral entry (Laquerre *et al.*, 1998).

Heparan sulfate is utilised as a tether in numerous members of the herpesvirus family, including HCMV (Kari & Gehrz, 1993), HHV-8 (Akula *et al.*, 2001) and BHV-4 (Vanderplasschen *et al.*, 1993).

EBV contains a gC homologue, gp350/220, which mediates the initial attachment of the virion to the host cell. EBV targets the CD21 (also known as CR2) receptor, a complement receptor which is highly expressed on the surface of B-lymphocytes and follicular dendritic cells (Prota *et al.*, 2002). Deletion of the gp350/220 gene from EBV does not abolish the ability of the virus to infect cells, although efficiency is reduced (Janz *et al.*, 2000).

1.1.4.2 Binding

Once tethered to the cell, the interaction of virion glycoproteins with host cell receptors allows binding of the virus to the cell surface. Individual herpesviruses use a specific receptor or group of receptors to bind to the host cell, and it is these differences in the host receptor(s) that lead to differences in cell tropism between members of the herpesvirus family.

Three classes of host entry receptors have been identified for HSV so far:

1. HVEM (herpesvirus entry mediator, a member of the TNF receptor family; also known as HveA).
2. Nectin-1 (HveC) and nectin-2 (HveB) (members of the immunoglobulin superfamily). These receptors are expressed on a large range of cell types, including epithelial cells, fibroblasts and neurons. Nectin-1 may be particularly important in direct cell-to-cell spread of the virus (Sakisaka *et al.*, 2001).
3. Specific sites in heparan sulphate (3-*O*-S HS) generated by certain 3-*O*-sulfotransferases (all three types of receptor reviewed by Spear, 2004; Campadelli-Fiume *et al.*, 2000).

The viral glycoprotein necessary for binding of HSV to these cell surface receptors is gD. Different regions of this protein are required for binding to different receptors – the HVEM and 3-*O*-S HS receptors require the presence of the N-terminus, while the nectins require other regions to allow successful binding. Evidence suggests gD is able to assume at least two conformations in complexes with receptors; one form able to bind HVEM and 3-*O*-S HS, and the other able to bind the nectins (Spear *et al.*, 2006). Once bound to the cell surface, the virus envelope then fuses with the cell membrane to release the capsid into the cell. This process requires the gH/gL glycoproteins (Roizman & Knipe, 2001).

In the case of EBV, the cell surface receptors necessary for binding to B cells are the HLA class II molecules. The virus is able to bind to all HLA-DR and –DP molecules, but is restricted in the HLA-DQ class to those molecules carrying a glutamic acid residue at amino acid 46 (Haan & Longnecker, 2000). The viral protein that mediates binding to HLA molecules is gp42. This protein, in complex with gp85 (gH) and gp25 (gL), is necessary for virus penetration of the cell membrane (Li *et al.*, 1997). Gp85 has been show to play a role in envelope fusion with cell membranes.

EBV entry into epithelial cells has different requirements to entry into B cells. There is no requirement for interaction of gp42 with HLA class II molecules, and instead glycoproteins gH and gL interact with a novel entry mediator (Molesworth *et al.*, 2000).

1.1.4.3 Transport to the Cell Nucleus

Following fusion with the cell membrane, the de-enveloped HSV virus is released into the cell cytoplasm. At this point certain tegument proteins (e.g. U_S11) remain in

the cytoplasm, while others travel to the nucleus either by association with the capsid, or by independent means. Host microtubules are required for successful transport of viral capsids to the nucleus, and evidence suggests proteins of the inner tegument are responsible for binding to host dynein motors which mediate transport towards the nucleus (Wolfstein *et al.*, 2006). Following transport, nucleocapsids associate with nuclear pore complexes. Viral DNA is released and passes into the nucleus, where it assumes a circular conformation (Roizman & Knipe, 2001).

1.1.4.4 Viral Gene Expression

Herpesvirus gene expression during lytic infection occurs sequentially (Honess & Roizman, 1974). The first genes to be transcribed are the immediate-early (IE-, or α-) genes. This group is defined by the presence of their transcripts immediately after infection and independently of *de novo* protein synthesis. In practice, these are genes that are still transcribed in the presence of inhibitors of protein synthesis such as cyclohexamide. The predominant role of this class appears to be in transactivation of other groups of viral genes.

In the case of HSV six IE genes have been identified. These are ICP0, ICP4, ICP22, ICP27, ICP47 and $U_S1.5$. These genes share similarities in their promoter region, including numerous binding sites for cellular transcription factors that are present upstream of a TATA box.

Immediate early gene transcription is initiated by a combination of viral and host proteins. Following entry of the virus into the cell, viral protein VP16 (ICP25, α-TIF) is transported into the cell nucleus by a cellular protein, HCF (host cell factor). This VP16-HCF complex is able to bind the host transcription activator Oct-1 to the viral DNA, allowing induction of IE-gene transcription.

Early (E, or β) gene expression is dependent on protein synthesis, as demonstrated by the absence of transcripts in the presence of inhibitors such as cyclohexamide. IE proteins are necessary for production of E gene transcripts, with ICP4 transactivating this process (Roizman & Knipe, 2001).

The early gene class consists largely of genes required for viral nucleic acid metabolism, including the thymidine kinase (TK) gene, a component of the viral ribonucleotide reductase (ICP6) and a DNA binding protein (ICP8).

Expression of late (L, γ) genes is reduced in the absence of DNA synthesis. This class can be further subdivided into two groups: the early-late (γ_1, leaky-late), where expression is enhanced by viral DNA synthesis; and the true late (γ_2) genes, which absolutely require DNA synthesis to occur prior to their expression. These subgroups largely contain genes encoding the structural components of the virion, including gC and gB.

1.1.4.5 Viral DNA Replication

Following onset of early gene expression, these gene products are able to localise to specific regions of the nucleus known as Nuclear Domain 10 (ND10) structures (Maul *et al.*, 1996). At these prereplicative sites viral DNA synthesis is initiated.

Seven viral gene products are essential for viral DNA replication. These are a polymerase (U_L30), a processivity factor for the polymerase (U_L42), a ssDNA binding protein (ICP8, or U_L29), an origin binding protein (U_L9) and three proteins that comprise a helicase-primase complex (U_L5, U_L8 and U_L52) (Uprichard & Knipe, 1997). Host factors such as DNA ligase and topoisomerase II are also likely to be involved (Roizman & Knipe, 2001).

The two most studied origins of replication in the HSV genome are *oriS* and *oriL*. *OriS* is present twice, on either side of the S compartment. *OriL* is found between ICP8 and the DNA polymerase sequence. Both types of origin contain palindromic sequence, with *oriL* being a 144bp palindrome and *oriS* slightly shorter at 45bp. Flanking the origin sequences are inverted repeats that act as binding sites for U_L9 (Roizman & Knipe, 2001).

Following binding of U_L9 to the origin, ICP8 then binds to this region, and in conjunction with U_L9 begins the unwinding of the dsDNA. The presence of U_L9 and ICP8 recruits the helicase-primase complex to the origin, and this complex generates a primer that allows the polymerase to begin synthesis of DNA (reviewed by Lehman & Boehmer, 1999).

Initially replication of circular viral DNA structures gives rise to theta replicative forms. As DNA synthesis progresses, replication switches from this theta mechanism to a rolling circle mechanism that generates concatemers. These molecules accumulate in the nucleus in structures called replication compartments.

In a manner extremely similar to HSV replication, the EBV lytic cycle requires seven viral genes – a DNA polymerase catalytic subunit (BALF5), a polymerase accessory subunit (BMRF1), a single stranded DNA binding protein (BALF2), an origin binding protein (BZLF1) and three proteins that together form a helicase-primase complex (BBLF4, BSLF1 and BBLF2/3). Initiation of replication occurs at the *oriLyt* site in the genome, and replication occurs in discrete replication compartments in the nucleus (reviewed by Tsurumi *et al.*, 2005).

1.1.4.6 Assembly of Virions: Capsid Formation and DNA Encapsidation

Formation of the viral capsid can occur following expression of the capsid genes, a subset of the late gene group. Initial assembly of some capsid proteins occurs in the cytoplasm prior to import into the nucleus for completion. VP5, VP26 and VP23 (U_L18) all require cytoplasmic association with other capsid or scaffold proteins such as VP19C (U_L38) or pre-VP22a before they can be imported into the nucleus.

VP5 is the major capsid protein, and forms hexons and pentons that make up the outer shell. Capsomeres are then linked by complexes of the minor capsid proteins VP19C and VP23.

Several different types of capsid are assembled in the nucleus. *C*-capsids contain viral DNA, and following budding through the nuclear membrane can go on to form infectious virions. *A*- and *B*-capsids both lack DNA, but B capsids contain the scaffold proteins VP22a and VP21 and the viral protease VP24. Successful encapsidation of DNA leads to removal of these proteins. *A*-capsids are believed to be failed capsids, unable to package DNA.

For encapsidation of viral DNA to occur, concatemers generated previously must first be cleaved. The viral DNA contains signals for cleavage and packaging of DNA, and these signals control site-specific breakage of DNA to generate single genomes.

1.1.4.7 Assembly of Virions: Envelopment and Egress

Capsids assembled in the nucleus must move into the cytoplasm before their eventual release from the cell as fully formed virions. The viral proteins U_L31 and U_L34 are located in the nuclear membrane and are necessary for movement of capsids from the nucleus to the cytoplasm. In the presence of these two proteins capsids are able to bud from the nucleus, forming a primary enveloped virion in the perinuclear space.

From this point onward the exact mechanism of envelopment and movement of the virus within the cell is disputed. Two pathways are suggested for virion egress, both shown in figure 1.2. In the first, the reenvelopment pathway, the enveloped nucleocapsid fuses with the outer nuclear membrane, releasing a deenveloped nucleocapsid into the cytoplasm. The particle subsequently buds into the trans-Golgi network and is ultimately released through secretory vesicles. In the second proposed pathway, called the lumenal pathway, the enveloped nucleocapsid moves through the cell in the lumen of the endoplasmic reticulum or in vesicles. The particle eventually transfers into the trans-Golgi network where maturation of the virion glycoproteins takes place (Roizman & Knipe, 2001).

The most recent evidence suggests the reenvelopment model is the most likely mechanism for virus egress. Infection with a HSV mutant where gD carries an ER retrieval sequence shows that the perinuclear virion envelopes contain gD, whereas extracellular virion envelopes do not. This suggests the virus acquires its final membrane in a compartment that excludes ER-retrieved gD (Skepper *et al.*, 2001). Electron microscopy further supports this hypothesis, showing several alphaherpesviruses (PrV, EHV-1 and HSV) undergoing fusion of the primary envelope with the outer nuclear membrane to release the deenveloped nucleocapsids into the cytoplasm. Microscopy further showed nucleocapsids undergoing reenvelopment in the area of the trans-Golgi network (TGN), and the role of the TGN in providing the secondary envelope for the nucleocapsid was confirmed by labelling with a TGN-specific antiserum (Granzow *et al.*, 2001). This evidence points to a deenvelopment-reenvelopment model of virus egress.

1.1.4.8 Tegumentation

Tegumentation may begin at two different locations, at either the cytosol or the future envelopment site. Numerous viral proteins are involved in formation of this structure, and these proteins are necessary for interactions between the capsid on one side and the envelope glycoproteins on the other. Closest to and interacting with the capsid is the U_L36 gene product, which forms an icosahedral structure. The U_L37 protein interacts with U_L36 to form the second layer of tegument covering the capsid. In the absence of these proteins virion maturation cannot progress. Subsequent stages in tegumentation are not clearly defined, and there appears to be functional redundancy

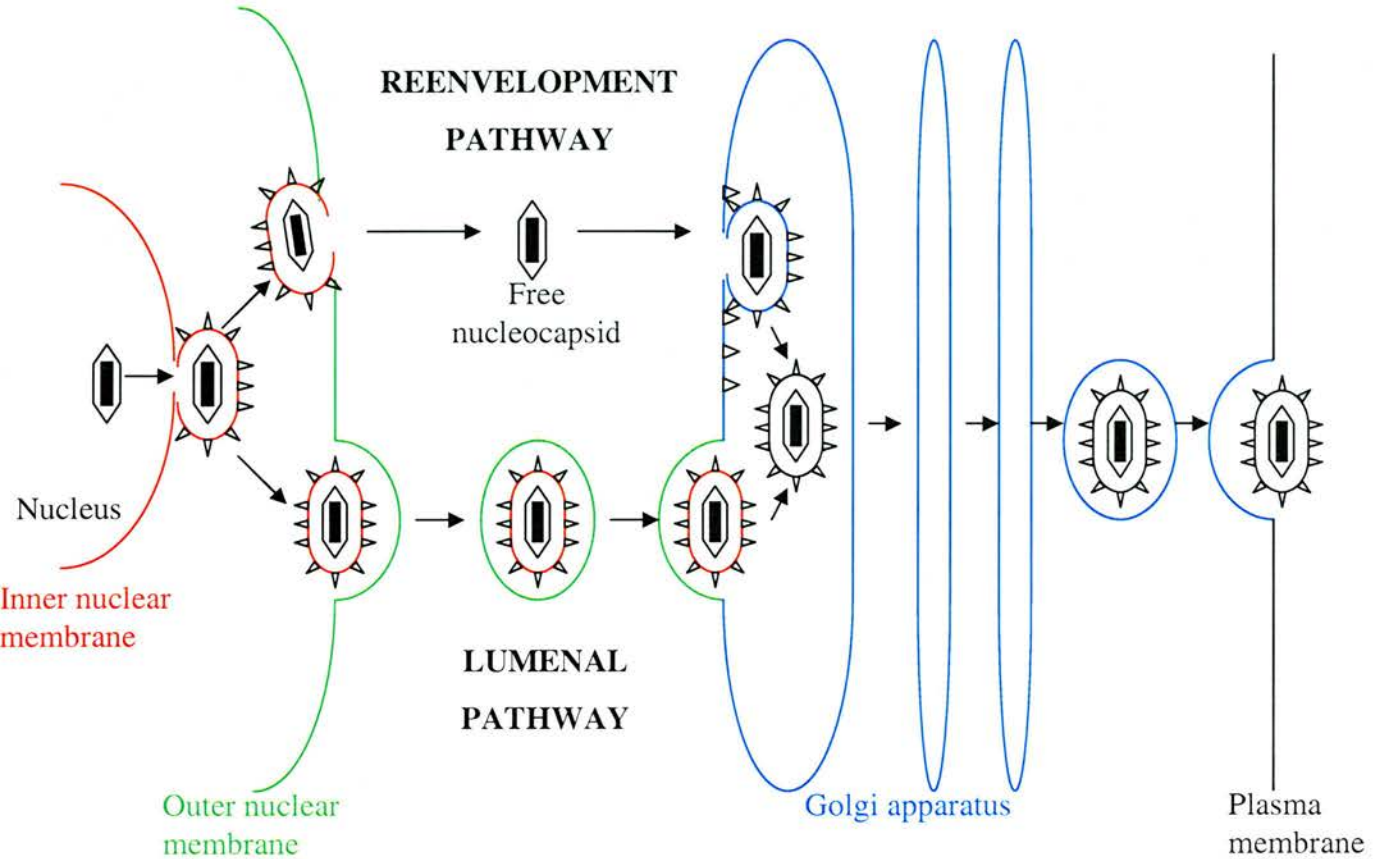

Figure 1.2 Virus Egress from the Nucleus. HSV nucleocapsids bud through the inner nuclear membrane. At this point two different pathways are proposed: the reenvelopment pathway, where the envelope of the nucleocapsid is lost when the virus buds into the cytoplasm and is regained following entry into the golgi pathway; and the lumenal pathway where the envelope is retained and the virion is transported through the Golgi apparatus to the cell exterior. Adapted from Roizman & Knipe, 2001.

in the proteins required for tegument formation (Mettenleiter, 2002b; Mettenleiter, 2004).

1.1.5 Herpesvirus Latency

Latency is a key feature of the herpesvirus family. The ability to remain relatively undetected in the host for extended periods of time allows the herpesviruses to persist in the host organism for a lifetime. Sporadic reactivation from the latent state allows transmission to susceptible individuals.

Different subfamilies of the herpesviruses and individual viruses themselves may have specific requirements for latency – some are discussed in further detail in sections 1.3.4.3-1.3.4.5. However, as before, research has focussed predominantly on the alphaherpesvirus HSV, and the features of latency discussed below relate predominantly to this virus.

Latency results when immediate early gene expression fails to occur. The exact mechanism by which this occurs is not clear, but mutant viruses deficient in IE gene expression undergo a quiescent infection and episomal genomes remain despite failure to undergo productive infection.

During latency a limited range of transcripts are expressed. In HSV these are designated the Latency Associated Transcripts (LATs), and are located in the repeats flanking the U_L region of the virus genome. The activity of viral transcription may be in part controlled by the acetylation state of histones associated with the genome. Acetylation of histones is associated with an 'open' conformation of chromatin and transcriptional activity, while a lack of acetylation is associated with condensed chromatin and a lack of transcription. During latent infection the latency-associated promoter is enriched with acetylated histone H3, while IE and E gene promoters show relatively lower levels of association with acetylated histones. During lytic infection the reverse is true, with acetylated histones associated with the active IE and E genes.

The role of the LATs may be in downregulation of viral gene expression (Garber *et al.*, 1997) or in prevention of virus-induced apoptosis (Perng *et al.*, 2000). Recent studies have shown the presence of a microRNA (miRNA) encoded by the LAT gene that confers resistance to apoptosis by interference with TGF-β signalling (Gupta *et al.*, 2006).

1.1.5.1 Reactivation from Latency

In its natural host, HSV may be reactivated after ultra-violet light, stress, hormone imbalances, injury to tissues innervated by latently infected neurons and potentially many other undefined triggers. The exact signal that initiates reactivation is unknown. *In vitro* mutation of many genes can result in impaired reactivation from latency. Mutations in virtually all genes required for viral replication result in this phenotype, as do mutations in the thymidine kinase, ribonucleotide reductase and ICP0 genes amongst others (Roizman & Knipe, 2001).

ICP0 has been implicated in several processes that may be involved in reactivation. ICP0 can reverse the repression of quiescent genomes, and in its absence reactivation is significantly reduced *in vivo*. The protein has a RING finger domain that allows E3 ubiquitin ligase activity and hence can target proteins for proteasome degradation. ICP0 can target ND10 proteins, including PML and Sp100, and degradation of these components may prevent ND10-induced silencing of viral gene expression. However ICP0 can interact with numerous other cellular and viral proteins, so the exact mechanism by which ICP0 is involved in de-repression of the viral genome is likely to be complex (reviewed by Efstathiou & Preston, 2005).

1.2 Gammaherpesviruses

1.2.1 Epstein Barr Virus

EBV was first discovered in 1964 in B lymphocytes cultured from Burkitt's lymphoma (Epstein *et al.*, 1964). Since its original discovery EBV has been found in association with a number of other tumour types, including Hodgkin's lymphoma, nasopharyngeal carcinoma, certain types of T cell lymphoma and a small percentage of stomach cancers (reviewed by D.Crawford, 2001). This association with disease is linked to the ability of EBV to infect and transform B-lymphocytes.

The genome of EBV was the first of the herpesviruses to be cloned into *E. coli*, and this enabled in-depth studies of the genome to be made (Arrand *et al.*, 1981). The genome consists of 172 kb of unique DNA flanked by repeated 0.5 kb terminal repeat sequences. The unique region is divided by four internal repeat sequences (Kieff & Rickinson, 2001).

1.2.1.1 Latent Gene Expression

EBV is able to infect primary human B lymphocytes derived from peripheral blood, tonsils or fetal cord blood. B lymphocytes at earlier stages of development can be infected albeit at lower efficiencies, and fully differentiated plasma cells are resistant to infection. A limited range of other cell types are susceptible to infection at low efficiencies, including T cells and NK cells (Kieff & Rickinson, 2001).

Infection of primary B lymphocytes *in vitro* results in approximately 10% of cells undergoing transformation to form lymphoblastoid cell lines (LCLs). These latently infected cells express a very limited range of viral proteins, incorporating the nuclear proteins (EBNA1-6) and integral membrane proteins (LMP1, LMP2A and LMP2B). Several viral RNAs are expressed - the EBERs and the BamHI A fragment rightward transcripts (BARTs). These viral gene products are able to drive previously resting B lymphocytes into continuous proliferation. These cells demonstrate an "activated" phenotype, with immunoglobulin secretion, expression of adhesion molecules and adherence to each other. It can be suggested that this activation acts to ensure growth transformation of the host cells and hence increase the number of latently infected B cells (Kieff & Rickinson, 2001).

EBV is able to restrict gene expression further during latency. The type of gene expression described previously is known as type III latency, and this program is seen following initial infection of naïve B lymphocytes in the tonsils (Tierney *et al.*, 1994) and during infectious mononucleosis (IM). During long-term infection the virus persists in long-lived memory B cells within the peripheral blood, and at present it is not clear exactly how B lymphocytes enter the memory compartment. One proposed hypothesis suggests EBV directly infects pre-existing memory cells (Young & Rickinson, 2004), although this does not explain the initial infection and proliferation of naïve B cells. An alternative hypothesis proposes the infected cells enter follicles and differentiate into resting memory cells through the process of germinal centre reaction. In this scenario viral genes in place of antigen drive this process (Babcock *et al.*, 2000). EBV may also persist in the epithelial cells of the tonsils in the absence of symptoms (Pegtel *et al.*, 2004), providing a possible explanation for the association of EBV with naso- and oropharyngeal epithelial carcinomas.

Two other patterns of gene expression have been described – latency I and latency II. In latency I only EBNA-1, EBERs and BARTs are expressed, while in latency II LMP-1 and LMP-2 are also expressed.

The differentiation of latently infected B cells occurs in conjunction with a change in the gene expression pattern, initially from latency III to latency II. This occurs due to a change in the viral promoter, from the Cp/Wp promoters used for the latency III program to the Qp promoter. This process is driven by methylation of the Cp/Wp promoter by host cell factors (Schaefer *et al.*, 1997).

Long-term viral gene expression is still a matter of debate. The latency I phenotype was first observed in Burkitt's lymphoma-derived B-lymphocytes *in vitro* (Gregory *et al.*, 1990). This limited pattern of gene expression allows evasion of CTL attack – the only viral protein present, EBNA1, interferes with antigen processing (Mukherjee *et al.*, 1998), although more recent evidence suggests this protein can still enter the MHC class I pathway (Lee *et al.*, 2004; Tellam *et al.*, 2004). However, within the long-lived memory B cell population *in vivo*, viral gene expression does not appear to be strictly limited to the latency I pattern – while most cells appear to only express EBERs and BARTs, occasional LMP2A expression is detectable, and EBNA1 is detected during cell division (Thorley-Lawson & Gross, 2004).

EBNA1 is expressed in all virus-infected cells. It is required for the maintenance and replication of the genome and is thought to act by tethering the virus to host chromosomes to ensure retention in daughter cells (Kanda *et al.*, 2001). EBNA1 has also been shown able to interact with certain viral promoters and hence regulate transcription, but *in vitro* only the genome maintenance function is essential for transformation of B cells (Humme *et al.*, 2003).

EBNA2 is involved in the transformation process. This protein interacts with the cellular protein RBP-Jκ (Jκ recombination binding protein) to activate both cellular (including CD23) and viral genes (including LMP1 and LMP2A). EBNA-LP also interacts with EBNA2 to allow efficient outgrowth of virus-transformed B cells *in vitro*, a process that is modulated by the EBNA3 proteins. The EBNA3 family includes EBNA3C, which can disrupt cell cycle checkpoints by interaction with cellular modulators of transcription (e.g. histone deacetylase 1) or proteins controlling cell cycle progression (e.g. cyclin A).

LMP1 is an oncogene that induces multiple changes in cells when expressed *in vitro*. These include induction of cell-surface adhesion molecules and activation antigens, and upregulation of anti-apoptotic proteins. LMP1 behaves as a constitutively activated member of the TNFR superfamily, activating several signalling pathways, and resulting in induction of the proteins mentioned previously. It is functionally similar to CD40, and can provide growth and differentiation signals to B cells (Thorley Lawson, 2001; Young & Rickinson, 2004).

LMP2A can drive the proliferation and survival of B cells in the absence of signalling through the B cell receptor. The protein is able to induce a range of genes, including those involved in cell cycle induction, apoptosis inhibition and suppression of cell-mediated immunity (Thorley Lawson, 2001; Young & Rickinson, 2004).

LMP2B is structurally very similar to LMP2A, although it lacks a 5' exon responsible for the signalling properties of LMP2A. Both genes are commonly expressed in EBV-associated malignancies such as Hodgkin's Disease and nasopharyngeal carcinoma. Both LMP2A and LMP2B have been shown to promote epithelial cell spreading and migration *in vitro*, a process that may contribute to the *in vivo* pathogenesis of epithelial-derived tumours (Allen *et al.*, 2005).

The non-coding EBERs are not essential for viral transformation of B-lymphocytes. However in conjunction with the proteins La and L22, the EBERs can bind to and potentially inactivate PKR (Nanbo *et al.*, 2002). EBERs are also involved in tumorigenicity, cell survival and IL-10 induction in Burkitt's lymphoma cell lines (Young & Rickinson, 2004). The protein products of the BARTs remain to be conclusively identified, but include the BARF1 protein, which is an early antigen expressed following induction of the lytic cycle. This protein has oncogenic properties when expressed *in vitro* (Young & Rickinson, 2004).

1.2.1.2 EBV Association with Disease

EBV is extremely prevalent in the human population, with more than 90% of adults being seropositive for the virus (Magrath, 1990), and this figure being closer to 100% in the developing world. Infection with EBV may occur at a young age with no obvious symptoms, and this pattern of infection is common in non-industrialised countries and in low socio-economic groups. In more affluent societies exposure to

the virus may be delayed until adolescence, where the virus is transmitted by kissing and related sexual behaviours (reviewed by Macsween & Crawford, 2003). Infection during adolescence is associated with development of infectious mononucleosis (IM) in between 50 and 74% of cases.

1.2.1.2.1 Infectious Mononucleosis

Following infection by the predicted salivary route, the virus is able to undergo productive replication in the oral cavity, as indicated by its presence in saliva. Evidence suggests this initial infection may occur in either epithelial cells or B cells (reviewed by Crawford, 2001). An initial incubation period of 30 days then occurs, with infected B cells circulating in the blood.

Primary infection induces both humoral and cell-mediated immune responses. IgM and IgG responses to nucleocapsid and envelope proteins are detectable at the time of presentation with symptoms, as well as IgG responses to some IE and E genes and EBNA2. Antibodies to the gp350 membrane protein are able to prevent binding to B cell CR2, but as these arise relatively late during primary infection they are unlikely to prevent viral spread in the early phase (reviewed by Callan, 2004; Moss *et al.*, 2001).

The T cell response is predominantly directed against viral lytic antigens. Uncontrolled T cell responses are damaging, as shown in the case of individuals affected by X-linked lymphoproliferative syndrome (XLPS). The gene affected in this case (SH2D1A, or SAP) is expressed in activated T cells, and inhibits the Signalling Lymphocyte Activation Molecule (SLAM), thereby controlling T cell activation. In individuals where no functional copy of the gene exists, infection with EBV results in a severe IM-like syndrome often resulting in death, or if the infection is survived, in development of B cell lymphoma and/or dysgammaglobulinaemia. It is thought that an uncontrolled CTL response to primary infection causes this syndrome (reviewed by Macsween & Crawford, 2003).

In the immunocompetent host there is a massive CD8+ T cell lymphocytosis, with clonal expansion of CD8+ T cells accounting for up to 30% of the entire CD8+ population. These expanded populations consist predominantly of cells responding to

EBV lytic antigens, with a much lower percentage responding to latent antigens. The high numbers of T cells are not maintained long-term, with most dying following resolution of primary infection (Callan, 2004). The CD8+ T cells produce large quantities of a number of cytokines, including lymphotoxin, TNFα, IL-1β and IL-6, and these may give rise to the symptoms of IM, including fever, lymphadenopathy, sore throat and fatigue (Crawford, 2001).

1.2.1.2.2 Burkitt's Lymphoma

In areas of equatorial Africa Burkitt's lymphoma (BL) is endemic, and in around 96% of cases these tumours contain EBV DNA. The tumours may be found in the jaw, ovary, mammary gland, liver, intestine and kidney, and are composed of rapidly proliferating small B cells. While the tumours arise in extra-nodal sites, the cells resemble germinal centre B cells.

In non-African BL the association of EBV with tumours is less strong, with virus present in tumour cells in around 20% of cases in Europe and North America, and between 50-70% in South America, North Africa and Russia.

The malignant B cells express only EBNA1, although the EBER and BamA transcripts are also present. It is thought that the tumour cells are derived from newly infected tonsillar B cells that have undergone virus-driven transformation and travelled to the lymph nodes. In this site the virus-infected malignant cells resemble centroblasts, a form of antigen-activated rapidly proliferating cells that give rise to germinal centres. Centroblasts are subject to somatic hypermutation events that act to increase the affinity of the B cell receptor for the antigen (reviewed by Crawford, 2001; Young & Rickinson, 2004).

Both virus- and non-virus-associated BL tumours all show one of three chromosome translocations, which results in the constitutive expression of the *c-myc* oncogene. This drives the cells into continuous proliferation and inhibits differentiation. Errors in the somatic hypermutation process mentioned above may allow these translocation events to occur, and hence causing malignant cells to form. The viral EBNA1 may promote cell survival and aid in the oncogenic process (Young & Rickinson, 2004).

The clustering of BL in Africa is closely linked to geographical areas of endemic malaria. It is suggested that recurrent bouts of malaria result in immunosuppression, which allows lytic EBV replication to occur. In conjunction with increased viral replication and further infection of B cells, malarial antigens can cause polyclonal activation of B cells, which may activate EBV-infected memory B cells and result in expansion of the infected B cell pool. Ultimately this leads to a disruption in control of persistent EBV in individuals who have had several attacks of malaria. These factors are also replicated by infection with the HIV virus, which causes both immunosuppression and polyclonal B cell activation (Crawford, 2001).

1.2.1.2.3 B Cell Lymphoproliferative Disease

BLPD occurs in immunodeficient individuals where a lack of EBV-specific CTLs allows proliferation of latently infected B cells. This is a well-noted effect in immunosuppressed transplant patients, giving rise to the alternative name Post-Transplant Lymphoproliferative Disease (PTLD). Between 5 and 30% of transplant recipients experience this disorder (Thompson & Kurzrock, 2004). Tumours arise usually within the first year following transplantation when immunosuppression is most severe. Tumour cells express the latency III programme of viral gene expression (Young & Rickinson, 2004).

BLPD is also common in HIV-positive individuals, particularly in the latter stages of AIDS when CD4+ T cell counts are low and immunosuppression is severe. Tumours are most commonly found in the brain and almost all tumours are EBV-positive (Crawford, 2001). In AIDS patients EBV is also associated with development of oral hairy leukoplasia (OHL), a benign lesion caused by viral replication in the superficial layers of the tongue epithelium (Greenspan *et al.*, 1985).

1.2.1.2.4 Hodgkin's Lymphoma

Approximately 65% of Hodgkin's lymphoma (HL) in the developing world are EBV-associated (Macsween & Crawford, 2003). Tumours are characterised by the presence of large multinuclear Reed-Sternberg cells and Hodgkin's cells (known collectively as HRS cells). HRS cells express the viral genes EBNA1, LMP1 and LMP2A. LMP1 and LMP2 are both implicated in enhanced cell survival and may contribute to the malignant phenotype – LMP1 constitutively activates the CD40

signalling cascade leading to cell proliferation (Lam & Sugden, 2003), while LMP2A mimics B cell receptor signalling to ensure cell survival (Young & Rickinson, 2004). EBV infection is an early event in tumour development, a factor that is consistent with an oncogenic role for the virus (Macsween & Crawford, 2003; Crawford, 2001).

HRS cells are derived from germinal centre B cells that contain functional Ig gene rearrangements but are defective in Ig transcription. The HRS cells only comprise a small percentage of the tumour but constitute the malignant element. The composition of the remaining part of the tumour allows classification into one of three subtypes: nodular sclerosing (NS), mixed cellularity (MC) and lymphocyte-depleted (LD) (Young & Rickinson, 2004).

1.2.1.2.5 Nasopharyngeal Carcinoma

Nasopharyngeal carcinoma (NPC) is common in areas of China and Southeast Asia. NPC arises from squamous epithelial cells and tumours can be classified by the degree of differentiation of the tumour – tumours are either undifferentiated, or non-keratinizing or squamous cell carcinomas. There is a 100% association between EBV and the undifferentiated form of the tumour (Crawford, 2001). EBV gene expression in NPC is restricted to EBNA1, LMP2A and 2B and the BamA transcripts. Approximately 20% of tumours also express LMP1 (Young & Rickinson, 2004). EBV infection takes place prior to outgrowth of the malignant cells.

The predisposition of certain ethnic groups to NPC has been mapped to an unidentified region of the MHC locus. Dietary and/or environmental factors may also contribute to the disease, such as salt fish dishes that contain carcinogenic nitrosamines, and traditional Chinese herbal snuff (Crawford, 2001).

1.2.1.2.6 Other Disease Associations of EBV

Gastric Carcinoma. EBV is found in approximately 10% of gastric carcinomas. These tumours express EBNA1, LMP2A and 2B, and the EBERs and BamA transcripts, similar to the pattern seen in NPC (Young & Rickinson, 2004).

Other tumours where EBV have been implicated include oral hairy leukoplakia, leiomyosarcoma (in conjunction with HIV infection), and potentially in tumours of the salivary gland and breast (reviewed by Thorley-Lawson *et al.*, 2004).

1.2.2 Kaposi's Sarcoma-Associated Herpesvirus

Kaposi's sarcoma (KS) was initially identified in 1872 by Moritz Kaposi, but the infectious agent causing this disease was not identified until 1994 (Chang *et al.*, 1994). KSHV (HHV-8) is a member of the gammaherpesvirus subfamily in the genus rhadinovirus. It is the only human rhadinovirus identified so far, and is closely related to herpesvirus saimiri.

KSHV distribution is dependent upon geographical and behavioural risk factors. In the USA virus can be detected in 0-10% of blood donors, while in Africa more than 50% of individuals are sero-positive (Moore & Chang, 2001). The mode of transmission is not known, but it can be detected in both semen and saliva. As homosexual men have a particularly high infection rate (up to 40% in some studies) a sexual mode of transmission has been suggested. In Africa infection in childhood is more common, suggesting a non-sexual route of transmission is more likely (Moore & Chang, 2001).

1.2.2.1 KSHV Molecular Biology

The KSHV genome consists of a unique region of 145 kb, flanked by a variable number of terminal repeats of 801 bp. The unique region consists of regions homologous to the other herpesviruses containing structural and metabolic proteins, interspersed with regions containing genes required for latency and host cell regulation (Moore & Chang, 2001).

In vitro KSHV tends to undergo latent replication. Virus can be propagated within primary effusion lymphoma (PEL) derived cell lines, and lytic replication can be induced by the addition of chemicals such as phorbol esters.

KSHV genes can be classified into 3 groups (Sarid *et al.*, 1998). The class I genes are truly latent and are not induced by chemical treatment. These consist of three genes located at the right hand end of the genome – LANA-1, v-cyclin, and vFLIP; and one gene lying outside this region, the LANA-2 gene. These genes have several different functions – LANA-1 is required for episome maintenance and tethering to host chromosomes; v-cyclin constitutively activates CDK6; v-FLIP inhibits Fas-mediated

apoptosis, and LANA-2 is a B-cell specific latency gene (reviewed by Jenner & Boshoff, 2002).

Class II genes are expressed at low levels in unstimulated cells but are phorbol-inducible and expressed during both lytic and latent infection. Class III gene transcripts are only detectable following phorbol treatment and consist of true lytic genes, including those for DNA replication and capsid assembly (Moore & Chang, 2001).

The ability of KSHV to cause tumours is a key feature in the diseases caused by the virus (see later for further details). Many viral genes are able to contribute to this process by interfering with the normal cell cycle progression and increasing the lifespan of the cell. Some examples of these genes are given below.

Numerous viral genes have been shown *in vitro* to have the ability to transform rodent cells. These include K1, vIL-6, vIRF1 and ORF74 (vGPCR). ORF72 (v-cyclin) is also involved in cell cycle regulation – v-cyclin closely resembles a D-type cyclin, and acts at the G1-S checkpoint to prevent cell senescence induced by pRB. LANA-1 can also interact with pRB to prevent cell cycle arrest (reviewed by Moore & Chang, 2001; Jenner & Boshoff, 2002).

Inhibition of apoptosis is an important process to prevent death of the infected cell before new virions can be produced to infect a new host. KSHV encodes several proteins able to alter host apoptotic pathways and hence increase cell survival.

Included in this group is the vBcl-2 (ORF16), which contains the anti-apoptotic BH1 and BH2 domains and is able to inhibit Bax-related apoptosis.

Viral FLIP (Fas-ligand interleukin converting enzyme [FLICE]-like caspase inhibitor) (ORF71) is able to act as an inhibitor of the Fas-TNF-receptor signalling pathway by preventing caspase 8 recruitment and hence inhibiting apoptosis.

Three different viral proteins target the pro-apoptotic host gene p53. Firstly, LANA-1 can bind p53 and repress its transcriptional activity and its ability to induce apoptosis. LANA-2 (ORF10.5) similarly is also able to inhibit p53-induced transcription and apoptosis. Viral IRF1 (ORF K9) acts in a similar manner to disrupt p53-induced apoptosis.

1.2.2.2 Disease Associations of KSHV

1.2.2.2.1 Kaposi's Sarcoma

KS is found in several distinct subgroups of the population: in immunosuppressed transplant recipients and AIDS patients; in HIV-negative individuals in Mediterranean countries (classic KS) and African countries (endemic KS), and also in HIV-negative homosexual men (Schulz *et al.*, 1998).

Classic KS affects predominantly elderly males, where it has a chronic course and rarely metastasises to other organs. It presents as multiple reddish-brown plaques and nodules on the lower extremities. Patients survive on average 10-15 years before death from unrelated causes. In contrast, endemic KS can present in a number of different ways: (1) as a benign nodular cutaneous disease in young men; (2) as an aggressive localised cutaneous disease invading soft tissue and bone, causing death within 5-7 years; (3) mucocutaneous and visceral disease, and (4) lymphadenopathic disease spreading to the lymph nodes and visceral organs, usually in the absence of skin lesions, and occurring in young children (Hengge *et al.*, 2002).

AIDS predisposes individuals already infected with KSHV to develop KS – the risk of developing symptoms is more than 20,000 times greater than the general population, and 300 times greater than other immunosuppressed patients. KS presents at multiple sites, with lesions frequently progressing to form tumours. With the development of improved treatment for AIDS in the western world AIDS-KS is rarely seen (Hengge *et al.*, 2002).

Early KS lesions consist of small endothelial-lined spaces surrounding normal blood vessels. As the disease progresses, these patches expand to form a spindle-celled vascular process that expands throughout the dermis. These processes further expand to form sheets of spindle cells and vascular spaces.

The malignant spindle cells that cause the disease are thought to derive from a multipotent precursor cell that under normal circumstances gives rise to hematopoietic and endothelial cells. During the early stages of disease only 10% of spindle and endothelial cells are positive for virus, but in late-stage lesions more than 90% of spindle cells contain virus, suggesting that virus provides a growth advantage to infected cells (reviewed by Jenner & Boshoff, 2002).

The role of KSHV in development in KS is not fully understood. Models suggest that virus reactivates from latently infected B cells following immunosuppression or as a

result of local cytokine production. The virus is then able to infect the precursor cells. KSHV has been shown able to induce differentiation of endothelial cells to lymphatic endothelial cells *in vitro*, and the same process may affect differentiation of spindle cells *in vivo* (Carroll *et al.*, 2004).

1.2.2.2.2 Body Cavity-Based Primary Effusion Lymphoma (BCB-PEL)

BCB-PEL is a rare, rapidly fatal malignancy first described in AIDS patients. The disease presents as a malignant peritoneal, pericardial or pleural effusion in the absence of an identifiable tumour mass.

KSHV-infected cells that comprise this lymphoma are often co-infected with EBV, in particular in the case of HIV-positive individuals. Lymphomas of HIV-negative people are more likely to carry only KSHV and not EBV (Leao *et al.*, 2002).

In this disease the cells harbouring the virus have been identified as preterminally differentiated, post-germinal-center-stage B cells. Virus is present in these cells at high copy number (50-150/cell) (reviewed by Boshoff & Chang, 2001). Gene expression is limited to the latent genes LANA, v-cyclin, v-FLIP and kaposin, as well as the vIL-6 homologue. This gene has been shown to promote B cell proliferation *in vitro* and may well perform the same function *in vivo* (Schulz, 2000). vFLIP may be particularly important for the survival of PEL cells – *in vitro* in the absence of this gene PEL cells undergo spontaneous apoptosis (Guasparri *et al.*, 2004).

1.2.2.2.3 Multicentric Castleman's Disease

MCD is a lymphoproliferative disease, causing lymphadenopathy, fever and splenic infiltration. KSHV is strongly associated (nearly 100%) with MCD in AIDS patients, and is present in approximately 50% of cases in HIV-negative individuals. The KSHV-positive MCD is characterised by the presence of large plasmablastic cells harbouring the virus. These plasmablasts are thought to originate from naïve B cells (reviewed by Jenner & Boshoff, 2002). The IL-6 receptor is expressed by the majority of KSHV-positive cells and a proportion of cells also express vIL-6 (Oksenhendler *et al.*, 2000). vIL-6 may drive differentiation of plasmablasts and the development of lymphoproliferative lesions.

1.2.3 Herpesvirus Saimiri

Herpesvirus saimiri (HVS) is the prototypic virus of the *rhadinovirus* genus. This virus is regularly found in squirrel monkeys (*Saimiri sciureus*) from the South and Central American rainforests (Melendez *et al.*, 1968). Infection of squirrel monkeys produces no obvious signs of disease; however experimental infection of other New World primates such as tamarins, common marmosets and owl monkeys can cause T-cell lymphoma as early as two months following infection.

Three main subgroups of HVS exist, named A, B and C (Medveczky *et al.*, 1984). These are classified according to pathogenic properties and sequence divergence in the non-repetitive terminal regions. Generally, subgroup C possesses the strongest oncogenic properties, and subgroup B the weakest. Differences also exist in the ability to infect different primate species – tamarins are susceptible to all three subgroups, whereas common marmosets do not show signs of disease following infection with HVS from subgroup B (reviewed by Fickenscher & Fleckenstein, 2001).

1.2.3.1 Molecular Biology of HVS

The genome of HVS is composed of 113 kb of unique sequence flanked by a variable number of 1444 bp terminal repeats (Albrecht *et al.*, 1992). The genome is similar to that of other *Rhadinoviruses*, including KSHV and MHV-68. Unlike many other gammaherpesviruses, HVS is able to undergo lytic replication *in vitro*, allowing study of productive replication, and the generation of recombinant viruses. HVS is able to infect a variety of human cells and persist at high copy number in episomal form.

The HVS genome contains large blocks of homology to the other gamma-2-herpesviruses, as well as blocks of genes unique to the virus. These unique blocks contain the transforming oncogenes as well as several homologues of cellular genes.
The transforming genes are located at the left-hand end of the genome. Variation in transforming genes is found between the three subgroups – A contains a single gene in this position, saimiri transformation-associated protein of subgroup A (stpA); the homologous gene in subgroup B (stpB) lacks transforming ability, and subgroup C carries two genes, stpC and tip (tyrosine kinase interacting protein). StpA and stpC share limited homology, but there is no obvious relationship between StpA and tip.

StpC is thought to mediate its oncogenic properties through its ability to activate NFκB. Both StpA and StpC have been shown to interact with TNF receptor-associated factors (TRAFs). These TRAFs are crucial for initiation of signalling pathways that ultimately result in activation of NFκB. Expression of StpC in conjunction with a TRAF protein in epithelial cells results in activation of NFκB, a process that is abolished if the TRAF is mutated to prevent binding of StpC. The non-transforming StpB can be converted to a transforming state if a region of StpC containing 18 collagen-like repeats is added. This alteration allows StpB to induce NFκB in epithelial cells.

StpC induces activation and subsequent phosphorylation and degradation of I-κB kinase (IKK) in both T-lymphoid and non-lymphoid cells. Evidence suggests that StpC binds to the TRAFs and activates NFκB-inducing kinase (NIK), which then activates IKK. This results in degradation of I-κB and activation of NFκB (reviewed by Tsygankov, 2005).

The tyrosine kinase interacting protein (Tip) of HVS is also able to stimulate T cells. Tip is thought to have many potential targets in the host cell and may affect a number of different pathways. Interaction of Tip with a host protein Lck (a Src-family protein tyrosine kinase) has been shown to lead to activation of Lck tyrosine kinase activity *in vitro*. Lck plays a role in T cell signalling, and constitutively active Lck mutants have oncogenic potential. This suggests the ability of Tip to activate Lck signalling may result in activation of T cells and lead to oncogenesis.

However not all evidence supports this hypothesis, and in fact in some cases this is directly contradicted. Expression of Tip in human Jurkat T cells causes downregulation of Lck-mediated signal transduction. Tip can also suppress the transforming ability of a constitutively active Lck mutant in fibroblast cells, a process that is enhanced by mutation of Tip that enhances binding to Lck. This evidence suggests that Tip functions in a manner similar to EBV LMP-2A – this protein inhibits B cell-receptor-mediated signalling and induces latency by blocking viral replication (reviewed by Fickenscher & Fleckenstein, 2001; Jung *et al.*, 1999).

Tip is also able to induce activation of STAT1 and STAT3 transcription factors in a Lck-dependent manner. When Tip binds to Lck, Lck is activated and in turn

phosphorylates Tip. This phosphorylation allows recruitment of STAT1 and STAT3, which are then tyrosine phosphorylated by Lck. However, removal of the tyrosine phosphorylation sites of Tip can still result in STAT3 activation. Therefore, while Tip is known to enhance Lck-dependent activation of STATs the mechanism is not yet clearly understood (reviewed by Tsygankov, 2005; Fickenscher & Fleckenstein, 2001).

Other transcription factors are known to be activated by Tip. NF-AT, a transcription factor with a role in T-cell stimulation, is activated by Tip, but the mechanism for this process is unclear. Some evidence points to a role for Lck in this process, but in the presence of protein tyrosine kinase inhibitors NF-AT activation can still occur, suggesting a Lck-independent mechanism (reviewed by Tsygankov, 2005).

Several other genes are present in the HVS genome that are involved in stimulating or enhancing T cell proliferation. These include the vIL-17 (ORF13) gene, which activates NF-κB and induces expression of IL-6, IL-8 and surface ICAM-1. Viral IL-17 enhances proliferation of primary T cells induced by PHA.The product of ORF14 (viral superantigen, vSag) binds to MHC class II molecules and stimulates T cell proliferation. It is not clear how essential the gene is for transformation *in vivo*.
The viral genome also contains anti-apoptotic genes such as ORF16 (Bcl-2 homologue) and ORF71 (vFLIP). Both genes are expressed during lytic infection and may prevent induction of apoptosis in lytically infected cells (Tsygankov, 2005; Fickenscher & Fleckenstein, 2001).

1.2.4 Gammaherpesviruses of Veterinary Importance

Malignant catarrhal fever is a generally fatal disease of cattle, deer, pigs and several other susceptible species. The cause of disease is infection with either alcelaphine herpesvirus-1 (AlHV-1) or ovine herpesvirus-2 (OvHV-2). In their natural hosts, the wildebeest and domestic sheep respectively, these viruses cause no overt signs of disease. However, in susceptible species the disease is characterised by hyperplasia of lymphoid organs, accumulation of T lymphocytes in many tissues, and vasculitis. These changes occur despite limited evidence of viral replication (reviewed by Coulter *et al.*, 2001).

Biological characteristics and preliminary sequence analysis allowed classification of the AlHV-1 virus as a rhadinovirus, and the sequencing of the genome in 1997 (Ensser *et al.*, 1997) confirmed previous findings. Of the 70 putative ORFs of AlHV-1, 61 show homology to HVS, the prototypic gamma-2-herpesvirus. Creation of a cosmid library of the OvHV-2 genome allowed sequencing of the genome (Rosbottom, 2003), confirming that while similar to AlHV-1, OvHV-2 is in fact a separate species.

AlHV-1 can be grown in tissue culture, allowing investigation of the function of viral genes *in vitro*. OvHV-2 can be propagated (but not easily isolated) in both bovine and rabbit T cell lines, with the bovine cells supporting predominantly latent infection, and the rabbit cells undergoing what appears to be an abortive productive infection (Rosbottom *et al.*, 2002).

Equine herpesvirus-2 (EHV-2) and equine herpesvirus-5 (EHV-5) were originally classified as β-herpesviruses based on their biological properties. Later sequence analysis resulted in their reclassification as γ-herpesviruses, with genome structures more closely related to HVS (a gamma-2-herpesvirus) than EBV (a gamma-1-herpesvirus) (Telford *et al.*, 1993; Telford *et al.*, 1995).

EHV-2 has been implicated in immunosuppression in foals, upper respiratory tract disease, conjunctivitis, general malaise and poor performance. An alternative role has been suggested in the reactivation of EHV-1 and EHV-4 (Welch *et al.*, 1992; Purewal *et al.*, 1992). EHV-2 may also be a predisposing factor for *Rhodococcus equi* infection of the respiratory tract (Nordegrahn *et al.*, 1996).

EHV-2 infection is common, with evidence showing infection of between 56 and 68% of tested horses in Sweden, and 71% of tested horses in England positive by PCR for the virus. By comparison infection with EHV-5 is substantially lower, with nearly 25% of English horses testing positive for the virus (Nordengrahn *et al.*, 2002).

Bovine herpesvirus-4 (BoHV-4) is found world-wide and has been isolated in a variety of clinical diseases as well as in healthy cattle. *In vitro* BoHV-4 is able to infect a broad spectrum of cells, including B-lymphocytes, T-lymphocytes, macrophages, endothelial cells, and liver, kidney and mammary gland cells. Most non-bovine cells do not support viral replication *in vitro* (reviewed by Ackermann,

2006), but *in vivo* it is able to infect cattle, buffalo (Dewals *et al.*, 2005), rabbits (Osorio *et al.*, 1982), lions and domestic cats (Kruger *et al.*, 2000).
Genome analysis shows BoHV-4 is a member of the gammaherpesvirus subfamily, and is more closely related to HVS than EBV (Lomonte *et al.*, 1996).

Porcine gammaherpesviruses PLHV-1, -2 and –3 are highly prevalent in domestic and feral pigs. PLHV-1 has been shown to be associated with lymphoproliferative disease in immunosuppressed and post-transplant pigs, and pathogenesis closely resembles the EBV-associated PTLD in humans.
Porcine herpesviruses are currently of interest because of developments in transplantation of organs from pigs to humans. Human herpesviruses are able to trigger graft rejection and transplant failure. Interactions between human herpesviruses and PLHV-1 have been demonstrated *in vitro*, indicating that xenotransplantation may be affected by interactions between human and porcine herpesviruses (Santoni *et al.*, 2006).

1.2.5 Animal Models of Gammaherpesvirus Infections

Initial infection with gammaherpesviruses is in many cases an asymptomatic process. The virus may persist for many years before symptoms become apparent, and while it is possible from this point to investigate the mechanisms of disease progression, it is not possible to determine what factors are involved prior to onset of symptoms.

In the case of EBV initial infection is apparent in the few individuals that develop infectious mononucleosis; in the majority of cases primary infection goes undetected. To overcome the lack of subjects for the study of acute infection and to allow investigation of factors preceding the numerous EBV-related lymphomas, the development of a suitable animal model is an important process. This allows investigation of the contribution of viral and host factors to the disease progression, as well as development of treatments and vaccines.

Initially attempts were made to develop models of infection using EBV infection of New World primates.
Inoculation of cotton-top tamarins (*Sagunis oedipus*) with EBV causes an acute polyclonal B cell proliferation, with some animals succumbing to lymphoproliferative

disease. This feature has allowed use of this model for post-transplant lymphoproliferative disease and potential vaccines (Epstein *et al.*, 1985). However, there are a number of differences to human infection with EBV. During acute infection disease progresses much more rapidly, with tumour formation occurring within 2-3 weeks following infection; and onset of lymphoproliferative disease occurs in the majority of animals infected (Shope *et al.*, 1973). These characteristics are not representative of acute EBV infection in humans, and while useful as a model for PTLD the cotton-top tamarin may not be as useful for the study of acute infection.
Infection of the common marmoset (*Calithrix jacchus*) causes an IM-like syndrome (Wedderburn *et al.*, 1984), but this does not replicate the B cell involvement of EBV in humans (Emini *et al.*, 1986) and no evidence of EBNA-1 expression (a characteristic feature of long-term persistence during EBV infection in humans) has been found at late time points (Farrell *et al.*, 1997). Therefore the common marmoset is not a suitable model for the study of long-term EBV persistence.

Attempts to infect Old World primates with EBV failed, possibly as a result of cross-reactive immunity from pre-existing Lymphocryptovirus (LCV) infection, use of a defective EBV isolate, problems with the route of inoculation, or a potential species restriction for efficient B cell immortalization by LCVs (Moghaddam *et al.*, 1998; Wang *et al.*, 2001).

Lymphocryptoviruses closely related to EBV have been known since the 1970s to infect Old World primates. The genomes of these viruses are colinear and encode highly homologous structural proteins. LCV-infected cell lines can be established from lymphocytes taken from both healthy and diseased primates, including chimpanzees, gorillas, orang-utans and various macaque species. These cell lines produce virus able to immortalise B cells, and during latent infection also express a nuclear antigen similar to the EBV EBNA proteins (reviewed by Wang *et al.*, 2001).

In vivo LCV infection resembles EBV infection in humans, with sero-conversion occurring in the majority of young animals. In the case of rhesus macaques (*Macaca mulatta*) infected with a rhesus LCV by an oral route, animals shed virus in oral secretions and harbour persistent, asymptomatic LCV infection in the peripheral

blood (Moghaddam *et al.*, 1997). These similarities allow investigation of acute and persistent infection in an animal virus analogous to EBV.

Simian LCVs have proved useful in understanding interactions between the virus and host during immunosuppression. Discovery of LCV-induced tumours (EB-like cynomolgus B-lymphotrophic herpesvirus) in cynomolgus monkeys immunosuppressed as a result of infection with SIV mirrors the development of EBV-positive B cell lymphomas in AIDS patients (Feichtinger *et al.*, 1992). This further emphasises the usefulness of Old World primate models in the study of EBV-related disease in both the immunocompetent and immunosuppressed host.

KSHV is difficult to study *in vivo* owing to the asymptomatic nature of primary infection – as yet no equivalent to the infectious mononucleosis disease caused by primary EBV infection has been detected. Investigation of events occurring during initial infection have been limited primarily to *in vitro* studies, and these are limited owing to the persistence of the KSHV genome in tissue culture predominantly in the latent state.

A number of viruses have been identified in primates that are closely related to KSHV and several of these have been identified as potential animal models for the study of KSHV. The rhadinovirus genus contains members that naturally infect both Old- and New-World primates. Amongst those that infect New World primates are herpesvirus saimiri and herpesvirus ateles (a virus of spider monkeys) (Melendez *et al.*, 1972), while those that infect Old World primates include rhesus monkey rhadinovirus (RRV) (Desrosiers *et al.*, 1997) and the PapRV2, a herpesvirus of baboons (Whitby *et al.*, 2003).

Advantages of the use of primate viruses for the study of KSHV include easy growth in tissue culture – the RV2mac virus, a rhadinovirus of macaques (*Macaca mulatta*) replicates lytically *in vitro* to produce high viral titres, allowing production of recombinant viruses and the study of individual viral genes within the context of an *in vitro* viral infection (reviewed by Damania & Desrosiers, 2001).
The presence of largely colinear genomes in a number of Old World primate rhadinoviruses allows investigation of both acute and chronic infection in an

analogous animal model. The RV2mac virus contains homologues to nearly all KSHV ORFs, with the exceptions of K3, K5, K7 and K12, and transcription profiles for both viruses are also very similar (Dittmer *et al.*, 2005).

As with EBV, the coinfection of macaques with SIV and one of the many rhesus rhadinoviruses allows *in vivo* modelling of the interactions between HIV and KSHV. Development of a disease closely related to the multicentric plasma cell variant of Castleman's disease has also been observed in rhesus macaques coinfected with SIV and a rhesus rhadinovirus, and hence more than one KSHV-associated disease can be studied in these primate models (Damania & Desrosiers, 2001).

While infection of Old World primates with their natural LCVs and rhadinoviruses may produce excellent models for the mechanisms of EBV and KSHV disease, the reality of keeping primates is much more difficult. High security, large expense and strict government regulations mean that use of primates in research is extremely limited. Added to this are the difficulties in generating transgenic animals for the investigation of viral-host interactions and the relative lack of understanding of many primate immune systems, and there are arguments for the development of more simple models of gammaherpesvirus infection.

Increasingly mice are the animal of choice for the study of gammaherpesviruses *in vivo* as they are small and easy to keep.

Murine models have been developed for both EBV and KSHV. In the case of EBV, SCID (severe combined immunodeficiency) mice inoculated with PBMC from EBV seropositive individuals develop EBV-positive BPLD-like tumours (reviewed by Johannessen & Crawford, 1999). However no murine model exists at present for the other EBV-related diseases. Similarly, a model for KSHV exists whereby SCID mice implanted with human fetal thymus and liver grafts are susceptible to infection and undergo an initial lytic infection followed by establishment of latency in CD19+ B cells (Dittmer *et al.*, 1999).

In addition to infection of mice with human viruses, it is also possible to infect with murine gammaherpesviruses. Murine gammaherpesvirus-68 (MHV-68) is able to cause both productive and latent infection in laboratory mice in a manner analogous to EBV infection (Sunil-Chandra 1992a; Sunil-Chandra, 1992b). The ease with which

recombinant viruses can be generated allows investigation of the role of individual genes *in vivo*, the majority of which are homologous to genes in the gammaherpesviruses EBV and KSHV. MHV-68 therefore provides a model system in which interactions between a gammaherpesvirus and its natural host can be studied, and from which parallels with EBV, KSHV and important veterinary gammaherpesviruses can be drawn.

1.3 Murine Gammaherpesvirus-68

MHV-68 was originally isolated from bank voles (*Clethrionomys glaroulus*) in 1980, along with the related viruses MHV-60 and MHV-72. At the same time two further viruses, MHV-76 and MHV-78 were isolated from wood mice (*Apodemus flavicollis*) (Blaskovic *et al.*, 1980). Suspensions of tissues (lung, spleen, liver, kidney and heart) were diluted and inoculated into the brains of newborn mice, and passaged from mouse to mouse. Different isolates were obtained from different passages. The isolated viruses were able to infect a range of cell lines derived from a number of different species (Svobodova *et al.*, 1982).

Initial studies of the virus led to classification of MHV-68 as an alphaherpesvirus. However later studies revealed MHV-68 was able to cause pneumonia in the lungs of newborn mice, with viral antigen detectable in a range of tissues and cell types. These mice failed to develop neurological disease (Rajcani *et al.*, 1985). Sequence analysis led to reclassification of MHV-68 as a gammaherpesvirus in the rhadinovirus genus (Efstathiou *et al.*, 1990), and this classification is further confirmed by the ability of the virus to establish latent infection in B lymphocytes, macrophages, dendritic cells and epithelial cells (Flano *et al.*, 2000; Sunil-Chandra *et al.*, 1992b; Weck *et al.*, 1999a; Stewart *et al.*, 1998).

MHV-68 is endemic in the UK wood mouse population (Blasdell *et al.*, 2003), and it is likely that this is the natural host species. More recently MHV-68 has been designated murid herpesvirus-4 (MHV-4) strain 68, with the other MHV isolates MHV-76, -60 and –72 similarly designated MHV-4 strain 76, -60 and –72.

1.3.1 MHV-68 Genome

The genome of MHV-68 consists of a single unique region of 118,237 bp DNA flanked by a variable number of 1,213 bp terminal repeats. The unique region consists

of 46% G+C, while the terminal repeats are composed of 77.6% G+C. Within the unique region are two internal repeats: a 40 bp repeat located at genome co-ordinates 26778 and 28191, and a 100 bp repeat located at co-ordinates 28981-101170. The strain of MHV-68 used for sequencing is designated γHV-68 WUMS (Virgin *et al.*, 1997).

The unique region of the MHV-68 genome is largely colinear with the genomes of other rhadinoviruses, including KSHV and HVS (see figure 1.3). The unique region comprises 73 open reading frames (ORFs) along with eight viral tRNA-like molecules and nine predicted microRNAs (Bowden *et al.*, 1997; Pfeffer *et al.*, 2005; Virgin *et al.*, 1997). As with other rhadinoviruses, MHV-68 possesses a number of cellular homologues, including a regulator of complement activation (ORF4), a Bcl-2 homologue (M11), a cyclin D homologue (ORF72) and a G-protein coupled receptor (ORF74) (Kapadia *et al.*, 1999; Wang *et al.*, 1999; van Dyk *et al.*, 1999 Wakeling *et al.*, 2001).

MHV-68 also contains a number of genes unique to this virus, with a significant number of these clustered at the left-hand end of the genome. These are M1, M2, M3 and M4. This region also contains the tRNA-like molecules and the predicted microRNAs (Bowden *et al.*, 1997; Pfeffer *et al.*, 2005). This region (the first 9.5 kb of the genome) is absent from the naturally occurring deletion mutant MHV-76 (Macrae *et al.*, 2001; Clambey *et al.*, 2002).

1.3.2 MHV-68 Virions

MHV-68 virion structure is similar to other herpesviruses (Ciampor *et al.*, 1981; Svobodova *et al.*, 1982). The capsid, tegument and glycoprotein genes homologous to those of other herpesviruses can be predicted to fulfil the same role in the MHV-68 virion. The composition of the MHV-68 capsid, tegument and envelope was investigated by Bortz *et al.* (2003). This study identified 5 capsid proteins (ORF25, ORF62, ORF26, ORF65 and ORF29); 3 tegument proteins (ORF75c, ORF45 and ORF11); 2 envelope proteins (ORF8 and ORF22); and 4 proteins of undetermined location (ORF20, ORF24, ORF48 and ORF52). In addition, several other studies have identified components of the MHV-68 envelope; these include M7 (Stewart *et al.*, 1996), ORF27 (May *et al.*, 2005b) and ORF28 (May *et al.*, 2005a).

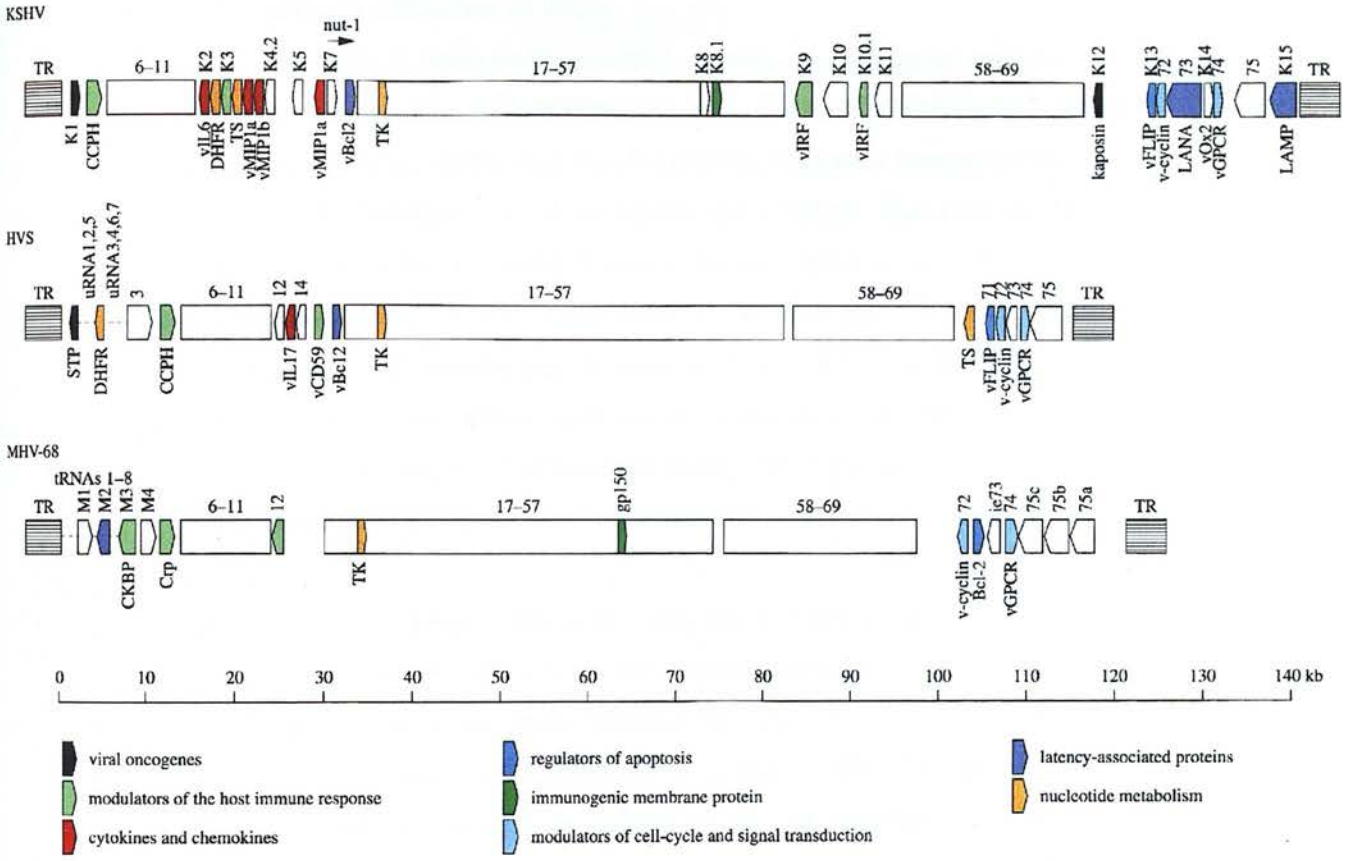

Figure 1.3 The Genome of MHV-68 is Largely Colinear with the Genomes of KSHV and HVS. Diagrammatic representation of the genome of MHV-68 aligned with the genomes of KSHV and HVS. Open boxes represent conserved gene blocks. Adapted from Nash et al, 2001.

1.3.3 MHV-68 Infection *In Vitro*

MHV-68 is able to infect and successfully replicate in a range of cell lines, including epithelial and fibroblast lines (Svobodova *et al.*, 1982). While MHV-68 undergoes productive infection in the majority of cell lines, there are a limited number of lines in which MHV-68 is able to establish a persistent infection. These include the NS0 line (derived from mouse myeloma B cells) (Sunil-Chandra *et al.*, 1993) and S11 cells (Usherwood *et al.*, 1996c). In the NS0 cell line both circular (episomal) and linear forms of the viral genome can be detected. Following treatment with acyclovir the amount of linear virus DNA molecules is substantially reduced, indicating the linear form of the genome is predominantly associated with lytic infection, whereas the episomal form is associated with latent infection (Sunil-Chandra *et al.*, 1993).

Many MHV-68 genes have been assigned functions based on their sequence homology to the genes of other herpesviruses whose roles are already known (Virgin *et al.*, 1997). However more recently the use of signature tagged transposon mutagenesis has identified conclusively a number of MHV-68 genes essential for the replication process, as well as several genes not essential but that significantly enhance viral replication (Moorman *et al.*, 2004; Song *et al.*, 2005). To date 41 genes have been shown essential for viral replication; these include 17 genes essential for replication in the α-, β- and γ-herpesvirus subfamilies, including MHV-68 ORF6 (a ssDNA binding protein), ORF8 (gB), ORF9 (DNA polymerase), ORF22 (gH) and ORF64 (tegument protein). A number of the essential genes have homologues only within the gammaherpesvirus subfamily: these include ORF45, a homologue of the KSHV IRF7 binding protein (Jia *et al.*, 2005).

Gene expression in MHV-68 occurs in a cascade fashion, with transcription of immediate early genes preceding early gene transcription, and late gene expression occurring subsequently to early gene expression (Ebrahimi *et al.*, 2003). MHV-68 transcription can be detected from 3 hours post-infection *in vitro*. The replication genes ORFs 6 (ssDNABP), 9 (DNA polymerase), 60 (ribonucleotide reductase subunit) and 61 (ribonucleotide reductase subunit) are transcribed with similar kinetics, with a defined early peak of transcription. Showing similar kinetics are the ORF57 and M6 genes. Other genes can be clustered into three general expression

patterns – one with a peak at 5 hours p.i., with a gradual decrease in transcript levels (including ORF50/Rta, ORF37 (alkaline exonuclease, and gL); a second group with a peak at approximately 8 hours p.i., including the structural genes ORFs 25 (capsid), 33 (tegument), 38 (membrane) and M7 (gp150), as well as several genes of unknown function (ORFs 20 and 52). The final group shows a peak of transcription at 12 hours post-infection, and includes a second group of structural proteins, including ORFs 19 (tegument), 66 (capsid), 68 (glycoprotein), and a gene of unknown function, M9 (Ahn *et al.*, 2002; Martinez-Guzman *et al.*, 2003). From this temporal analysis of viral gene expression it is possible to build up a profile of the events of MHV-68 replication, and also to hypothesis about the functions of unknown genes such as M6 and M9 based on similarities of their expression pattern to genes of known function.

Along with the essential replication proteins, a number of non-essential genes are also expressed during *in vitro* infection. The M4, K3 and ORF73 genes are expressed with immediate early kinetics, while the cellular homologues (ORF72, M11 and ORF74) are expressed with early-late kinetics. The early-late group also includes the abundantly expressed M3 gene, which encodes a chemokine binding protein.

Following the assembly of new virions in a manner that has not been investigated (but is assumed analogous to the process observed for HSV-1), MHV-68 can exit the cell into the extra-cellular space, or can infect adjacent cells. The M7 (gp150) gene of MHV-68 encodes a glycoprotein necessary for viral egress into the extra-cellular space (de Lima *et al.*, 2004; Stewart *et al.*, 2004). In contrast, the ORF27 (gp48) gene has been identified as involved in the process of egress directly into adjacent cells (May *et al.*, 2005c). gp48 must be localised to the plasma membrane for efficient movement of virions into new cells, a process that requires the viral ORF58 product (May *et al.*, 2005b).

1.3.4 MHV-68 Infection *In Vivo*

Investigation of the virus revealed MHV-68 was able to infect inbred laboratory strains of mice. In 1992 Sunil-Chandra *et al.* demonstrated that MHV-68 was able to infect BALB/c mice and cause disease reminiscent of EBV infection (Sunil-Chandra *et al.*, 1992a).

1.3.4.1 Initial Infection

The intranasal route of infection is commonly used as an experimental method of inoculation. An alternative strategy is infection via the intraperitoneal (i.p.) route (Weck *et al.*, 1996). The natural route of transmission of the virus has not been conclusively determined. The discovery of virus in the lungs of the postulated natural host of MHV-68, the wood mouse, would suggest that the aerosol route of transmission may occur in the wild. However the housing of infected mice with uninfected mice does not easily result in transmission of the virus, suggesting the intranasal route may not be the most efficient (Gaspar-Smith & Bost, 2004). Other potential natural routes of transmission are via breast milk (Raslova *et al.*, 2001), or via the digestive system (Peacock & Bost, 2000).

Following inoculation by the intranasal (i.n.) route, mice develop an infection of the lung, with virus detectable as early as 1 day post-infection, the peak of replication occurring on d3-5, and clearance of the virus by d10. While virus cannot be detected by plaque assay after d10, detection by PCR is possible for extended periods following infection (Stewart *et al.*, 1998).

MHV-68 localises to the alveolar epithelium and mononuclear cells (Sunil-Chandra *et al.*, 1992a). In these cells gene expression is similar to expression during *in vitro* infection, with detection of both lytic and latent transcripts (Martinez-Guzman *et al.*, 2003). A number of genes not required during acute infection *in vitro* have however been shown to play a role during acute infection *in vivo*. These include the thymidine kinase (ORF21) gene (Coleman *et al.*, 2003), the dUTPase (ORF54) gene (Song *et al.*, 2005), ORF73 (Moorman *et al.*, 2003a; Fowler *et al.*, 2003) and ORF75a (Song *et al.*, 2005).

Thymidine kinase (TK) and dUTPase are both required for nucleic acid metabolism, producing dTMP and dUMP respectively, both of which can be converted to dTTP. Cellular dTMP can be synthesised *de novo*, with the methylation of dUMP by thymidylate synthase, or it can be salvaged from dT by thymidine kinase. This second pathway predominates, and the process is limited by the presence of cellular TK, which is restricted to S phase. In non-cycling cells cellular TK is not present, and hence the supply of dTMP is limited and viral replication cannot occur. The presence of a viral thymidine kinase overcomes this restriction and allows viral replication in

non-cycling cells. *In vitro* a TK-deficient virus shows no replication deficit, most likely due to the presence of pre-existing dTMP pools. However *in vivo* the TK-deficient virus is severely impaired during acute infection of the lung, with viral replication 10,000 times lower than that of the wild-type MHV-68 (Coleman *et al.*, 2003). This implies that during acute infection the virus is infecting cells without a pre-existing dNTP pool, which suggests the virus is infecting fully differentiated epithelial cells that have exited the cell cycle.

ORF73 shows homology to the KSHV LANA-1 gene (Virgin *et al.*, 1997). The LANA-1 protein of KSHV is multifunctional, involved in episome maintenance and tethering to host chromosomes, as well as prevention of apoptosis and disruption of cell cycle control (reviewed by Jenner & Boshoff, 2002). The MHV-68 gene is 24.2% homologous to the KSHV gene (Virgin *et al.*, 1997), and it has not been determined if the MHV-68 ORF73 shares all properties of LANA-1. Following low-dose infection (1×10^3 pfu) with an ORF73-deficient virus, delayed replication kinetics were observed (Moorman *et al.*, 2003a). However at higher doses (1×10^4 pfu) the absence of ORF73 does not appear to affect acute infection in the lung (Fowler *et al.*, 2003; Moorman *et al.*, 2003a).

ORF75a is a tegument protein of unknown function, and it is not clear how this influences acute replication *in vivo* while having no effect during *in vitro* infection (Song *et al.*, 2005).

The deletion mutant MHV-76 also shows an attenuated phenotype in the lung following intranasal infection. This virus, lacking M1-M4 and 8 vtRNAs, produces lower viral titres in the lung and is cleared more rapidly than MHV-68 (Macrae *et al.*, 2001). This phenotype has not been attributed to any individual gene missing from the MHV-76 genome, and may result from a combined effect of the missing genes and/or tRNAs (see section 1.3.5.1 for further discussion).

Infection of the lung is accompanied by an infiltration of lymphoid cells into the peribronchiolar, perivascular and interstitial areas (Sunil-Chandra *et al.*, 1992a). This infiltrate consists predominantly of T cells, monocytes and macrophages (Sarawar *et al.*, 2002), with the T cell population consisting predominantly of CD8+ T cells. CD8+ T cells have been shown to play a key role in control of MHV-68 acute infection in the lung – depletion of CD8+ T cell subsets by antibody results in elevated viral titres at early time points accompanied by a failure to clear the virus.

CD4+ T cell depletion does not have such an extreme effect during initial infection – the virus does not replicate to the extremely high titres observed in CD8+-depleted mice, and while acute infection is prolonged the virus is eventually cleared (Ehtisham *et al.*, 1993).

The type I interferon response is extremely important in the initial response to infection. Infection of mice lacking a functional type I interferon receptor (IFN-α/β-$R^{-/-}$) causes significant mortality (80%) at the usually non-lethal dose of 4 x 10^5 pfu. Infection of these mice with the lower dose of 4 x 10^3 pfu still results in 50% mortality within 7-8 days of infection. IFN-α/β-$R^{-/-}$ mice have 100- to 1000-fold higher viral titres in the lungs, and those that survive past 8 d.p.i. still harbour infectious virus in the lungs at 3 weeks post-infection, indicating impaired clearance (Dutia *et al.*, 1999). Virus is also able to disseminate to other organs such as the adrenal gland and liver (Dutia *et al.*, 1999; Barton *et al.*, 2005).

1.3.4.2 Viral Dissemination

The next stage of infection is the trafficking of MHV-68 to the mediastinal lymph node. This process is most likely mediated by the dendritic cells (S. Selverajah, unpublished data). Preformed infectious virus cannot be detected in the MLN at this point and therefore the virus is most likely cell-associated (Stevenson & Efstathiou, 2005). Infected dendritic cells, macrophages and B cells can all be detected in the MLN (Nash *et al.*, 2001); however in the absence of B cells virus still reaches the MLN but fails to disseminate to other lymphoid organs, suggesting the B cell is the major cell type required for trafficking of the virus to other organs (S. Selverajah, 2001).

1.3.4.3 Acute Phase Latency in the Spleen

Upon reaching the spleen MHV-68 establishes a latent infection, with MHV-68 detected within germinal centre B cells, macrophages and dendritic cells (Flano *et al.*, 2000). During establishment of latency there is a rapid expansion of germinal centre B cells, a process that is dependent on the presence of CD4+ T cells. In the absence of CD4+ cells there is a substantial reduction in the ability of the virus to establish latency (as measured by infectious centre assay) as well as an absence of the

splenomegaly characteristic of MHV-68 infection (Ehtisham *et al.*, 1993; Usherwood *et al.*, 1996a). Splenomegaly usually peaks on d10, and the increase in cell number is due to an expansion of the B cell, CD8+ and CD4+ T cell subsets (Usherwood *et al.*, 1996a). Splenomegaly is driven by viral factors located in the left-hand end of the genome – following infection with MHV-76 splenomegaly fails to occur, indicating the 9.5 kb deleted region is important for this feature of infection (Macrae *et al.*, 2001). The exact gene or genes required for this process have yet to be identified. Following the peak of latency, numbers of latently infected cells decline to levels at the limit of detection (Sunil-Chandra *et al.*, 1992a).

In addition to the increase in both B and T cells that result in splenomegaly, there is an increased number of circulating T cells, specifically the Vβ4+CD8+ subtype. This increase is observed from d21 and is reminiscent of the infectious mononucleosis observed during EBV infection. A viral superantigen has been suggested to drive this rapid proliferation of CD8+ T cells in conjunction with CD4+ cell-derived cytokines (Tripp *et al.*, 1997; Coppola *et al.*, 1999). While this process does not occur following infection with MHV-76, the exact viral factor(s) that drive this process have not yet been identified.

The type II interferon response is also important in control of pathology in the spleen. In the absence of a functional type II response, both the spleen and MLN of mice infected with MHV-68 show fibrosis and atrophy at 17 days post-infection. Absence of a type II IFN response results in altered levels of some cytokines – IL-1β, TNF-α and TGF-β1 are elevated in the spleens of IFNγR$^{-/-}$ mice, all of which are involved in induction of fibrosis. Other chemokines are present at reduced levels in the spleens of IFNγR$^{-/-}$ mice – IP-10 and MIG (both involved in T cell recruitment) are both downregulated. IP-10 is also known to inhibit fibroplasia and deposition of extracellular matrix proteins, so a reduction in levels may contribute to the phenotype observed in IFNγR$^{-/-}$ mice (Ebrahimi *et al.*, 2001).

IFNγ is also involved in control of persistent replication in the PECs and to a lesser effect in the spleen. In the absence of IFNγ significant levels of persistent replication are detected in the PECs from d16 to d42, but in the spleen only on d16 (Tibbetts *et al.*, 2002). This suggests an alternative mechanism may control persistent replication

in the spleen. Reactivation from latency is an important factor in maintenance of persistent replication in IFNγ$^{-/-}$ mice (discussed in section 1.3.4.6).

The switch from lytic to latent infection requires a change in gene expression patterns. During latency the genes involved in viral replication and production of new virions are not required and transcription must be curtailed; other genes necessary to maintain the virus in a quiescent state must be activated. Host factors such as NF-κB have been identified as able to inhibit MHV-68 lytic replication and drive the virus into a latent state (Brown *et al.*, 2003). This process may occur by the interaction of NF-κB with the MHV-68 RTA.

RTA (Replication and Transcription Activator), or ORF50, plays a key role in the lytic-latent switch. Upregulation of the gene by alteration of the promoter region results in accelerated lytic growth *in vitro*, and a deficit in latency establishment in the spleen *in vivo*. Virus was also cleared more rapidly from the lung (May *et al.*, 2004; Rickabaugh *et al.*, 2004). Infection with an ORF50.stop virus is difficult as this virus is not replication competent; however *in vivo* infection shows that in the absence of RTA viral persistence is established in the lungs, although when measured at d42 lung viral load is reduced compared to mice infected with wild-type virus. By 4 months post-infection the situation is reversed, with the ORF50.stop virus resulting in a higher viral load than the wild-type virus. At no time point was virus detected in the spleen (Moser *et al.*, 2006). This result suggests that while lytic replication is not essential to seed persistent virus in the lungs, it may be required in order for the virus to traffic to the spleen.

Both over- and under-expression of the RTA gene causes a failure in establishment of latent infection in the spleen. This suggests that initial lytic replication is essential for virus to traffic to the spleen, and that upon reaching the spleen RTA expression must be downregulated to allow for normal establishment of latency.

Several other genes have been implicated in the establishment of latency in the spleen. ORF73 is one of the few viral genes identified as absolutely essential for the establishment of latency. By homology to the LANA-1 protein of KSHV, the ORF73 gene product is involved in maintenance of the viral episome, and this function has

been confirmed for the MHV-68 ORF73 *in vitro* (Fowler *et al.*, 2003). In the absence of ORF73, MHV-68 fails to establish latency in the spleen following inoculation by either the intranasal or intraperitoneal route (Fowler *et al.*, 2003). I.p. vaccination with an ORF73-deficient virus can protect against a later intranasal challenge with wild-type virus, with no evidence of establishment of latency in either the lung or the spleen following the challenge (Fowler *et al.*, 2004).

M1 is one of the unique genes of MHV-68. M1 has been suggested to affect establishment of latency in the spleen following i.p. inoculation. Infection with a virus where M1 is disrupted by a LacZ cassette results in reduced viral titres at d4 and d9 post-infection; however these results were not reproduced when infecting with an M1 deletion mutant. This suggests the observed phenotype may be due to the presence of a large expression cassette in the M1.LacZ virus rather than a true attribute of the M1 gene (Clambey *et al.*, 2000).

The M2 gene of MHV-68 is also involved during acute-phase latency. M2 is dispensable for replication *in vitro*, but is one of the few viral genes expressed in the latently infected S11 cell line (Husain *et al.*, 1999). Following intranasal (but not intraperitoneal) inoculation, M2 is required for establishment of normal viral load. Infection with an M2-deficient virus results in a 10-fold deficit in viral load compared to infection with wild-type MHV-68 at 16 days post-infection (Jacoby *et al.*, 2002), although splenic lymphocytosis is unaffected (Macrae *et al.*, 2003). This suggests that proliferation of latently infected cells and uninfected cells may occur independently or are driven by different viral factors. M2 also plays a role in long-term control of viral load in the spleen, and this is discussed later.

M3 is a broad-spectrum chemokine binding protein, able to bind to CC, CXC, C and CX_3C chemokines (Parry *et al.*, 2000). Expression of M3 can prevent chemokine-induced chemotaxis and may interfere with the migration of lymphoid cells (Jensen *et al.*, 2003). M3 is consistently expressed in the spleen from d7 to d10, with transcripts rarely detectable by d21 (Simas *et al.*, 1999). Studies where M3 is disrupted by the presence of a LacZ cassette have shown the virus to be deficient in establishment of latency – the M3-deficient virus shows evidence of initial lymphoid colonisation, but entry into germinal centres is impaired, and at d13 and d21 there is a substantial

reduction in the number of splenic follicles harbouring virus (Bridgeman *et al.*, 2001). This suggests a further role for immune evasion in latency amplification; however a later study where M3 is disrupted by a more subtle process (the insertion of a stop codon) revealed no requirement for M3 in the spleen (van Berkel *et al.*, 2002).

M4, one of the unique left-hand end genes of MHV-68, is necessary for establishment of normal viral load in the spleen (Evans *et al.*, 2006; Geere *et al.*, 2006 Townsley *et al.*, 2004). The M4 ORF encodes a secreted glycoprotein of unknown function (Evans *et al.*, 2006). While M4 is dispensable for *in vitro* replication, *in vivo* in the absence of the gene splenic viral load is reduced between 10 and 100-fold from as early as 14 days post-infection. This deficit appears to be resolved by 42 days post-infection. Reports vary as to whether M4 contributes to splenomegaly; however it is clear that M4 contributes to viral expansion during acute-phase latency.

K3 encodes a protein able to cause inhibition of MHC class I antigen presentation. Several homologues exist amongst the other gammaherpesviruses, including the K3 and K5 genes of KSHV, the major immediate early protein of BoHV-4 and HVS ORF12 (Stevenson *et al.*, 2000). MHV-68 K3 is an ER-associated protein able to ubiquitinate H-2Db, -2Kb, -2Dd and –2Kd, and target them for degradation by the proteasome (Boname & Stevenson, 2001). K3 is required for expansion of latently infected cells in germinal centres, and in the absence of the gene a reduction in infective centres is observed during establishment of latency (d13 and d17) in conjunction with reduced viral load compared to wild-type virus. The absence of K3 also leads to an increased number of virus-specific CD8+ CTLs (Stevenson *et al.*, 2002). This suggests that immune evasion of CTLs is an important requirement for latency expansion in the spleen.

1.3.4.4 Long-Term Viral Persistence in the Spleen

Long-term latency in the spleen is maintained in both memory and germinal centre B cells (Flano *et al.*, 2002). Low levels of latent virus are also detectable in splenic macrophages and dendritic cells (Flano *et al.*, 2003), and this maintenance of virus in non-B cells correlates with other studies demonstrating the persistence of virus in the spleens of B cell (MuMT)-deficient mice (Weck *et al.*, 1996). Maintenance of latency is dependent on the development of memory B cells, as shown by the progressive loss

of latency in CD40$^-$ B cells (CD40 is required to deliver survival signals to germinal centre B cells that allows them to become memory B cells) (Kim *et al.*, 2003).

CD4+ T cells are important for long-term control of the infection. MHC class II$^{-/-}$ mice (I-A$^{b-/-}$) are constitutively CD4+-deficient. Infection of these mice with MHV-68 initially produces a disease similar to that observed in wild-type mice, with the virus cleared with only a small delay from the lung, and subsequent establishment of latency in the spleen. However from d22 onwards virus was consistently detected in the lungs of the MHC class II$^{-/-}$ mice, with increasing titres detected until 135 days post-infection, by which point most mice had died from a wasting disease (Cardin *et al.*, 1996). In this situation despite a functional CD8+ T cell population, infection cannot be controlled (Belz *et al.*, 2003). Viral evasion of CD8+ T cells has been linked to the development of this wasting syndrome, specifically viral inhibition of MHC class I antigen presentation by the K3 gene (Stevenson & Efstathiou, 2005).

M2 is required for the long-term control of viral load in the spleen. The requirements for M2 during establishment of latency were mentioned previously; however despite an initial reduction in viral load following infection with an M2-deficient virus, viral load at late time points post-infection (up to d46) is significantly higher than wild-type virus (Macrae *et al.*, 2003; Jacoby *et al.*, 2002). It would appear that in the later stages of infection M2 is involved in inhibition or prevention of over-expansion of virus-infected cells. As this phenotype is not observed following infection with MHV-76, it is likely dependent on the action of another region of the left-hand end of the genome.

1.3.4.5 Alternative Sites of Long Term Persistence

Several other sites of long-term viral persistence exist. At three months post-infection these include the blood, brain, kidney, liver, bone marrow, nasopharyngeal-associated lymphoreticular tissue (NALT) and lungs. The frequency of genome positive cells in the majority of these organs and tissues is low – 1/120,000 for bone marrow, and 1/63,000 in the NALT, in contrast to 1/7,700 in the spleen at the same time point (Flano *et al.*, 2003). It has not been shown conclusively that this virus present at low levels is not an artefact present as a result of an abortive infection.

In 1996 the lung was shown to harbour low levels of viral DNA up to 1 month post-infection even in the absence of any detectable infectious virus (Usherwood *et al.*, 1996b). The presence of virus in the lungs in latent form was later demonstrated by Stewart *et al.* (1998). MHV-68 was shown to persist in the lungs of both wild-type (C57/Bl6) and B cell deficient (MuMT) mice as late as 12 months post-infection. As only episomal forms of the virus were detectable, and vtRNAs were detectable by *in situ* hybridisation in the absence of indicators of lytic replication (in this case hybridisation to viral thymidine kinase), this was taken to indicate ongoing latent infection. Latent virus was detected in both wild-type and MuMT mice, indicating that persistence in the lung could occur independently of the presence of B cells. The cell type identified as harbouring the virus in MuMT mice was the epithelial cell.
Further evidence to support the presence of a latent infection in the lung came from the treatment of infected mice with 4'-S-EtdU (an antiviral compound that causes inhibition of DNA synthesis by chain termination, in a manner similar to Acyclovir) for a month prior to sampling of the lungs. Treatment did not abolish the presence of virus in the lungs of wild-type or MuMT mice up to 2 months post-infection, indicating viral persistence is maintained even in the absence of lytic replication.

Flano *et al.* (2003) confirmed the importance of the lung as a site of viral persistence by demonstrating that the lung has the highest frequency of genome positive cells (1/21,000) outside the spleen (1/7,700) of any organ investigated thus far. While agreeing with the findings of Stewart *et al.* (1998) that the lung is an important site of latency, this study suggested an alternative site to the epithelial cell as harbouring latent virus. This study involved the separation of the different populations of lung cells by FACS and investigation of frequency of genome positive cells. Results showed while initially all populations (B cells, macrophages, dendritic cells and "null" [predominantly stromal and epithelial] cells) harboured virus, long-term persistence was maintained only in the B cell population. This controversy remains to be resolved.

1.3.4.6 Reactivation from Latency

At times in the viral life cycle it is predicted that the virus must reactivate from the latent state to produce new virions for transmission to other hosts. The exact trigger for reactivation is unknown; however again the RTA gene is known be involved.

Expression of RTA in the latently infected S11 cell line is sufficient to disrupt latency and initiate lytic gene expression. This ultimately leads to viral DNA replication and production of infectious viral particles (Wu *et al.*, 2000).

The type I interferon response is important in control of viral reactivation. Despite establishing normal levels of latency, IFN-α/β-$R^{-/-}$ mice display substantially higher levels of reactivation in both the spleen (5-fold) and PECs (40-fold) than immunocompetent mice at 28 days post-infection. *In vivo* depletion of IFN-α/β in wild-type mice prior to sampling produces a similar result, with depleted mice showing greater levels of reactivation than undepleted mice. However at later time points (161 d.p.i.) the role of type I interferon appears to diminish, with both wild-type and IFN-α/β-$R^{-/-}$ mice showing similar levels of virus reactivation (Barton *et al.*, 2005).

Type II interferon is similarly involved in control of viral reactivation. *In vitro* experiments have demonstrated that latently infected cells reactivate virus at reduced levels when incubated in the presence of IFNγ. *In vivo* depletion of IFNγ following establishment of latency increases the frequency of cells that reactivate virus, confirming the role of type II interferon in control of reactivation from latency in PECs (Steed *et al.*, 2006).
In the absence of a functional type II interferon response, reactivation is essential for persistent replication of MHV-68. Infection of IFNγ$^{-/-}$ mice with reactivation-deficient viruses (M11- and v-cyclin-deficient viruses, see below for details) results in significantly lower levels of persistent replication in the PECs. This suggests persistent replication in IFNγ$^{-/-}$ mice is a distinct process to acute replication, with different genetic requirements (Gangappa *et al.*, 2002).

Reactivation is not an essential factor in maintaining long-term viral load in the memory B cells of the spleen. Infection of wild-type mice with a reactivation-deficient virus does not affect viral load in the spleen at late time points (up to 6 months) post-infection. In contrast, B cell deficient mice are unable to maintain viral load in the absence of reactivation, indicating that viral reactivation is only essential in the absence of B cells (van Dyk *et al.*, 2003).

Several viral genes have been implicated in reactivation.

ORF72 (v-cyclin) is a homologue of mammalian D-type cyclins. V-cyclin is required for reactivation from latency in both splenocytes and PECs (van Dyk *et al.*, 2000). As mentioned previously, failure to reactivate from latency has no bearing on long-term viral load in the spleens of immunocompetent mice (van Dyk *et al.*, 2003). MHV-68 v-cyclin can bind to cellular cdk2 and cdc2, and through interactions with these proteins can drive the cell into S phase (Upton *et al.*, 2005), a stage of the cell cycle conducive to viral replication.

ORF74 has previously been identified as a latency-associated transcript (Virgin *et al.*, 1999), and by homology to KSHV and HVS has been identified as a G protein-coupled receptor (GPCR). ORF74 is expressed at late time points post-infection (up to 10 months), but is one of the rare genes where transcription occurs predominantly in the lungs and less frequently in the spleen. MHV-68 ORF74 has transforming ability *in vitro*, an ability also observed in the KSHV GPCR (Wakeling *et al.*, 2001). Disruption of ORF74 leads to a reduction in reactivation from latency (Moorman *et al.*, 2003b).

M11 is a partial bcl-2 homologue, containing the anti-apoptotic but not the pro-apoptotic capabilities of bcl-2 (Wang *et al.*, 1999). As with ORF74, M11 has been identified as a latency-associated transcript, and can be detected as a bicistronic transcript with ORF74 (Virgin *et al.*, 1999; Wakeling *et al.*, 2001). Perhaps unsurprisingly given its association with ORF74, M11 is another gene expressed at relatively high levels in the lung at late time points post-infection (Roy *et al.*, 2000). Disruption of M11 does not affect establishment of latency in the spleen or the PECs, but reactivation from the PECs is 4-5 fold less efficient than wild-type virus (Gangappa *et al.*, 2002).

The M1 gene of MHV-68 has been implicated in control of viral reactivation. Sequence analysis shows putative homology to a poxvirus serpin homologue (Virgin *et al.*, 1997), although the MHV-68 M1 gene lacks certain conserved regions important for serpin function (Clambey *et al.*, 2000). Following deletion of M1, the virus exhibits enhanced reactivation from latency in the PECs and the spleen at d42-

50 (Clambey *et al.*, 2000). This suggests M1 plays an important role in suppression or control of viral reactivation.

1.3.4.7 MHV-68 Association with Lymphoproliferative Disease

Long-term *in vivo* infection can produce lymphoproliferative disease in mice. Over the course of a 3 year study, 9% of mice developed lymphoproliferative disease. These disorders predominantly affected the spleen, mesenteric lymph nodes, liver, lung and kidney, and clinical signs of illness were detectable from 165 to 825 days post-infection. Development of lymphomas was associated with an increased number of latently infected genome-positive cells compared to latently infected but clinically normal mice. Occasional positive cells resembling lymphoid cells were seen in the tissue parenchyma, suggesting a possible route of spread (Sunil-Chandra *et al.*, 1994). Host factors have been identified that control development of lymphoproliferative disease – infection of BALB mice deficient in β2-microglobulin (and hence deficient in MHC class I antigen presentation) results in development of disease at a significantly higher rate (67%) and at earlier time points than in wild-type BALB/c mice (22%) (Tarakanova *et al.*, 2005).

1.3.5 Other Strains of Murid Herpesvirus-4

The isolation of a number of related viruses at the same time as MHV-68 has provided opportunities to investigate naturally occurring deletion mutants of MHV-68 that are able to persist *in vivo*.

1.3.5.1 MHV-76

MHV-76 was isolated from the yellow-necked wood mouse (*Apodemus flavicollis*) (Blaskovic *et al.*, 1980). Characterisation of this strain of MHV-4 showed the viral genome is essentially identical to MHV-68, with the exception of a deletion of the first 9,538 bp at the left-hand end of the unique region of the genome. This region contains the genes M1, M2 and M3; most of the 5' end of M4, and the 8 vtRNA-like molecules. MHV-76 most likely arose during *in vitro* culture of MHV-68 – the genome of MHV-76 is identical over several thousand base pairs to MHV-68, indicating an extremely close relationship. *In vitro* growth of MHV-76 shows no significant difference to growth of MHV-68, indicating that none of the genes

contained in the missing region are essential for replication (Macrae *et al.*, 2001; Clambey *et al.*, 2002).

In vivo MHV-76 replicates to lower levels in the lung than MHV-68, viral titres peak slightly earlier (d4 rather than d6), and is cleared more rapidly (d10 rather than d12). Splenomegaly is reduced compared to an MHV-68 infection, and latency is established at much lower levels. At late time points post-infection (up to 5 months p.i.) MHV-76 is able to persist in the spleen but less efficiently in the lung (Macrae *et al.*, 2001).

The inflammatory response to MHV-76 is much greater in the lungs during acute infection than the response to MHV-68. This response starts earlier and is much more severe, although it is resolved with similar kinetics. No obvious differences have been observed in the spleen (Macrae *et al.*, 2001).

These results indicate that in the left hand region of the genome is a factor involved during acute replication in the lung, and a factor potentially involved in immune evasion; there is also a factor involved in driving splenomegaly, and a factor involved in establishment of latency in the spleen. There may also be a factor involved in long-term persistence in the lung. Work is ongoing to establish the exact role of the unique genes and the tRNAs in pathogenesis (as mentioned previously). It is possible that some of the features of MHV-76 infection may be due to a combination of unique genes, as no single gene mutation can account for some of the characteristics of infection.

It is also possible that factors exist in the left-hand end of the genome that have yet to be characterised. Work by Dutia *et al.* (2004) has identified two transcripts of 4.3 and 3.2 kb that do not correspond to any previously identified transcript. These may contribute to viral pathogenesis, and the deletion of the left-hand end of the genome in MHV-76 may abolish these transcripts, accounting for some of the differences between MHV-68 and MHV-76.

1.3.5.2 MHV-72

MHV-72 was isolated from the bank vole (*Clethrionomys glareolus*) (Blaskovic *et al.*, 1980). This virus lacks approximately 7000 bp of unique sequence from the left-hand end of the genome. The remaining sequence is very similar to the genome of MHV-68; however MHV-72 lacks genes M1-M3 as well as the viral tRNA-like molecules (Oda *et al.*, 2005).

In vivo infection with MHV-72 fails to cause splenomegaly up to 1 month post-infection. This is similar to the phenotype of a mutant virus, MHV-76inM4, where the M4 gene has been inserted into the genome of MHV-76 (Townsley *et al.*, 2004), resulting in a similar genome composition to MHV-72. This confirms that M4 is not involved in induction of splenomegaly.

However the inclusion of approximately 2.5 kb in the genome of MHV-72 that is absent in the genome of MHV-76 confers on MHV-72 the ability to induce tumour formation and lymphoproliferative disease, a characteristic not observed in MHV-76 infection (Oda *et al.*, 2005). This suggests that either M4 or the sequence 5' of the ORF has tumorigenic properties. A very similar isolate to MHV-72, MHV-Sumava, also possesses the ability to cause tumour formation *in vivo* (Mistrikova *et al.*, 2004).

1.3.5.3 MHV-60

MHV-60 is the third virus along with MHV-68 and MHV-72 to be isolated from the bank vole (Blaskovic *et al.*, 1980). Unlike MHV-76, MHV-60 is able to induce splenomegaly and is also implicated in development of lymphoproliferative disorders and/or tumours (Pappova *et al.*, 2004).

1.4 Project Outline

As shown above, the *in vivo* pathogenesis of MHV-68 has been extensively studied. However there remain a number of factors about which relatively little is known. The aim of the project was to further the understanding of MHV-68 pathogenesis in three separate but related areas: firstly in the study of MHV-68 persistence in the lung, and the viral genes required for this process; secondly in the study of an MHV-68 mutant carrying a mutation in an apparently non-coding region of the left end of the genome that causes altered pathology during acute infection of the lung; and finally in the investigation of the role of the viral M1 gene during *in vivo* infection.

Chapter 2: Materials & Methods

2.1. Extraction of DNA

2.1.1.From Bacteria

2.1.1.1 Small scale isolation of plasmid DNA using a QIAprep Miniprep kit (Qiagen)

Plasmid DNA was purified using a QIAprep spin miniprep kit (QIAGEN, UK) according to the manufacturers instructions. A single isolated bacterial colony was transferred to 5 ml of sterile LB containing the required antibiotic (100μg/ml, either ampicillin, kanamycin or chloramphenicol) before overnight incubation at the appropriate temperature (30°C or 37°C) with orbital shaking. The culture was pelleted by centrifugation at 4000 x g for 6 minutes and the supernatant discarded. The pellet was resuspended in 250 μl of buffer P1 and transferred to a microfuge tube. 250 μl buffer P2 was added and the tube contents mixed by inversion. 350 μl buffer N3 was added and the tube contents mixed by inversion prior to centrifugation for 10 minutes at ~17,900 x g. The resulting supernatant was transferred to a QIAprep spin column and the DNA bound to the membrane by centrifugation (~17,900 x g, 1 minute). The membrane was then successively washed with 0.5 ml of buffer PB (~17,900 x g, 1 minute) and 0.75 ml of buffer PE (~17,900 x g, 1 minute) before the membrane was dried (~17,900 x g, 3 minutes) and the plasmid DNA eluted into 20 μl of buffer EB.

2.1.1.2 Large Scale Preparation of Plasmid DNA (Maxiprep)

Large scale preparation of plasmid DNA was carried out using a Qiagen Plasmid Maxi kit. Briefly, following a modified alkaline lysis procedure the plasmid DNA is bound to QIAGEN Anion-Exchange Resin under low-salt low-pH conditions. RNA and proteins are removed by medium-salt washing and plasmid DNA is then eluted in a high-salt buffer. Finally the DNA is concentrated and desalted by isopropanol precipitation.

A single colony was used to inoculate 5mls of LB containing the appropriate antibiotic. Following incubation for 8 hours at 37°C with orbital shaking the culture was then diluted 1 in 50 in fresh LB (with antibiotic) to a final volume of 250 ml. This culture was incubated at 37°C with orbital shaking for 16 hours. Cells were pelleted by centrifugation at 6000 x *g* for 15 minutes at 4°C. Resuspension in 10 ml of buffer P1 (50 mM Tris-Cl; 10 mM EDTA; 100 μg/ml RNase A) was followed by lysis with the addition of 10 ml buffer P2 (200 mM NaOH; 1% SDS (w/v)) followed by a 5

minute incubation at room temperature. This reaction was neutralized by the addition of 10 ml pre-chilled buffer P3 (3.0 M potassium acetate, pH 5.5) followed by a 20 minute incubation on ice. The cell lysate was then centrifuged at 4°C and 20,000 rpm for 30 minutes. The supernatant containing the plasmid DNA was removed and centrifuged again (4°C, 20,000 rpm, 15 minutes). During this period a Qiagen-tip 500 anion-exchange column was equilibrated by the addition of 10 ml buffer QBT (750 mM NaCl; 50 mM MOPS, pH 7; 15% isopropanol (v/v); 0.15% Triton® X-100(v/v)). Addition of the lysate to the Qiagen-tip 500 was followed by two washes of the column with 30 ml buffer QC (1.0 M NaCl; 50 mM MOPS, pH 7; 15% isopropanol (v/v)). DNA was eluted in 15 ml buffer QF (1.25 M NaCl; 50 mM Tris-Cl, pH 8.5; 15% isopropanol (v/v)), precipitated by the addition of 10.5 ml isopropanol and centrifuged at 15,000 x *g* for 30 minutes at 4°C to pellet the DNA. The pellet was washed in 70% ethanol (v/v) and centrifuged again at 15,000 x *g* for 10 minutes. Following removal of the ethanol the plasmid DNA was resuspended in 200 µl Tris-EDTA (pH 8.0).

2.1.1.3 Small Scale Isolation of BAC DNA using a PhasePrep BAC DNA kit (Sigma)

BAC DNA was purified using the PhasePrep BAC DNA kit according to the manufacturer's instructions. A single colony was added to 10 ml LB containing the appropriate antibiotic and the cells were grown overnight at 37°C with orbital shaking. Cells were pelleted by centrifugation at 5000 x g for 10 minutes and resuspended in 250 µl resuspension buffer. The bacteria were lysed by addition of 250 µl lysis buffer with a 5 minute incubation period at room temperature. Addition of 250 µl chilled neutralisation buffer with a 5 minute incubation period on ice terminated the lysis reaction. The sample was then centrifuged at 16,000 x g for 5 minutes at 4°C to pellet the cell debris. Supernatant was then transferred to a fresh tube and 450 µl isopropanol added to precipitate the DNA. The sample was centrifuged at 16,000 x g for 20 minutes at 4°C to pellet the DNA. The pellet was washed in 70% ethanol and resuspended in 500 µl elution solution. Residual RNA was digested by the addition of 1 µl of RNase cocktail followed by a 5 minute incubation at 60°C. 40 µl sodium acetate buffer solution (3 M, pH 7.0) was added to adjust the salt concentration. Endotoxins were removed by the addition of 100 µl

endotoxin removal solution followed by a 5 minute incubation on ice then a 5 minute incubation at 37°C. The sample was centrifuged for 3 minutes at 16,000 x g to separate the phases, and the clear upper phase containing the BAC DNA was transferred to a fresh tube. DNA was precipitated by the addition of 540 µl DNA precipitation solution and pelleted by centrifugation at 16,000 x g for 20 minutes at 4°C. The pellet was washed with 70% ethanol, centrifuged again at 16,000 x g for 5 minutes at 4°C and the supernatant discarded. The pellet was allowed to air dry for 5 minutes to remove any excess ethanol before resuspension in 15 µl of dH_2O.

2.1.2 From Animal Tissues

2.1.2.1 Extraction of DNA from Animal Tissues using a Qiagen DNeasy Tissue Kit

Animal tissues previously frozen and stored at –80°C were defrosted and the DNA extracted according to the manufacturer's instructions. Briefly, up to 25 mg tissue (10 mg if extracting DNA from spleen) was incubated overnight at 55°C in Buffer ATL in the presence of proteinase K (0.4 mg) to lyse the cells. Following addition of 200 µl Buffer AL samples were incubated at 70°C for 10 minutes. Addition of 200 µl ethanol precipitated the DNA and the lysate was loaded onto the DNeasy mini column. Centrifugation at 6000 x *g* for 1 minute bound the DNA to the membrane. The membrane was washed once with buffer AW1 (6000 x *g* for 1 minute) and once with buffer AW2 (14,000 x *g* for 3 minutes to allow the membrane to dry). DNA was eluted by addition of a total of 200 µl buffer AE.

2.1.2.2 Extraction of DNA from Whole Lungs

The protocol was adapted from Molecular Cloning: A Laboratory Manual (Sambrook & Russell). Lungs were homogenised in 10 volumes (w/v) of lysis buffer (10 mM Tris-Cl, pH 8.0; 0.1M EDTA, pH 8.0; 0.5% (w/v) SDS). Proteinase K was added to a final concentration of 100 µg/ml and the lysate was incubated overnight at 50°C in a sterile 15 ml polypropylene tube (Nunc). Approximately 200 µl of the lysate was then treated using the Qiagen DNeasy Tissue Kit as stated above, starting from the addition of buffer AL.

2.1.2.3 Modification of "Extraction of DNA from animal tissues using a Qiagen DNeasy Tissue Kit" for use with Lung Homogenate

Lungs were previously homogenised in 2 ml Glasgow's Medium and stored at –80°C until required. 400 µl homogenate was lysed overnight at 55°C in 0.8 mg proteinase K and 180 µl buffer ATL. Samples were then processed as before.

2.2. Manipulation of DNA

2.2.1 DNA Digestion with Restriction Endonucleases

Restriction enzymes were purchased from New England Biolabs and were used in conjunction with the manufacturers buffer. Digests were performed for 3 hours in a 10-50 µl final volume at a temperature recommended by the manufacturer (usually 37°C). 10 units of restriction endonuclease were used per reaction. For all reactions the volume of enzyme was always less than 10% of the final reaction volume. At the end of the digestion period the enzyme was inactivated by heating for 15 minutes at 70°C.

2.2.2 Blunt Ending Restriction Fragments

T4 DNA Polymerase (Invitrogen) was used to fill the restriction endonuclease termini. 5 units of polymerase were used in conjunction with the manufacturers buffer to incorporate dNTPs (Roche) at a concentration of 1 mM into the ends of the fragment. Reaction volume was made up to 100 µl using sterile distilled water (Sigma). The reaction was performed for 15 minutes at 11°C.

2.2.3 DNA Purification

DNA was purified by phenol: chloroform extraction. A phenol:chloroform:iso-amyl alcohol mixture (25:24:1 ratio respectively) equilibrated to pH 7.8 was added to an equivalent volume of DNA solution in the presence of 0.1 volumes 3 M sodium acetate (pH 5.2) and vortexed thoroughly. Following centrifugation at >15,000 x g for 4 minutes, the aqueous phase was removed whilst avoiding contamination with either the organic phase or interphase. The aqueous phase was dispensed to a fresh tube and an equivalent volume of chloroform added. The sample was then subject to one round of chloroform extraction to remove any contaminating phenol.

2.2.4 Ethanol Precipitation

DNA was precipitated by the addition of 2.5 volumes of ice-cold 96% ethanol (v/v) directly to the sample. The sample was vortexed prior to incubation at –20°C for 1 hour to enhance precipitation. DNA was recovered by centrifugation for 20 minutes at 17,000 x g. The supernatant was discarded and 1 volume of 70% ethanol (v/v) was added to the sample before a further centrifugation step (4 minutes, 17,000 x g). The supernatant was removed and the open tube was left at 37°C until any remaining ethanol evaporated. The DNA pellet was resuspended in the required volume of dH_2O.

2.2.5 Ligation of Blunt-Ended DNA

T4 DNA ligase (Promega) was used in conjunction with the manufacturers buffer to attach linker sequences to blunt-end DNA fragments (see appendix for linker sequences). 500 picomoles of linker were added to 1 μg of fragment and ligation was carried out overnight at 17°C in the presence of 3 units of T4 ligase in a final volume of 20 μl. The reaction was terminated by heating at 70°C for 15 minutes.

2.2.6 Agarose Gel Electrophoresis

2.2.6.1 Standard Protocol

DNA was electrophoresed on gels consisting of 1% agarose (SeaKem, Flowgen, UK). Gels were cast with TAE buffer containing 0.5 μg/ml (w/v) ethidium bromide (Sigma, UK). DNA samples were diluted to a final volume of 20 μl with dH_2O before the addition of 0.1 volumes of loading buffer per sample (15% (w/v) Ficoll type 400 and 0.25% (w/v) orange G in TAE buffer). Electrophoresis was performed at 50 V in a horizontal electrophoresis apparatus containing TAE buffer. DNA fragment sizes were estimated by comparison to known DNA molecular weight standards using 2-log DNA ladder (New England Biolabs). Following electrophoresis, agarose gels were visualized with a short wave UV transilluminator.

2.2.6.2 For Separation of BAC DNA Digested Fragments

DNA was electrophoresed on gels consisting of 0.8% agarose and cast with TAE buffer. DNA samples were diluted to a final volume of 20 μl with dH_2O before the addition of 0.1 volumes of loading buffer per sample (as above). Electrophoresis was

performed at 40 V in a horizontal electrophoresis apparatus containing TAE buffer. DNA fragment sizes were estimated by comparison to known DNA molecular weight standards using 2-log DNA ladder (New England Biolabs). Following electrophoresis, agarose gels were post-stained by immersion in 1 l TAE containing 100 µl ethidium bromide for 90 minutes with gentle agitation. Non-specific staining was removed by washing twice in TAE buffer for 1 hour with gentle agitation. Gels were then visualized with a short wave UV transilluminator.

2.2.7 Isolation of DNA Fragments from Agarose using a QIAquick Gel Extraction kit (Qiagen)

DNA fragments of interest were excised with a sterile scalpel blade under long-wave UV light. The gel fragment was placed into a microfuge tube and incubated for 10 minutes at 50°C in 3 volumes (w/v) of buffer QG (100 mg ~100 µl). Following incubation 1 gel volume (w/v) of isopropanol was added and the mixture transferred to a QIAquick spin column. Centrifugation (17,900 x g, 1 minute) bound the DNA to the silica membrane. The membrane was then successively washed with 0.5ml of buffer QG and 0.75ml of buffer PE before the membrane was dried (17,900 x g, 3 minutes) and the DNA eluted into 20 µl of buffer EB.

2.2.8 Ligation of DNA Fragments into Vector Plasmids

Ligations were performed with approximately 100 ng of vector DNA, with variable concentrations of insert DNA such that the insert to vector ratio was typically 3:1. Reactions contained 3 units of T4 ligase in conjunction with the manufacturers buffer and were made up to a final volume of 10 µl with dH_2O. Ligation reactions were incubated overnight at 17°C.

2.2.9 Quantification of DNA

DNA concentration was assessed by spectrophotometry (CE 2041, Cecil Instruments). DNA was diluted 1 in 100 in dH_2O and absorbance measured at wavelengths of 260 nm and 280 nm. The concentrations of the unknown samples were calculated using the equation: OD_{260} x 50 x 100 = DNA concentration (ng/µl).

2.2.10 Southern Blotting

2.2.10.1 Extraction of High-Molecular Weight Viral DNA

BHK cells were infected at an MOI of 1 and incubated for 90 minutes at 37°C on an orbital shaker (225 rpm). Cells were added to T175 flasks (1 x 10^7 cells/flask) in a final volume of 40 ml and incubated for 6 days at 37°C. Infected cells were removed with a cell scraper (Nunc) and cell suspensions pooled into 250 ml polypropylene conical centrifuge flasks. Suspensions were spun for at 1912 x *g* for 20 minutes at 4°C to pellet the cells. The pellet was resuspended in 4 ml cold sterile PBS and dounce homogenised 20 times on ice. The homogenate was then transferred to a universal and centrifuged at 1912 x *g* for 20 minutes at 4°C. The supernatant was then stored on ice while the pellet was resuspended again in 1ml of cold sterile PBS and dounce homogenised 20 times. After centrifugation again at 1912 x *g*, 20 minutes, 4°C the supernatant was added to the previously saved supernatant and the pellet was discarded.

Virus was purified further by ultracentrifugation through 20% D-sorbitol. 30 ml of 20% D-sorbitol in sterile PBS were placed in SW28 thin walled tubes and virus supernatant was layered on top. Tubes were filled to the brim with SPBS. Tubes were ultracentrifuged using a Beckman L8-70M at 28,000rpm for 80 minutes. The supernatant was discarded and the pellet was resuspended in 0.5 ml 50 mM Tris pH 8.0.

Viral DNA was extracted using high molecular weight buffer (0.25 M EDTA, 0.5% SDS, 0.2 M Tris pH 8.0). 5 ml of buffer was added along with proteinase K (100 µg/ml) and samples were incubated overnight at 53°C.

An equal volume of phenol:chloroform:IAA (25:24:1) was added and samples were mixed on a tilting platform for 30 minutes at room temperature. Centrifugation at 1500 x g for 5 minutes separated the mixture. The aqueous phase containing viral DNA was retained, and the phenol:chloroform extraction was repeated a further 3 times. After the fourth centrifugation the aqueous phase was added to an equal volume of chloroform and was mixed and centrifuged as before. 1/3 volume of ammonium acetate (7.5 M) was then added to the aqueous phase, followed by 2 volumes of 96% ethanol at room temperature. Samples were mixed gently and incubated at –20°C until a precipitate appeared. After transfer to a glass 30 ml corex tube samples were centrifuged at 8000 x g for 30 minutes at 4°C. Supernatant was

removed and samples were washed 3 subsequent times in 70% ethanol with centrifugation at 8000 x *g* for 10 minutes at 4°C. After briefly allowing the pellet to air dry the sample was resuspended in 400 µl TE buffer (pH 8.0) and stored at 4°C until required.

2.2.10.2 Digestion of High Molecular Weight DNA

10 µg DNA was digested by the addition of 100 U of the appropriate enzyme and 40 µl of the corresponding enzyme buffer and made up to a final volume of 400 µl using H_2O. Samples were incubated for 6 hours at the appropriate temperature.

DNA was reprecipitated by the addition of 2 volumes 96% ethanol and placed at -20°C for 30 minutes. Samples were centrifuged at 10,000 x *g* for 20 minutes to pellet the DNA. Pellets were washed twice with 70% ethanol (with centrifugation at 10,000 x *g* for 10 minutes). The supernatant was discarded and the pellet was briefly allowed to air dry before resuspension in 10 µl TE buffer (pH 8.0).

2.2.10.3 Electrophoresis and Transfer to Blot

Loading buffer was added to samples prior to separation of DNA fragments on a 0.7% w/v agarose-TAE gel (15 cm) run at 4 v/cm. The gel was rinsed in deionised H_2O and transferred into denaturation solution (0.5M NaOH, 1.5M NaCl) for 45 minutes with gentle agitation. Following a second rinse in dH_2O the gel was transferred into neutralisation buffer (1M Tris-HCl (pH 7.5), 1.5M NaCl) for 25 minutes with gentle agitation. Buffer was removed and replaced with fresh neutralisation buffer for another 20 minutes. For transfer to the nylon membrane the apparatus was set up as follows: a large electrophoresis tank (BioRad, UK) was partially filled with 10x SSC. Two layers of 3MM filter paper (Whatman), presoaked in 10x SSC, were placed in the tank so the ends were immersed in the 10x SSC. The gel was placed face-down on the filter paper and a single sheet of uncharged nylon membrane (Hybond N+, Amersham Biosciences, UK), pre-wet for 5 minutes in dH_2O, was placed on top of the gel. This was covered by three layers of filter paper (pre-soaked in 10x SSC) cut to the size of the gel. The gel was surrounded by parafilm to prevent short-circuiting of the blotting apparatus. A stack of dry paper towels was placed on top of the filter paper to ensure capillary transfer of the DNA. A glass plate with a 500g weight on top was placed on top of the towels to ensure uniform pressure and even transfer of the

DNA to the membrane. Following overnight transfer the membrane was removed and the DNA was cross-linked to the membrane using a Stratalinker 1200 (Stratagene, UK). The membrane was then wrapped in saran wrap and stored at –70°C until required.

2.2.10.4 Radiolabelling of a dsDNA Probe

25-50ng of the dsDNA to be used as the probe was denatured by heating at 100°C for 2 minutes. The volume was made up to 45 µl using TE buffer and the sample was placed on ice. DNA was then added to 1 ready-to-go DNA labelling bead (Amersham, UK) and left to dissolve. 5 µl (α-32^P)dCTP (2000Ci/mmol) was added to the sample and mixed gently by pipetting. The mixture was incubated for 30 minutes at 37°C and subsequently denatured by heating at 100°C for 2 minutes.

2.2.10.5 Purification of the Probe

Micro-bio-spin chromatography columns (BioRad) were used according to the manufacturer's instructions. Briefly the tip of the column was removed and the column was placed in a 1.5 ml microfuge tube prior to centrifugation for 4 minutes at 1000 x *g* to remove the buffer solution. After placing the column in a clean 1.5 ml eppendorf tube the probe was added to the centre of the column and centrifuged for 4 minutes at 1000 x *g*. The used column was discarded, leaving the labelled probe in the microfuge tube.

2.2.10.6 Prehybridisation and Hybridisation

Ultrahyb buffer (Ambion) was prewarmed to 68°C. The membrane was transferred to a roller bottle and 10 ml of preheated Ultrahyb buffer (Ultrahyb) was added. Prehybridisation was carried out for 30 minute at 42°C.

For hybridisation 25 µl of the probe was added to the roller bottle and hybridisation was carried out overnight at 42°C. High-stringency washes were used to remove any probe bound non-specifically to the membrane. All solutions were preheated to 42°C. The hybridisation buffer containing the probe was removed and replaced with 2 x SSC, 0.1% SDS for 2 minutes. This wash buffer was removed and replaced fresh buffer (2 x SSC, 0.1% SDS) for 5 minutes. This wash was repeated using fresh buffer again. Finally the blot was washed twice with 0.1 x SSC, 0.1% SDS for 15 minutes.

All washes were carried out at 42°C. For detection of the radiolabelled probe the membrane was wrapped in saran wrap and placed in a cassette with a sheet of Kodak Xomat film (Sigma, UK). The cassette was stored overnight at –80°C prior to development of the film in an X-ray developer.

2.3 Transformation of Competent Cells with Vector DNA

Escherichia coli (ElectroMAX™ DH10B™ cells, Invitrogen, UK) were transformed with plasmid DNA according to the manufacturers directions. 2.5 µl of ligation reaction was added to 20 µl of electrocompetent cell suspension. The mixture was then electroporated using a BioRad MicroPulser. 1 ml of S.O.C. medium was then added to the cell suspension before incubation for 2 hours at 30°C with orbital shaking. The suspension was then centrifuged for 1 minute at 4000 x g to pellet the cells and the excess media removed. Cells were then resuspended in a small volume (approx 10 µl) of S.O.C. medium and plated onto an LB agar plate containing the appropriate antibiotic (30 µg/ml kanamycin, Sigma, UK). Plates were incubated in an inverted orientation overnight at 30°C, before long-term storage at 4°C (up to six weeks).

2.4. RNA Extraction and Manipulation

2.4.1 RNA Extraction from Cells Cultured *In Vitro* using a Qiagen RNeasy Mini Kit

RNA was isolated from cells cultured *in vitro* according to the manufacturer's protocol. Cells were lysed directly in the culture dish by the addition of 1 volume (600 µl) Buffer RTL (containing β-mercaptoethanol). Samples were homogenised by passage through a QIAshredder spin column at 18,000 x *g* for 2 minutes. 1 starting volume of 70% ethanol was added to adjust binding conditions. Samples were then loaded onto RNeasy mini columns and centrifuged for 15 seconds at 8000 x *g*. The RNA was washed once with Buffer RW1 (8000 x *g*, 15 seconds) and once with Buffer RPE (8000 x *g*, 15 seconds). The membrane was washed one final time in Buffer RPE and centrifuged at 18,000 x *g* for 2 minutes to dry the membrane. RNA was eluted by the addition of 30 µl RNase-free H_2O to the spin column followed by centrifugation at 8000 x *g* for 1 minute.

2.4.2 RNA Extraction from Animal Tissues using a Qiagen RNeasy Mini Kit

Samples previously stored at –80°C in RNAlater (Ambion) were defrosted and a 20 µg section was removed from the RNA*later* and homogenised in 1 volume (600 µl) Buffer RTL (containing β-mercaptoethanol). The protocol was then followed as given previously for extraction of RNA from cultured cells (section 2.4.1).

2.4.3 Quantification of RNA

RNA was quantified using spectrophotometry as for DNA. The concentrations of RNA in the unknown samples were calculated using the equation: OD_{260} x 40 x 100 = RNA concentration (ng/µl).

2.4.4 Reverse Transcription of RNA

RNA was initially treated using a DNA-*free* DNase kit (Ambion) to remove any contaminating DNA. The reaction consisted of 5 µg of RNA, 1 µl DNase I buffer and 2 units of DNase I and the mixture was made up to a final volume of 13 µl using nuclease-free water. Samples were incubated for 1 hour at 37°C. The DNase enzyme was inactivated by the addition of 1.3 µl DNase Inactivation Reagent followed by incubation for 2 minutes at room temperature. Samples were then spun for 1 minute at 6000 x *g* to pellet the Inactivation Reagent.

5.5 µl DNase-treated RNA was used in the subsequent reverse transcription step, with the remaining RNA to be kept for use as a –RT control. RNA was added to 1 µl Oligo-dT primer (Invitrogen), 1 µl 10mM dNTPs (Invitrogen) and 8.5 µl of nuclease-free H_2O (Ambion). Samples were incubated for 5 minutes at 65°C followed by a brief cooling period on ice. 4 µl 5x First Strand Buffer, 2 µl 0.1 M DTT and 1 µl RNaseOUT (Invitrogen) were added to the RNA and the samples were incubated for 10 minutes at room temperature and 2 minutes at 42°C. 1µl SuperScript II Reverse Transcriptase was then added and samples were incubated at 42°C for 1 hour. The reverse transcriptase was inactivated by incubation at 70°C for 15 minutes.

2.4.5 Northern Blotting

2.4.5.1 RNA Extraction from Cells Cultured *In Vitro* using TRI Reagent

For extraction of large quantities of RNA from cultured cells RNAwiz (Ambion, UK) was used. 4-5 x 10^7 cells were harvested by trypsinisation and frozen at –80°C until required. Cells were later defrosted and the RNA isolated according to the protocol given by the manufacturer. Briefly cells were resuspended in 5 ml TRI reagent. The mixture was incubated for 5 minutes at room temperature to dissociate the nucleoproteins from the nucleic acids. 1 ml of chloroform was added, samples were shaken for 20 seconds and left to incubate at room temperature for 10 minutes. The mixture was centrifuged at 12,000 x *g* for 15 minutes at 4°C and the resulting aqueous phase transferred into a clean tube. 5 ml DEPC-treated H_2O was added, followed by 5 ml isopropanol. After mixing samples were incubated at room temperature for 10 minutes. Samples were spun for 15 minutes at 10,000 x *g* and 4°C to pellet the RNA. The supernatant was removed and the pellet washed by the addition of 1 ml 75% ethanol followed by centrifugation at 10,000 x *g* for 5 minutes at 4°C. The supernatant was again removed and pellet was allowed to air dry for 3 minutes. Finally the pellet was resuspended in 50 µl DEPC-treated H_2O.

2.4.5.2 Purification of Poly A+ RNA from Total RNA using a Qiagen Oligotex mRNA Mini Kit

Up to 0.25 mg of RNA was added to 250 µl Buffer OBB and 15 µl Oligotex Suspension solution and the final volume made up to 515 µl using RNase-free water. Samples were incubated at 70°C for 3 minutes to disrupt the secondary structure of the RNA. Subsequent incubation for 10 minutes at room temperature allowed the poly-A tails of mRNAs to able to hybridise to a dT oligomer ($dC_{10}T_{30}$) covalently linked to the surface of polystyrene-latex particles. The oligotex-mRNA complex was pelleted by centrifugation for 2 minutes at 18,000 x *g* and the supernatant removed. The pellet was resuspended in 400 µl Buffer OW2 and the sample was added to a spin column. Centrifugation at 18,000 x *g* for one minute allowed removal of contaminating unbound rRNA and tRNAs. The spin column was washed again by addition of 400 µl Buffer OW2 followed by centrifugation at 18,000 x *g* for one minute. Poly-A RNA was dissociated from the oligotex particles by the addition of 35 µl hot (70°C) Buffer OEB. Centrifugation at 18,000 x *g* for one minute eluted the mRNA. Another 35 µl hot Buffer OEB was added to the column and centrifuged again to ensure complete elution of mRNA.

2.4.5.3 Electrophoresis and Blotting

RNA samples were made up in a total volume of 20 µl. 5 µl loading buffer (16 µl saturated aqueous bromophenol blue, 80 µl EDTA (0.5M, pH 8.0), 720 µl 37% formaldehyde, 2 ml 100% glycerol, 3.084 ml formamide, 4 ml 10x MOPS buffer, 100 µl dH_2O) was added to each sample. This was followed by incubation at 65°C for 5 minutes and subsequent chilling on ice. 200 ml 1.2% agarose was melted and cooled to 65°C whereupon 3.6 ml 37% formaldehyde and 2 µl 10mg/µl ethidium bromide were added. The gel was run at 30 V for 30 minutes with recirculating running buffer (100 ml 10x MOPS buffer, 20 ml 37% formaldehyde, made up to 1 l with RNase-free H_2O) prior to loading samples. After loading, samples were electrophoresed at 5-7 V/cm overnight. 5 µg of an RNA molecular weight marker was loaded alongside the samples as a reference. The gel was then visualised and photographed under short-wave UV light before rinsing in RNase-free H_2O. This was followed by washes in 0.05 M NaOH (20 minutes) and 20 x SSC (40 minutes with agitation). The protocol then continued as stated previously for southern blotting with the following alterations: transfer occurred in the presence of 20 x SSC and was allowed to continue for no more than 4 hours. Paper towels were replaced every 30 minutes to enhance transfer. After transfer the membrane was soaked in 6 x SSC (5 minutes with agitation). The RNA was cross-linked to the membrane using a Stratalinker 1200 and stored at –70°C until required.

2.4.5.4 Prehybridisation and Hybridisation

Northern blots were prehybridised and hybridised as for Southern Blots using dsDNA probes. After overnight hybridisation the probe solution was removed and replaced with 1 x SSC, 0.1% SDS at room temperature and washed for 10 minutes in the roller bottle. This was replaced with 2 x SSC at room temperature and washed for 15 minutes. Successive washes were carried out in 2 x SSC, 0.1% SDS (5 minutes, twice) and 0.1 x SSC, 0.1% SDS (10 minutes, twice) all at 42°C. The membrane was exposed to X-ray film using the protocol given for Southern Blotting in section 2.10.6.

2.5 Polymerase Chain Reaction

2.5.1 Components of Standard PCR Reactions

Standard PCR reactions were typically performed in a 50 µl final volume, and consisted of

PCR reaction buffer (Invitrogen, UK)

3 mM $MgCl_2$ (Invitrogen, UK)

100 µM each of dATP, dCTP, dGTP and dTTP (set of deoxynucleosides, PCR Grade, Roche)

50 pmol of each primer (MWG Biotech, Germany,)

1 U of *Taq* DNA polymerase (Invitrogen, UK).

100 ng of template DNA was used for each reaction. PCR reactions were performed in 0.5ml thermotubes (Abgene) in an Omnigene thermal cycler (Thermohybaid). Negative control reactions containing dH_20 in place of template DNA were always performed. A modified hot-start procedure was used to increase the specificity of amplification. Reactions (minus *Taq* polymerase) were overlaid with mineral oil (Sigma, UK) before heating to 95°C for 5 minutes. Reactions were held at 80°C while *Taq* polymerase was added. PCR programmes typically consisted of 45 seconds denaturing at 95°C, 45 seconds annealing time at a primer-pair specific temperature and extension for 2 minutes at 72°C. Following 37 cycles reactions were incubated at 72°C for 10 minutes before cooling to room temperature.

2.6 Real Time PCR

2.6.1 Generation of Standards for Use in Real Time PCR

2.6.1.1 Generation of Standards for Absolute Quantification

2.6.1.1.1 Cloning of PCR Products

PCR products were cloned using a TOPO TA Cloning® Kit for Sequencing (Invitrogen) according to the manufacturer's instructions.

Briefly, linearized pCR®4-TOPO® vector (with single 3' thymidine (T) overhangs) is able to ligate to the PCR insert (with single 3' adenosine (A) residues added by Taq polymerase during the PCR reaction) by base pairing. Topoisomerase I covalently linked to the vector is released by the pairing of vector with insert, allowing re-circularisation of the vector.

The reaction was carried out using 4 µl of PCR product, 1 µl salt solution (1.2 M NaCl, 0.06 M $MgCl_2$) and 10 ng pCR®4-TOPO® vector in a final volume of 6 µl. The reaction mixture was gently mixed and incubated at room temperature for 30 minutes prior to transformation of One Shot TOP 10 chemically competent cells (Invitrogen, UK).

2.6.1.1.2 Transformation of One Shot TOP 10 Chemically Competent *E.coli*

One Shot TOP 10 chemically competent cells (Invitrogen, UK) were transformed according to the manufacturers directions. A 50 µl aliquot of competent cells was thawed on ice and 2 µl of the TOPO cloning reaction added. The mixture was incubated on ice for 30 minutes prior to heat shocking at 42°C for 30 seconds. The sample was then immediately replaced on ice and 250 µl S.O.C. medium added before incubation with agitation at 37°C for 1 hour. 10 µl and 50 µl aliquots were spread onto LB-kanamycin plates and incubated in an inverted orientation at 37°C overnight. Colonies were subsequently picked and analyzed further by miniprep and PCR and/or restriction endonuclease digestion.

2.6.1.1.3 Quantification of Plasmid Copy Number

DNA concentration was assessed by spectrophotometry (CE 2041, Cecil Instruments). DNA was diluted 1 in 100 in dH_2O and absorbance measured at wavelengths of 260nm and 280nm. The concentrations of the unknown samples were calculated using the equation: OD_{260} x 50 x 100 = DNA concentration (ng/µl).

The number of copies of plasmid in a microlitre was determined using the following:

The molecular weight of a dsDNA molecule = (number of base pairs) x (660 Da/bp)

Copies DNA per µl = (6.023×10^{23} x mass per µl)/ Molecular weight

Appropriate dilutions were then made to give solutions containing 1×10^7 down to 1×10^1 plasmid copies per µl.

2.6.1.2 Generation of Standards for Relative Quantification

A set of primers encompassing the entire region of interest plus approximately 30-40 bp at each end were used to amplify template DNA according to the protocol given for standard PCR (see section 5). The resulting product was run on a 2% w/v agarose

gel and the band gel extracted using a Qiagen QiaQuick Gel Extraction Kit according to the manufacturer's instructions (see section whatever) and eluted into 30 µl buffer EB. The product was then serially diluted to by a factor of 10 to produce a series of standards for use in quantitative PCR.

2.6.2 Components of Real Time PCR Reactions

Real time PCR analysis was performed using a Rotorgene (Corbett Research, Australia) using the intercalating dye SYBR Green to determine levels of dsDNA product. Reactions were performed in a 20 µl final volume, and consisted of:

PCR reaction buffer containing $MgCl_2$ (20mM)

10 mM each of dATP, dCTP, dGTP and dTTP (set of deoxynucleosides, PCR Grade, Roche)

50 pmol of each primer (MWG Biotech, Germany),

0.75 U of FastStart Taq DNA Polymerase (Roche)

0.7 µl of SYBRGreen (Biogene Ltd).

Each reaction contained 100 ng DNA template. Negative reactions performed in parallel with dH_2O used in place of template DNA. Standard dilution reactions were similarly performed in parallel with plasmid DNA or primary PCR product used as template. Reactions were carried out in 0.1ml tubes (Corbett Research).

Following a hot start at 95°C for 10 minutes to activate the hot-start Taq polymerase samples were amplified for 45 cycles. Cycles consisted of 95°C for 30 seconds, 30 seconds at the appropriate anneal temperature for the primer pair (see appendix whatever) and 72°C for 30 seconds. Reactions were carried out using a RotorGene 3000 (Corbett Research). Fluorescence level was measured at the end of the 72°C extension phase. After cycle 45 a melt curve analysis was performed to determine the specificity of PCR products; fluorescence was measured during an incremental increase of temperature from 65°C to 95°C. All samples including standard dilutions and negative controls were run in duplicate or triplicate to assess accuracy during reaction set-up.

2.6.3 Normalisation of Samples

The quality and amount of the template DNA or cDNA was assessed by performing a real-time PCR reaction on the template using primers for a cellular housekeeping

gene, and any variation in the results owing to differing amounts or quality of input DNA was corrected by normalisation.

β-actin was used as a control for normalisation of both DNA and cDNA. Each sample was allocated a ratio of its β-actin content in relation to the 75th percentile of the β-actin levels of all samples assayed. This ratio was used to normalise the levels of the genes of interest (method according to McKimmie, 2005; an example from this work is given in Table 1).

Sample Name	**Assayed level of gene X**	**Level of house-keeping gene**	**Ratio to 75th percentile**	**Normalised level of gene x**
	(Copies/reaction)	**(Copies/reaction)**	**Column C/71.25**	**Column B/D**
1	10	40	0.561	18
2	50	200	2.807	18
3	12	45	0.632	19
4	10	10	0.14	71
5	8	40	0.561	14
	75th percentile	**71.25**		

Table 2.1 Normalisation using a housekeeping gene to determine levels of gene X (from McKimmie, 2005). Illustrated above is the effect that template variation can have on apparent levels of the unknown gene. Sample 2 appears to contain far higher levels of X; however level of the housekeeping gene is far higher than in any other sample, indicating the elevated level of X is due to a higher amount of starting template DNA. Normalisation corrects this, revealing sample 2 contains similar levels of X to those in samples 1, 3 and 5. Conversely the level of starting template in sample 4 is far lower than other samples, and normalisation reveals the relative level of X in this sample is elevated compared to the other samples.

The 75th percentile value is used as a reference in place of measures such as the mean average because this value is less affected by outliers that may skew the results. A ratio is determined for each sample that measures the deviation of each sample from the 75th percentile. Levels of the unknown gene (in this case X) are then altered on the assumption that the ratio of the housekeeping gene to gene X is uniform.

2.7 Cell Culture

2.7.1 Maintenance of Cell Cultures

All cells were grown at 37°C, 5% humidified CO_2 in sterile plasticware (Nunc). Baby Hamster Kidney fibroblasts (BHK-21) were grown in Glasgow's Modified Eagles Medium (GMEM) containing 10% new-born calf serum (Invitrogen), 10% tryptose phosphate broth (Invitrogen), 2mM L-glutamine (Merck BDH), 100 U/ml penicillin (Merck BDH) and 100 U/ml streptomycin (Merck BDH). Owl Monkey Kidney epithelial cells (OMK) were maintained in Dulbecco's Modified Eagles Medium (DMEM) containing 10% fetal calf serum (Invitrogen), 2 mM L-glutamine (Merck BDH), 100 U/ml penicillin (Merck BDH) and 100 U/ml streptomycin (Merck BDH).

2.7.2 Harvesting and Counting of Cells

Adherent cells were removed from tissue-culture flasks by trypsinisation. Growth medium was removed and the cells were washed in 0.02% versene. Incubation with 0.25% trypsin (Invitrogen) caused the cells to detach from the plasticware. An equal volume of fresh medium was added to inactivate the trypsin and cells were centrifuged for 450 x *g* for 5 minutes. The supernatant was discarded and the cell pellet was resuspended in fresh medium. A 50 µl sample was added to an equal volume of 0.1% trypan blue and unstained cells were counted prior to reseeding.

2.7.3 Reconstitution of Infectious Virus from BAC-cloned MHV-68

Cre 3T3 cells were seeded at $2x10^4$ cells/well in a 96 well plate. 24 hours post-seeding cells were transfected with the MHV-68 BAC using Effectene (QIAGEN) according to the manufacturer's instructions and plates were incubated for 10 days at 37°C with 5% humidified CO_2. Infected cells were pipetted up and down to detach them from the plate and break up any clumps. Following 3 freeze-thaw cycles infected cells were added to subconfluent 3T3 cells previously seeded in 24 well plates. Plates were then incubated for 7 days at 37°C with 5% humidified CO_2. Wells containing colourless plaques were selected and infected cells from these wells were harvested again and passaged twice more through 3T3 cells, first in a 24 well plate and subsequently in a 6 well plate. Virus was then titrated on BHK cells (see section 9.5.1 for method) and subsequently infected into BHK cells at low MOI. Virus harvested from these cells was subsequently used to prepare a virus stock.

2.7.4 Preparation of Virus Stocks

BHK-21s were harvested and counted as described before. Cells were resuspended to a final concentration of 1 x 10^7 cells/ml and infected with an MOI of 0.001. After incubation with shaking for 1 hour (37°C, 225 rpm) infected cells were reseeded into T175 flasks at 4 x 10^6 cells/flask in a final volume of 40 ml of growth medium. Cells were then incubated at 37°C until complete cytopathic effect was evident (5-6 days post-infection). Supernatant was decanted and pooled into 250 ml conical centrifuge tubes; infected cells were removed from flasks using a cell scraper (Nunc) and added to the supernatant. After centrifugation (2000 x *g* at 4°C for 20 minutes) the supernatant was discarded and cell pellets were resuspended in a minimal volume of PBS. The cell suspension was then homogenised using a chilled dounce homogeniser and subsequently sonicated in a glass universal for 15 minutes at. After centrifugation (2000 x *g*, 4°C, 20 minutes) the supernatant (containing virus) was decanted into a fresh universal and stored on ice. The pellet was resuspended in a minimal volume of PBS and homogenised again with the dounce homogeniser. Following centrifugation (2000 x *g*, 4°C, 20 minutes) the supernatant was added to the previously stored supernatant. Aliquots of the supernatant were frozen and stored at –80°C.

2.7.5 In Vitro Assays

2.7.5.1 Titration of Virus Stocks

BHKs were harvested and counted as before and resuspended to a concentration of 1 x 10^7 cells/ml in GMEM. 44 µl virus stock was defrosted and added to 4 ml GMEM in a sterile plastic bijou and mixed thoroughly to give a 10^{-1} dilution of virus. Serial ten-fold dilutions of virus were made by adding 440 µl of the dilution to 3.96 ml of GMEM. 2 x 10^6 BHK-21 cells in a volume of 0.2 ml were added to each dilution and samples were shaken (225 rpm) for 1 hour at 37°C. 2 ml from each dilution was then added to 3 ml of medium and plated out into a 60 mm petri dish. The remaining 2 ml were then plated out in the same way to give a replica. Plates were incubated for 4 days at 37°C, 5% CO_2. The medium was discarded and the plates were each fixed with 3 ml of 10% neutral buffered formalin for at least 30 minutes. The formalin was then discarded and plates were stained with 0.1% toluidine blue. Plates were scored

microscopically for cytopathic effect and virus titre was calculated using the equation: viral titre = (plaque number x dilution)/2.

2.7.5.2 One-Step and Multi-Step Growth Curves

Single- and multi-step growth in vitro was analysed by infection of BHK cells. Cells in suspension were infected for 90 minutes at an MOI of 5 for single-step or 0.05 for multi-step. Cells were pellet by centrifugation (450 x *g*, 5 minutes) and resuspended in complete Glasgow's medium four times to remove unbound virus. 2 x 10^6 (one-step) or 1 x 10^6 (multi-step) cells were seeded into 24 well plates. At specific time points post-infection cells were harvested by pipetting up and down several times, freeze-thawed three times and infectious virus determined by plaque assay. All infections were performed in duplicate, with each infection titration duplicated.

2.7.6 In Vivo Assays

2.7.6.1 Animal Infections

Animals were purchased from B&K Universal (Hull, UK) or bred in-house. Female BALB/c mice purchased from B&K Universal were infected at 6-8 weeks of age. IFNγR-/- mice on a 129/Sv/Ev background and 129 Sv/Ev (wild-type) mice were bred in-house and infected at 1-3 months of age. All mice were housed in specific pathogen free conditions. Following halothane anaesthesia mice were infected by intranasal inoculation with 4 x 10^5 pfu of virus in a total volume of 40 µl PBS (unless otherwise stated). At specific times post-infection mice were euthanised by CO_2 asphyxiation and specific organs were harvested.

2.7.6.1.1 Lung perfusion

When it was necessary to remove blood from the lungs prior to death mice were kept under heavy halothane sedation while 30 ml sterile PBS was injected into the right ventricle. During this procedure the heart would stop beating and the required organs could then be removed.

2.7.6.2 Titration of Infective Virus in Tissues

For titration of infectious virus in tissues the protocol was identical to that for titration of virus stocks (section 2.7.5.1) with the following variations: samples were

homogenised in 1.8 ml medium prior to a freeze-thaw to disrupt cell membranes. The thawed sample was centrifuged at 2000 x *g* for 5 minutes to pellet debris. 440 µl supernatant was then added to 3.96 ml medium and serial dilutions were made and the protocol continued as before.

2.7.6.3 Infective Centre Assay for the Detection of Latently Infected Splenocytes

This assay was used to determine the frequency of reactivation of virus from latently infected cells. Spleens were harvested and stored in 5 ml RPMI medium containing 10% fetal calf serum, 2 mM L-glutamine, 100 U/ml penicillin, 100 U/ml streptomycin and 50 µM 2-mercaptoethanol. Spleen cells were separated using a scalpel blade to produce a single-cell suspension in 5 ml RPMI. This was transferred to a pre-rinsed universal tube and centrifuged at 450 x *g* for 5 minutes at 4°C. The supernatant was removed and the pellet was resuspended in the remaining liquid. 1 ml of sterile dH_2O was added to lyse erythrocytes and equilibrium was reestablished by the addition of 9 ml sterile PBS. Any debris was allowed to settle and the cell suspension was then transferred to another pre-rinsed universal tube. After centrifugation (450 x *g*, 5 minutes, 4°C) the supernatant was discarded and the pellet resuspended in 5 ml complete RPMI. Splenocyte cell numbers were determined and 10-fold dilutions were plated out with 1 x 10^6 BHK cells (in 5 ml complete RPMI) in 60 mm petri dishes (Nunc). Each dilution was plated in duplicate. After incubation for 5 days at 37°C with 5% CO2 plates were fixed and counted as before (see section 2.7.5.1).

2.8 Histology

2.8.1 Preparation of Samples for Histology

Mice were euthanised as before without perfusion. Lungs were removed and inflated by the insertion of a 21-gauge needle into the trachea and injection of 10% neutral buffered formalin. The trachea was tied off with cotton to prevent escape of formalin and lungs were stored in 10% neutral buffered formalin until sent for processing to the Veterinary Pathology Unit, Easter Bush Veterinary Centre. Here samples were paraffin-embedded and 5 µm sections cut and placed onto uncoated slides. Sections were stained by staff at Easter Bush with hematoxylin and cosin.

2.8.2 Immunostaining using a Vectastain ABC kit

Paraffin embedded sections were dewaxed by immersion in xylene for 15 minutes and rinsed in 100% ethanol for 2 minutes. Slides were treated with 0.3% H_2O_2 in methanol for 30 minutes to quench endogenous peroxidase activity. After rehydration through alcohol (100, 95, 80 then 70% ethanol, 2 minutes for each step) slides were rinsed twice in dH_2O for 1 minute and treated with protease (Sigma, 0.001 g/ml) for 5 minutes. After a 5 minute rinse in TBS slides were blocked for 30 minutes at room temperature using 5% normal goat serum (NGS, Vectastain) in TBS. Excess blocking serum was blotted onto a paper towel and replaced with the primary antibody (Rabbit B polyclonal MHV-68) diluted 1/500 in 2% blocking serum for 60 minutes at room temperature. After two 2 minute washes in TBS the secondary antibody (goat anti-rabbit, 0.5% in 2% blocking serum, Vectastain) was added and slides were incubated for 60 minutes at room temperature. ABC reagent was made according to the manufacturer's instruction (2 drops A and 2 drops B in 2.5 ml TBS) and left to stand at room temperature for 30 minutes. Excess secondary antibody was removed by washing in TBS for 2 minutes and ABC reagent was added to the slides and incubated for 30 minutes at room temperature. Excess ABC reagent was removed by washing in TBS for 2 minutes. NovaRed (Vector Labs) was used according to the manufacturer's instructions to develop the stain. This was followed by two washes of 2 minutes in dH_2O. Slides were counterstained with hematoxylin (Vector Labs)(1 minute) and washed twice in TBS for 2 minutes. Slides were dehydrated by two washes in 100% ethanol for two minutes, and then cleared by placing in xylene for 2 minutes. Slides were mounted using Vectamount Permanent Mounting Medium.

2.9 Statistical Analysis

All data were analysed using Graphpad Prism software (Graphpad, San Diego, CA). Real time data were assessed for statistical significance using the non-parametric Mann-Whitney test or the Student's t test in Minitab.

Appendix

A.1 Oligonucleotides Utilised in the Study

A.1.1 Primers Used for PCR and Real Time PCR

A1.1 External Primers for Generation of Standard Templates

Sense (for) Antisense (rev)	Primer pair	Anneal Temp	Amplified Region
M4A-for M4B-rev	5'-GCG CGG ATC CGA CAC CTG GAG AAG ATG ATG ATA TTC-3' 5'-CGC GGA ATT CGG TTC TAG AAA GTC ATA AAT CTC AAT-3'	50	MHV-68 Spans entire M4 ORF 1169bp product
M3clone-for M3clone-rev	5'-CCA GCC TGT ACT GTT GCC CCT-3' 5'-GGC CTT CCT ATC CAC ACT AGG-3'	50	MHV68 Spans entire M3 ORF 1198bp product
Bactin1-for Bactin1-rev	5'-GTG GCA TCC ATG AAA CTA CA-3' 5'-GTA CTC CTG CTT GCT GAT CC-3'	62	Murine β-actin 272bp product

A1.2 Internal Primers for Quantification

Sense (for) Antisense (rev)	Primer pair	Anneal Temp	Amplified Region
M3RT-For M3RT-Rev	5'-TGG CAC TCA AAC TTG GTT GTG G-3' 5'-TAA CAG GCA GAT TGC CAT TCC C-3'	65	MHV-68 M3 fragment.
M4RT-For M4RT-Rev	5'-CAC CTG AGA TCA AGT CTA-3' 5'-GTC GCA TAA CCA TGT CCA CG-3'	65	MHV-68 M4 fragment
RTA3mod-for RTA3mod-rev	5'-GGC ACA TTT GCT GCA GAA CCC AG-3' 5'-GAA CGG CGC CTG TGT ACT CAA AGG	65	MHV-68 ORF50 fragment. 357bp product
Bactin2-for Bactin2-rev	5'-CGT TGA CAT CCG TAA AGA CC-3' 5'CTG GAA GGT GGA CAG TGA-3'	62	Murine β-actin 202bp product

A.1.2 Oligonucleotides Utilised Not Including PCR Primers

Name	Sequence	Modifications
Bamlinker	5'-CGC GGA TCC GCG-3'	5' phosphate
Kpnlinker	5'-GGG TAC CC-3'	5' phosphate

Appendix 2.1 pLXSN

pLXSN with the entire ORF50 gene (1400bp)cloned into the MCS was obtained from Dr Bernadette Dutia.

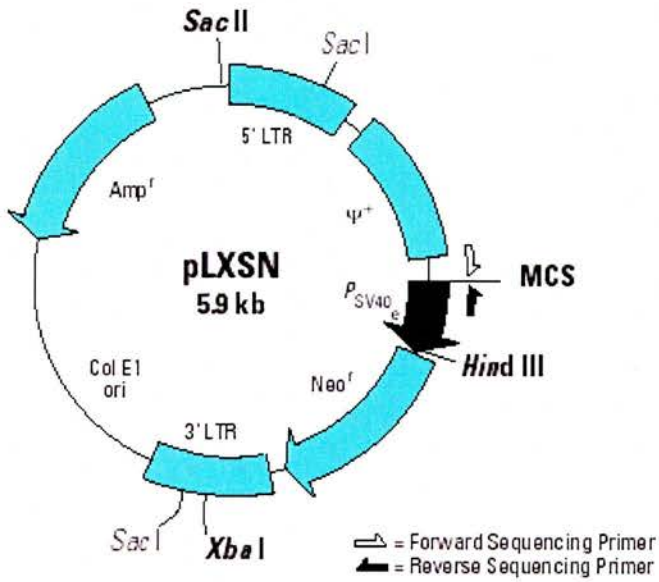

Appendix 2.2 pCR®4-TOPO

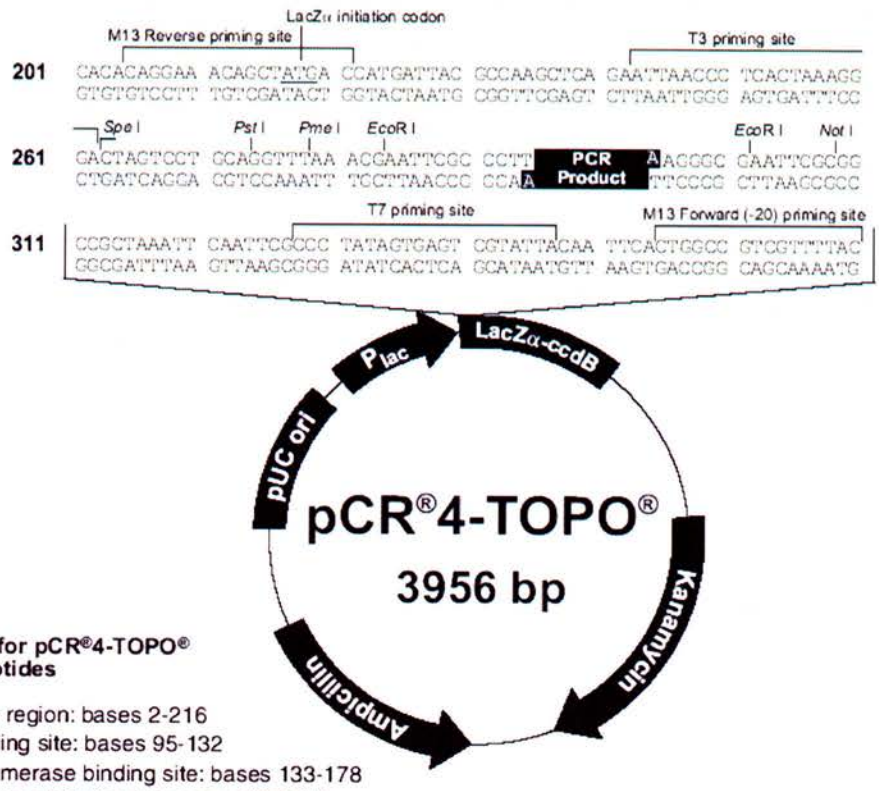

Comments for pCR®4-TOPO®
3956 nucleotides

lac promoter region: bases 2-216
  CAP binding site: bases 95-132
  RNA polymerase binding site: bases 133-178
  Lac repressor binding site: bases 179-199
Start of transcription: base 179
M13 Reverse priming site: bases 205-221
LacZα-*ccdB* gene fusion: bases 217-810
  LacZα portion of fusion: bases 217-497
  *ccd*B portion of fusion: bases 508-810
T3 priming site: bases 243-262
TOPO® Cloning site: bases 294-295
T7 priming site: bases 328-347
M13 Forward (-20) priming site: bases 355-370
Kanamycin promoter: bases 1021-1070
Kanamycin resistance gene: bases 1159-1953
Ampicillin (*bla*) resistance gene: bases 2203-3063 (c)
Ampicillin (*bla*) promoter: bases 3064-3160 (c)
pUC origin: bases 3161-3834
(c) = complementary strand

Appendix 2.3 pST76k_SrE

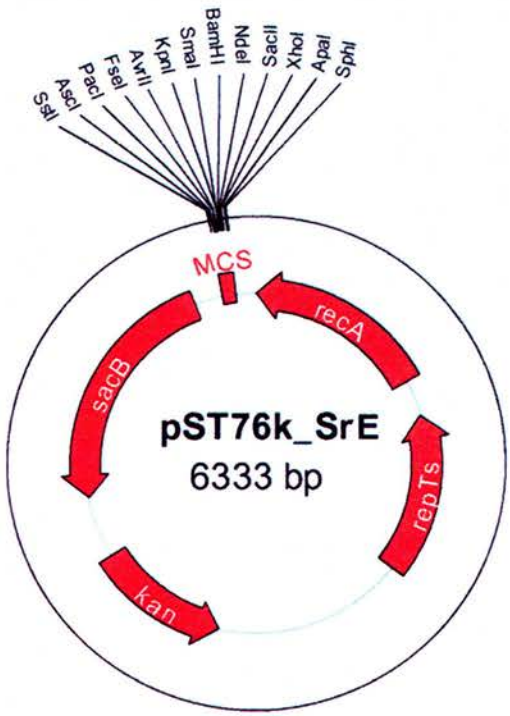

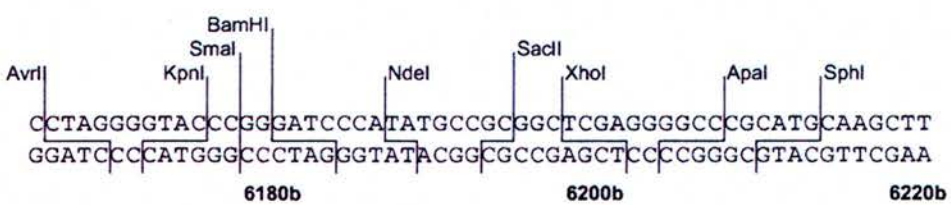

Appendix 2.4 pBluescript SK-

f1 (–) origin 24–330
β-**galactosidase** α-**fragment** 463–816
multiple cloning site 653–760
lac *promoter* 817–938
pUC origin 1158–1825
ampicillin resistance (*bla*) ORF 1976–2833

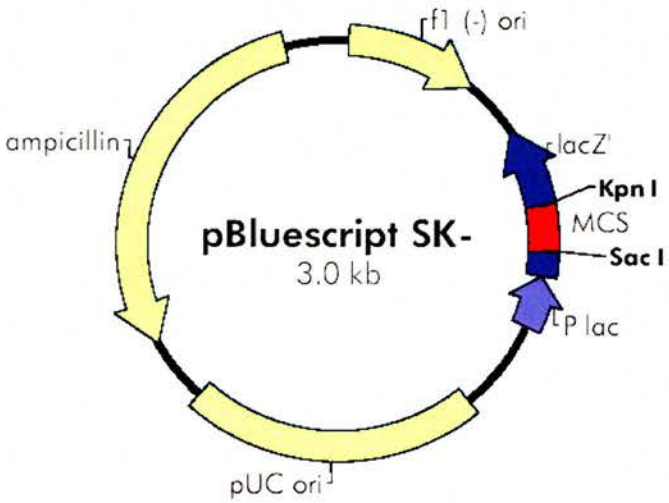

pBluescript SK (+/–) Multiple Cloning Site Region (sequence shown 601–826)

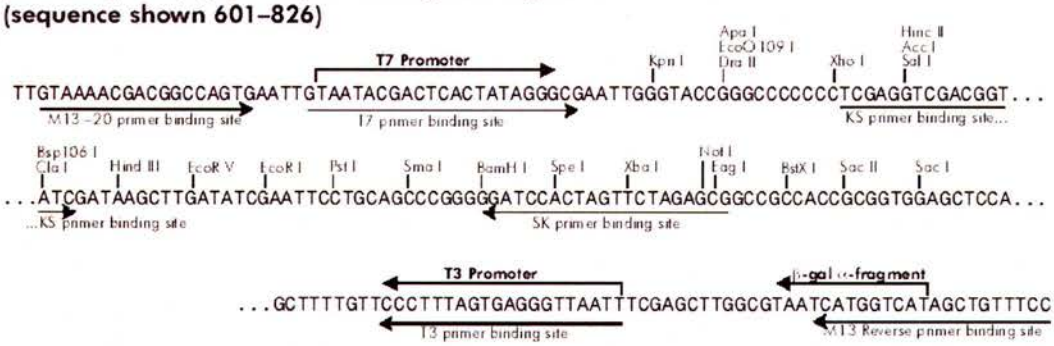

A.3 Stock Solutions Used in this Study

TE buffer	10 mM Tris-HCl (pH 8.0) 1 mM EDTA
TAE buffer	0.04 M Tris-acetate 1 mM EDTA
Luria-Bertani (LB) medium	1% (w/v) tryptone 0.5% (w/v) yeast extract 1% (w/v) NaCl
LB agar	1 x LB broth, 1.5% (w/v) bacto-agar
SOC medium	1 x LB broth, 20 mM glucose, 20 mM $MgCl_2$
20 x SSC	3 M NaCl, 300 mM sodium citrate (pH 7.0)
Phosphate-buffered saline (PBS)	150 mM NaCl, 2.5 mM KCl, 10 mM $Na_2H_2PO_4$, 1 mM KH_2PO_4 (pH 7.4)
RNase-free H2O	dH_2O, 0.1% diethylpyrocarbonate, autoclave.
Tris-buffered saline	1% (w/v) NaCl, 0.025% (w/v) KCl, 0.4% (w/v) Tris (pH 7.4)

A.4 Commercial Suppliers of Reagents and Equipment Used in this Study

ABgene, ABgene UK (Head Office, ABgene House, Blenheim Road, Epsom, KT19 9AP, UK. www.abgene.com

Ambion Inc., Ambion (Europe) Ltd., Ermine Business Park, Spitfire Close, Huntingdon, Cambridgeshire, PE29 6XY, UK. www.ambion.com

Amersham, Amerhsal Place, Little Chalfont, Buckinghamshire, HP7 9NA, UK www.amershambiosciences.com

B & K Universal, Grimston, Aldbrough, Hull HU11 4QE, UK, www.bku.com

BioRad Laboratories Ltd., BioRad House, Maylands Avenue, Hemel Hempstead, Hertfordshire, HP2 7TD, UK www.bio-rad.com

Corbett Research, 14 Hilly Street, Mortlake, Sydney, Australia, NSW 2137 www.corbettlifescience.com

Flowgen, Wilford Industrial Estate, Ruddington Lane, Wilford, Nottingham, NG11 7EP, UK www.flowgen.co.uk

Invitrogen Ltd., 3 Fountain Drive, Inchinnan Business Park, Paisley, PA4 9RF, UK www.invitrogen.com

Merck BDH, Boulevard Industrial Park, Padge Road, Beeston, Nottingham, NG9 2JR, UK www.merckbiosciences.co.uk

MWG Biotech (UK) Ltd., Anzignerstr. 7a, 85540 Ebersberg, Germany www.mwgbiotech.com

New England Biolabs (NEB), 240 County Road, Ipswich, MA 01938-2723, USA www.neb.com

Nunc, Kamstrupvej 90, Postbox 280, DK-4000, Roskilde, Denmark. www.nuncbrand.com

Promega UK, Chilworth Science Park, Southampton, SO16 7NS, UK www.promega.com

QIAGEN Ltd., Boundary Court, Gatwick Road, Crawley, West Sussex, RH10 9AX, UK www.qiagen.com

Roche, Bell Lane, Lewes, East Sussex, BN7 1LG, UK www.roche-applied-science.com

Sigma, Sigma-Aldrich Company Ltd., Dorset, England, UK www.sigmaaldrich.com

Stratagene, 11011 N. Torrey Pines Road, La Jolla, CA 92037, USA www.stratagene.com

Thermohybaid, Action Court, Ashford Road, Ashford, Middlesex, TW15 1XB, UK www.thermohybaid.com

Vector Laboratories, Ltd., 3 Accent Park, Bakewell Road, Orton Southgate, Peterborough, PE2 6XS, UK www.vectorlabs.com

Chapter 3: Investigation of genes important for viral persistence in the lung

3.1 Background to the Study

The lung has been identified as a site of persistence for a number of herpesviruses. MCMV is able to establish a persistent infection in the lungs, and recurrence of the virus in this location is associated with development of interstitial pneumonia (Balthesen *et al.*, 1993; Kurz *et al.*, 1999; reviewed by Reddehase *et al.*, 2002). CMV, EBV, HHV-7 and HHV-8 have all been implicated in development of idiopathic pulmonary fibrosis (Tang *et al.*, 2003; Stewart *et al.*, 1999). The association of clinical disease with herpesvirus persistence in this organ makes the lung an important area for study. Identification of key viral genes required for persistence may allow for development of vaccination and/or treatment strategies.

MHV-68 has been shown to establish a long-term infection of the lung. Following intranasal inoculation with the virus laboratory mice initially develop an acute infection in the lung which is cleared by approximately 10-12 days post-infection. A persistent infection is then established in the lung that can still be detected as late as 12 months post-infection and possibly beyond (Stewart *et al.*, 1998). This study further showed that in the absence of B cells viral DNA was still maintained in the lungs at late time points post-infection. Using a combination of *in situ* hybridisation and staining for viral lytic gene products, the cell type identified as harbouring the virus in this situation was the epithelial cell. This technique did not exclude the possibility that other cell types such as macrophages or dendritic cells were able to harbour latent virus.

A later study by Flano *et al.* (2003) used FACS to separate the different populations of lung cells, and subsequently the frequency of cells harbouring virus within each population was determined by a limiting dilution PCR assay. This method showed that at 3 months post-infection only the B cell population had a significant pool of MHV-68 infected cells (1/17917), while all other populations (macrophages, dendritic cells and null [including epithelial] cells) had frequencies lower than 1 in 2 x 10^5 cells. This study did not investigate the effect of anti-viral treatment on viral persistence, so there is a possibility that a percentage of detectable virus may be lytic rather than latent.

Both studies agree that the presence of virus at late time points is consistent with latent rather than chronic lytic infection. This was demonstrated by Stewart *et al.* (1998) by demonstration of the continued presence of viral DNA in the lungs of μMT mice following treatment with 4'-S-EtdU, and following treatment only episomal (and not linear) forms of the genome were detectable, indicating a latent infection. However, both wild-type and μMT untreated mice have both linear and episomal forms of the genome at late time points, indicating that ongoing lytic infection or reactivation may be a normal feature of MHV-68 infection in the lung. Preformed infectious virus was similarly detected by Flano *et al.* (2003), albeit at extremely low levels (<100 PFU/tissue) and not in every mouse studied. These studies did not determine whether viral load in the lung was reduced following anti-viral treatment, which would indicate whether viral replication is required to maintain normal viral load in this organ.

3.1.1 Viral Genes with a Potential Role in Persistence in the Lung

The majority of studies on viral genes involved in establishment and maintenance of MHV-68 latency have focused on the spleen, and several genes have been identified as important in these processes. These include M2, M4 and ORF72.

M2 is a B cell associated antigen implicated in control of viral expansion in spleen lymphocytes. Disruption of the gene results in high levels of persistence at later time points (up to d70 post-infection studied) (Macrae *et al.*, 2003; Jacoby *et al.*, 2002).

M4 plays a role during establishment of latency in the spleen. During acute-phase latency (14-21 days post-infection) the absence of the M4 gene product results in a 10-100-fold reduction in the number of genome positive spleen cells (Townsley *et al.*, 2004), although by d42 viral levels are equivalent in both wild-type and M4-knockout viruses (Evans *et al.*, 2006).

ORF72 (v-cyclin) is required for efficient reactivation from latency (van Dyk *et al.*, 2000). V-cyclin interacts with cellular cdks to drive cell cycle progression in order to establish the S-phase environment thought to be required for viral replication (Upton *et al.*, 2005).

Immune evasion may also play a role in maintenance of a persistent infection, and several viral genes are known to be involved in this process. These genes include M3, K3 and ORF4.

The **M3** gene product is a secreted chemokine binding protein, able to block binding of host chemokines to cell surface receptors. Previous studies utilising a virus with M3 disrupted by insertion of a LacZ cassette showed a disruption in establishment of latency in the spleen, with a decline in latent load due to immune clearance of the virus (Bridgeman *et al.*, 2001). However these results were not reproduced on infection with an M3.stop virus, where establishment and reactivation from splenic latency occurred as for wild-type virus (van Berkel *et al.*, 2002).

K3 is able to bind to and downregulate surface MHC class I expression and so prevents or reduces CTL recognition of infected cells. Following infection with a K3-deficient virus establishment of normal latent load is impaired and long-term (up to 180 days post-infection) viral load appears lower than in wild-type-infected mice (but this difference is not statistically significantly different) (Stevenson *et al.*, 2002).

ORF4 (Regulator of Complement Activation, RCA) inhibits complement C3 activation in both the classical and alternative pathways (Kapadia *et al.*, 1999). Complement plays a role in regulation of viral latency, and in its absence a higher frequency of reactivation is observed in the spleen and PECs. The RCA protein is also required for efficient persistent replication in IFNγR-/- mice (Kapadia *et al.*, 2002).

Loss of the left-hand end of the genome of MHV-68 (incorporating genes M1, M2, M3, M4 and 8 vtRNAs) has given rise to the naturally occurring deletion mutant **MHV-76**. The virus replicates at lower levels and is cleared more rapidly from the lung, and establishes latency in the spleen at lower levels than wild-type virus (Macrae *et al.*, 2001; Clambey *et al.*, 2002).

Amongst the studies on viral persistence in the lung one paper identifies a gene transcribed at late time points post-infection in the lung. **M11** is an anti-apoptotic Bcl-2 homologue, and transcripts of this gene can be detected in the lungs at 10 months post-infection, suggesting an important role for this gene in long-term persistence (Roy *et al.*, 2000). This gene has also been implicated in reactivation from latency in

the spleen, but this function has not been investigated in the lung (Gangappa *et al.*, 2002).

3.1.2 The Host Immune Response and its Role in Viral Persistence

Interactions between the host immune response and the virus may also play a role in determining the level of virus persistence. Type I interferon has previously been shown to play a role in clearance of the virus from the lung, with IFN-α/β $R^{-/-}$ mice harbouring infectious virus in the lung up to 21 days post-infection (Dutia *et al.*, 1999). Reactivation of latent virus from spleen and peritoneal cells in these mice is enhanced, demonstrating a role for type I interferon in control of latent infection (Barton *et al.*, 2005).

Type II interferon is important for control of both latent and persistent replication. Treatment of latently infected PECs *in vitro* with IFNγ reduces the frequency of cells that reactivate virus (Steed *et al.*, 2006). In the absence of IFNγ pre-formed (i.e. lytic) virus can be detected up to d42 post-infection in peritoneal cells but not in the spleen. Similarly, reactivation from latency in the PECs is enhanced in IFN-$\gamma^{-/-}$ mice (Tibbetts *et al.*, 2002), and *in vivo* depletion of IFN-γ in wild-type mice also increases the frequency of cells that reactivate virus (Steed *et al.*, 2006).

In the absence of the immune response involved in control of persistence or latency in the lung, levels of persistence (and hence viral load) may be altered.

3.2 Using Viral Load to Measure the Contribution of Particular Genes to Viral Persistence in the Lung

The above genes were selected for further study into their involvement in establishment or maintenance of a persistent infection in the lung. Real time PCR was used to quantify viral load in the lungs at late time points post-infection to see if the absence of any of these genes affected this measure. Figure 3.1 shows the MHV-68 mutants used in the study.

3.2.1 Background to Real Time PCR

Real time PCR is an established method for the quantification of viral load in vivo (reviewed by Niesters). Several different strategies can be employed to detect PCR amplification in real time, all of which utilise the production of a fluorescent signal

M1Δ - M1 deletion mutation

1170 bp deletion with a 190 bp insertion.

Unpublished data, see results chapter 4 for further details

76(RΔM2) - M2 frameshift mutation

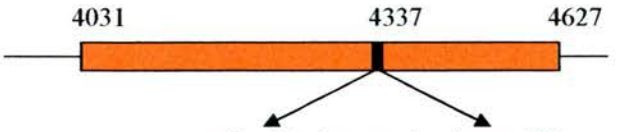

4bp deletion causing frameshift

Macrae et al, 2003

γHV68-M3.stop - M3 stop mutation

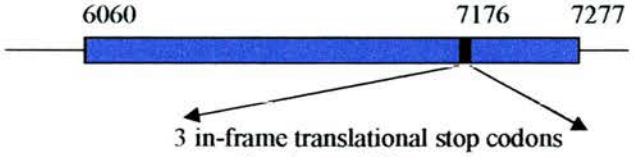

3 in-frame translational stop codons & a frameshift mutation

Van Berkel et al, 2002

M4Stop - M4 stop mutation

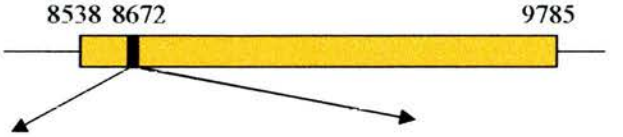

3 in-frame translational stop codons

Geere et al, 2006

γHV68-RCAstop - ORF4 stop mutation

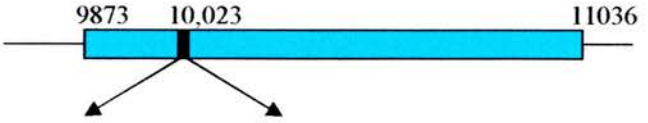

Translational stop codon

Kapadia et al, 2002

ΔK3TET⁻ - K3 insertion mutation

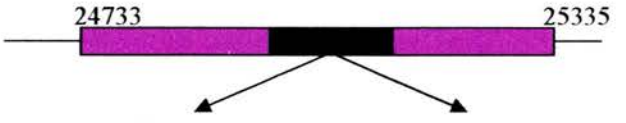

FRT site plus 165bp plasmid sequence

Stevenson et al, 2002

V-cyclin.stop - ORF72 stop mutation

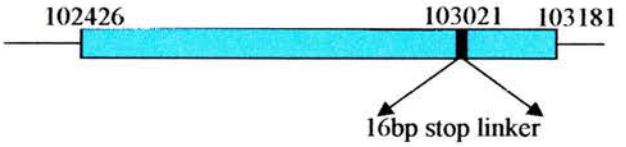

16bp stop linker

Van Dyk et al, 2000

MHV-76

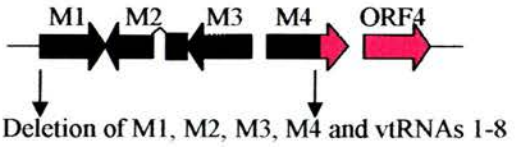

Deletion of M1, M2, M3, M4 and vtRNAs 1-8

Macrae et al, 2001

Figure 3.1a - Mutant viruses used in the initial study. Genes with a potential role in latency or immune evasion were identified and the corresponding mutant viruses were obtained. The figure shows the name, specific mutation and origin of each virus used. Thanks to B.M. Dutia, A.I. Macrae, P.G. Stevenson and H.W. Virgin IV for the kind gift of these viruses.

TK$^-$Kan$^-$ - Thymidine kinase deletion mutant

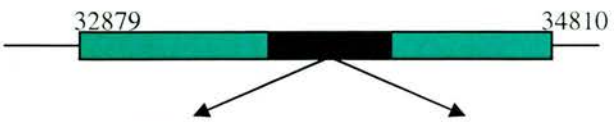

FRT site plus 165bp plasmid sequence, minus 150bp of viral genome

Coleman et al, 2003

27- STOP - ORF27 stop mutant

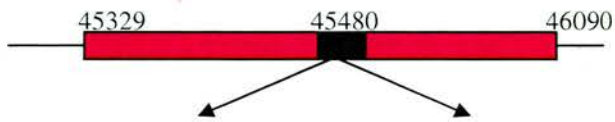

Stop codons in all reading frames

May et al, 2005a

FS73 - ORF73 frameshift mutation

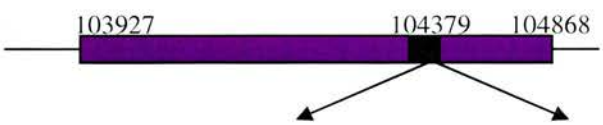

5bp insertion causing frameshift

Fowler et al, 2003

Figure 3.1b - Mutant viruses used during investigation of the role of lytic genes during long term persistence in the lung. Genes with a role during acute infection in the lung were identified and the corresponding mutant viruses were obtained. The figure shows the name, specific mutation and origin of each virus used. Thanks to P.G. Stevenson and S. Efstathiou for the kind gift of these viruses.

once a PCR product is formed (reviewed by Bustin, 2005; Mackay *et al.*, 2002). Hydrolysis probes (e.g. the TaqMan™ system) utilise the 5'-nuclease activity of the DNA polymerase to hydrolyse a probe bound to the target amplicon. This releases a fluorescent reporter dye previously quenched by a second fluorescent dye located at the 3' end of the probe and allows detection of amplified product. Hybridisation probes require two separate probes to bind to the target sequence in a head-to-tail arrangement. One probe will carry the donor fluorophore (usually fluorescein) and the other an acceptor fluorophore. Binding brings the two probes into close proximity, allowing fluorescence resonance energy transfer from donor to acceptor and resulting in emission of red fluorescent light. Molecular beacons utilise a third strategy. Hybridisation probes are generated that form a stem-and-loop structure, with the loop complementary to the target sequence. In solution the stem structure maintains a fluorescent reporter dye in close proximity to a quencher molecule located at the other end of the probe. When bound to the target the stem-loop structure separates and the quencher and reporter are distant enough that the reporter signal can be detected. These methods are highly specific and sensitive but are also expensive. A significantly less expensive method uses sequence non-specific DNA-binding fluorophores. SYBR green I fluoresces when associated with dsDNA which is exposed to a suitable wavelength of light. While much cheaper, this method requires the primers used in the PCR reaction to be highly specific as formation of other products or primer dimer will give an over-estimate of the amount of specific product.

3.2.2 Development of a Real Time PCR Assay to Measure Viral Load

An assay was developed using the SYBR-green method of detection. Primers were designed and optimised to allow amplification of the target sequence in the absence of any non-specific product or primer dimer. Primers specific to the ORF50 gene (RTAmod) were selected as fulfilling the above criteria. To generate a standard curve serial dilutions of plasmid pLXSN with the ORF50 gene cloned in (pLXSN+RTA, obtained from Dr Bernadette Dutia) were generated. Initially the DNA content of the plasmid stock was determined by spectrophotometry and the plasmid copy number determined using the equation given in Materials & Methods section 2.6.1.1.3. Plasmid pLXSN+RTA had a total size of 7.3kb, giving a single copy of the plasmid a mass of 4.818×10^6 Da.

Figure 3.2a shows the range of the qPCR platform. The DNA template containing 1 x 10^6 copies per µl (i.e. 5 x 10^6 copies per reaction) was amplified first, with each subsequent dilution amplified at intervals of 4 cycles until the DNA template was diluted by 4 orders of magnitude. Quantitation of the amount of target in the unknown samples is achieved by measuring C_T (the *threshold cycle*, or cycle number at which the fluorescence increases above background level) and using the standard curve to determine starting copy number. C_T is determined by software analysis and is set at a point where all curves represent logarithmic growth.

Figure 3.2b shows the specificity of the RTA primers when used to amplify lung DNA one month post-infection. Melt-curve analysis was used to determine the specificity of each qPCR. The temperature at which PCR products melt varies over a large range, and because of length differences non-specific products usually melt at a lower temperature than desired PCR products. Following qPCR amplification the mixture was heated from 65°C to 95°C in increments of 0.1°C. The presence of a specific PCR product was detected by a sudden loss of fluorescence as the uniform population of DNA strands melted. Non-specific products such as primer dimer were detected by irregular decreases in fluorescence. Both plasmid and lung DNA produced a single peak of the same size, corresponding to the amplification of the same region of template DNA.

3.2.3 Normalisation of Samples

Normalisation is used to correct sample-to-sample variation. For RT real time PCR this reduces variation as a result of differences in initial RNA quantity or quality, or as a result of experimental treatment such as reverse transcription. Real time PCR results are usually normalised against a control gene that may also act as a positive control for the reaction. The ideal housekeeping gene (or genes) for this process has been investigated and reviewed many times and is often controversial (see chapter 5 for further discussion). However this debate is not an issue when normalising samples for DNA rather than cDNA levels. Any cellular gene or region of DNA present consistently in all cell types can be used as a template. Normalisation of DNA samples is carried out to reduce error due to variation in input DNA quantity or quality.

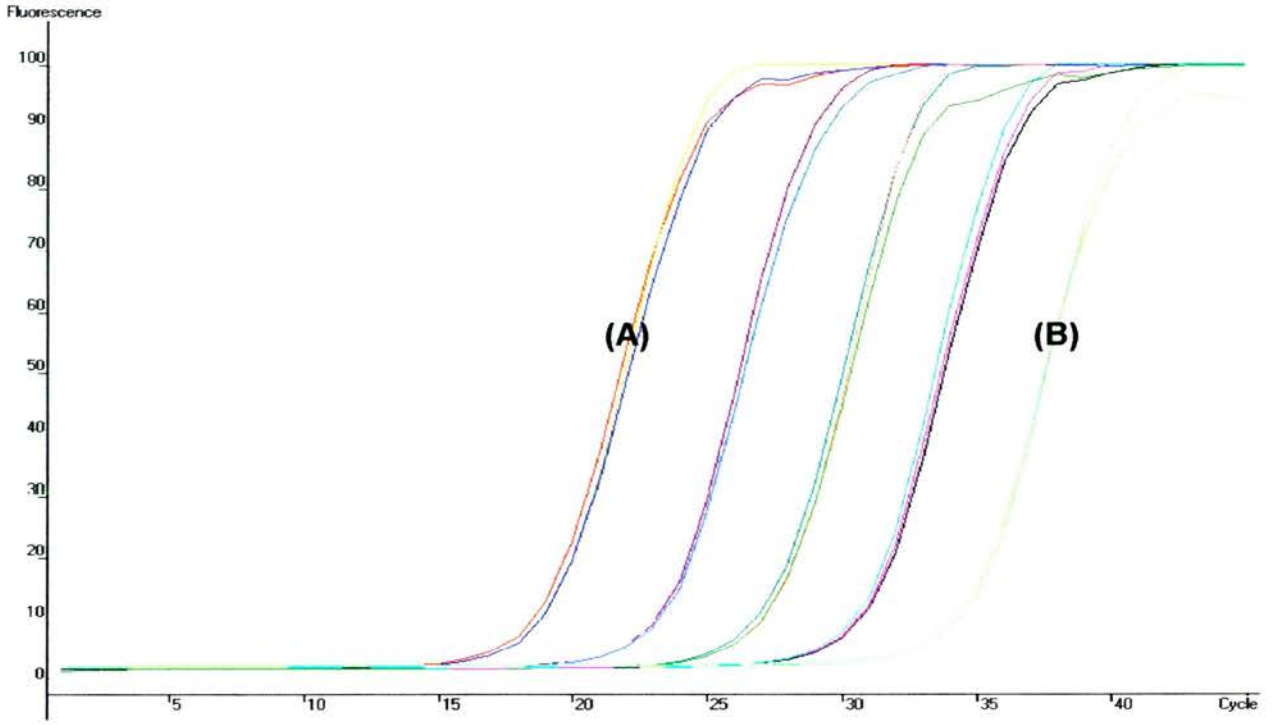

Figure 3.2a - qPCR platform for the RTA assay using 10-fold dilutions of the pLXSN+RTA plasmid. Reactions containing 5 x 10^6 copies of the plasmid are amplified first (marked A), with subsequent 10-fold dilutions amplified at intervals of 4 cycles to a minimum of 5 x 10^2 copies (marked B).

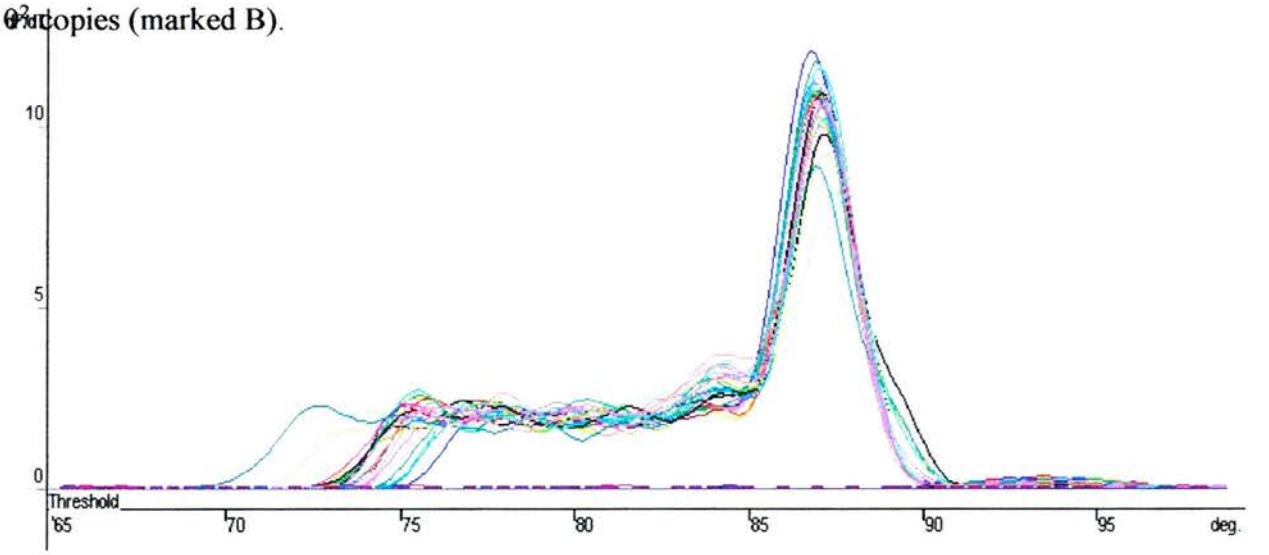

Figure 3.2b - Melt curve analysis of pLXSN+RTA and DNA from infected lung samples 1 month post-infection. PCR reactions are heated from 65°C-95°C in increments of 0.1°C. The presence of a single peak at approximately 87°C indicates a single specific PCR product is produced in reactions containing either plasmid or lung DNA as template.

The β-actin gene was selected as the normalisation gene because this assay had already been developed and optimised for use in real-time PCR by Clive McKimmie (PhD thesis, 2005). Standards for this reaction were made using uninfected mouse lung DNA as a template. β-actin 1 primers were used to amplify the target region by PCR to generate a fragment of 272 bp. PCR samples were run on a 1% agarose-TAE gel and visualised using a long wave UV transilluminator. The band was excised and DNA extracted using a QIAquick Gel Extraction kit and resuspended in 30 µl Buffer AE. Serial 10-fold dilutions were made using Buffer AE down to 1/10,000,000.

For the qPCR reaction the β-actin 2 primers (which are internal to the region amplified by the β-actin 1 set) were used, with the platform shown in figure 3.3a. The sensitivity of this reaction extends from a 1/1000 dilution of the β actin-1 template down to 1/10,000,000. As before melt curve analysis was used to determine the specificity of the qPCR reaction (shown in figure 3.3b).

Quantification for the β-actin PCR is relative – the absolute copy number in each of the standard dilution series is not determined, and hence the copy number for unknown samples is a value relative to the standard dilutions, not an absolute value. As this assay is used only to confirm that levels of β-actin are similar in all samples an absolute value is not necessary.

3.3 Experimental Protocol

A previous study showed that BALB/c mice show greater levels of MHV-68 gene expression and higher viral titres in the lung during acute infection compared to C57BL/6 mice (Weinberg *et al.*, 2004). This corresponds to our own results – an initial study involving infection of C57BL/6 mice failed to produce useful data because at later time points the level of viral DNA in the lungs fell below the limit of detection of our assay. BALB/c mice were used in all subsequent experiments because their increased susceptibility to infection meant the viral load in the lungs at late time points was above the limit of detection of the assay, and therefore it was likely any difference in phenotype would be more easily detected.

Female BALB/c mice aged 5-6 weeks were infected intranasally with 4×10^5 PFU of virus. For each of 3 time points (1, 3 and 6 months post-infection) three mice per time point per virus were infected. Mice were thoroughly perfused with SPBS and the

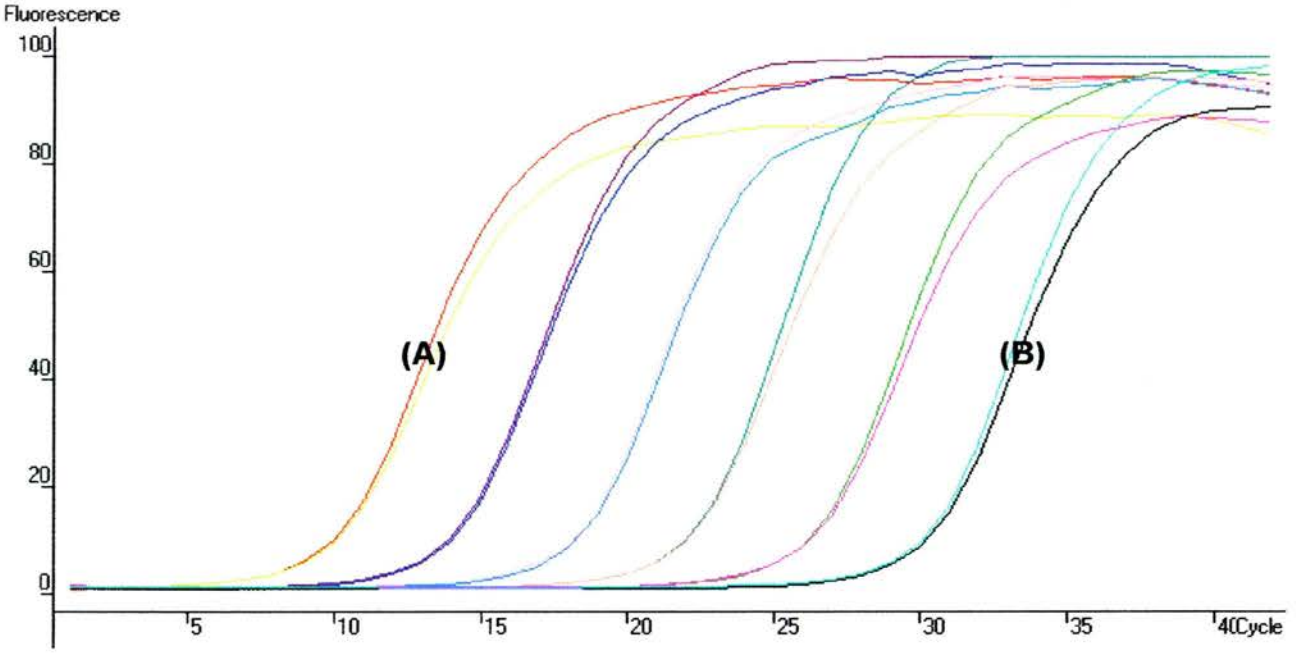

Figure 3.3a - qPCR platform for the β actin assay using 10-fold dilutions of the β actin-1 amplified template. Reactions containing 1/100 dilution of the β actin-1 template (marked A) are amplified first, with subsequent 10-fold dilutions amplified at intervals of 4 cycles to a 1/100,000,000 dilution of the template (marked B).

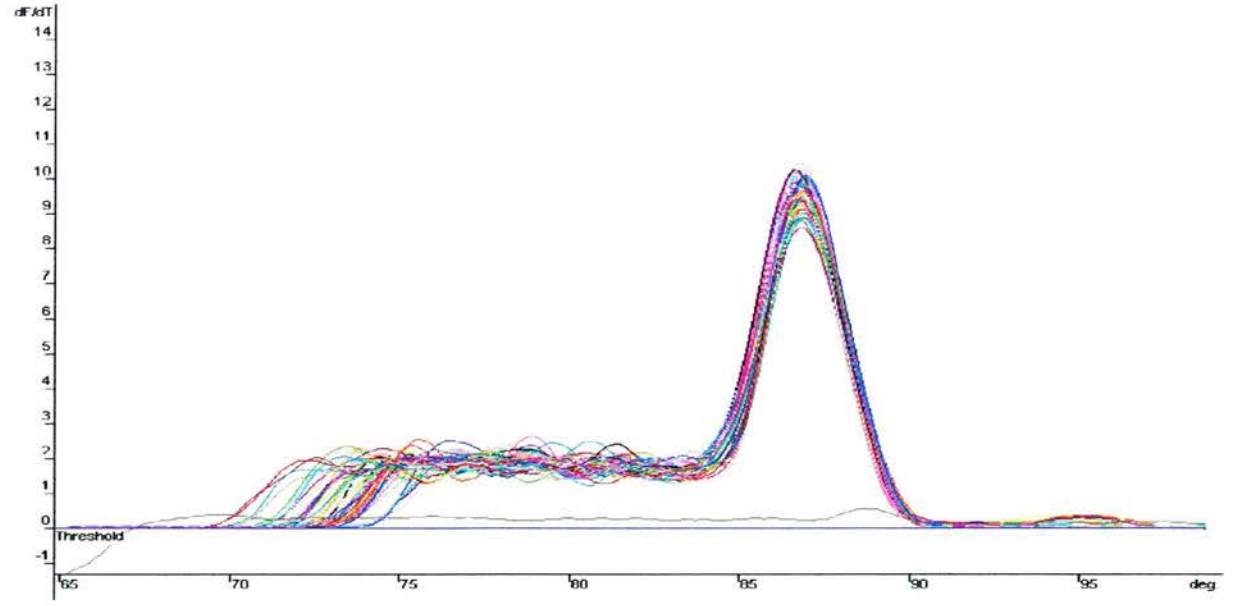

Figure 3.3b - Melt curve analysis of β actin qPCR using β actin-1-amplified product or infected lung DNA 1 month post-infection as template. PCR reactions are heated from 65°C-95°C in increments of 0.1°C. The presence of a single peak at approximately 87°C indicates a single specific PCR product is produced in reactions containing either β actin-1 PCR product or lung DNA as template.

lungs were removed. DNA was extracted using the protocol for an entire lung detailed in section 2.1.2.2 of Materials and Methods. This method ensures that there is less chance of error due to sampling effect that could occur when using the standard Qiagen DNeasy protocol and extracting DNA from only 25 mg of lung tissue.

Initially the viral load in all samples was quantified using the RTA real time assay. Comparison of samples between different real time runs is not advisable as differences in mastermix composition and threshold level may introduce error into the results. To overcome this each real time run contained all three wild-type MHV-68-infected samples as well as the mutant virus under investigation. All samples and standard dilutions were run in triplicate to increase the accuracy of the results. The mean viral load for each sample was calculated from the replicates. Quantification of β-actin for each sample was carried out using the β-actin real time PCR. Samples and standards were run in duplicate. RTA levels were then normalised to the level of β-actin using the method given previously (Materials and Methods section 2.6.3).

3.3.1 Initial Results

Figure 3.4 shows the melt curve analyses for RTA real-time reactions using 6 month samples. At 1 and 3 months post-infection a single product is detected. However when amplifying DNA from the 6 month lungs levels of viral DNA in some samples were too low to be detected by the RTA assay and non-specific amplification was observed. Viral load in the 6 month samples were therefore quantified using a more sensitive qPCR assay that uses primer set M4RT (primer sequences shown in Appendix 1.2). The lowest copy number that can be accurately measured by this assay is 10^1 copies/µl (compared to 10^2 for the RTA assay). Figure 3.5 shows the platform and the melt curve analysis for the 6 month samples using the M4 assay. A single peak at 84°C can be seen in the melt curve, indicating specific amplification of the M4 gene. The M4RT primers bind to a region of the M4 gene distal to the mutation in the M4.stop virus and therefore viral load can still be measured in mice infected with this virus. In MHV-76 the region these primers bind to is absent so it was not possible to measure viral load in MHV-76-infected mice.

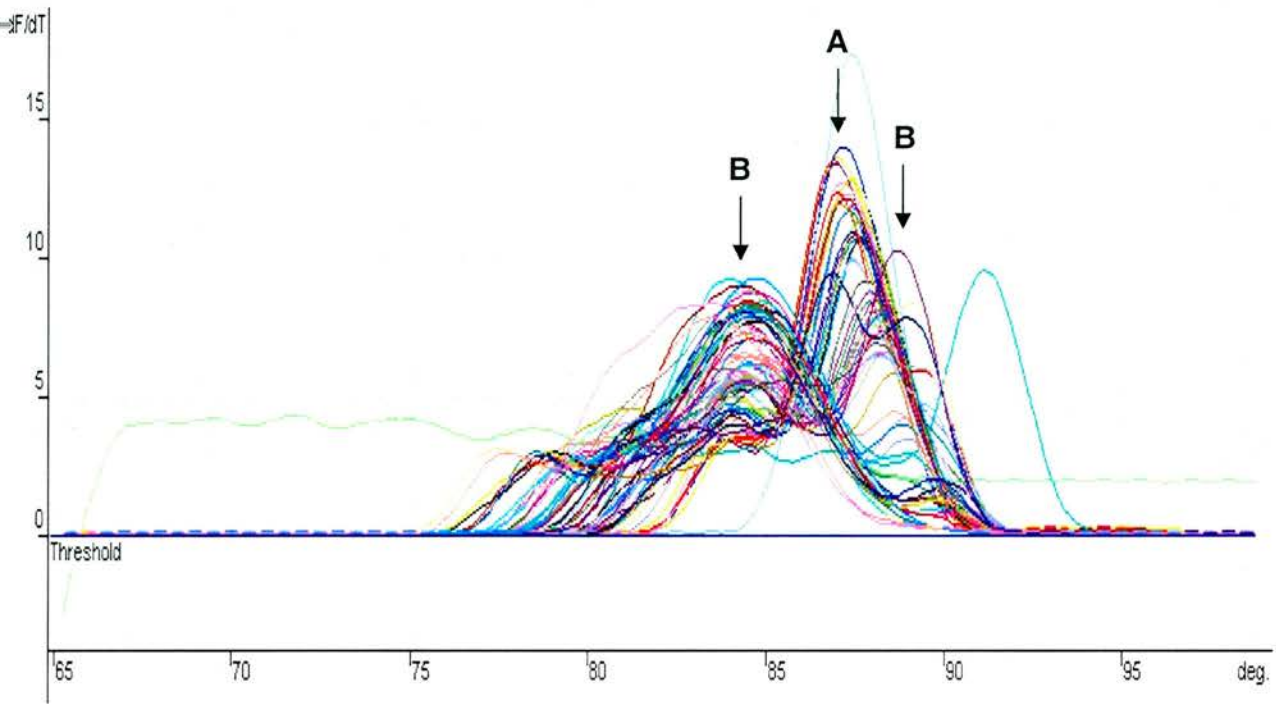

Figure 3.4 - Melt curve analysis of an RTA qPCR using either pLXSN+RTA or DNA from infected lung 6 months post-infection. Curves contain a peak at approximately 87°C (marked A) which corresponds to amplification of the pLXSN+RTA template, ranging from 5 x 10^6 to 5 x 10^2 copies per reaction. The majority of the 6 month infected lung samples show more than one peak (the most obvious are marked B), indicating non-specific amplification of template DNA. Quantification of viral load in these samples is not possible because the dsDNA present does not correspond to the specific RTA-amplified region of the viral genome.

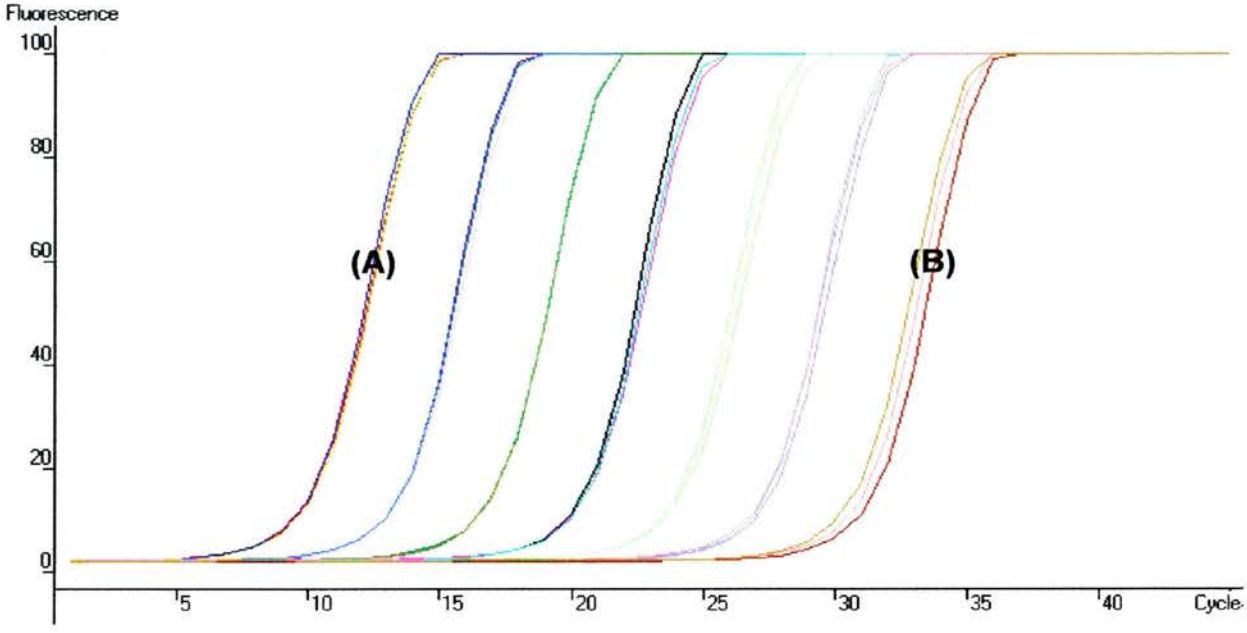

Figure 3.5a - qPCR platform for the M4 assay using 10-fold dilutions of the M4 plasmid. Reactions containing 5 x 10^7 copies of the plasmid (marked A) are amplified first, with subsequent 10-fold dilutions amplified at intervals of 4 cycles to a minimum of 5 x 10^1 copies (marked B).

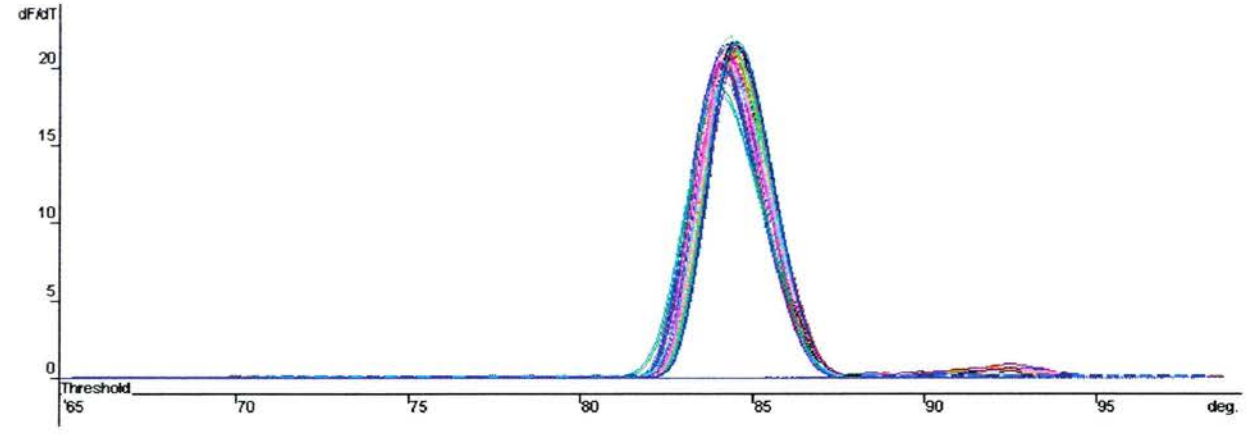

Figure 3.5b - Melt curve analysis of the M4 assay using either M4 plasmid or lung DNA 6 months post-infection. The presence of a single peak at approximately 83°C indicates a single specific PCR product is produced in reactions containing either plasmid or lung DNA as template. The non-specific amplification seen previously when amplifying the same template lung DNA does not occur when using the M4RT primer set.

Figure 3.6 shows normalised viral load results for all viruses at all time points investigated. At some time points there may appear to be differences in viral load between mutant- and wild-type-infected mice (of note are the ORF72-infected mice at 3 and 6 months post-infection, and the M11-infected mice at 6 months post-infection). However statistical analysis was carried out using the non-parametric Mann-Whitney test and at no time point did any of the viruses studied show any significant difference to the wild-type virus.

During the course of the experiment a virus with a potential role in immune evasion (and hence with a possible role in persistence in the lung) became available. The role of M1 during MHV-68 infection is discussed in detail in chapter 4 and has previously been implicated in reactivation in the spleen (Clambey *et al.*, 2000). Our data also indicates a potential role during acute infection of the lung. As before 3 mice per time point were infected intranasally with 4 x 10^5 PFU of M1Δ virus, with the same number of mice infected with wild-type MHV-68 for comparison. At 3 weeks post-infection one mouse infected with MHV-68 died of causes unrelated to viral infection. One month post-infection 3 mice infected with M1Δ and 2 mice infected with wt virus were sacrificed and lung viral load quantified using the RTA assay as before.

Prior to the 3-month time point, results became available for the 6-month time point for all other viruses. The small sample sizes had made statistical analysis difficult and it was decided in the case of the M1Δ experiment to omit the 3 month time point in favour of a larger sample group at the 6 month time point. The viral load in mice 6 months post-infection was determined as before using the M4 assay.

Results for the M1Δ experiment are also shown in figure 3.6. Statistical analysis using the Mann-Whitney test showed no significant difference at the 1 and 6 month time points between the M1Δ and wild-type viruses. The increased sample size did however allow for greater confidence in the results.

3.3.2 Investigation of the Role of Type I and Type II Interferons in Long Term Persistence in the Lung

A single 6-month time point was selected. Previous studies had not shown any difference in viral load at the intermediate time points of 1- and 3-months post-infection so these were omitted.

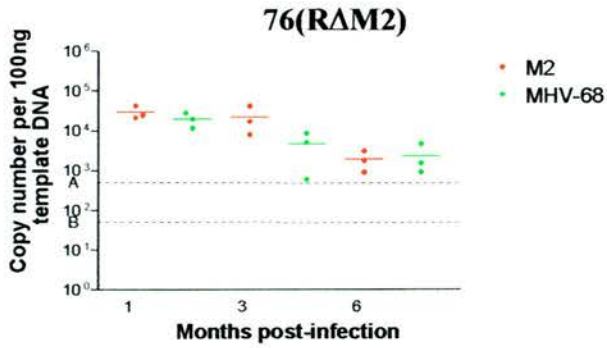
76(RΔM2)
Copy number per 100ng template DNA
M2
MHV-68
Months post-infection

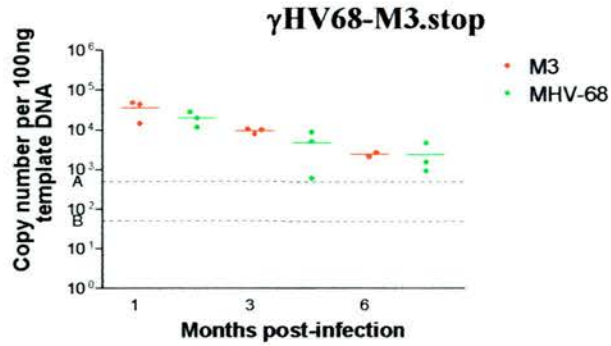
γHV68-M3.stop
Copy number per 100ng template DNA
M3
MHV-68
Months post-infection

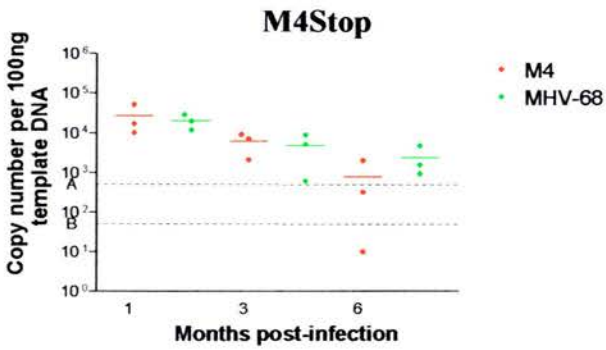
M4Stop
Copy number per 100ng template DNA
M4
MHV-68
Months post-infection

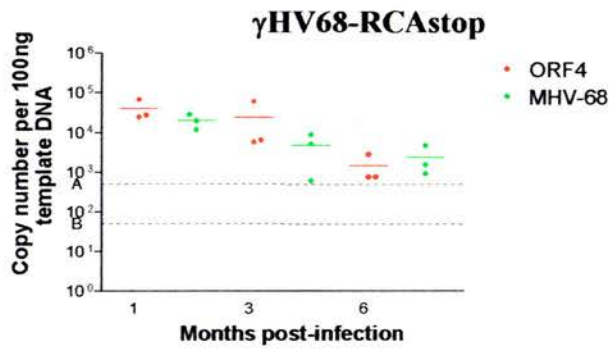
γHV68-RCAstop
Copy number per 100ng template DNA
ORF4
MHV-68
Months post-infection

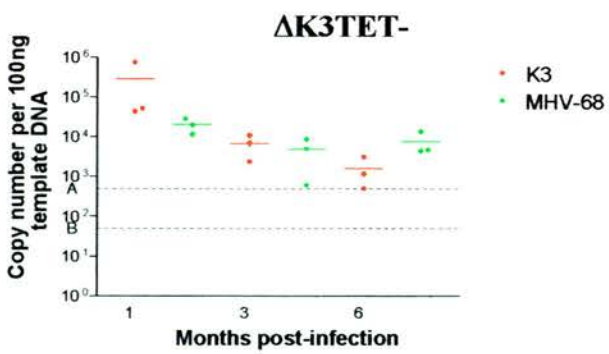
ΔK3TET-
Copy number per 100ng template DNA
K3
MHV-68
Months post-infection

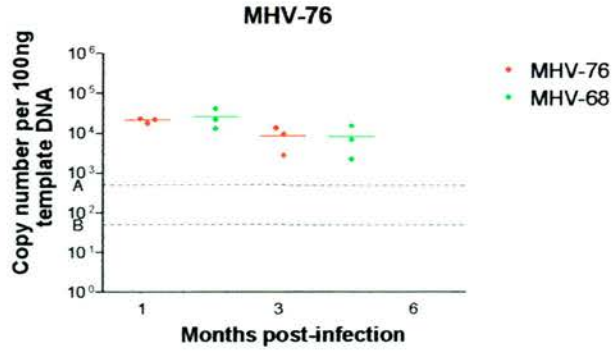
MHV-76
Copy number per 100ng template DNA
MHV-76
MHV-68
Months post-infection

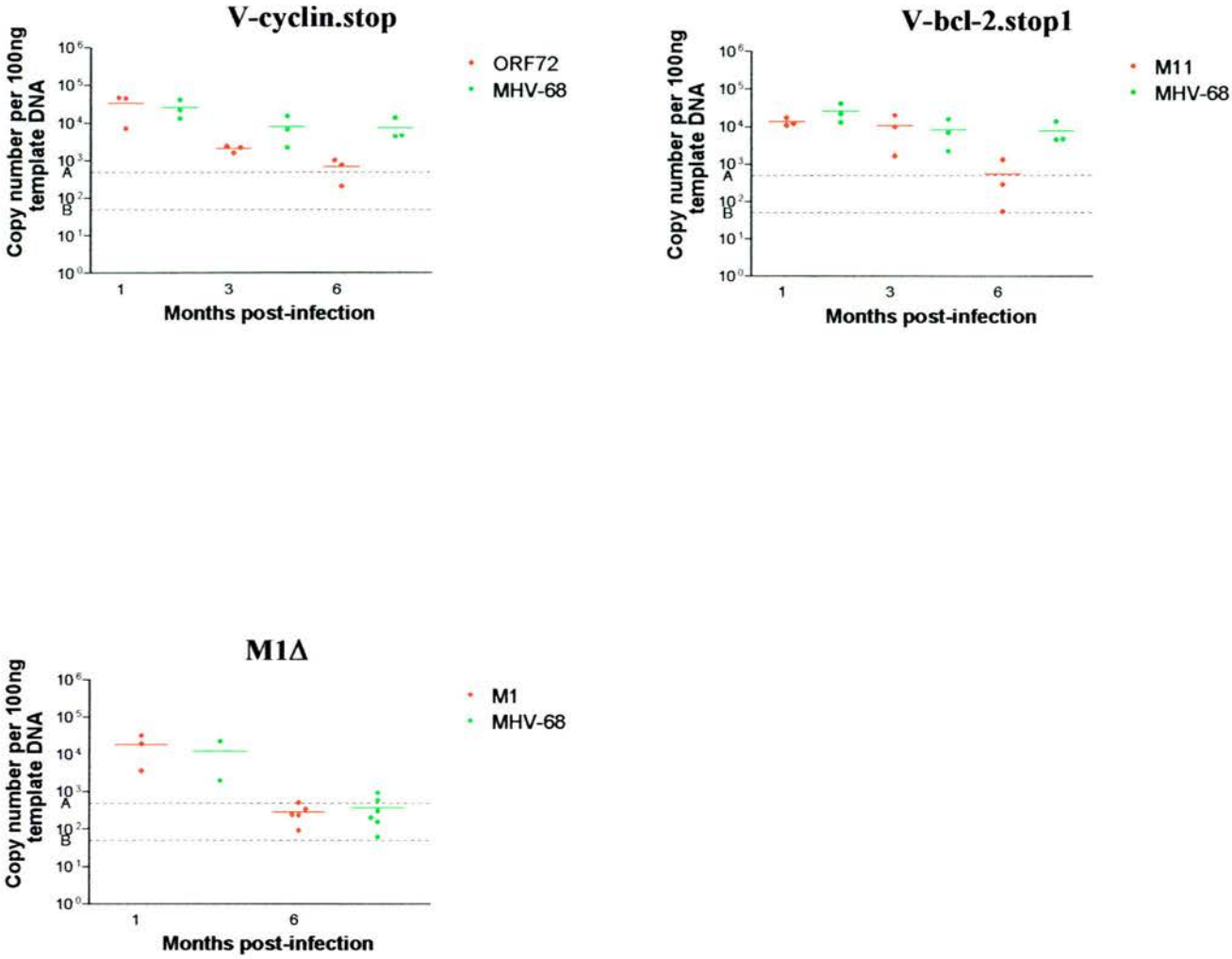

Figure 3.6 – Viral load in the lungs at 1-, 3- and 6-months post-intranasal infection with 4 x 10^5 PFU of the stated mutant virus. Viral load is quantified using real time PCR DNA was extracted from infected lungs and 100 ng used per PCR reaction. At 1- and 3-months post-infection primers specific to the RTA gene were used to amplify viral DNA in infected lungs. At 6 months the more sensitive M4 assay was used. Samples were subsequently normalised to the amount of β-actin in the sample (previously determined by a separate qPCR reaction using β-actin-specific primers) . The line labelled A is the limit of detection using the RTA assay; the line labelled B is the limit of detection using the M4 assay.

Previous data has shown that IFN-α/β $R^{-/-}$ mice (Muller *et al.*, 1994) are highly susceptible to infection with MHV-68, with 80% mortality following intranasal infection with 4 x 10^5 PFU of virus. Infection with 4 x 10^3 PFU results in 50% mortality before d13, with mice surviving past this point remaining in good health (Dutia *et al.*, 1999).

IFN-α/β $R^{-/-}$, IFNγ$R^{-/-}$ and control 129 SV/EV mice were infected intranasally at 5-6 weeks of age with 4 x 10^3 PFU of wild-type MHV-68. 12 IFN-α/β $R^{-/-}$ and 6 each of the IFNγ$R^{-/-}$ and 129 SV/EV mice were infected, with the expectation that ~50% of the IFN-α/β $R^{-/-}$ mice would die before the 6 month time point was reached. By 6 months post-infection 8/12 IFN-α/β $R^{-/-}$ mice were dead, a figure slightly higher than previously stated, and likely to result from the small sample group used in this experiment. All IFNγ$R^{-/-}$ and 129 mice survived. At 6 months mice were perfused and sacrificed as before, and lung viral load was quantified using the M4 assay.

Results for this experiment are shown in figure 3.7. At 6 months post-infection viral load for IFNγ$R^{-/-}$ mice infected with MHV-68 is higher than for wt mice similarly infected, although this difference is not statistically significant. Average viral load in the lungs of IFN-α/β $R^{-/-}$ mice is higher than for both IFNγ$R^{-/-}$ and wt mice, although again this is not a statistically significant difference.

3.4 Investigation of Viral Genes with a Role during Lytic Replication in the Lung

Genes were previously selected on the evidence of their involvement in immune evasion or establishment and/or maintenance of latency, factors thought likely to be key in viral persistence in the lung. However given that the genes appeared to have no effect on viral load at late time points post-infection it was decided to investigate several other candidates. Two genes had previously been identified as playing a role during lytic infection in the lung, and the corresponding mutant viruses were obtained from Dr. Philip Stevenson at the University of Cambridge. The thymidine kinase (TK^-) virus is severely impaired in lytic replication in the lungs but by one month post-infection normal levels of splenic latency have been established. The ORF27 gene encodes a glycoprotein (gp48) required for intercellular viral spread. Mutation of this gene results in a phenotype intermediate between that of the TK- and wild-type

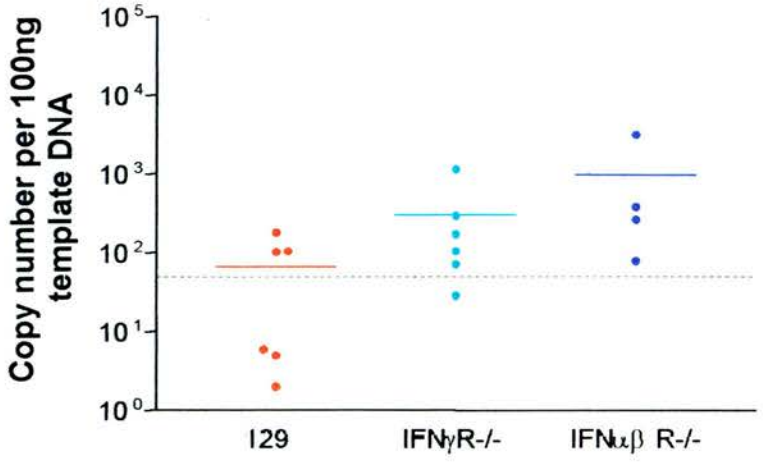

Figure 3.7 – Viral load in the lungs of wild-type 129, IFNγR$^{-/-}$ or IFNαβR$^{-/-}$ mice at 6 months post-intranasal infection with 4 x 10^3 PFU of wild-type MHV-68. As before, viral load was quantified using the M4 real time PCR assay to quantify viral copy number in 100 ng template DNA. Samples were normalised to the amount of β actin in the sample. The dashed line denotes the limit of detection of the assay.

viruses, with a deficit in lytic replication in the lungs compared to wild-type virus but not as extreme as that observed for the TK- virus. Similarly there is a reduction in the initial amount of latent virus in the spleen but this is resolved by one month post-infection.

To determine if latency plays any role in maintenance of persistent lung infection an ORF73-deficient virus was obtained from Dr. Stacey Efstathiou at the University of Cambridge. ORF73 is involved in episome maintenance, and the absence of this gene in MHV-68 results in complete failure to establish latency in the spleen (Fowler 2003, Moorman 2003).

3.4.1 Experimental Protocol

Initially the ORF73 virus (shown in figure 3.1b) was used to set up an experiment as before with time points at 1, 3 and 6 months post-infection and 3 mice per virus per timepoint. Wild-type MHV-68 virus was also used to infect mice as a control. Mice were infected with 4 x 10^5 PFU of virus intranasally. By 7 days post-infection all mice infected with the ORF73 virus were dead, and were disposed of before autopsies were possible. All mice infected with wild-type MHV-68 survived and appeared healthy at d10 but were culled at this point as they were no longer required. Previous studies using the ORF73 virus involved intranasal infection at 1 x 10^4 PFU and did not report any unexpected deaths (Fowler *et al.*, 2003).

To test the hypothesis that lytic replication may be important for viral persistence in the lung BALB/c mice were infected with the TK, ORF27, ORF73 or wild-type virus (virus mutants shown in figure 1b). Mice were infected with 1 x 10^4 PFU intranasally to avoid any of the complications seen previously when infecting with a higher dose. Owing to time constraints a single time point at 2.5 months was chosen. 6 mice per virus were used to aid statistical analysis. One mouse infected with ORF73 died at 1 month post-infection of causes unrelated to viral infection. At 2.5 months post-infection lungs were harvested and assayed as before using the M4 real time assay.

3.4.2 Results for Investigation of Genes with a Role During Lytic Infection

Figure 3.8 shows the normalised results for the TK, ORF27 and ORF73 viruses compared to the wild-type MHV-68 control. Statistical analysis using the non-parametric Mann-Whitney test shows viral load in mice infected with the TK virus is significantly different to mice infected with the wild-type virus ($p<0.0051$), as is the ORF73 virus ($p<0.0225$), but no significant difference was observed on infection with the ORF27 virus.

To determine if normal latent infection was established in the spleen following infection with viruses that had altered viral load in the lungs the viral load of spleens from the TK, ORF27, ORF73 and wild-type MHV-68-infected mice were quantified using real time PCR. DNA was extracted using the standard protocol for the Qiagen DNeasy kit (Materials & Methods section 2.1.2.1) and viral load quantified as before using the M4 real time assay. In all cases the viral load fell below the limit of detection of the assay and hence viral load could not be quantified using this technique (data not shown).

3.5 Discussion

Prior to 1998 the lung was not considered an important site for MHV-68 persistence. Stewart *et al.* (1998) first demonstrated persistence of the virus in the lung at late time points post-infection, and using μMT (B cell-deficient) mice demonstrated persistence in the absence of B cells. In both wild-type and μMT mice episomal and linear forms of the genome were found, indicating a non-B cell type was able to harbour latent virus. This alternative cell type was identified by *in situ* hybridisation as the lung epithelial cell.

Since 1998 debate has continued about the cell type harbouring latent virus in the lung, with evidence presented by Flano *et al.* (2003) that the B cell is the predominant site of latency at late time points with little or no contribution from epithelial cells.

However, while the focus has centred on the site of persistence of the virus, little attention has been paid to the possibility that latent infection is not the only means of maintaining the virus in the lungs. Evidence exists in other herpesviruses that there is the potential for chronic lytic infection existing below the detection limit of infectivity assays. In the case of cytomegalovirus the lung is a known site of viral persistence,

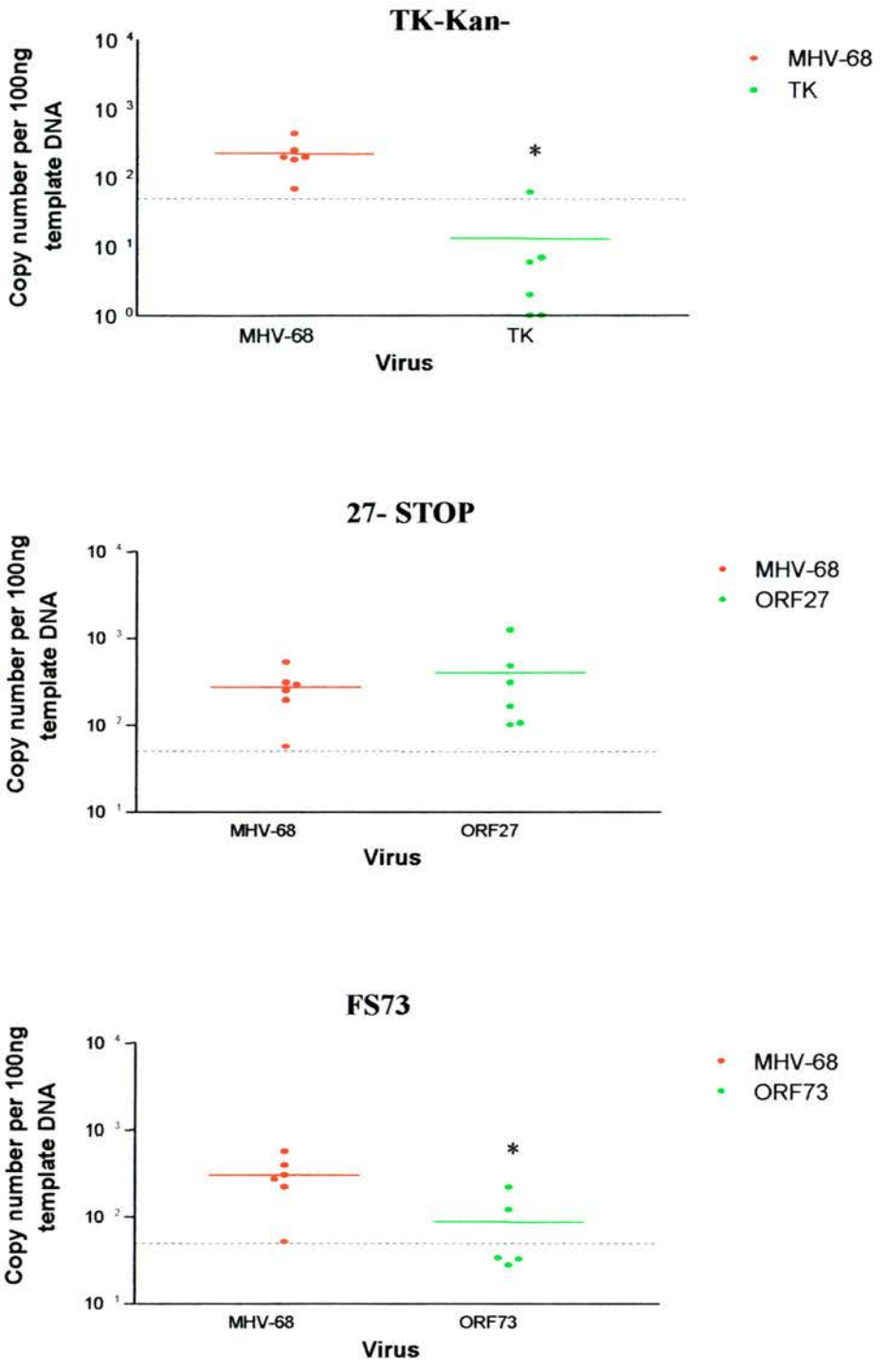

Figure 3.8 – Viral load in the lungs at 2.5 months post-intranasal infection with 1 x 10^4 PFU of the stated mutant virus. As before, viral load was quantified using the M4 real time PCR assay to quantify viral copy number in 100 ng template DNA. Samples were normalised to the amount of β actin in the sample. The dashed line denotes the limit of detection of the assay. Mutant virus samples marked * have viral load significantly different to mice infected with wild-type virus (as determined using the non-parametric Mann-Whitney test).

but debate continues as to whether this is a true latent infection or if low level persistence is occurring (reviewed by Reddehause *et al.*, 2002). Previous studies on long-term MHV-68 infection in the lung cannot discount the possibility of a chronic infection occurring alongside latency.

In our study we assessed the contribution of both lytic and latent genes in maintaining a long-term infection of the lung to determine the likelihood of chronic versus latent infection.

M2 is a latently expressed gene that functions in a tissue-specific manner – it is required for establishment of normal levels of latency in the spleen but not in the peritoneal exudate cells (Jacoby *et al.*, 2002). Similar to the PECs, the absence of the M2 gene did not result in any alteration in viral load in the lung. M2 is required for colonisation of splenic follicles and exiting of infected germinal centre B cells into the memory B cell compartment (Simas *et al.*, 2004), and this process may not be necessary for maintenance of viral load in the lung.

In the absence of the M3 gene no effect is seen on viral load at late time points in the lung. No previous role has been identified for M3 during latency, either *in vitro* (Husain *et al.*, 1999; Martinez-Guzman *et al.*, 2003) or *in vivo* (van Berkel *et al.* 2002). A single *in vitro* study has shown the presence of an RTA-responsive element in the M3 promoter region which could link M3 transcription to the latent-lytic switch (Martinez-Guzman *et al.*, 2003) but no obvious role in reactivation has been shown *in vivo*. Vaccination with an M3-containing construct protects during lytic infection in the lung but has no effect on latent infection, suggesting M3 is expressed only during the lytic cycle or in a very limited number of latently infected cells (Obar *et al.*, 2004). There may still be a role for genes involved solely in lytic replication in maintenance of viral persistence - preformed infectious virus can still be detected at late time points post-infection (Flano *et al.*, 2003), suggesting the possibility of ongoing chronic lytic replication or reactivation from latency. However at this point there is no clear role for M3 either in latency or in maintenance of a chronic lytic infection.

Despite a clear role for M4 in establishment of latency in the spleen again there is no obvious role in maintenance of infection in the lung. While levels of long-term splenic latency are independent of M4, differences in viral load are still apparent at 1 month post-infection (Townsley *et al.*, 2004). This difference was not replicated in the lungs, with viral load unaffected by the loss of M4 at 1-, 3- and 6-months post-infection.
M4 has been shown to act in a tissue-specific manner, with no requirement for the gene in establishment of latency in the PECs (Evans *et al.*, 2006). Similarly there appears to be no role in establishment or maintenance of latency in the lung. This may be due to the tissue-specific requirements mentioned above, or alternatively viral persistence in the lung may not depend on latent infection to the same extent as in the spleen. Interestingly minor effects have been noticed during acute infection of the lung. Infection with MHV76inM4 (MHV-76 with the complete M4 gene inserted into the left-hand end) causes higher viral titres on days 1-3 compared to both MHV-76 and MHV-68 (Townsley *et al.*). Higher viral lung titres are reported on d9 following infection with an M4.stop mutant (Evans *et al.*) but this result has not been replicated following infection with a very similar M4.stop mutant (Geere *et al.*, 2006). If any small differences do exist these do not appear to have any impact on long-term viral load in the lungs.

Complement is known to play a role in regulation of several aspects of B cell biology (Ochsenbein *et al.*, 1999; Carroll & Fischer, 1997). As lung B cells are one of the suggested sites of MHV-68 persistence the interaction between complement and B cells may impact viral persistence. A previous role for the MHV-68 RCA (Regulator of Complement Activation) gene during viral persistence has been demonstrated in the spleens of IFN$\gamma R^{-/-}$ mice. However in wild-type mice the lack of a role for RCA during latency in the spleen is mirrored by the absence of an obvious role for the gene during persistence in the lung. Complement (but not the RCA gene) has been shown to affect viral latency in both the spleen and PECs, and while our studies have not investigated the effect of complement deficiency on persistence in the lung we conclude that there is no obvious role for RCA in maintenance of viral load at this site.

Many viruses use avoidance of MHC class I antigen presentation as a mechanism to subvert the immune response. Herpesviruses, poxviruses and retroviruses all encode proteins capable of targeting MHC class I molecules for degradation (reviewed by Furman and Ploegh, 2002), acting at different points in the MHC biosynthesis and antigen presentation pathway to prevent viral antigen presentation at the cell surface. While the mechanism of KSHV genes K3 and K5 action have been studied in detail *in vitro* (Lorenzo *et al.*, 2002; Hewitt *et al.*, 2002; reviewed by Fruh *et al.*, 2002) little is known about its role *in vivo*. The presence of a close homologue in the MHV-68 genome, K3, allows study of the role of K3 *in vivo*, and we have focussed on the role of K3 in maintenance of viral load in the lungs.

While infection with a K3-deficient virus results in a lack of expansion of latently infected cells in germinal centres and ultimately a reduction in viral load in the spleen the same effect is not observed in the lung. At no time point studied was the viral load statistically significantly different between mice infected with wild-type or K3-deficient viruses.

Interestingly Stevenson *et al.* (2002) report a slight elevation of viral lung titres in K3-infected mice at days 8-10 post-infection, although the virus is subsequently cleared with normal kinetics by d15. While not statistically significant, at 1 month post-infection viral load in mice infected with the K3 virus is elevated compared to wild-type. This brings into question the validity of results where such a small sample group is used, and the only way to confirm if the mild enhancement during acute lung infection has any impact on long-term load would be to repeat the experiment using a much larger sample group.

In the case of the M11 gene, high levels of transcription in the lung but not the spleen at 10 months post-infection would indicate an important role for this gene during persistence in the lung (Roy *et al.*, 2000). At 1 and 3 months post-infection there is no obvious difference in viral load in mice infected with wild-type or M11-deficient virus. However at 6 months there is an indication that viral load is reduced in the M11-infected mice compared to the wild-type-infected mice, although owing to the small sample group this is not statistically significant.

Previous studies have shown that the M11-deficient virus is able to establish latency in the spleen and PECs at normal levels (as measured by viral load). The phenotype observed for the M11.stop virus is a reactivation deficit in PECs (Gangappa *et al.*,

2002). Therefore it is possible that while the M11 virus can establish latency at normal levels, reactivation in the lungs may be impaired in the absence of the gene. If the deficit observed at 6 months can be reproduced in a larger sample group this would indicate reactivation is important for maintenance of viral load at late time points.

An alternative role has been demonstrated for the M11 gene in maintenance of persistent (not latent) infection of IFNγR$^{-/-}$ mice. These mice characteristically show persistent replication, with large vessel vasculitis and premature death (Weck *et al.* 1997; Dal Canto *et al.*, 2000). The M11.stop virus is attenuated in these mice, with decreased incidence of arteritic lesions and a threefold greater survival rate (Gangappa *et al.*, 2002). This study involved i.p. infection so effects in the lung were not investigated. However if persistent replication is important for maintenance of viral load, intranasal infection of IFNγR$^{-/-}$ mice with the M11.stop virus may show differences compared to infection with wild-type virus. This would be an interesting study to undertake but time constraints did not permit it.

The viral cyclin gene has been shown to play a key role in reactivation from latency (Van Dyk *et al.*, 2000; Van Dyk *et al.* 2003). At 6 months post-infection mice infected with a v-cyclin-deficient virus show normal viral load in both splenocytes and PECs but show impairment in viral reactivation (Van Dyk *et al.*, 2003). At all time points studied viral load in the lungs was not statistically significant different in mice infected with v-cyclin or wild-type virus. However at both 3 and 6 months post-infection there appears to be a trend towards a reduction in viral load in the v-cyclin infected mice. Owing to the small sample sizes it is impossible to tell if this apparent reduction in viral load is a true difference or merely a result of the sample size.

Several possibilities arise as a result of the lack of clarity in the results. If the difference observed at 6 months post-infection is a true reduction in viral load through loss of v-cyclin this would suggest reactivation from latency is important in maintenance of viral load at late time points. Alternatively if the difference at 6 months is merely a result of sample variation and viral load in the v-cyclin-infected mice is in fact the same as in wild-type-infected mice this would indicate reactivation is not important for maintenance in the lung.

Viral reactivation is involved in maintenance of viral load in MuMT mice. Mice infected with the v-cyclin-deficient virus establish latency at similar levels to wild-type infected mice but by 6 months post-infection viral load in the spleen is relatively lower (Van Dyk *et al.*, 2003). Reactivation and reseeding in these mice is key to maintenance of viral load in the spleen, and may also be much more important in the lungs of immunocompetent mice than previously thought.

The results for the M11 and v-cyclin viruses together suggest a possible requirement for reactivation in maintenance of viral load in the lung at late time points. However these experiments will have to be repeated with greater numbers of mice to test this hypothesis.

MHV-76 replicates to lower levels, is cleared more rapidly and shows an earlier and larger immune response in the lungs compared than that seen following infection with MHV-68. 5 months post-infection viral DNA can only be detected in the lungs of 1/4 mice, compared to 4/4 in the spleen (Macrae *et al.*, 2001). This failure to detect viral DNA in the lungs suggested a potential defect in long-term persistence. However at 1- and 3-months post-infection there is no obvious difference in viral load as measured by real-time PCR. The assay used by Macrae was sensitive to 1-10 copies of the viral genome in 1 µg DNA, which is considerably more sensitive than the 500 copies per 100 ng used in the RTA real-time assay.

Given the lack of a significant change in viral load between 3- and 6-months post-infection in mice infected with the individual M1-M4 mutants it seems unlikely that a significant difference in viral load would be detected at 6 months post-infection for mice infected with MHV-76. Unfortunately this was not tested owing to sensitivity problems with the RTA assay below 500 copies/100ng template DNA. The absence of the M4 gene meant the more sensitive M4 assay could not be used, and the cost of developing a real time assay for gene outside the deleted region is too large for use at one time point in one set of samples.

Previous studies involving M1 have involved disruption of M1 with a LacZ cassette, a method that may result in distorted phenotypes (Jacoby *et al.*, 2002). The phenotype reported for the M1.LacZ virus was a deficiency in reactivation, a phenotype common in viruses carrying the LacZ cassette. Our more recent studies indicate loss of M1

results in a disruption in the acute phase of latency, characterised by the absence of splenomegaly and a reduction in the number of latently infected cells in the spleen at d14. In the lung our data indicates M1 controls acute infection in the lung, and following deletion of the gene higher viral titres and delayed clearance from the lung are observed. However despite differences during acute infection of the lung and acute phase latency in the spleen, there is no alteration in long term persistence at 1- or 6-months post-infection.

Of the genes previously shown to be important for latency in the spleen, none showed the same requirement in the lung. This suggests a different gene expression programme is required for maintenance of latency in the lung, or that latency is not a key feature of viral persistence.

To determine if lytic replication in the lung has any effect on long-term viral load the TK$^-$ and ORF27-deficient viruses were used to inoculate mice. At the same time the ORF73-deficient virus also became available.

At the single time point tested the TK$^-$ virus showed a significantly reduced viral load compared to wild-type virus. This was a very surprising result as previous studies in the lung have focussed on the role of latency during long-term infection, and the TK$^-$ deficient virus is able to establish latency in the spleen at normal levels by 1 month post-infection (Coleman *et al.*, 2003). Two possible conclusions can be drawn from these results: either a certain level of lytic replication is required to establish normal latent levels of virus, or lytic replication is largely responsible for maintaining viral load in the lungs and latency is a relatively insignificant part of this process.

In the case of herpes simplex virus TK$^-$ viruses have been used to demonstrate that impaired lytic infection results in a reduction in the number of neurons carrying the latent viral genome and also in a fewer copies of the latent genome per infected cell (Slobedman *et al.*, 1994; Thompson & Sawtell, 2000). However these experiments did not measure if latent load increased to wild-type levels at later time points, as is the case for TK$^-$ MHV-68 levels in the spleen.

Vaccination with MHV-68 lytic cycle proteins produces a similar effect to infection with a TK$^-$ virus. The initial lytic infection in the lung is substantially reduced following vaccination, and establishment of latent infection in the spleen is similarly impaired, although by 1 month post-infection levels in the spleen are comparable to

non-vaccinated mice. Vaccination with a latent epitope (M2) caused no deficit during initial lytic replication in the lung, and while initial levels of latency in the spleen were reduced long-term latency was established at normal levels (Woodland *et al.*, 2001). Use of lytic epitope vaccination could be used to further test our hypothesis that normal lytic replication in the lung is necessary for establishment of normal long-term viral load.

The ORF27-deficient virus is deficient in intercellular viral spread (May *et al.*, 2005a; 2005b). Following intranasal infection the virus shows reduced lytic replication in the lung, although not to the same extent as the TK$^-$ virus. In contrast to the TK$^-$ virus this initial deficit does not affect long-term viral load. This suggests two possibilities: there is a threshold level of initial lytic replication required for normal establishment of latency, with the TK$^-$ virus falling below this level and the ORF27 virus above it; or the different mechanisms in which the two viruses are deficient affect establishment of latency differently. The ORF27 virus shows no growth deficit *in vitro* following high M.O.I. infection, while low M.O.I. resulted in impaired growth in BHK-21 cells. If single-cycle replication can result in establishment of latency there would be no expectation of a deficit in establishment of latency by the ORF27 virus. Either of the above possibilities may explain the lack of a role for ORF27 in long term persistence in the lung.

The KSHV ORF73 homologue (LANA) has been shown to have multiple functions (reviewed by Viejo-Borbolla & Schulz, 2003), including segregation of episomes to progeny cells during cell division, repression of RTA promoter activity and control of cell cycle progression. The ORF73 of HVS is similarly involved in targeting and inactivation of cell cycle control proteins (Borah *et al.*, 2004). In the case of MHV-68 the ORF73 gene sequence analysis would suggest functional similarities to the KSHV protein this awaits confirmation. However the MHV-68 gene has been shown essential for establishment of latency in the spleen following intranasal inoculation (Fowler *et al.*, 2003).

Use of the ORF73-deficient virus helps determine if latency is a requirement for viral persistence in the lung. Mice infected with the ORF73 virus had reduced viral load 2.5 months post-infection compared to infection with wild-type virus, indicating a requirement for latency during long-term infection. This would suggest that in the

case of the TK⁻ infected mice a certain level of lytic replication is required in order to seed a sufficient number of latently infected cells, although it does not entirely eliminate the possibility of ongoing chronic lytic replication assisting in maintenance of viral load.

In order to confirm that latency in the spleen had been established at normal levels by the TK⁻ and ORF27 viruses and failed in the case of the ORF73 virus, real-time PCR was used to quantify viral load in the spleens. However all spleens including those infected with wild-type virus fell below the 50 copy limit of detection. Given that 100ng of template DNA corresponds to DNA from approximately 347,222 cells (data from Jackson Laboratories, www.informatics.jax.org), and the number of infected cells is approximately 1/1,000,000; it is not surprising that detection of viral DNA is problematic. Early attempts to use nested PCR to enhance the sensitivity of quantification were unsuccessful as this process introduced a large degree of variation into the replicates, indicating the nested reaction did not occur uniformly in all samples and therefore potentially distorting results (data not shown). A better option would have been to use a reactivation assay, or to develop an assay where more than 100ng template DNA can be used.

While indicating a significant role for latency in maintenance of viral load, we have not eliminated the possibility that ongoing lytic replication is a factor. As mentioned previously, Stewart *et al.* (1998) investigated the effect of inhibiting viral replication by treatment with 4'-S-EtdU, but did not measure the impact of treatment on viral load. A reduction in viral load following anti-viral treatment would indicate viral replication (whether from reactivation or chronic lytic infection) is an important factor in long-term persistence in the lung. An ongoing lytic infection would also help to explain the importance of the TK gene in maintenance of viral load. This would be an interesting experiment, but time constraints did not permit it to be carried out.

Mice deficient in the type I interferon response show 100- to 1000-fold higher viral titres during acute infection of the lung. Our previous work has shown that a lytic replication deficiency results in a reduction in the viral load in the lung at late time points post-infection. An obvious hypothesis might therefore be that enhanced lytic replication may lead to establishment of latency at higher levels and hence increase

viral load at late time points. This was not the case however for the M1 virus, and similarly in IFN-α/β $R^{-/-}$ mice this does not appear to happen. The initially high lytic titres do not result in a higher viral load at 6 months post-infection. This is mirrored by the situation in the spleen, where IFN-α/β $R^{-/-}$ mice eventually establish latency at normal levels despite the presence of virus considerably earlier and at 10-fold higher levels compared to wild-type mice.

Depletion of interferon in wild-type mice following resolution of acute infection results in increased reactivation in the PECs, showing that interferon continues to play a role after acute infection. Barton *et al.* (2005) have shown that type I interferon is important in control of virus reactivation during the early phase of virus latency but is dispensable at later time points. If the same is true in the lung potential differences during early latency may not have been detected by measuring a single time point at 6 months post-infection.

Type II interferon is not involved in viral clearance from the lung during acute infection – mice deficient in the type II interferon response are able to clear the virus from the lungs. Our studies show IFNγ$R^{-/-}$ mice are able to maintain long-term infection of the lung at similar levels to wild-type mice, indicating that IFNγ does not have an obvious role during acute or long-term infection of the lung.

Interferon-γ has previously been implicated in control of reactivation in the PECs but not in the spleen. Reactivation has not been definitively shown to be important for maintenance of infection in the lung, but our initial experiments suggest that it appears likely to be involved. The lack of a role for interferon-γ in control of reactivation in the spleen suggests other host mechanisms must be in place to control this process, and these mechanisms may also be functioning in the lung.

Our results would suggest a model whereby an initial level of lytic replication during acute infection is required to seed latent infection at normal levels in the lung. Once latent infection is established, viral load can initially be maintained in the absence of any reactivation. However at later time points (from 3 months post-infection) reactivation from latency is necessary to reseed the lung tissue and maintain viral load.

In conclusion we have identified that initial levels of lytic infection may play an important role in establishing sufficient levels of latency to maintain viral load at late time points. Reactivation may play a role in maintenance of viral load but further studies are required to determine if this is the case. With the exception of ORF73, genes identified as necessary for establishment and maintenance of viral load in the spleen did not show the same effect in the lung. We still have not conclusively ruled out the presence of an ongoing chronic infection in the lung, but have demonstrated that establishment of latency is necessary for maintenance of normal viral load.

Chapter 4: Characterisation of the M1 Gene of MHV-68

4.1 Background to the Study

The left end of the MHV-68 genome has been an area of considerable interest for some time. This part of the genome contains four open reading frames (M1-M4) and 8 viral tRNA-like molecules which are unique to MHV-68. While these genes are dispensable for replication *in vitro*, several have been shown to play an important role in MHV-68 pathogenesis *in vivo*.

Of the four unique genes M1 is the least investigated. Initial sequence analysis identified this gene as a potential serpin homologue (Bowden *et al.*, 1997). Serpins (serine proteinase inhibitors) have multiple regulatory functions *in vivo* (reviewed by Potempa *et al.*, 1994) but are also found in the poxvirus family of viruses. Poxvirus serpins have been shown to inhibit apoptosis (Brooks *et al.*, 1995; Macen *et al.* 1996), a function which may allow infection of a wider range of cells (Moon *et al.*, 1999). Viral serpins are also involved in regulation of inflammation (Ray *et al.*, 1992).

Several previous attempts have been made to investigate the role of M1 using M1 deletion viruses. The V2 (Simas *et al.*, 1998) and LHΔgfp (Dutia *et al.*, 2004) viruses have deleted part or the entire M1 gene and replaced it with a reporter gene (LacZ or GFP) under CMV promoter control. These viruses both lack several of the tRNA-like molecules found at the left-hand end of the genome. The M1.LacZ virus generated by Clambey *et al.* (2000) has 480bp of the M1 gene and 131bp of upstream sequence replaced by an expression cassette containing LacZ under the CMV immediate-early promoter.

There are problems associated with disruption of MHV-68 genes with large expression cassettes, and Clambey *et al.* (2000) did note that an M1 deletion virus (M1Δ511) without an expression cassette had a slightly different phenotype to the M1.LacZ virus. Previous changes in phenotype attributed to the loss of M1 were later shown to be a result of the LacZ insertion rather than any change in M1.

4.2 Generation of M1Δ and M1ΔRev Viruses

4.2.1 Generation of the M1Δ Virus

Previous work in our lab produced a virus with a large deletion in the M1 region. This virus lacks 1170 bp of the M1 gene, corresponding to genome co-ordinates 2022-

3193. This removes the majority of the M1 ORF, which is located at genome co-ordinates 2023-3283. During the BAC mutagenesis procedure, 190 bp of sequence was also introduced into this region, consisting of M13 sequence and an FRT site.

4.2.2 Generation of the M1ΔRev Virus

To confirm that any change in phenotype observed following infection with the M1Δ virus was due to the targeted mutation and not a distal mutation in the MHV-68 genome, a marker rescue virus (M1ΔRev) was constructed in which the M1 ORF sequences were restored in M1Δ.

As the M1Δ virus was created by mutagenesis of the MHV-68 BAC (Adler *et al.*, 2000) the revertant was generated using the two-step replacement procedure previously described for BAC-derived viruses (Borst *et al.*, 1999; Messerle *et al.*, 1997; O'Connor *et al.*, 1989). The process is illustrated in figure 4.1.

The Hind E fragment of the MHV-68 genome cloned into pUC13 (Efstathiou *et al.*, 1990) was used as a template to repair the lesion in the M1 gene. This fragment incorporates the first 6.1 kb of the left-hand end of the genome including the complete M1 gene plus flanking sequences.

The shuttle plasmid pST76k_SrE contains a limited number of restriction endonuclease sites within the multiple cloning site. As none of the sites present were also found at the termini of the Hind E fragment it was necessary to add linker sequences to the ends of Hind E to allow cloning into one of the restriction sites.

Initially a sample of pUC13+Hind E was removed from a glycerol stock previously frozen at –80°C and spread on an agar plate containing ampicillin. Following overnight incubation at 37°C a single colony was isolated and grown overnight in LB containing ampicillin. Following enzymatic digestion with HindIII the sample was run on a 1% agarose gel and the 6.1kb fragment corresponding to Hind E was gel extracted using a Qiagen Qiaquick Gel Extraction Kit. Nucleotides were then added to the restriction termini of the Hind E fragment using T4 polymerase to create blunt ends. The blunt-ended Hind E DNA was then purified using phenol:chloroform to remove any contaminating T4 polymerase.

Figure 4.1 BAC Mutagenesis Procedure in *E. coli* DH10B cells (adapted from O'Connor et al, 1989)

1. Formation/selection of cointegrates

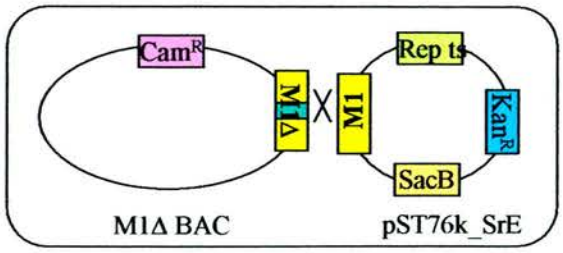

Transfection of the shuttle plasmid pST76k_SrE, (Materials & Methods section A.2.3) containing the corrected copy of M1 into *E. coli* containing the M1Δ BAC allows homologous recombination mediated by recA to occur.

The shuttle plasmid replicates most efficiently at 30°C so incubation of transfected cells is carried out at at this temperature. RecA is active at this temperature so recombination can occur.

Growth on kanamycin- and chloramphenicol-containing agar plates selects for cells containing both the M1Δ BAC and the shuttle plasmid.

After 24-28 hours plates are moved to 43°C- this prevents replication of the shuttle plasmid and only cells containing cointegrates will form colonies.

2. Resolution of cointegrates

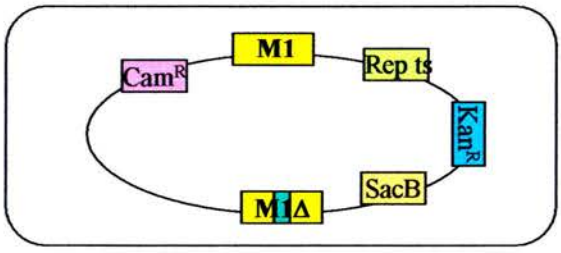

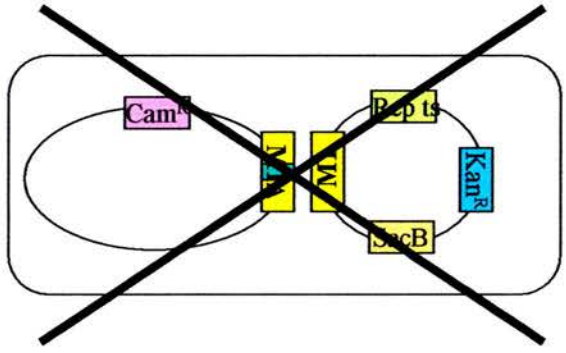

After incubation at 43°C individual colonies are streaked onto plates containing chloramphenicol and incubated at 30°C. RecA is active at this temperature, allowing resolution of cointegrates.

Resolved cointegrates are selected by incubation on plates containing chloramphenicol and 5% sucrose. Plates are incubated for 24-48 hours at 30°C.

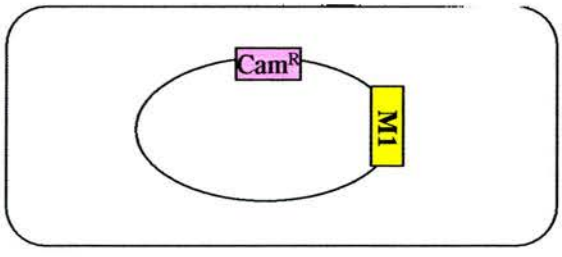

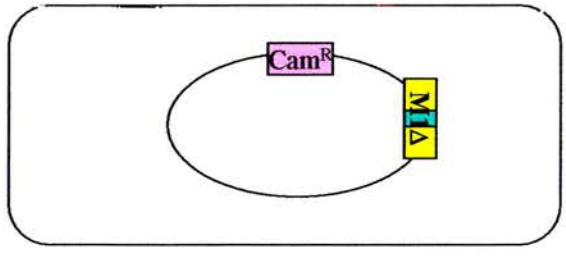

Confirmation of kanamycin sensitivity is achieved by plating colonies in parallel on

kanamycin and chloramphenicol plates.

This can be checked by restriction enzyme mapping or PCR analysis.

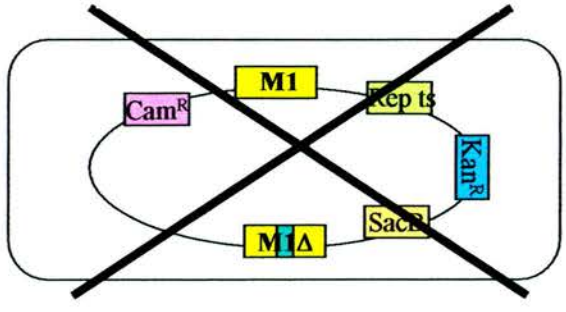

BamHI linkers (sequence given in Materials & Methods section A.1.2) were added to the blunt ends using T4 DNA ligase. The Hind E fragment was then digested using BamHI, and PCR-purified using the Qiagen QIAquick kit to remove any unattached linkers.

pST76k_SrE was also digested using BamHI and treated with calf intestinal phosphatase (CIP) to prevent self-annealing. The Hind E fragment and pST76k_SrE were then ligated overnight using T4 DNA ligase. This DNA was electroporated into electrocompetent DH10B cells. Bacteria were spread on agar plates containing kanamycin to select for the presence of recombinant plasmids and incubated overnight at 30°C.

This protocol was attempted numerous times but at no point were any recombinant plasmids formed. A similar strategy using Kpn linkers (Materials and Methods section A.1.2) in place of BamHI was attempted (with pST76k_SrE digested with Kpn1) with similarly poor results. A third strategy involving the blunt ending of the Hind E fragment (and no linkers added) followed by ligation into the Sma1 site of pST76k_SrE also did not work.

To test if addition of BamHI linkers to the Hind E fragment was occurring successfully it was decided to attempt cloning of the Hind E/BamHI fragment into another plasmid containing a BamHI site in the multiple cloning site. pBluescript SK- was digested with BamHI and incubated overnight at 17°C with the Hind E/BamHI fragment in the presence of T4 DNA ligase. Following electroporation into DH10B cells bacteria were spread on plates containing ampicillin and incubated overnight at 37°C. Many colonies were formed, and individual colonies were used to inoculate 5 ml LB containing ampicillin. After overnight incubation at 37°C plasmid DNA was extracted from cultures using a Qiagen Miniprep kit. DNA was digested using BamHI and run on a 1% gel. Figure 4.2 shows the presence of a 3 kb and a 6.1 kb band, corresponding to the 3 kb plasmid fragment and the 6.1 kb Hind E fragment.

Having determined that BamHI linkers could successfully be added to Hind E to allow cloning into pST76k_SrE, the ligation of Hind E to the shuttle plasmid was determined to be the flawed step in the protocol. Having initially attempted a 3:1 ratio of insert

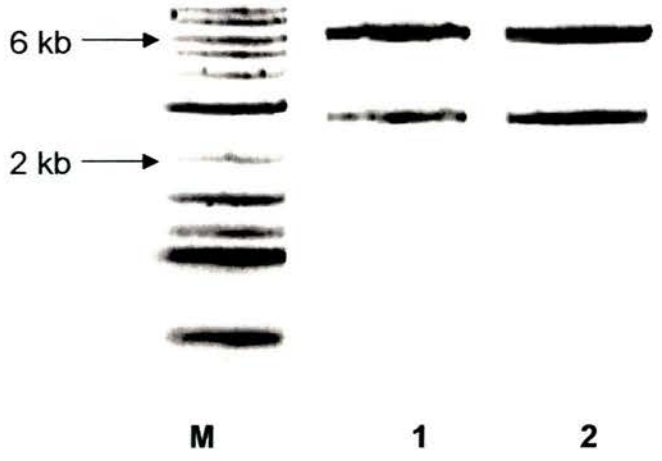

Figure 4.2 The HindE fragment of MHV-68 was successfully cloned into pBluescript. Following blunt-ending of the HindE fragment and subsequent addition of BamH1 linkers, HindE was cloned into the BamH1 site of pBluescript. Individual bacterial colonies were grown overnight in LB and plasmid DNA extracted. Following plasmid digestion with BamH1, fragments were run on a 1% gel and stained with ethidium bromide. The presence of a 3.1 kb band and (corresponding to the pBluescript plasmid) and 6.1 kb band (corresponding to the HindE fragment) indicated the successful cloning of HindE into pBluescript. Digests from two independent colonies are shown (marked 1 and 2). Band sizes were determined relative to a 2 log ladder (marked M) (NEB).

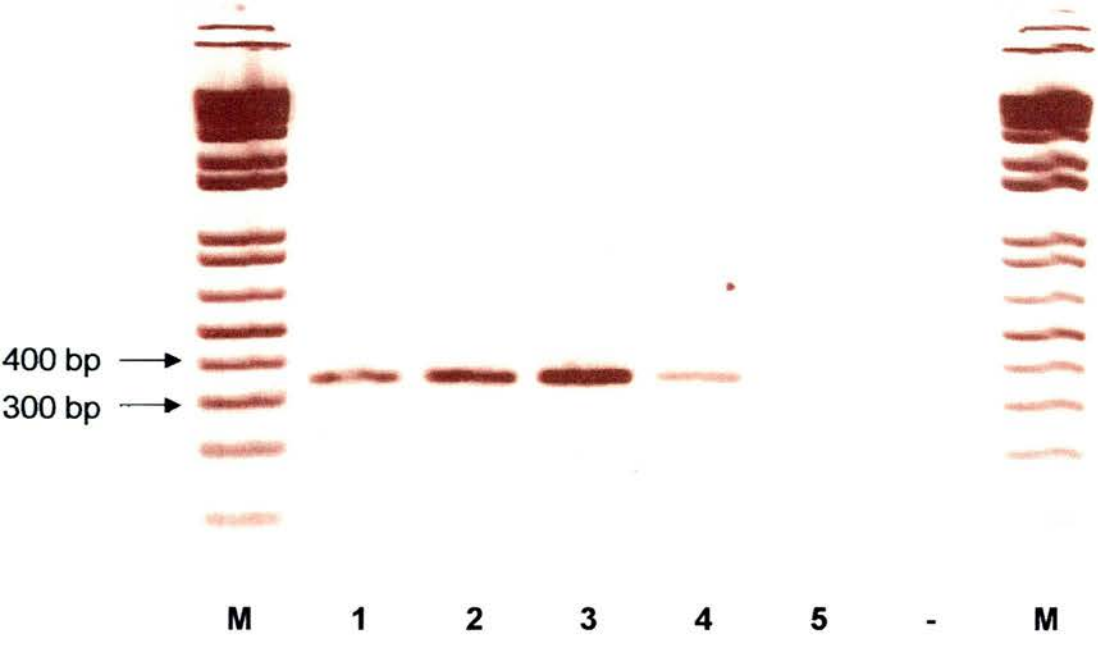

igure 4.3 HindE (including the M1 gene) was successfully cloned into pST76k_SrE. The presence of indE in pST76k_SrE was confirmed by by PCR using primers specific for the gene (bdgene4 and 115'race) which give a product of 340 bp. 5 separate colonies are shown above (numbered 1-5), as well s a negative control (-). Band sizes were determined relative to a 1 kb+ ladder (marked M) (NEB).

(Hind E) to vector (pST76k_SrE), different ratios were used, from 1:1 up to 6:1. After numerous attempts the original 3:1 ratio produced colonies containing recombinant pST76k_Sre with Hind E. PCR using primers specific to the M1 gene confirmed the presence of the M1 gene in the plasmid (shown in figure 4.3).

From this point onwards the protocol proceeded as demonstrated in figure 4.1. Briefly, the pST76k_SrE+Hind E was electroporated into DH10B cells containing the M1Δ BAC. DH10Bs containing both the BAC and the shuttle vector were selected by plating in the presence of kanamycin and chloramphenicol. After incubation at 30°C to allow formation of cointegrates, selected colonies were replated at 43°C where the shuttle cannot replicate and only cells containing a cointegrate will form colonies. Colonies growing at 43°C were replated at 30°C to allow resolution of cointegrates – the bacterial recA is active at this temperature. As the resulting colonies were likely to be a mixture of either resolved BACs or cointegrates, cointegrates were selected against by plating at 30°C in the presence of 5% sucrose. Confirmation of kanamycin sensitivity was achieved by plating colonies in parallel on kanamycin and chloramphenicol plates.

Individual colonies were selected and grown overnight in 5 ml LB containing chloramphenicol. Colonies known to contain PHA3 (wild-type BAC) and M1Mbac (the M1Δ BAC) were also grown to allow for comparison. BAC DNA was extracted using the Sigma BAC DNA kit and eluted into a final volume of 15 µl.

Infectious M1ΔRev virus was then reconstituted from BAC DNA. BAC vector sequences must be removed from the virus prior to use *in vivo* as failure to remove these sequences results in attenuation of the virus (Adler *et al.*, 2001). As the vector sequence is flanked by *lox*P sites, passaging the virus through Cre 3T3 cells expressing Cre recombinase results in excision of the BAC vector DNA. As the vector sequence contains gfp under control of the CMV IE promoter it is possible to differentiate between viral plaques which have excised the vector sequence (colourless) and those which have not (green)(Adler *et al.*, 2000). Following isolation of M1ΔRev virus lacking BAC vector DNA, viral stocks were grown and titrated.

Confirmation of the reintroduction of the complete M1 gene into the M1ΔRev genome was achieved using southern blotting.

To make the radioactive probe for the M1 gene HindE in pUC13 was digested with HindIII and the resulting fragments run on a 1 % agarose gel. The band corresponding to HindE (6.1 kb) was isolated and the DNA extracted using the Qiagen QIAquick gel extraction kit. This DNA was then radiolabelled with (α-32^P)dCTP according to the protocol given in Materials & Methods 2.2.10.4-5.

BHK-21 cells were infected with M1Δ, M1ΔRev or PHA4 (wild-type MHV-68) viruses according to the protocol given in 2.2.10.1. Viral DNA was extracted from the BHK-21s and digested with EcoRV. In the case of PHA4 and M1ΔRev digestion with this enzyme was predicted to produce fragments of 6216 bp and 2901 bp, while digestion of M1Δ was expected to produce bands of 4774, 2901, 444 and 20 bp (as shown in figure 4.4). After separation of the DNA fragments by electrophoresis the DNA was transferred to nylon membrane and probed with the radiolabelled HindE fragment.

Figure 4.4c shows the southern blot of EcoRV-digested M1Δ, M1ΔRev and PHA4 DNA. As predicted, both PHA4 and M1ΔRev show an identical restriction fragment pattern, with bands of the predicted size. M1Δ shows the predicted alteration, with a reduction in size of the 6216 bp band to 4774 bp, and a new band at 444 bp (the predicted band at 20 bp was not visible). The band at 2901 bp is still present in M1Δ.

4.3 *In Vitro* Characterisation of the M1Δ and M1ΔRev Viruses

4.3.1 M1Δ and M1ΔRev Replicate Equivalently to PHA4 *In Vitro*

Previous studies involving viruses with a deficiency in the M1 gene have not indicated any requirement for M1 during *in vitro* growth (Clambey et al, 2000; Simas et al, 1998; Dutia et al, 2004). Analysis of single and multiple rounds of replication in BHK-21 cells demonstrated that all viruses replicated equivalently, confirming M1 is dispensable for *in vitro* replication and does not affect cell-to-cell spread. One- and multi-step growth curves are shown in Figure 4.5.

Confirmation of the reintroduction of the complete M1 gene into the M1ΔRev genome was achieved using southern blotting.

To make the radioactive probe for the M1 gene Hind E in pUC13 was digested with HindIII and the resulting fragments run on a 1 % agarose gel. The band corresponding to Hind E (6.1 kb) was isolated and the DNA extracted using the Qiagen QIAquick gel extraction kit. This DNA was then radiolabelled with (α-32^P)dCTP according to the protocol given in Materials & Methods 2.2.10.4-5.

BHK-21 cells were infected with M1Δ, M1ΔRev or PHA4 (wild-type MHV-68) viruses according to the protocol given in 2.2.10.1. Viral DNA was extracted from the BHK-21s and digested with EcoRV. In the case of PHA4 and M1ΔRev digestion with this enzyme was predicted to produce fragments of 6216 bp and 2901 bp, while digestion of M1Δ was expected to produce bands of 4774, 2901, 444 and 20 bp (as shown in figure 4.4). After separation of the DNA fragments by electrophoresis the DNA was transferred to nylon membrane and probed with the radiolabelled Hind E fragment.

Figure 4.4c shows the Southern blot of EcoRV-digested M1Δ, M1ΔRev and PHA4 DNA. As predicted, both PHA4 and M1ΔRev show an identical restriction fragment pattern, with bands of the predicted size. M1Δ shows the predicted alteration, with a reduction in size of the 6216 bp band to 4774 bp, and a new band at 444 bp (the predicted band at 20 bp was not visible). The band at 2901 bp is still present in M1Δ.

4.3 *In Vitro* Characterisation of the M1Δ and M1ΔRev Viruses

4.3.1 M1Δ and M1ΔRev Replicate Equivalently to PHA4 *In Vitro*

Previous studies involving viruses with a deficiency in the M1 gene have not indicated any requirement for M1 during *in vitro* growth (Clambey *et al.*, 2000; Simas *et al.*, 1998; Dutia *et al.*, 2004). Analysis of single and multiple rounds of replication in BHK-21 cells demonstrated that all viruses replicated equivalently, confirming M1 is dispensable for *in vitro* replication and does not affect cell-to-cell spread. One- and multi-step growth curves are shown in Figure 4.5.

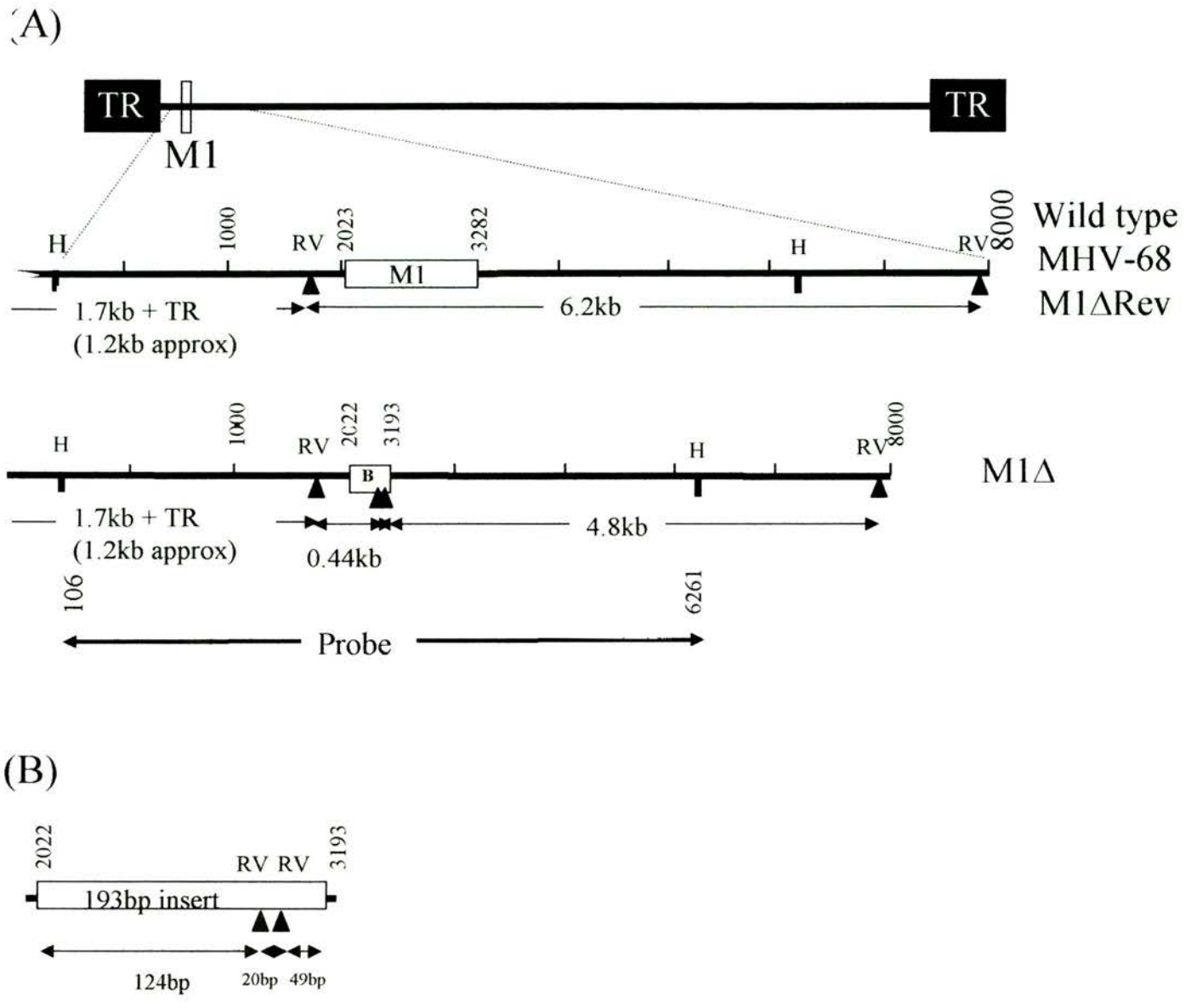

Figure 4.4a & b Construction and confirmation of the genome structure of M1Δ and M1ΔRev. (A) Structure of the region encoding M1. The diagram shows the site of the deletion in M1Δ, the restriction fragments generated by digestion with EcoRV (RV) and the position of the probe used for the Southern Blot analysis. (B) The M1Δ insertion. A 193 bp insert containing two EcoRV sites (RV) replaces genome co-ordinates 2022-3193.

(C)

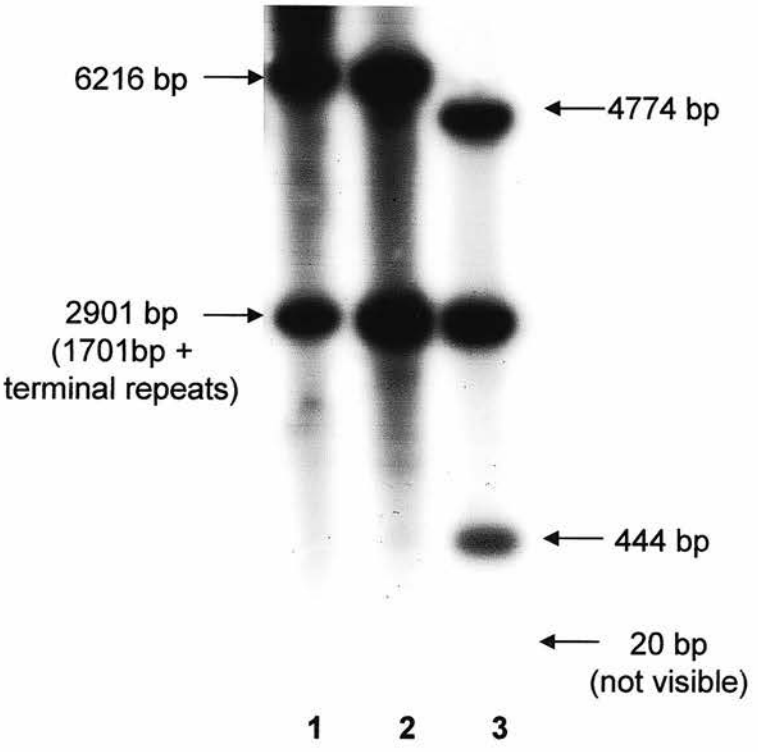

Figure 4.4c Southern Blotting shows the deletion of approximately 1 kb in the HindE region of the M1Δ virus and the subsequent restoration of this region in the M1ΔRev virus. Viral DNA was extracted from BHK-21 cells infected with M1Δ, M1ΔRev or PHA4. DNA was digested with EcoRV, and the fragments were separated by gel electrophoresis and subsequently transferred by southern blotting to a nylon membrane. Probing with (α-32^{P})dCTP-labelled HindE revealed identical band patterns for the M1ΔRev (lane 2) and PHA4 (lane 1) DNA, with two bands (2901 bp and 6216 bp) observed as predicted. The M1Δ virus (lane 3) retained the 2901 bp band, showed a reduction in size of the 6216 bp fragment to 4774 bp, and contained two further bands of 444 bp and 20 bp (not visible) as predicted by the deletion of 1171 bp and the introduction of 193 bp.

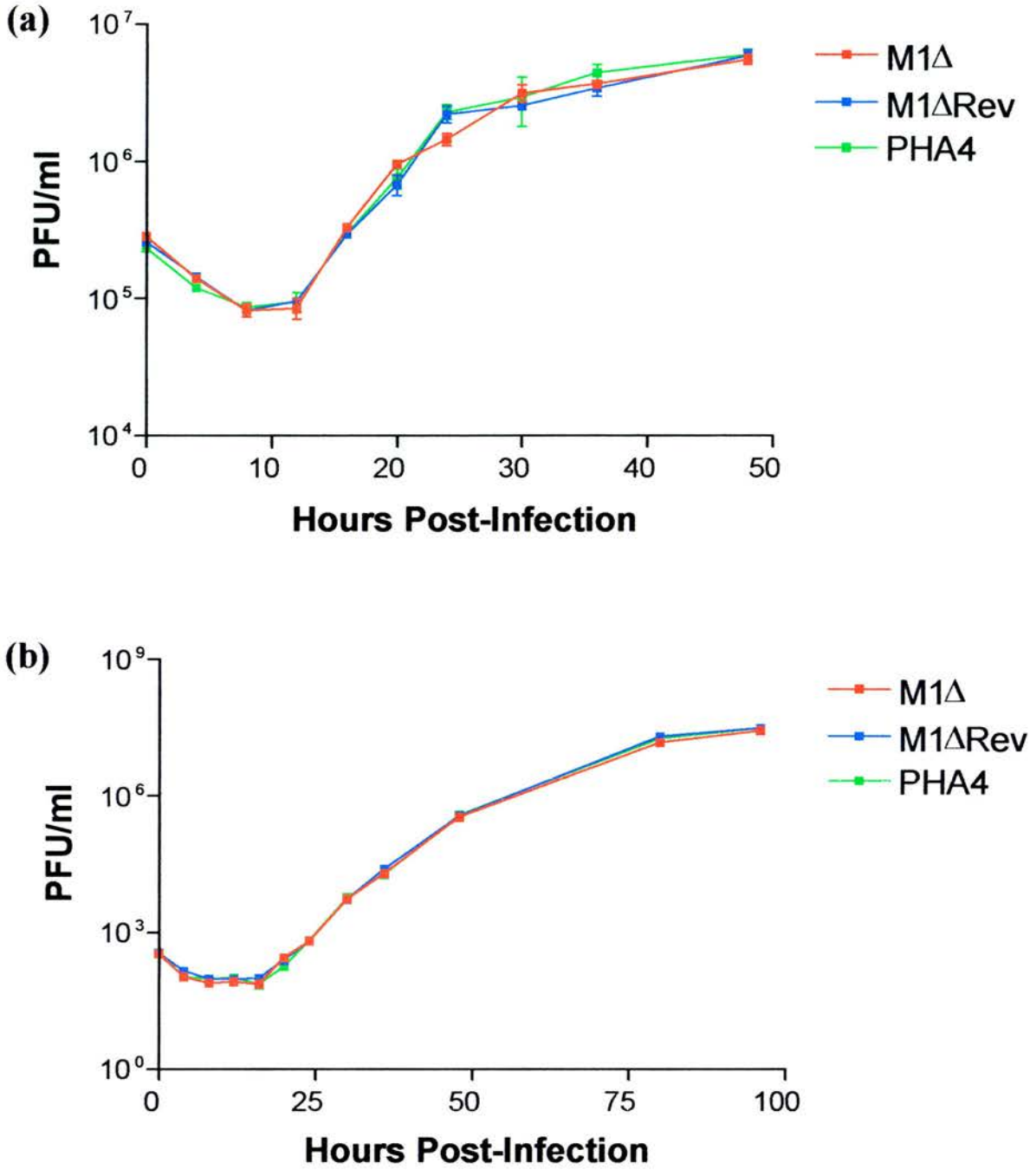

4.5 The M1Δ virus replicates with the same kinetics as wild-type and revertant viruses *in vitro*. BHK-21 cells were infected with 5 p.f.u. per cell (one-step, a) or 0.05 p.f.u. per cell (multi-step, b) and harvested at specific time points post-infection. Infected cells were lysed by freeze-thawing and virus titres were determined on BHK-21 cell monolayers. All infections and titrations were carried out in duplicate. The data represent the mean±SD.

4.4 *In Vivo* Characterisation of the M1Δ and M1ΔRev Viruses

4.4.1 Infection with M1Δ Results in Increased Lung Titres Following Intranasal Infection

Previous studies investigating the role of M1 have focussed primarily on the spleen. Following intranasal infection with MHV-76, a reduction is seen in viral titres compared to infection with MHV-68, and MHV-76 is cleared more rapidly from the lung (Macrae *et al.*, 2001). This phenotype has not been attributed to the individual action of genes M2, M3 or M4, or the viral tRNA-like molecules (Macrae *et al.*, 2003; Jacoby *et al.*, 2002; van Berkel *et al.*, 2002; Evans *et al.*, 2006; Geere *et al.*, 2006; A. Cliffe, 2005). This suggests a potential role for M1 in modulating infection in the lung. To test this hypothesis female BALB/c mice aged 5-6 weeks were infected intranasally with 4 x 10^5 PFU of M1Δ, M1ΔRev or PHA4. 4 mice were infected per virus per time point. At the appropriate time mice were sacrificed by CO_2 asphyxiation and the lungs and spleen removed.

Lung titres were determined using plaque assays according to the protocol given in Materials & Methods section 2.7.6.2. Time points assayed were 3, 5, 8 and 10 days post-infection. As shown in Figure 4.6, M1Δ infection results in significantly elevated lung titres at days 5 ($p<0.05$), 8 ($p<0.005$) and 10 ($p<0.01$) days post-infection compared to both M1ΔRev and PHA4, although not at day 3.

These findings suggest that M1 is important during productive infection with MHV-68. Previous data (figure 3.6) indicates that the initial elevation in lung titres does not affect long-term levels of viral persistence in the lung, and the role for M1 in the lung appears to be limited to the acute phase of infection.

4.4.2 M1 Plays a Role in Stimulation of Lymphoid Cell Proliferation

Clambey *et al.* (2000) identified a role for M1 in reactivation from latency in the PECs following intraperitoneal infection. No statistically significant difference was observed in the spleen, although the frequency of reactivation was slightly higher for M1.LacZ at late time points.

To determine if differences in reactivation were reproduced following infection with M1Δ and also if intranasal infection affected establishment, maintenance or reactivation from latency, BALB/c mice were infected intranasally with 4 x 10^5 PFU

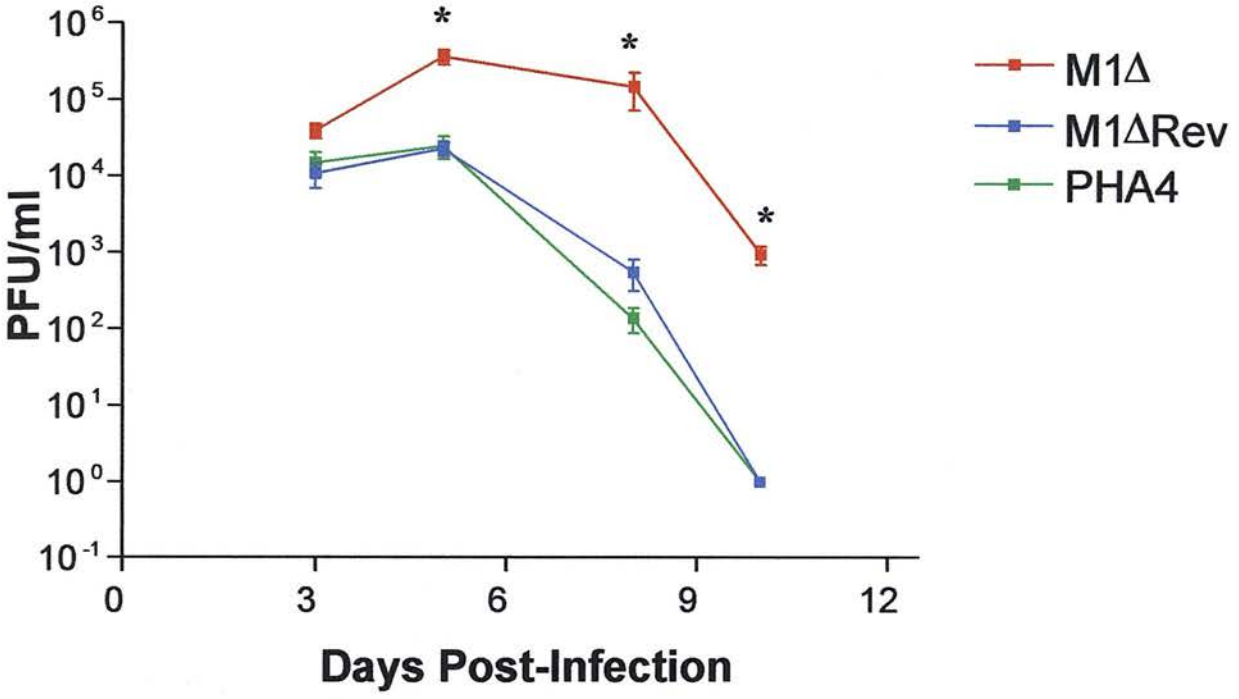

Figure 4.6 The M1Δ virus replicates to higher titres in the lung. BALB/c mice were infected intranasally with 4 x 10^5 PFU of either the M1Δ, M1ΔRev or PHA4. Lungs were harvested at various times post-infection and virus titres were determined on BHK-21 cell monlayers. The data shown represent the mean±SD for 4 mice. A significant difference was observed between M1Δ and both M1ΔRev and PHA4 at days 5, 8 and 10 post-infection ($P<0.05$, Students's *t*-test).

of either M1Δ, M1ΔRev or PHA4. Spleens were removed at specific time points post-infection and weighed.

Mice infected with M1ΔRev or PHA4 showed increasing spleen mass from day 5 to a peak at d15, with mass returning to an approximately normal level by d22 (shown in figure 4.7a). This rise and fall in spleen mass is mirrored by the number of splenocytes – again there is 6-7- fold rise in number from d5 to d15 followed by subsequent return to normal levels (figure 4.7b).

Changes in spleen mass failed to occur following infection with M1Δ, with proliferation of lymphocytes severely impaired and showing only a two-fold rise in numbers. This is similar to the deficit observed following infection with MHV-76, where splenocyte numbers fail to rise to the same levels as seen on infection with MHV-68 (Macrae *et al.*, 2001). This phenotype has not been observed in MHV-68 mutants lacking M2 (Macrae *et al.*, 2003), M3 (Van Berkel *et al.*, 2002), M4 (Geere *et al.*, 2006) or the tRNA-like molecules (A. Cliffe, 2005). This aspect of the MHV-76 phenotype is therefore likely to be solely due to the actions of the M1 gene.

Levels of latent virus in the spleen were to be measured by the ex-vivo reactivation assay (Materials & Methods section 2.7.6.3). However owing to an unfortunate infection in the BHK-21 cells the only time point at which the assay was performed was at d15. Figure 4.8 shows the results for this single time point. Despite the comparatively low splenocyte numbers there are a greater number of infective centres (i.e. cells reactivating latent virus) in M1Δ-infected spleens compared to M1ΔRev- or PHA4-infected spleens ($p<0.05$). This suggests either a higher number of infected cells in the spleens of M1Δ-infected mice, or an equivalent or reduced number of cells reactivating virus at an increased level. To determine what process was driving the increased levels of infective centres quantitative PCR was used to determine the viral load in the spleens of M1Δ- and control-infected mice.

4.4.3 Quantification of Viral Load in the Spleens of M1Δ-, M1ΔRev- and PHA4-infected Mice

Splenocytes previously stored at -80°C (excess remaining from the ex-vivo reactivation assay) were used to quantify levels of viral DNA in the spleen during the course of the experiment. At each time point 4 M1Δ samples and 2 each of M1ΔRev-

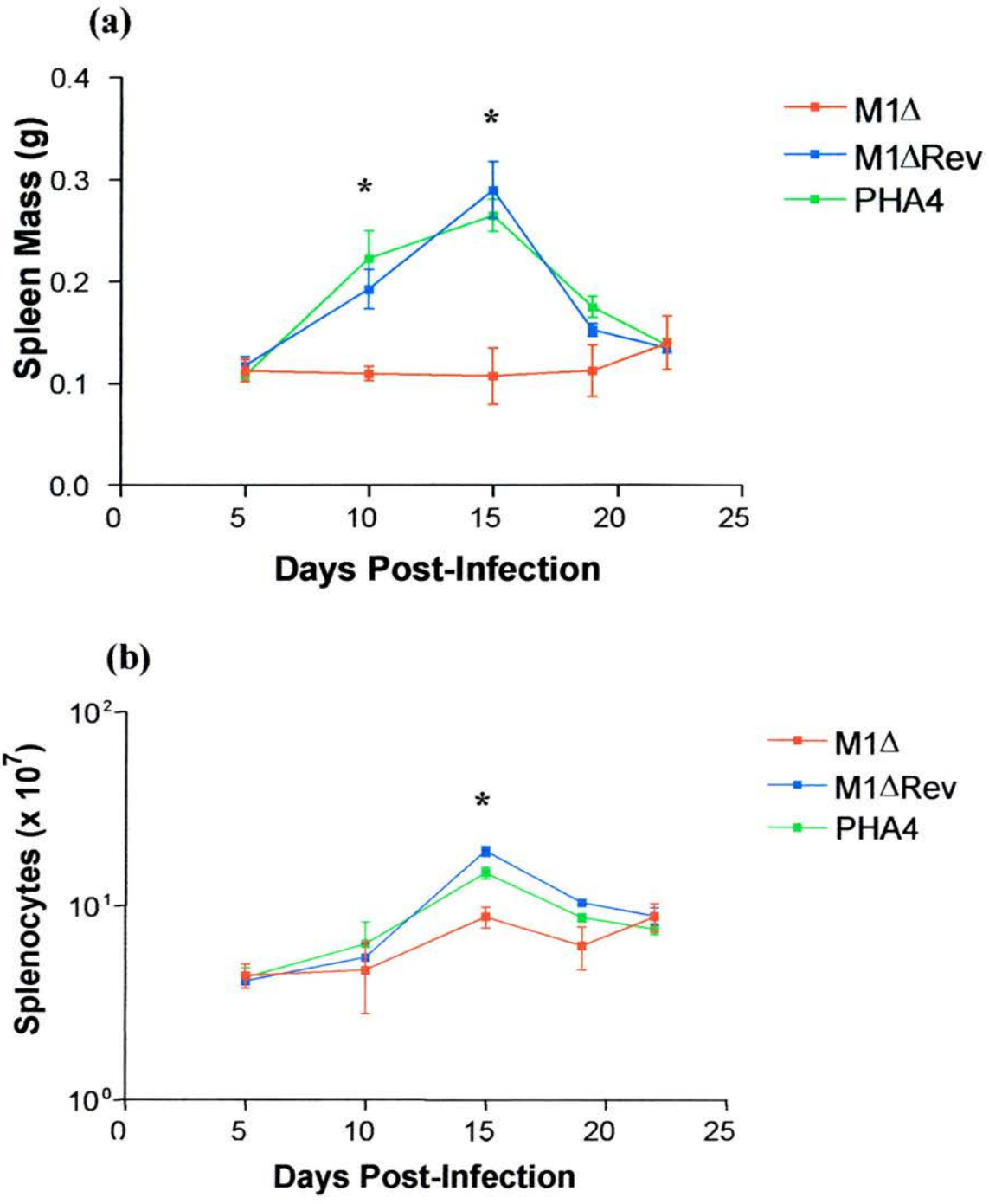

Figure 4.7 M1 is necessary for lymphocyte expansion and the corresponding increase in spleen mass. BALB/c mice were infected with 4 x 10^5 p.f.u M1Δ, M1ΔRev or PHA4. At various times post-infection spleens were removed and weighed (a) and the number of splenocytes counted (b). The data shown represent the mean±SD. A significant difference was seen between M1Δ and the control viruses (M1ΔRev and PHA4) in spleen mass at d10 ($p<0.01$) and d15 ($p<0.005$), with the M1Δ virus failing to show any increase in mass at these time points. This corresponds to a failure of the M1Δ virus to drive lymphocyte expansion, with a significant difference in splenocyte number between M1Δ and the control viruses observed at d15 ($p<0.05$) (Student's *t*-test).

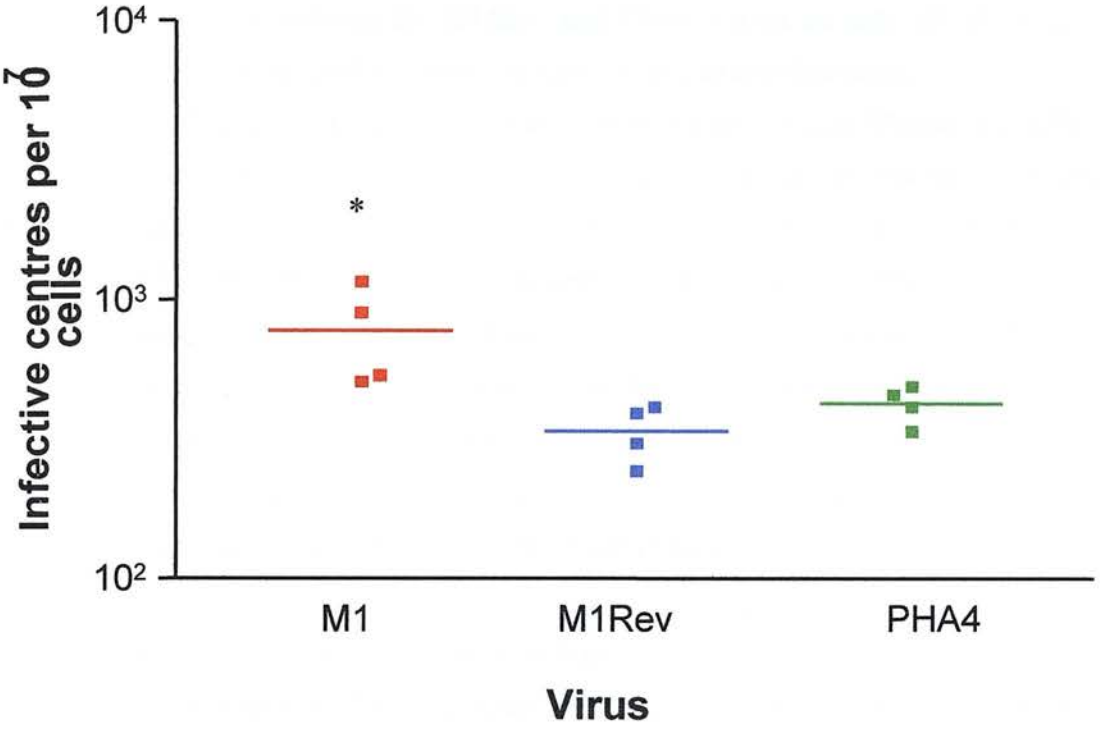

Figure 4.8 At d15 deletion of M1 results in increased reactivation from latency. BALB/c mice were infected intranasally with 4 x 105 p.f.u of either M1Δ or control (M1ΔRev or PHA4) viruses. Each data point represents 4 mice. Mice were sacrificed 15 days post-infection. The M1Δ virus shows a significant increase in the number of infective centres at d15 compared to control viruses ($p<0.01$, Student's *t*-test).

and PHA4-infected samples were studied. No differences have been observed *in vitro* or *in vivo* between the M1ΔRev and PHA4 viruses so only 4/8 of the available samples were used for quantification of viral load to reduce costs.

DNA was extracted from splenocytes using the Qiagen DNeasy kit. DNA was quantified and 100 ng template DNA was used in the M4 real-time PCR assay to quantify viral load. As before (see chapter 3) viral load was normalised to the levels of β-actin DNA in the samples to correct for any variation in quantity or quality of the template DNA. Figure 4.9 shows the results for this experiment. At d10 both M1Δ and control (M1ΔRev or PHA4) infected samples show similar viral loads. However at d15 mice infected with the M1Δ virus show an approximately 5-fold reduction in virus levels compared to controls. By d19 post-infection the viral load is again equivalent in the M1Δ- and control-infected samples.

Results from these experiments indicate that there appears to be a failure of the M1Δ virus to drive lymphocyte expansion, resulting in a lack of increase in spleen mass. Viral DNA load is significantly reduced on d14 compared to wild-type virus, which may or may not be as a result of the absence of lymphocyte expansion. Levels of reactivating virus are significantly higher following infection with M1Δ, indicating that control of reactivation is impaired. While the frequency of infected splenocytes is equivalent in M1Δ-, M1ΔRev- and PHA4-infected mice, the frequency of reactivation of virus in M1Δ-infected mice is approximately 5-fold higher. The real time PCR assay cannot determine whether a reduction in viral load is a result of fewer infected cells, or if the number of infected cells remains constant and the viral copy per cell is reduced. A reduction in viral copy number per cell would account for the similar frequencies of infected splenocytes observed in M1Δ-, M1ΔRev- and PHA4-infected mice despite the apparent differences in viral load.

In order to confirm the results observed above and to determine if enhanced reactivation of the M1Δ virus is observed at times other than d14, the experiment was repeated.

Female BALB/c mice were infected as before with either M1Δ or M1ΔRev viruses (PHA4 was omitted as the results were expected to match those of M1ΔRev). Mice were to be sacrificed at 10, 15 and 20 days post-infection and the spleens investigated

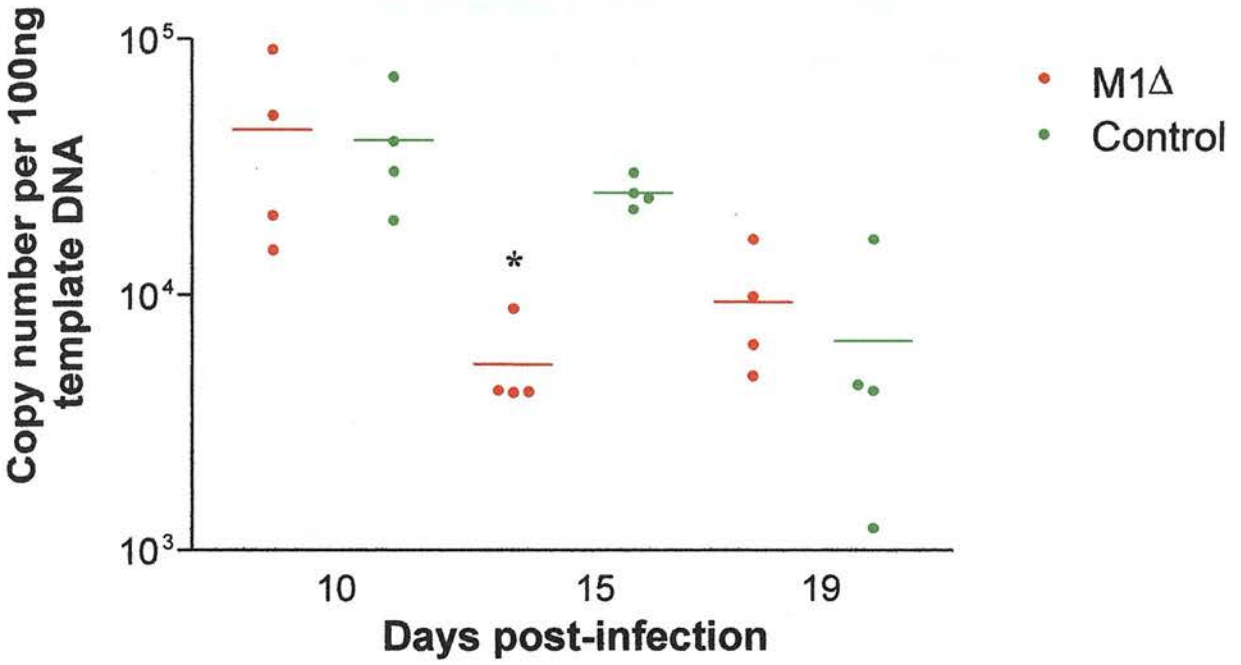

Figure 4.9 Deletion of M1 results in failure to establish normal viral load at d15. DNA was extracted from the spleens of the mice used in the previous experiment (figures 4.9-10) and viral load was quantified using real time PCR. At d15 viral load in mice infected with M1Δ was significantly reduced ($p<0.0001$, Student's *t*-test).

for levels of reactivating virus and for quantification of viral load. However for unclear reasons a number of mice succumbed to the virus several days after infection. While the mice were infected at the same age as in the previous experiment, there is a possibility the mice used in the repeat experiment were smaller, and this reduction in size in some way increased susceptibility to viral infection.

Figure 4.10 shows the survival curve for mice infected with either M1Δ or M1ΔRev. All mice infected with M1Δ survived, while 8/12 mice infected with M1ΔRev died between 9 and 13 days post-infection. This indicates the M1 virus is attenuated *in vivo* compared to the wild-type virus

Owing to the deaths of the M1ΔRev-infected mice the experiment continued with only 2 M1ΔRev-infected mice per time point, and only d10 and d15 investigated. However, the extremely small sample sizes coupled with the likelihood that a number of mice were presenting with clinical symptoms at the point of sacrifice made repetition of the previous experiments difficult. While a number of experiments were attempted (shown in figures 4.11-4.13) the results were likely to have been skewed by the inclusion of sick mice at the time points investigated. As such, the results obtained previously were not reproduced in this second experiment and it was not possible to validate our findings.

4.5 Discussion

These data show a distinct role for the M1 gene in the pathogenesis of MHV-68. Preliminary results indicate a role for M1 during acute infection of the lung, as well as confirming a previously identified role during virus reactivation in the spleen.

Our data show loss of M1 results in a significant increase in viral titres at early time points in the lung and delayed clearance. No previous studies involving M1-deficient viruses (Clambey *et al.*, 2000; Simas *et al.*, 1998; Dutia *et al.*, 2004) have investigated viral replication in the lung and this is the first indication of a role in this organ. Infection of mice with the deletion mutant MHV-76 which lacks M1 as well as M2, M3, M4 and 8 vtRNA-like molecules does not result in the elevated lung titres observed following infection with M1Δ (Macrae *et al.*, 2001). In fact MHV-76 infection results in a significant reduction in lung titres following intranasal infection,

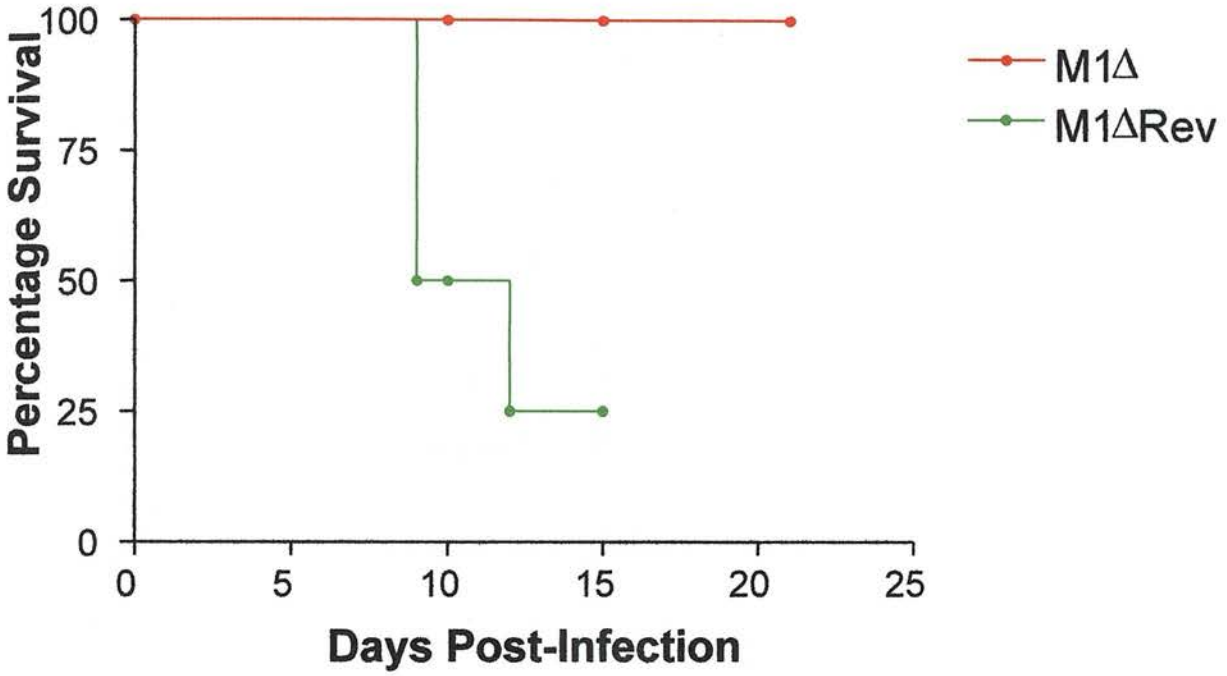

Figure 4.10 The M1Δ virus is attenuated *in vivo* compared to the wild-type revertant virus M1Δ Rev. BALB/c mice aged 5-6 weeks were infected intranasally with 4 x 105 p.f.u. of either M1Δ or M1ΔRev virus. The Kaplan-Meier analysis shows the deaths of 8/12 M1ΔRev-infected mice between 9 and 12 days post-infection. All M1Δ-infected mice survived, indicating attenuation of the virus.

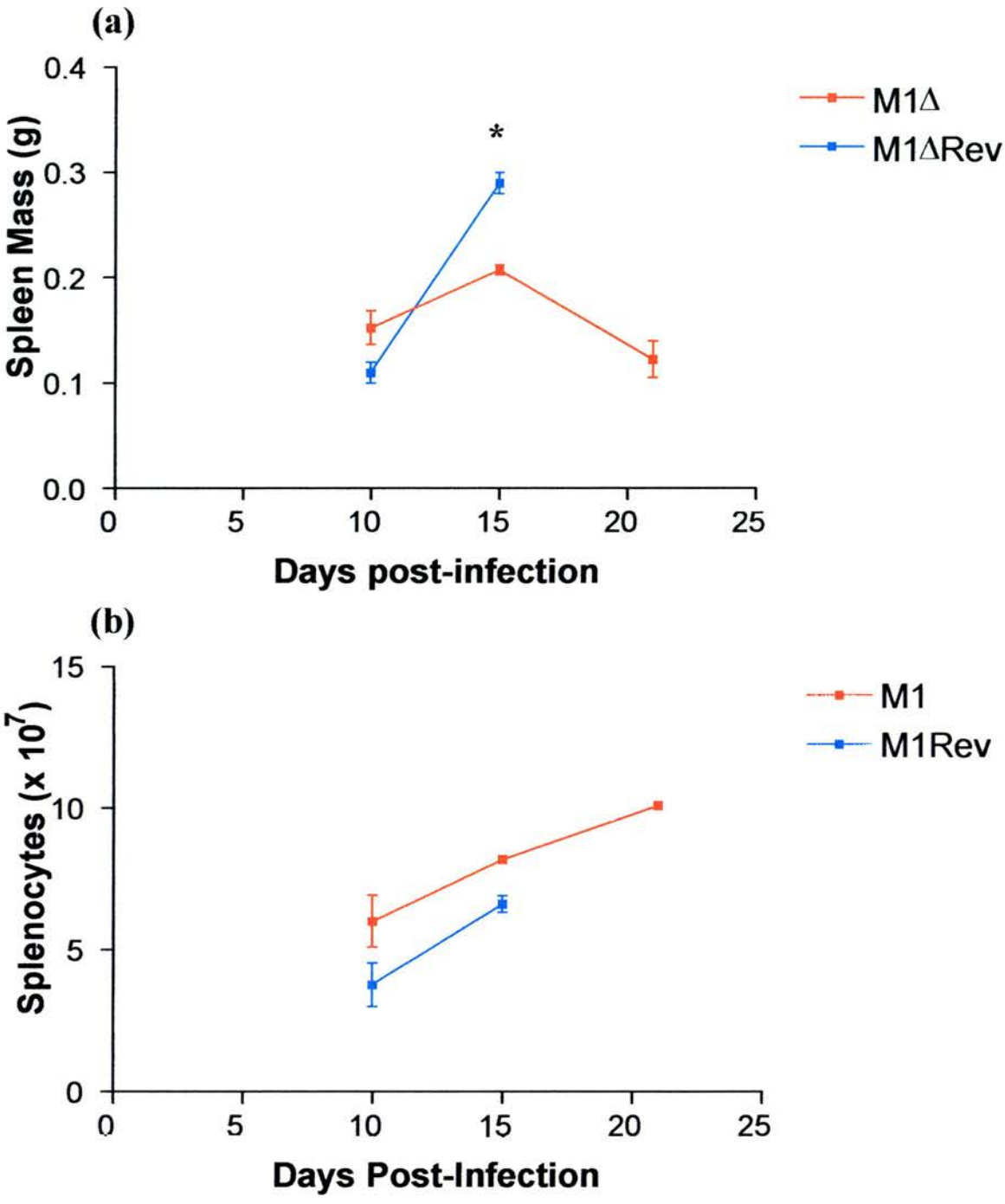

Figure 4.11 M1Δ fails to cause an increase in spleen mass at d15 but this does not correlate with a failure to cause lymphocyte expansion. As shown previously in figure 4.9a the control virus (M1ΔRev) shows a peak in spleen mass at d15, while the M1Δ virus fails to stimulate this peak (a). However the previous difference between viruses at d10 is not seen, possibly due to the ill-health of the M1Δ Rev mice at this point. Unlike the previous experiment the peak in spleen mass in the M1ΔRev virus is not accompanied by a peak in splenocyte numbers (b). Data points for the M1Δ virus correspond to 4 mice; data points for the M1ΔRev virus correspond to 2 mice. Data were analysed using the Student's *t*-test.

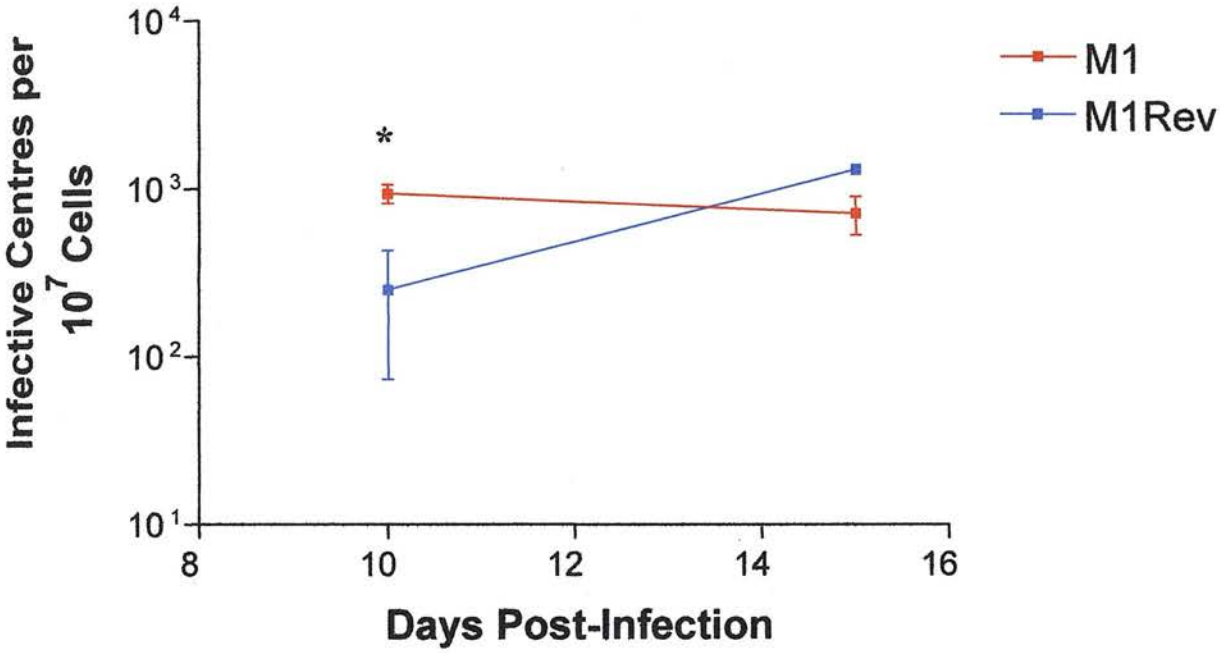

Figure 4.12 Deletion of M1 results in increased reactivation from latency. Spleens taken previously from BALB/c mice (see figure 4.14) were assayed for the level of reactivating virus. At d10 the M1Δ virus shows a significantly higher level of reactivating virus compared to the M1ΔRev virus ($p<0.05$, Student's *t*-test). By d15 levels of reactivation are equivalent for the two viruses.

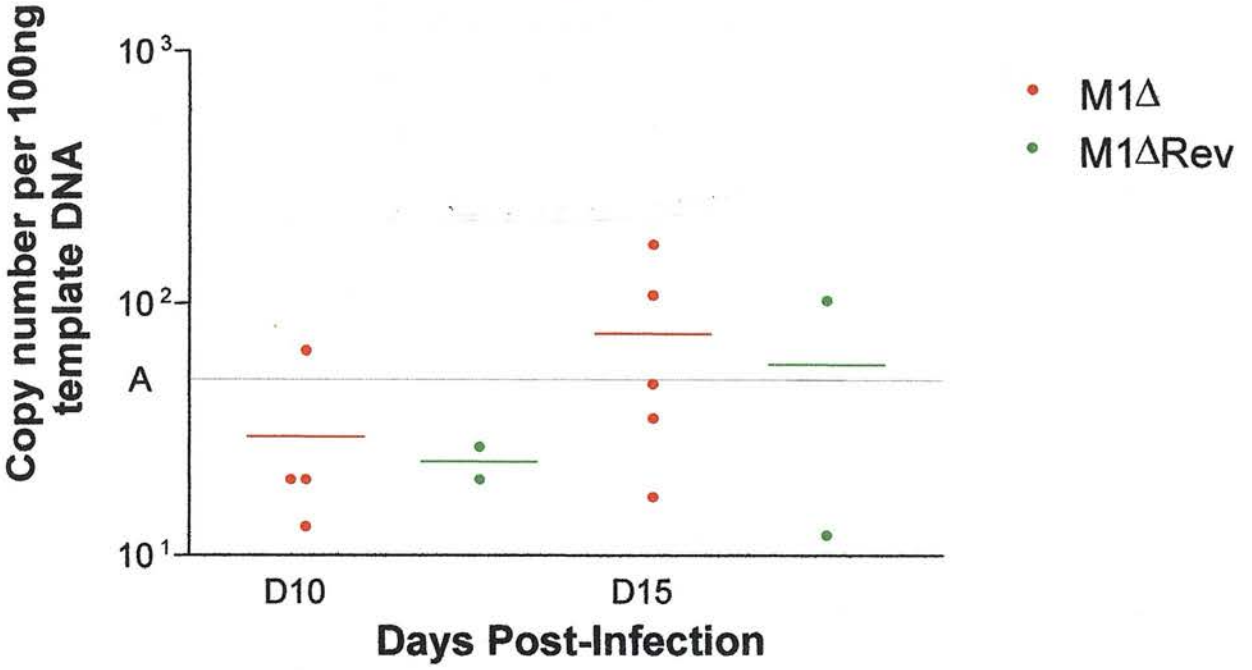

Figure 4.13 Spleen viral load is below the limit of detection following intranasal infection with either M1Δ or M1Δ Rev. Female BALB/c mice aged 5-6 weeks were infected intranasally with 4 x 105 p.f.u. of either M1Δ or M1ΔRev. Owing to the deaths of a number of M1ΔRev-infected mice, 4 mice per time point were used for M1Δ-infected mice and 2 mice per time point for M1ΔRev-infected mice. The majority of samples fall below the limit of detection of the assay (indicated by the line A) making accurate comparison of viral load between the two viruses difficult.

along with earlier clearance from the lung, a direct contrast to the M1Δ virus. This suggests another part of the left-hand end of the genome is also involved in maintaining normal viral titres in the lung. Mutation of any of the other unique genes or the tRNAs individually does not affect lung titres (Jacoby *et al.*, 2002; van Berkel *et al.*, 2002; Bridgeman *et al.*, 2001; Evans *et al.*, 2005; Geere *et al.*, 2006; A Cliffe, personal communication). This suggests a combination of genes and/or tRNAs in the unique region are responsible for normal viral titres in the lung, and the combined loss results in the reduction in lung titres in MHV-76 that are not observed in any single unique gene mutant

Previous studies have shown M1 plays a role in viral reactivation. Clambey *et al.* (2000) found 1/3 PECs reactivating virus following infection with M1.LacZ compared to 1/15 following infection with wild-type virus at 6 weeks post-infection. At this time point spleen cells demonstrated a small increase in frequency of reactivation compared to wild-type virus. Our initial experiment demonstrated a 5-fold increase in the frequency of spleen cells reactivating virus at d15. Whether this difference was maintained at other time points remains to be determined – it is possible by 6 weeks post-infection similar results to those obtained by Clambey *et al.* may be reproduced.

Data from the first experiment showed that a peak in spleen mass was linked to increased number of splenocytes in M1ΔRev- or PHA4-infected mice, a common characteristic of MHV-68 infection (Sunil-Chandra *et al.*, 1992a; Sunil-Chandra *et al.*, 1992b). Following infection with M1Δ, neither of these features were observed. Spleen mass and lymphocyte expansion following infection with M1-deficient viruses has previously been studied by Dutia *et al.* (2004) using the V2 virus that lacks M1 and vtRNAs 1 and 2 (Simas *et al.*, 1998). This study showed that following infection of wild-type 129 SV/EV mice with V2, spleen numbers at d13 are lower than in mice infected with wild-type virus. However, spleen cell numbers in V2-infected mice continue to rise from d13 until at least d29 (the last time point investigated). In this study splenomegaly appears delayed rather than abolished, and it is possible that in the BALB/c mice this phenomenon is repeated, albeit with a longer initial delay.

MHV-76 infection also fails to cause splenomegaly (Macrae *et al.*, 2001; Clambey *et al.*, 2002), a characteristic not attributed to any other of the unique genes. This suggests this aspect of the MHV-76 phenotype is due to the loss of M1 from the viral genome.

In the case of the second experiment a large number of M1ΔRev-infected mice died, leading to the conclusion that the M1Δ virus was relatively attenuated. This attenuation was also noted by Clambey following infection of C.B-17 SCID and IFNγR-deficient mice with the M1.LacZ virus. The most likely explanation for the deaths of the M1ΔRev-infected mice was a reduction in size compared to the previous experiment.

The repeat experiment produced a number of confusing results, a problem compounded by the small sample sizes in the M1ΔRev-infected group owing to the deaths.

At d10 spleen masses and splenocyte numbers were marginally lower in M1ΔRev-infected mice compared to M1Δ, most likely because the M1ΔRev-infected mice were terminally ill at this point. At this time point M1Δ was able to reactivate virus at higher levels. By d15 spleen masses of M1ΔRev-infected mice had increased to a level higher than that of M1Δ-infected mice, reproducing results from the previous experiment. However this was not linked to a significantly higher level of splenocytes in M1ΔRev-infected mice, which either suggests spleen mass is not directly related to splenocyte number, or that the splenocytes were miscounted. There is a possibility that spleen mass is influenced by factors independent of cell number, such as fluid content. However the second option appears more likely as it is not clear how spleen mass could increase in the absence of either an increased number or a massively increased size of cells, and an increased size of cells was not observed.

Reactivation at d15 is equivalent for both viruses, and it is not possible to tie this to any difference in viral load because almost all samples measured fell below the limit of detection of the real time assay.

This experiment was useful in that it confirmed Clambey's previous findings that M1-deficient viruses are attenuated *in vivo*, but owing to the extremely small sample sizes in the M1ΔRev-infected group few conclusions can be drawn from the remaining assays.

Previous sequence analysis indicated sequence homology of the M1 gene to the poxvirus serine proteinase inhibitor (serpin) SPI-1 gene (Virgin *et al.*, 1997), although M1 lacks clear homology to the functionally important hinge domain and reactive site loop of the poxvirus serpins (Bowden *et al.*, 1997). As mentioned previously, the role of the poxvirus SPI-1 gene appears to be inhibition of apoptosis (Brooks *et al.*, 1995; Moon *et al.*, 1999). A role in inhibition of apoptosis has not yet been demonstrated for M1, although the presence of another anti-apoptotic gene in the MHV-68 genome has been widely documented. The M11 gene is a bcl-2 homologue that is able to inhibit Fas- and TNF-induced apoptosis (Wang *et al.*, 1999; Roy *et al.*, 2000) and is required for efficient reactivation from latency (Gangappa *et al.*, 2002). However, the properties of M1-deficient viruses do not mirror the properties of M11-deficient viruses, which suggests that if M1 is an inhibitor of apoptosis it is acting at a different point during infection to the known anti-apoptotic M11 gene.

Further sequence analysis has demonstrated similarities between the M1 and M3 genes of MHV-68 (van Berkel *et al.*, 1999). The M3 gene shows no significant homology to the poxvirus SPI-1 gene, and functions as a secreted chemokine binding protein to modulate the host immune system (van Berkel *et al.*, 1999; Parry *et al.*, 2000; van Berkel *et al.*, 2000;). Structural analysis of M3 and M1 have shown that M1 and M3 may share folding features, but that the M3 chemokine contact residues are rarely conserved in M1, indicating that an unrelated function for M1 is likely (Alexander *et al.*, 2002).

This study also indicates that the M4 gene of MHV-68 may share folding features with both M3 and M1, indicating a possible relationship between M1 and M4. The function of the M4 gene of MHV-68 is also yet to be elucidated; however, it encodes a secreted glycoprotein required for establishment of normal viral load during acute phase latency (Evans *et al.*, 2006; Geere *et al.*, 2006). This defect in viral load during acute phase latency mirrors our findings following *in vivo* infection with the M1 deletion virus. However, despite some similarities disruption of M4 does not produce an identical phenotype *in vivo* to disruption of M1 (Evans *et al.*, 2006; Geere *et al.*, 2006; Clambey *et al.*, 2000). This indicates that while possibly related, the functions of these two genes are not redundant.

One of the key features following deletion of M1 is the enhanced reactivation from latency in the spleen. This is a phenomenon also observed in B cell-deficient mice (Weck *et al.*, 1999). It is tempting to speculate that in the absence of M1 an interaction with B cells fails to occur, and as a result B cells in immunocompetent mice fail to control reactivation.

In conclusion our preliminary results confirm findings previously shown. M1 appears to play a role in virus reactivation in lymphoid tissue, and loss of M1 from the virus genome results in attenuation as determined by reduced virulence in young or small mice. Our results also show a number of previously unidentified characteristics of an M1-deficient virus, including an increase in lung titres during acute infection, and a failure to drive splenomegaly. These data are only preliminary, however due to time constraints it was not possible to repeat all experiments to confirm the results. While structural similarities appear between the M1 gene and the other MHV-68 unique genes M3 and M4, the functions of these genes do not appear to be redundant, indicating a unique function for the M1 gene during acute infection of the lung and establishment of latency in the spleen.

Chapter 5: *In Vivo* Characterisation of the M4In1 Virus

5.1 Background to the Study

The left end of the MHV-68 genome has long been known to play a role in pathogenesis of the virus (Nash *et al.*, 2001). The region contains four unique genes and eight viral tRNA-like molecules, all of which have been studied to investigate their roles during infection.

As well as the coding DNA sequence, an amount of apparently non-coding DNA is contained within the left end of the genome. This includes a 1.2 kb region located between the M3 and M4 genes. Little is known about the importance of this region in viral pathogenesis, but it is conserved in the naturally occurring deletion mutant MHV-72. This virus is similar to the MHV-76 virus, but while MHV-76 is lacking the first 9.5 kb of the left end of the genome, MHV-72 misses only the first 7 kb. As a result, while MHV-76 lacks genes M1-M4 and the vtRNAs, MHV-72 still carries the complete M4 gene as well as sequences upstream of this gene. The presence of an extra 2.5 kb of sequence in the MHV-72 genome results in a slightly altered phenotype compared to MHV-76. Mice infected with MHV-72 are prone to development of tumours at late time points post-infection, a characteristic not associated with MHV-76 infection (Oda *et al.*, 2005). This suggests that M4 and/or the upstream sequences may play a role in tumorigenesis.

5.2 Generation of the M4In1 and M4In1Rev Viruses

The M4 gene has been a focus of interest for some time. Initial studies identified the start of the M4 gene at genome co-ordinate 8409 bp (Virgin *et al.*, 1997). To investigate the role of M4 during MHV-68 infection, an M4 mutant virus was generated using the MHV-68 BAC system developed by Adler *et al.* (2000). Shuttle recombination (method from Wagner & Koszinowski, 2004) was used to insert a 19bp region of DNA containing 3 in-frame stop codons into the start of the M4 gene at genomic co-ordinate 8409. The aim was to prevent translation of the M4 gene, and this virus was known as the M4In1 virus. To confirm that any change in phenotype observed following infection with the M4In1 virus was due to the targeted mutation and not a distal mutation in the MHV-68 genome, a marker rescue virus (M4In1Rev) was constructed in which the wild-type M4 sequences were restored in M4In1 (Geere, 2004).

Prior to characterisation of the M4In1 virus, studies on the M4 gene revealed the start codon was in fact located at genomic co-ordinate 8526 (Townsley *et al.*, 2004). This indicated that the mutation had been introduced into an apparently non-coding region of the genome between the M3 and M4 genes.

However despite the location of the mutation in an intergenic region, the M4In1 virus showed an altered phenotype following intranasal infection of IFNγR$^{-/-}$ mice. Of note were the lungs of these mice at 12 days post-infection, where a substantial increase in pathology was observed in M4In1-infected mice compared to MHV-68-infected mice. The initial *in vivo* study of this virus was limited to a small group of mice at a limited number of time points (Geere, 2004).

To further characterise the M4In1 virus we conducted a number of *in vivo* studies to determine how the mutation altered pathogenesis of the virus.

5.3 *In Vivo* Characterisation of the M4In1 Virus

5.3.1 Intranasal Infection of Wild-Type 129 SV/EV Mice Results in Increased Viral Lung Titres at Early Time Points Post-Infection.

Previous observations suggested the M4In1 virus resulted in an altered phenotype in the lung following intranasal infection of IFNγR$^{-/-}$ mice. To investigate if this phenotype occurs in conjunction with an alteration in viral levels in the lung 3-4 month old IFNγR$^{-/-}$ and wild-type 129 mice were infected intranasally with 4×10^5 p.f.u. of either M4In1 or control viruses (M4In1Rev or PHA4). At various time points post-infection mice were sacrificed and organs were removed and stored at –80°C until required. Infectious virus was determined by plaque assay (Materials & Methods section 2.7.6.2) and the results are shown in figure 5.1. At 3 days post-infection the virus titre is significantly higher in 129 mice infected with M4In1 compared to 129 mice infected with either of the control viruses (M4In1Rev or PHA4). No significant difference was observed following inoculation of IFNγR$^{-/-}$ mice with M4In1 or control viruses.

Townsley *et al.* (2004) found that following insertion of the M4 gene into the MHV-76 genome elevated lung titres were observed 1 day post-infection relative to MHV-76 and MHV-68, although by day 5 this difference has resolved. This finding led to

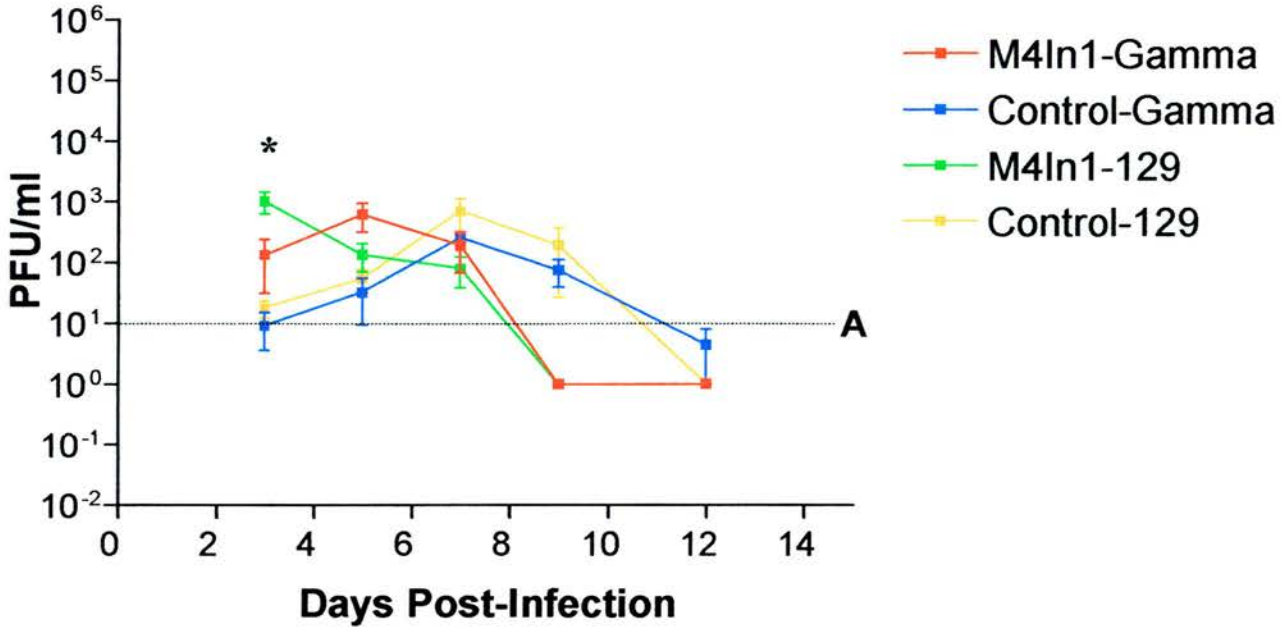

Figure 5.1 The M4In1 Virus causes increased lung titres at early time points in wild-type 129 mice but not in IFNγR$^{-/-}$ mice. 3-4 month old mice were infected intranasally with 4 x 10^5 p.f.u. of either M4In1 or a control virus (50% of mice infected with M4In1Rev and 50% with PHA4). At 3 days post-infection 129 mice infected with M4In1 showed significantly increased viral titres in the lung compared to mice infected with the control viruses ($p=0.04$, Student's *t*-test). This difference was not observed following intranasal infection of IFNγR$^{-/-}$ mice. At all other time points no significant difference was observed between mice infected with M4In1 or control viruses. Each data point represents four mice. The limit of detection of the assay is labelled **A**.

speculation that the mutation upstream of the M4 gene may be resulting in a similar phenotype in the M4In1 virus, potentially due to upregulation of the M4 gene.

5.3.2 M4In1 is Attenuated *In Vivo* Following Infection of Juvenile IFNγR$^{-/-}$ Mice

The M4 phenotype is most obvious in the spleen, with a 10-100-fold deficit in viral load observed during acute phase latency (Evans *et al.*, 2006; Geere *et al.*, 2006). This deficit is observed between days 14 and 17, and is resolved by d42. To test if viral load in the spleen was altered at these time points both wild-type 129 and IFNγR$^{-/-}$ mice were infected intranasally with 4 x 10^5 p.f.u. of either M4In1 or M4In1Rev (no study has indicated a difference between M4In1Rev and PHA4, so PHA4 was not included for cost reasons). The previous *in vivo* study had involved infection of mice aged 3-4 months, but owing to time constraints mice were subsequently infected at 5 weeks of age. The aim was to quantify viral load at the time points 15, 20 and 40 days post-infection, with 4 mice per virus per time point. However there was an unexpected consequence of infecting IFNγR$^{-/-}$ mice at a younger age. At 12 days post-infection 8/12 IFNγR$^{-/-}$ mice infected with M4In1Rev died (shown in Figure 5.2). M4In1-infected IFNγR$^{-/-}$ mice all survived until d40, as did the remaining 4 M4In1Rev-infected mice. All 129 mice survived regardless of the virus they were infected with.

It is not entirely surprising that infection of immunocompromised mice at such a young age resulted in premature death for many of the mice. However, interestingly none of the mice infected with M4In1 succumbed to infection despite being in all respects identical to the mice infected with M4In1Rev. This suggests that M4In1 is attenuated *in vivo*, indicated by the reduced mortality of these mice compared to wild-type infected mice.

5.3.3 Investigation of M4In1 Pathogenesis in Juvenile Mice

In order to carry out previously planned experiments and also to repeat previous experiments to verify results, 6 week old IFNγR$^{-/-}$ and 129 mice were infected intranasally with 4 x 10^5 p.f.u. of either M4In1 or M4In1Rev.

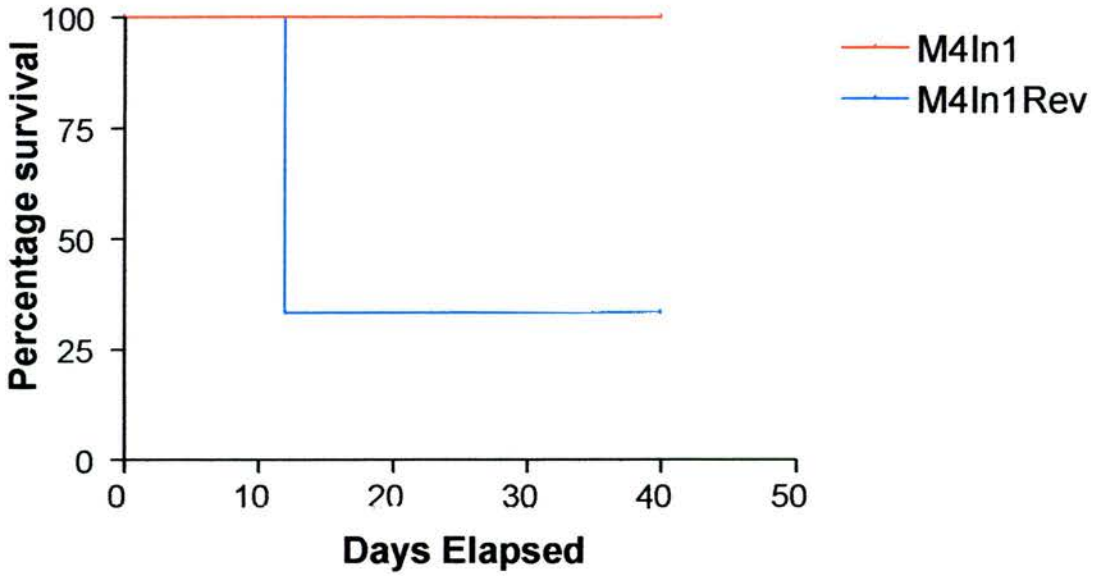

Figure 5.2 M4In1 is attenuated following intranasal infection of juvenile IFNγR$^{-/-}$ mice. 5 week old IFNγR$^{-/-}$ mice were infected intranasally with 4 x 10^5 p.f.u. of either M4In1 or M4In1Rev viruses. 12 mice per virus were infected in total. By d12 8/12 mice infected with M4In1Rev had died from infection. All mice infected with M4In1 survived. The remaining mice remained healthy until d40, when the experiment was ended.

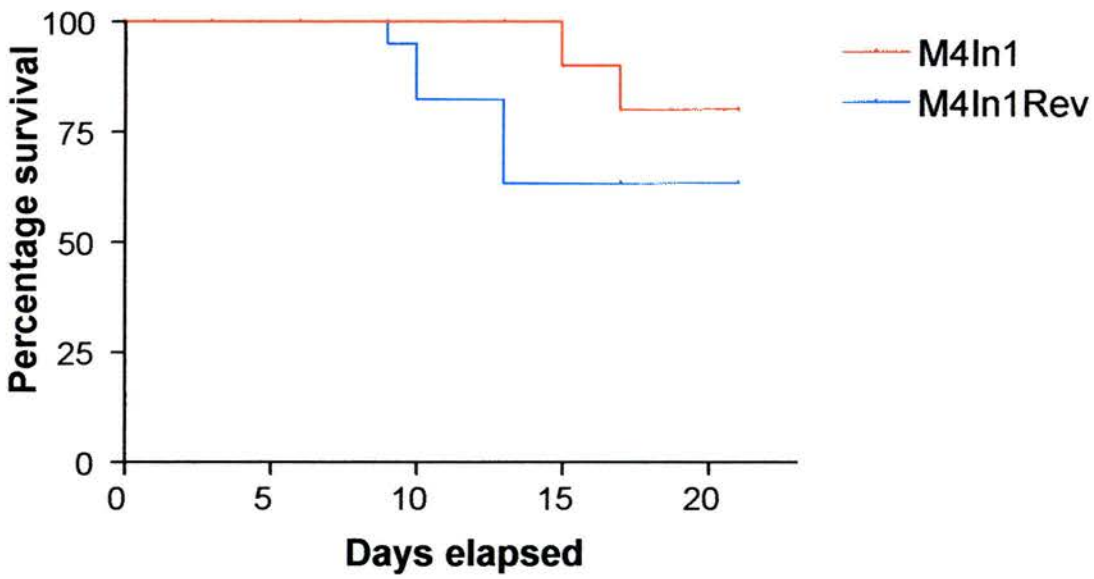

Figure 5.3 M4In1 is attenuated following intranasal infection of 6 week old IFNγR$^{-/-}$ mice. 6 week old IFNγR$^{-/-}$ mice were infected intranasally with 4 x 10^5 p.f.u. of either M4In1 or M4In1Rev viruses. Between days 9 and 13 6/32 mice succumbed to infection. Unexpectedly 2/32 mice infected with M4In1 died between days 15 and 17.

During the course of the experiment IFNγR$^{-/-}$ mice infected with M4In1Rev again began to fall ill and die as a result of infection. Between days 9 and 13, 6/32 mice infected with the revertant virus died (shown in figure 5.3). This 19% death rate is a significant reduction on the previous figure of 67% for 5 week old mice but still suggests that the remaining immune system in these mice is not developed enough at 6 weeks old to control MHV-68 infection.

2/32 mice infected with M4In1 succumbed to infection, although at later time points than M4In1Rev-infected mice. This was an unexpected result because in the previous experiment involving younger mice no deaths were observed in this group. However the percentage of deaths was still greatly reduced compared to M4In1Rev-infected mice, leading to the conclusion that M4In1 is attenuated in IFNγR$^{-/-}$ mice up to 6 weeks of age.

Despite the deaths of mice in both groups there were still sufficient numbers remaining to carry out the majority of planned experiments, albeit with reduced numbers at certain time points. To further investigate if the M4In1 virus showed elevated titres at very early time points in the lung, infected mice were sacrificed at 1, 3, 6, 9 and 13 days post-infection and the lungs removed. Viral titres were determined as before using a plaque assay. Figure 5.4 shows the results for this experiment. Unlike the previous results (figure 5.1) no difference was seen in M4In1 and M4In1Rev viral titres in either 129 or IFNγR$^{-/-}$ mice at very early time points post-infection (d1 or d3). However at d9 IFNγR$^{-/-}$ mice infected with M4In1Rev show significantly higher titres than M4In1-infected mice. This time point corresponds to the onset of death in this particular group of mice and indicates that an inability to control infection was causing death. By d13 virus was cleared by M4In1Rev-infected mice, indicating that mice still alive at this time point were able to recover from infection. In contrast, M4In1-infected IFNγR$^{-/-}$ mice had not completely cleared the virus from the lungs by d13. A number of mice from this group went on to die shortly after this time point, suggesting that some mice were unable to control infection. It is not known if this is coupled to a lack of clearance of the virus from the lung.

At no time point were differences observed in 129 mice infected with either M4In1 or M4In1Rev. This contrasts with the previous experiment where M4In1 infection resulted in higher viral titres at d3. This suggests that the younger mice are unable to

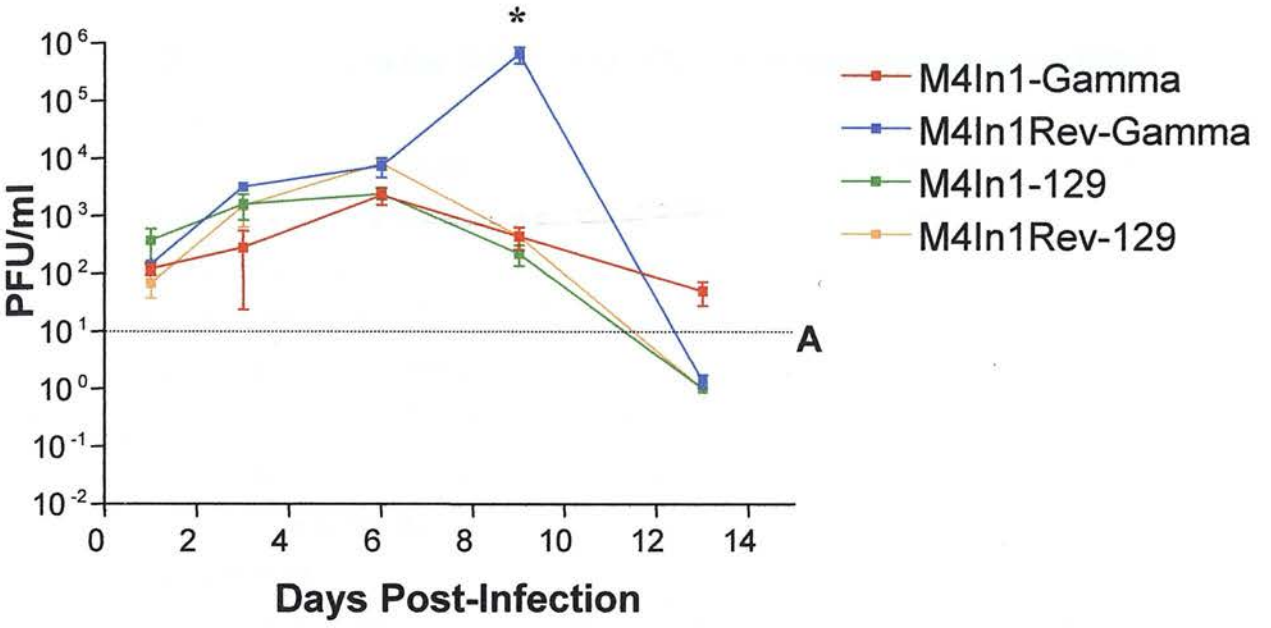

Figure 5.4 The M4In1 Virus is attenuated at d9 relative to wild-type virus in IFNγR$^{-/-}$ mice but not in wild-type 129 mice. 6 week old mice were infected intranasally with 4 x 10^5 p.f.u. of either M4In1 or M4In1Rev. Unlike the previous experiment no difference in viral titres was seen at very early time points post-infection in either 129 or IFNγR$^{-/-}$ mice, although at d9 IFN γR$^{-/-}$ mice infected with M4In1 showed significantly lower titres compared to mice infected with M4In1Rev. Each data point represents four mice. The limit of detection of the assay is labelled **A**.

control infection, and this lack of control masks the differences observed following infection of older mice.

5.3.4 Viral Load in the Spleen is Unaffected by the Insertion in the M4In1 Virus

M4 is essential for establishment of normal latent load in the spleen following intranasal infection (Townsley *et al.*, 2004; Evans *et al.*, 2006; Geere *et al.*, 2006). To determine if viral load was affected by the presence of a small insertion upstream of the M4 start codon, viral load was quantified using real-time PCR. DNA was extracted from the spleen using a Qiagen DNeasy kit (Materials & Methods section 1.2.1) and real-time PCR was carried out according to the protocol given in Materials & Methods section 2.6. The M4 assay (using primers distal to the mutation in M4In1) was used. Normalisation was used to correct for variation in quality and quantity of template DNA.

Spleen samples from both experiments (infection of 5- or 6-week old mice) were used for quantification. As shown in figure 5.5, at no time point studied was a difference in viral load observed between M4In1 and M4In1Rev for either IFNγR$^{-/-}$ or 129 mice. This indicated that M4 activity was not significantly altered in the spleen and suggests that the lung phenotype is unlikely to be related to M4. However given that differences in the lung observed in older mice were not detected following infection of younger mice, there is a possibility that a difference between M4In1 and wild-type viruses could go undetected in this experiment.

To determine if M4 expression was altered in the M4In1 virus a reverse transcriptase real-time PCR assay was developed to quantify M4 transcription. Given that previous results did not indicate any effect of the M4In1 insertion on M4, it was decided to investigate if M3 was in any way affected. While the M3 gene is much further from the site of the mutation than M4 there was still the possibility of an effect on M3 expression.

5.3.5 Development of Real-Time PCR Assays to Quantify M3 and M4 Transcription

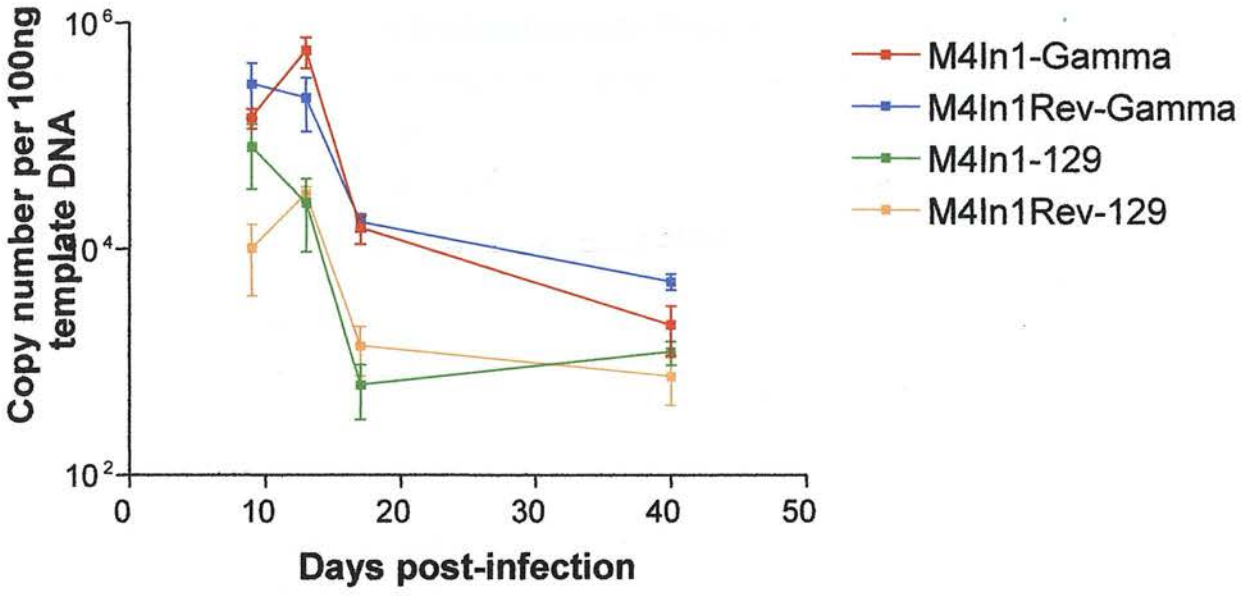

Figure 5.5 Viral load in the spleen is unaffected by the mutation in the M4In1 virus. 6 week old IFNγR$^{-/-}$ and 129 mice were infected intranasally with 4 x 10^5 p.f.u. of either M4In1 or M4In1Rev. At various time points up to d17 post-infection mice were sacrificed and the spleens removed. 5 week old mice were infected as above and at d40 mice were sacrificed and the spleens were removed. Real-time PCR was used to quantify viral load. Each data point represents at least 4 mice, with the exception at d17 (the point corresponding to IFNγR$^{-/-}$ mice infected with M4In1Rev represents only 2 mice). At no point is the viral load for mice infected with M4In1 different to the control virus for both IFNγR$^{-/-}$ and 129 mice.

In order to determine if M3 or M4 transcript levels were affected by the presence of the mutation at genome co-ordinate 8409, real time assays were developed for both genes. The assay was developed using the SYBR-green method of detection.
For the real time assay primers were designed that fell within the region of the M3 or the M4 transcript (shown in Materials & Methods appendix 1.2). To generate standards for absolute quantification plasmids were made containing either the complete M3 or M4 gene. Initially the gene (either M3 or M4) was amplified by PCR from viral DNA (see Materials & Methods section 5). PCR products were then cloned into pCR4®-TOPO® vector and the plasmid copy number per µl was determined by spectrophotometry. Serial ten fold dilutions were made to generate the standard dilution series for use in the real time PCR reaction.

Figures 5.6 and 5.7 show the range of quantification of the M3 and M4 assays. In both cases the DNA template containing 1×10^7 copies per µl (i.e. 5×10^7 copies per reaction) was amplified first, with each subsequent dilution amplified at intervals of 4 cycles until the DNA template was diluted by 6 orders of magnitude. Quantitation of the amount of target in the unknown samples was achieved as before by measuring C_T and using the standard curve to determine starting copy number. Melt curve analysis was used to demonstrate the specificity of the primers.

5.3.5.1 Normalisation of cDNA Samples

The amount of cDNA in a given sample can vary owing to factors such as RNA degradation, quantity of RNA present in the reverse transcription reaction, and reaction efficiency during reverse transcription.
To reduce variation RNA was quantified by spectrophotometry prior to reverse transcription. Normalisation of samples was also used to correct for any otherwise undetected variation, for example due to degradation of either the RNA or cDNA.
The use of housekeeping gene to normalise input levels of template is a widely used practice. However the ideal gene for use in this process is the subject of much debate (Thellin *et al.*, 1999; Suzuki *et al.*, 2000; Vandesompele *et al.*, 2002; reviewed by Huggett *et al.*, 2005). Commonly used genes include β-actin, GAPDH and 18s rRNA amongst others. Ideally several housekeeping genes are used to normalise the sample

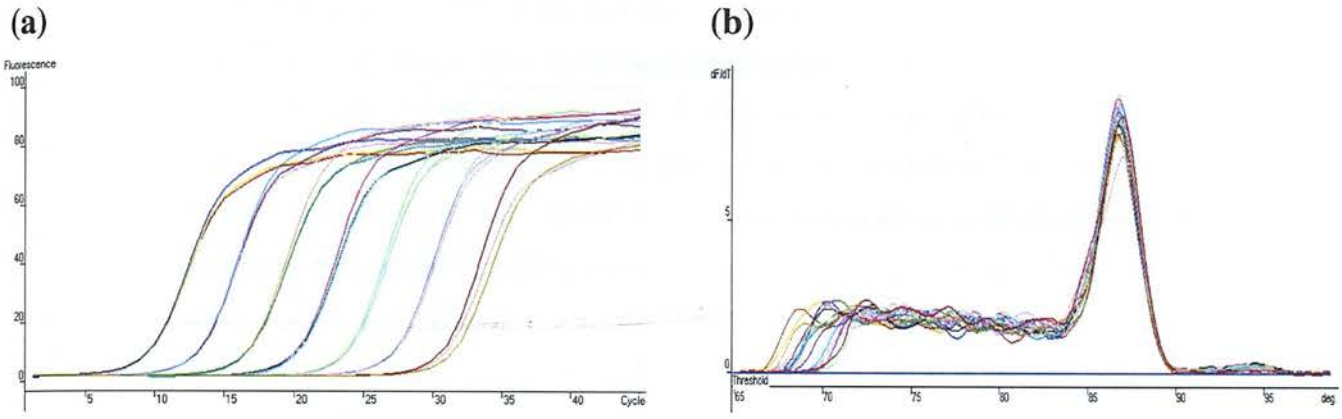

Figure 5.6 The M3 real time assay platform. The M3 assay can quantify viral load in the range 50 - 50,000,000 copies per 100 ng template DNA (a). Reactions containing 5 x 10^7 copies are amplified first, with subsequent 10-fold dilutions amplified at 4-cycle intervals. The PCR reaction is amplifying a single specific product that melts at 86°C (b).

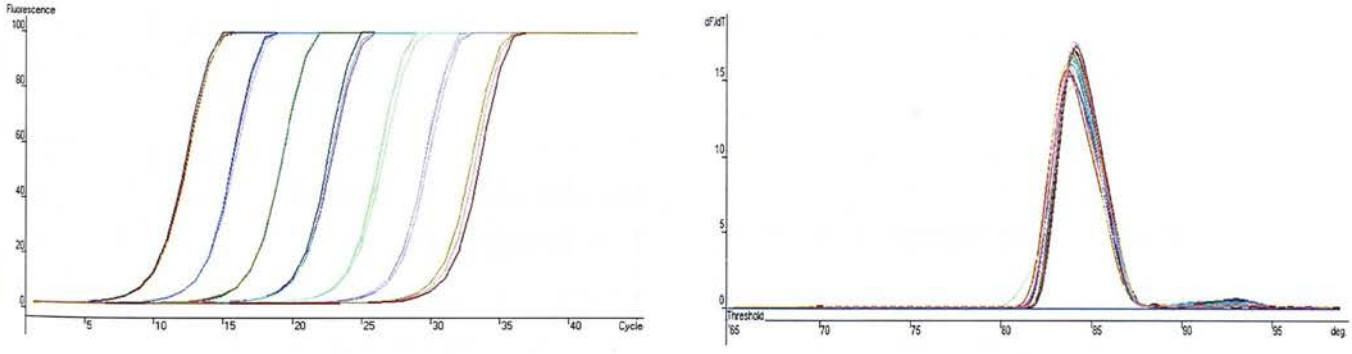

Figure 5.7 The M4 real time assay platform. The M4 assay can quantify viral load in the range 50 - 50,000,000 copies per 100 ng template DNA (a). Reactions containing 5 x 10^7 copies are amplified first, with subsequent 10-fold dilutions amplified at 4-cycle intervals. The PCR reaction is amplifying a single specific product that melts at 83°C (b).

(Vandesompele *et al.*, 2002), but time and cost made this an unrealistic proposition. Therefore we selected β-actin as the housekeeping gene for normalisation.

Viral infection of cells often results in host shutoff and hence impairment of housekeeping gene transcription. This affects the normalisation process as levels of the normalisation gene are skewed in infected compared to uninfected cells. To determine how levels of β-actin were affected by MHV-68 infection, BHK-21 cells were infected with either M4In1 or M4In1Rev. 2 x 10^6 cells were infected at 5 p.f.u. per cell and incubated at 37°C. Mock-infected cells were set up in parallel. 4 samples were set up for each of the viruses and the uninfected controls. At 17 hours post-infection RNA was harvested and reverse transcribed. Levels of β-actin were determined using real time PCR.

At the time point investigated β-actin levels were approximately 100-fold lower in infected cells compared to uninfected cells, and samples infected at different MOIs also showed variation in β-actin levels at the time point investigated (data not shown). However within samples infected at the same MOI, β-actin levels were very similar. Therefore provided *in vitro* samples are infected at the same MOI, β-actin levels are constant between samples and β-actin is a suitable housekeeping gene for normalisation.

In vivo infections are much more complicated as the level of infection (and hence the level of β-actin downregulation) shows much more variation between samples. However at 16 days post-intranasal-infection the level of genome positive cells in a spleen infected with wild-type virus is approximately 1/300 (Evans *et al.*, 2006). At this frequency β-actin levels are unlikely to be substantially affected by MHV-68 infection, and variation in levels of infection between samples are also unlikely to alter β-actin levels significantly. On this basis we decided that β-actin was a suitable housekeeping gene for normalisation of *in vivo* samples.

5.3.6 Transcription of M3 and M4 *In Vitro* are Unaffected by the M4In1 Mutation

BHK-21 cells were infected at a M.O.I. of 5 with either M4In1 or M4In1Rev and incubated at 37°C. At various time points post-infection cells were harvested and the RNA extracted. RNA was reverse transcribed and the resulting cDNA was used in

real time PCR assays to quantify the levels of M3 and M4 transcription. Samples were normalised to the level of β-actin RNA.

Figure 5.8 shows the results for this experiment. Samples were taken at 4, 8, 12 and 24 hours post-infection. At no time point studied was any difference detected in M3 or M4 transcription between M4In1 and M4In1Rev. This suggests the phenotype observed following infection with M4In1 is not due to an alteration in transcription of the neighbouring genes. However to confirm this is the case during *in vivo* infection this experiment was repeated using samples taken from infected mice.

5.3.7 M3 and M4 Transcription *In Vivo* Are Not Affected by the M4In1 Mutation

Previous study of the M4In1 virus had identified a phenotype in the lung, and therefore it would seem obvious to start investigation of alteration in transcription in this organ.

To determine if a different phenotype is observed following infection of IFNγR$^{-/-}$ mice, both wild type 129 SV/EV and IFNγR$^{-/-}$ 6-week old mice were infected intranasally with 4 x 10^5 p.f.u. of either M4In1 or M4In1Rev (these mice were used in other experiments shown in figures 5.4 and 5.5). At various times post-infection 4 mice per virus were sacrificed. Spleen samples were stored in RNALater to preserve RNA until it could be extracted. At d13 an extra 4 mice per time point were sacrificed (the lungs from the first four mice being required for the lung titration, figure 5.4) and the lungs inflated with 10% neutral buffered formalin. This was to allow for histological sections to be taken as well as RNA to be extracted.

To determine if M3 or M4 levels were altered in the lungs following infection with M4In1, the organs were embedded in paraffin and 5 μm sections were cut and placed onto slides. Sections were then scraped off slides using a clean scalpel blade, and RNA was extracted using the method given in Materials & Methods section 2.4.2. However all RNA extracted in this way was degraded, as demonstrated by a failure to amplify the β-actin gene by PCR following reverse transcription in any samples tested (data not shown). This failure was most likely due to a delay in processing from formalin to paraffin (Ben-Ezra *et al.*, 1991; O'Leary *et al.*, 1994). While a number of kits are available for optimised extraction of RNA in this way, time constraints did not allow for investigation of these kits and optimisation of the procedure. It was

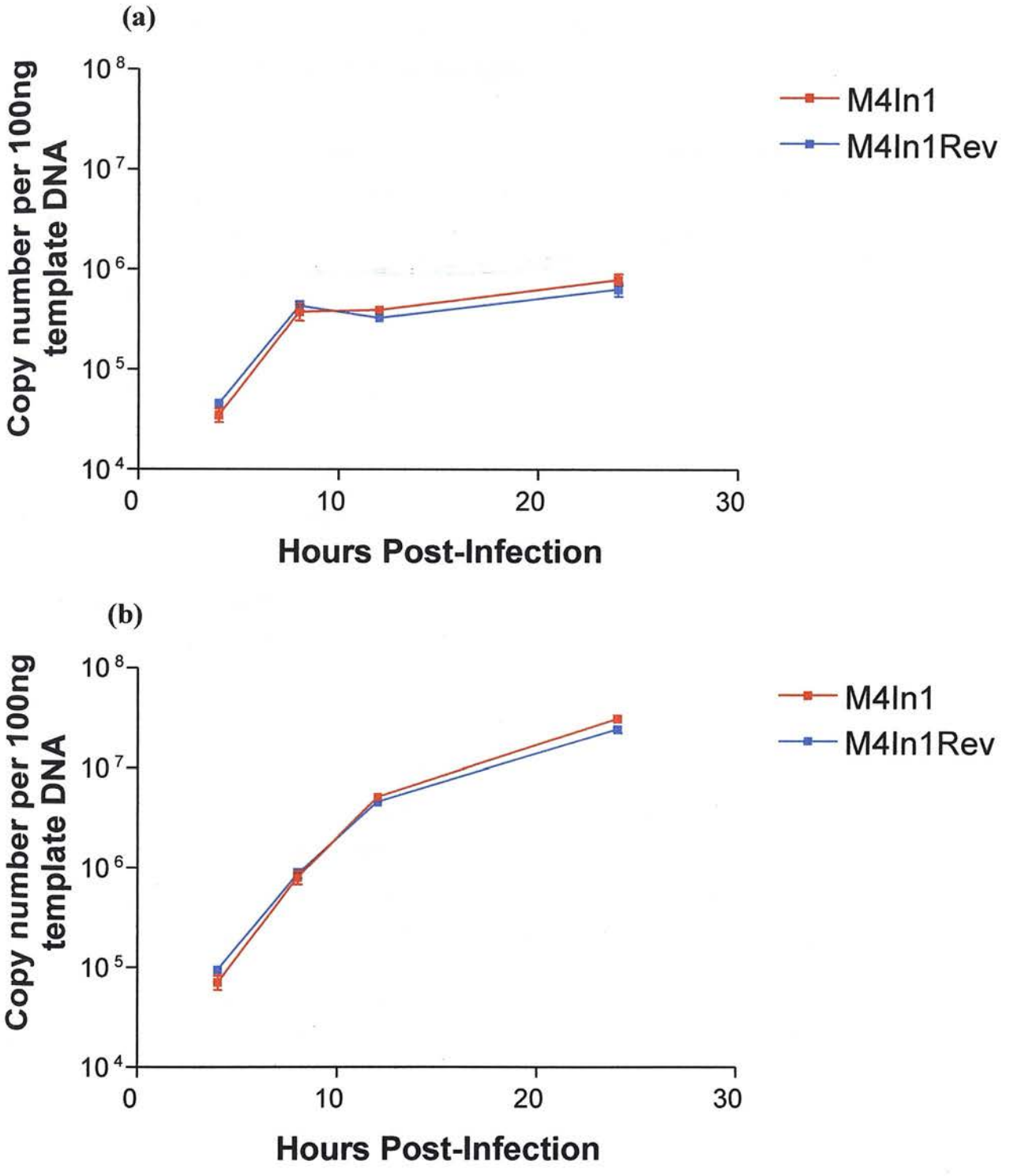

Figure 5.8 The M4In1 mutation does not affect *in vitro* transcription of M4 or M3. Levels of both M4 (a) and M3 (b) transcripts following *in vitro* infection of BHK-21 cells with M4In1 were comparable to levels in cells infected with M4In1Rev at all time points studied (up to 24 hours post-infection).

therefore not possible to determine if M3 or M4 transcription was altered in the lungs of M4In1-infected IFNγR$^{-/-}$ or 129 mice.

As spleen samples had been preserved in RNAlater, extraction of RNA presented no problems. Figure 5.9 shows levels of M3 and M4 transcripts in the spleens of IFNγR$^{-/-}$ and 129 mice infected with either M4In1 or M4In1Rev. At no time point studied was a significant difference observed in transcript levels between M4In1 and M4In1Rev in either IFNγR$^{-/-}$ or 129 mice.

As the RNA extraction from the lung was unsuccessful it is not possible to conclusively prove that M3 or M4 transcription is not in some way altered following infection with M4In1. Given the lack of an alteration in viral load in the spleen it appears unlikely the mutation is affecting M4.

5.3.8 M4In1 Infection Results in Attenuated Pathology in the Lungs of Both IFNγR$^{-/-}$ and Wild-Type 129 Mice

IFNγR$^{-/-}$ and 129 mice were infected at 6 weeks of age with 4 x 10^5 p.f.u. of either M4In1 or M4In1Rev. At 13 days post-infection lungs were removed and inflated with 10% neutral buffered formalin. Lungs were embedded in paraffin and 5 μm sections were cut, placed on slides and stained with H & E.

At the same time slides previously analysed were obtained for comparison with our more recent work. The original slides were made from the lungs taken from 3-4 month old mice infected intranasally with 4 x 10^5 p.f.u. of either M4In1, M4In1Rev or PHA4, and sacrificed at d12. Lungs were inflated with formalin and embedded in paraffin prior to sections being cut and stained with H & E.

Sections were assessed for both the type of pathology present and also scored blind for severity of pathology. Sections were scored on a scale of 0-4, with 0 indicating no pathology, 1 for mild pathology, 2 for moderate, 3 for severe and 4 for extremely severe pathology.

In the initial investigation into the pathogenesis of M4In1 *in vivo*, the report suggested an increase in pathology in IFNγR$^{-/-}$ mice infected with M4In1 compared to control-

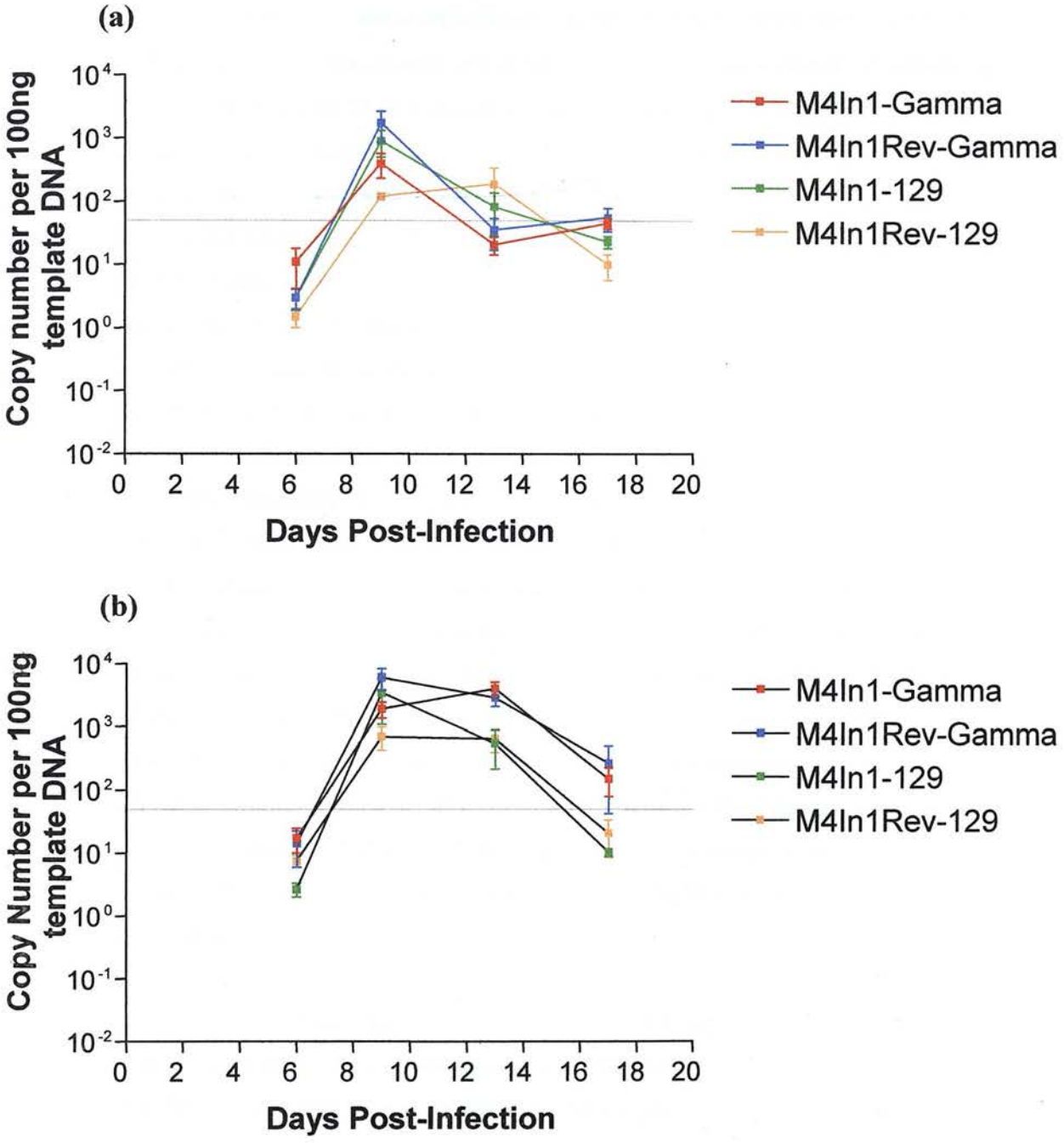

Figure 5.9 The M4In1 mutation does not affect *in vivo* transcription of M4 or M3. Levels of both M4 (a) and M3 (b) transcripts following *in vivo* infection of IFNγR$^{-/-}$ or 129 mice with M4In1 were comparable to levels in IFNγR$^{-/-}$ or 129 mice infected with M4In1Rev at all time points studied (up to 17 days post-infection).

infected mice. Our subsequent reanalysis of the slides indicates this may not be the case.

Figures 5.10 and 5.11 show representative areas of M4In1-, M4In1Rev-, and PHA4-infected mice from the original experiment. In IFNγR$^{-/-}$ mice (figure 5.10) infected at 3-4 months old with M4In1 one of the two samples exhibits almost no pathology, while the other exhibits unusual pathology not found in any other sample – inflammation is found around the airways and the vasculature, and is predominantly non-supperative and PMN inflammation. Owing to the sample size of 2 it is difficult to draw conclusions from this.

In the case of control-infected 3-4 month old mice (2 infected with M4In1Rev; 2 with PHA4) the results are much more consistent. Moderate to extremely severe reactions are observed in the four mice, with 3 out of 4 rated severe or extremely severe. The airways for all four mice show peribronchiolar non-supperative inflammation, and all mice show non-supperative lymphocyte-dominated vasculitis.

Our later study involving infection of 6 week old IFNγR$^{-/-}$ mice showed similar results, albeit with younger mice showing greater pathology compared to the corresponding 3-4 month old samples. The 4 mice infected with M4In1 aged 6 weeks all show the peribronchial non-supperative inflammation and vasculitis observed in many other samples. However this group showed extensive fibrosis in the interstitium, a characteristic not obvious in the corresponding older mice.

In the case of the 6 week old M4In1Rev mice the pathology observed was similar to that in the M4In1-infected mice, but all samples were scored as having extremely severe pathology. This indicates again that the M4In1 virus has an attenuated phenotype *in vivo*.

Surprisingly, the wild type 129 mice recapitulated the phenotype of the M4In1 virus, a result that had not been detected previously (shown in figure 5.11).

In the case of mice infected aged 3-4 months, all samples showed evidence of peribronchiolar non-supperative inflammation and vasculitis. Again, the M4In1-infected mice showed evidence of a reduction in pathology compared to M4In1Rev- or PHA4-infected mice, but this is a relatively small difference, and the small sample size does not easily allow for conclusions to be made.

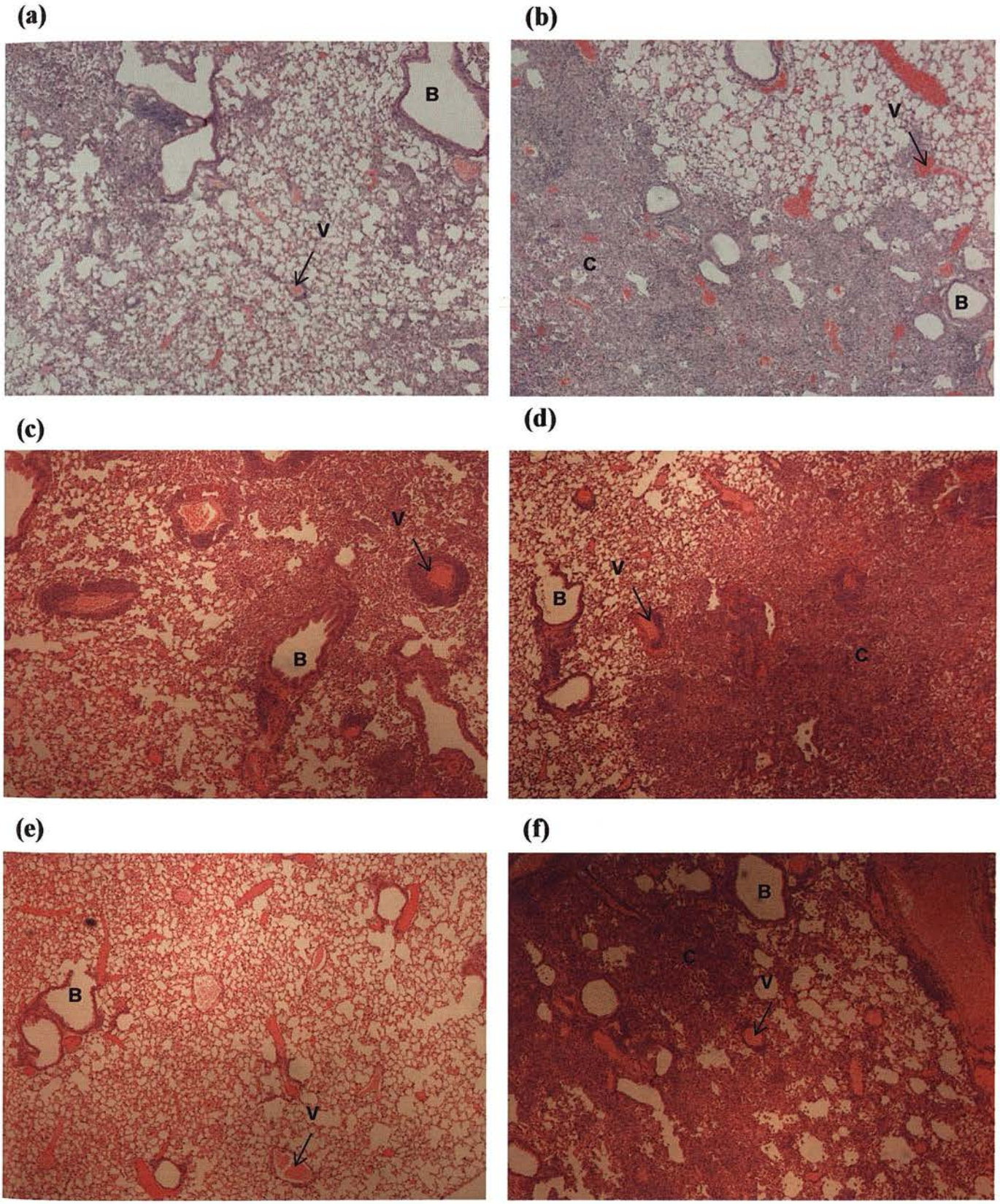
(a)
B
V
(b)
V
C
B
(c)
V
B
(d)
V
B
C
(e)
B
V
(f)
B
C
V

Figure 5.10 M4In1 shows attenuated pathology following intranasal infection of IFNγR$^{-/-}$ mice. At 12 or 13 days post-infection lungs were removed from mice infected with either M4In1, M4In1Rev or PHA4 and fixed with formalin. Samples were embedded in paraffin wax, and 5 μm sections were cut and stained with H&E. In both mice 6 weeks old (a) or 3-4 months old (c, e) at time of infection the M4In1 virus shows reduced pathology compared to 6 week old mice infected with M4In1Rev (b) or 3-4 month old mice infected with M4In1Rev (d) or PHA4 (f).

Four mice were available per virus for the 6 week old mice, with consistent results within the sample groups - the M4In1Rev-infected mice showed extensive fibrosis and areas of consolidation (marked **C**) within the interstitium. Non supperative inflammation was observed around the bronchioles (marked **B**) and the vasculature (marked **V**).

Two mice were available per virus (M4In1, M4In1Rev or PHA4) for the 3-4 month old mice. Results were consistent for the control-infected viruses, with extensive non supperative vasculitis and peribronchiolar inflammation. Results were inconsistent for M4In1-infected mice, with one showing very little inflammation (e) and one **showing** a reaction not observed in any other sample, with thick perivascular cuffs of non supperative and mixed PMN inflammation (c).

(a)

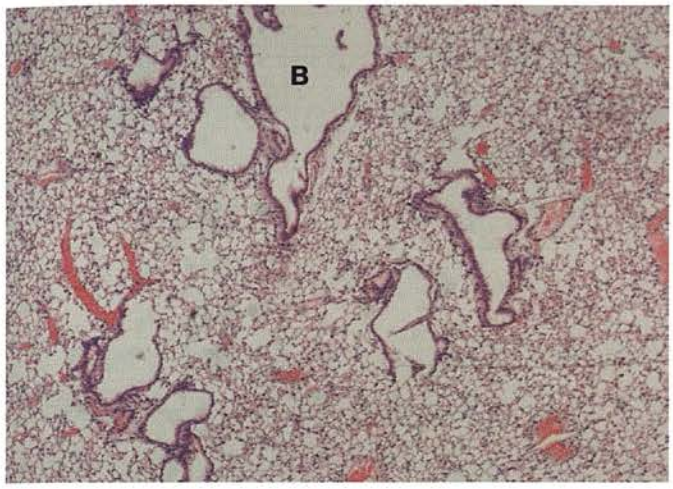

(b)

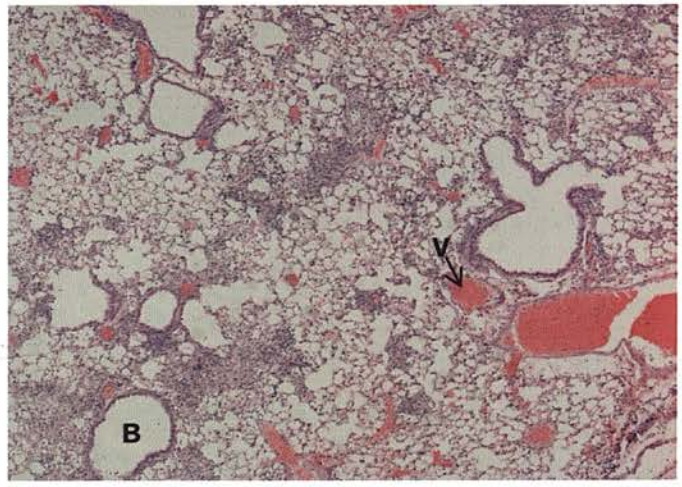

(c)

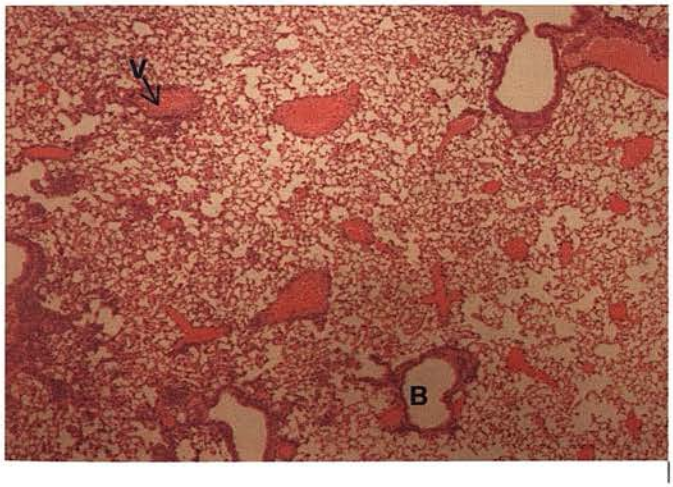

(d)

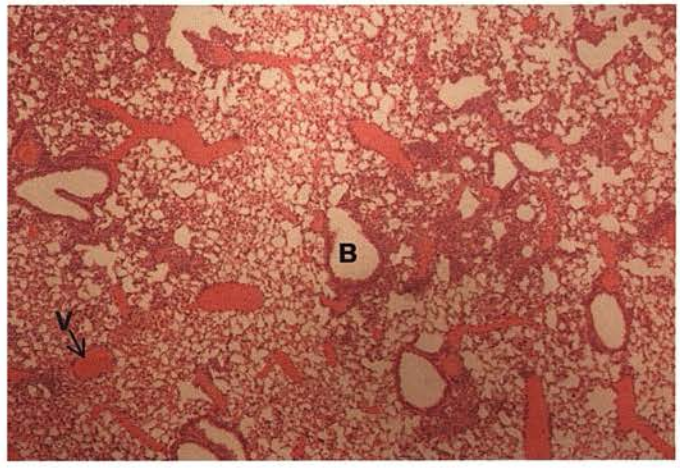

(f)

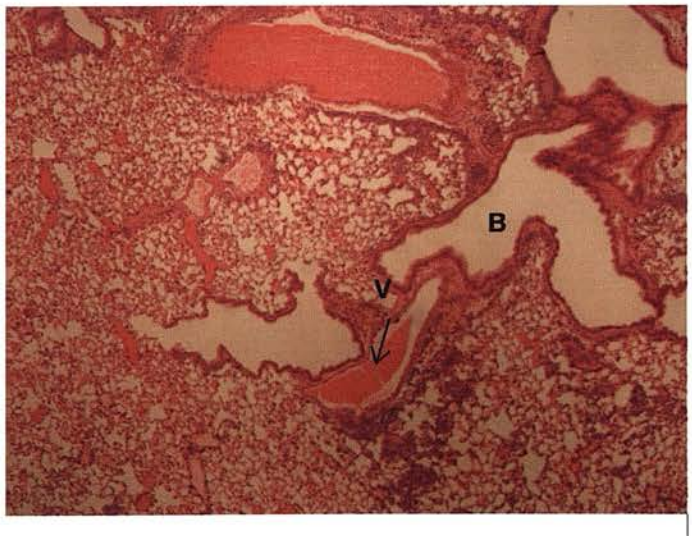

Figure 5.11 M4In1 shows attenuated pathology following intranasal infection of wild-type 129 mice. At 12 or 13 days post-infection lungs were removed from mice infected with either M4In1, M4In1Rev or PHA4 and fixed with formalin. Samples were embedded in paraffin wax, and 5 μm sections were cut and stained with H&E. In both mice 6 weeks old (a) or 3-4 months old (c) at time of infection the M4In1 virus shows reduced pathology compared to 6 week old mice infected with M4In1Rev (b) or 3-4 month old mice infected with M4In1Rev (d) or PHA4 (e).

Two mice were available per virus for the 6 week old mice, with consistent results within the sample groups - the M4In1Rev-infected mice showed fibrosis and consolidation on a reduced level to that observed for IFN γR-/- mice infected with the same virus. M4In1-infected mice showed focal small areas of inflammation, with very little pathology overall.

Two mice were available per virus (M4In1, M4In1Rev or PHA4) for the 3-4 month old mice. M4In1Rev- and PHA4-infected mice showed similar results (d,e), with moderate non supperative inflammation around the bronchioles and vasculature. M4In1-infected mice showed the same type of reaction (c) but at slightly reduced levels to those seen for M4In1Rev- or PHA4-infected mice.

In the case of the mice infected at 6 weeks, sections from only 2 mice per virus were available. All mice showed mild periobronchiolar non-supperative inflammation and vasculitis, although as before the M4In1-infected mice appeared to have less severe pathology. Again, owing to the small sample size it is difficult to draw conclusions from these results.

Figure 5.12 shows the scores for both the IFNγR$^{-/-}$ and129 mice infected with M4In1, M4In1Rev or PHA4. In the case of the IFNγR$^{-/-}$ mice large variation was observed within all sample groups. The 3-4 month old mice appear to exhibit a reduction in pathology compared to the 6-week old mice, possibly because the increased age at time of infection gives more time for development of the remaining aspects of the immune system. It appears that in the case of both the 3-4 month and the 6-week old mice the M4In1Rev and PHA4 viruses exhibit a greater level of pathology. There is no statistical difference between the M4In1 virus and the control viruses; however the small sample sizes make any analysis extremely difficult.

For wild type 129 mice infected with M4In1, M4In1Rev or PHA4, the results are similar – again, the M4In1Rev- and PHA4-infected mice show on average higher levels of pathology compared to the M4In1-infected mice. However, again the very small sample groups make any statistical analysis difficult, and while this evidence is suggestive of attenuation of the M4In1 virus in the lung, it is not conclusive.

5.3.9 Investigation of Novel Transcripts in the Region of the M4In1 Mutation

Following infection of BHK-21 and OMK cells with MHV-68, Dutia *et al.* (2004) identified a number of novel transcripts that are detectable with a probe spanning part of the left end of the genome (nt 106-1517). These include 4.3 kb and 3.2 kb transcripts present in low abundance in the mRNA fraction. Introduction of mutations into the left hand end of the genome in the region of the vtRNAs and M1 can result in the disruption of these transcripts and the presence of alternative sized RNA molecules, potentially as a result of aberrant processing.

To determine if these transcripts are disrupted by the mutation in the M4In1 virus OMK cells were infected at a M.O.I. of 5 with either M4In1, M4In1Rev, MHV-76,

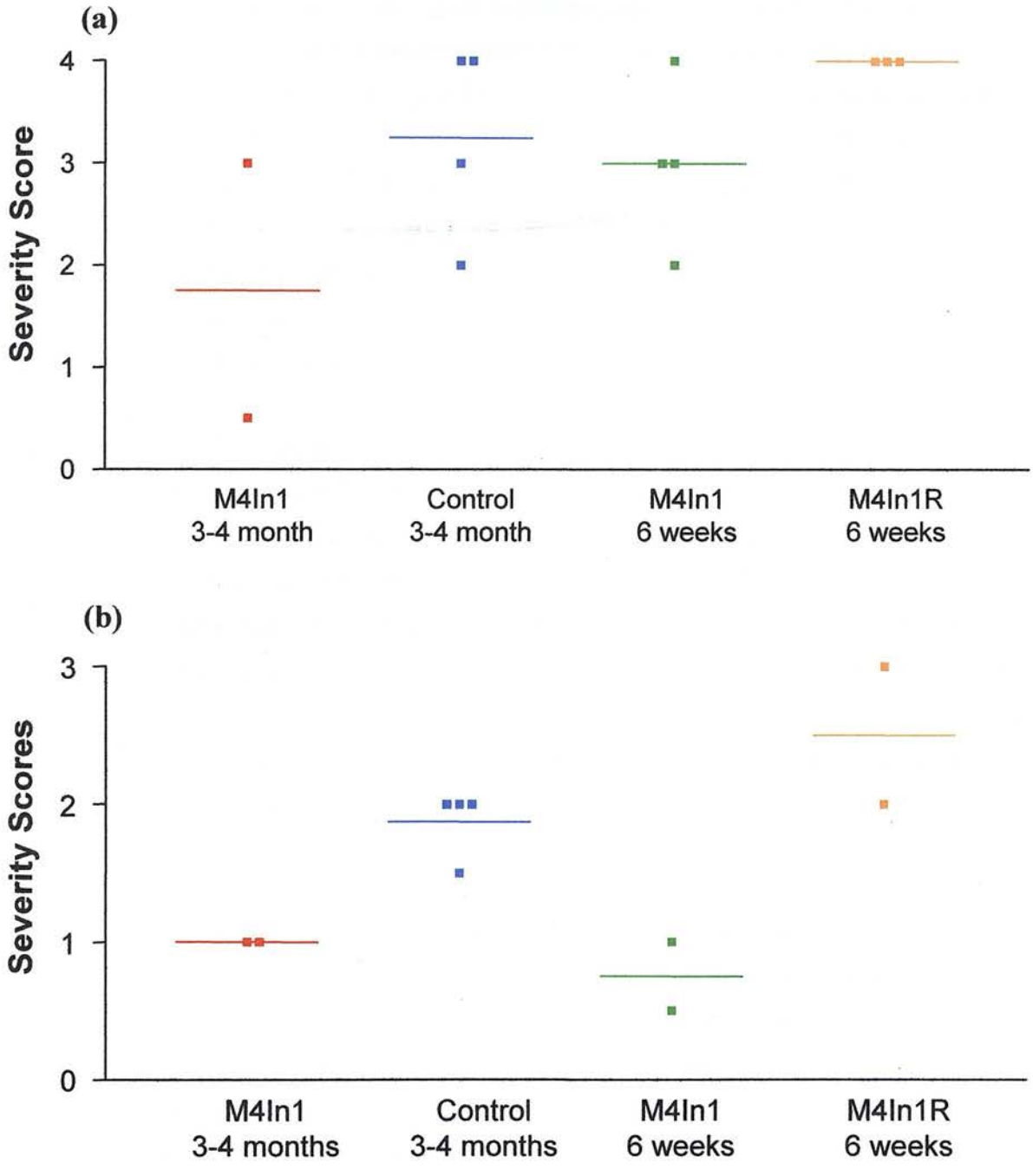

Figure 5.12 The M4In1 virus causes attenuated pathology in the lungs following infection of both IFNγR-/- and 129 mice. Mice aged 3-4 months or 6 weeks old were infected intransally with either M4In1, M4In1Rev or PHA4 (samples labelled "control" consist of 2 M4In1Rev- and 2 PHA4-infected mice). At 12-13 days post-infection lungs were removed and sections prepared that were stained with H&E. Sections were then scored blind for the severity of pathology. For both IFNγR-/- (a) and 129 (b) mice the M4In1 virus showed attenuated pathology in both mature and juvenile mice.

MHV-68 (g2.4) or PHA4. Uninfected control cells were set up in parallel. OMK cells were used because these appear to produce higher levels of the unidentified transcripts (B Dutia, personal communication). Cells were incubated overnight before the RNA was harvested and prepared for Northern blotting according to the method given in chapter 2 section 4.5. The blot was probed using pEH1.4 (Dutia *et al.*, 1999), corresponding to genome co-ordinates 106-1517. Despite washing the blot under increasingly stringent conditions it was impossible to remove large amounts of non-specific hybridisation and therefore the unique transcripts could not be detected. It was not possible to determine if these transcripts had been altered by the presence of the M4In1 mutation.

5.4 Discussion

Previous studies on the pathological features of MHV-68 controlled by the left end have focussed on the clearly defined open reading frames. We have shown that mutation in a presumed non-coding region can alter the pathogenesis of MHV-68. This region does not appear to control transcription levels of neighbouring genes and yet is capable of substantially altering pathology in the lung. The phenotype observed does not correspond to any phenotype previously observed in any of the other unique genes of MHV-68. It is possible that the mutation has disrupted one of the more recently identified transcripts in this region but our studies were unable to determine if this is the case.

The role of the region at genomic co-ordinate 8409 seems to primarily affect pathology in the lung at around 12-13 days post-infection. The M4In1 mutation results in attenuation of pathology at this time point, although this difference is less apparent by d20 and no difference is observed by d40 (previous unpublished study by B. Gangadharan following infection of 3-4 month old mice with M4In1, M4In1Rev or PHA4, data not shown). This suggests the role for the region around co-ordinate 8409 is limited to the acute phase of the infection.

Following infection of 3-4 month old mice, increased viral titres are detected in M4In1-infected 129 mice at d3. By d5, no significant difference is detectable between M4In1- and control-infected 129 mice. However, M4In1 is cleared by d9, while wild-type controls are not completely cleared until d12. While not shown in this

experiment to be statistically significantly different, this phenotype would appear to be reiterated in IFNγR$^{-/-}$ mice. This suggests that M4In1 may have initial replication advantage, which is followed by more rapid clearance from the lung.
Similar results have been obtained previously following infection of BALB/c mice aged 4-5 weeks (B. Dutia, unpublished data). Intranasal infection with M4In1 produces higher viral titres at d1 compared to infection with M4In1Rev, indicating an initial replication advantage. Unlike in the 129 mice, there are no obvious differences in viral titres by d3, and both M4In1 and M4In1Rev are cleared by d10. This could be due to a difference in the host response as a result of strain differences, however as this experiment has not been repeated it is difficult to draw conclusions on this apparent difference.

The pathology observed in the lungs of M4In1-infected mice aged 3-4 months is less severe than that observed in the control-infected mice at d12 in both IFNγR$^{-/-}$ and 129 mice. However, differences between 129 mice infected with M4In1 or a control virus are small, and repetition of this experiment using a larger sample group is necessary to determine if M4In1 is attenuated in the lungs of these mice.

The repetition of this experiment using juvenile mice produced results that are difficult to interpret. The high viral titres in M4In1Rev-infected IFNγR$^{-/-}$ mice at d9 is most likely due to the use of extremely sick mice at this time point rather than a true difference between M4In1 and M4In1Rev. The lack of clearance of M4In1 from the lungs of IFNγR$^{-/-}$ mice at d13 is again most likely a feature of the onset of severe disease rather than a true difference between M4In1 and M4In1Rev. However, it is worth noting that the onset of disease in M4In1-infected IFNγR$^{-/-}$ mice was delayed compared to M4In1Rev-infected mice, which would indicate that M4In1 is attenuated compared to wild-type virus. M4In1-infected IFNγR$^{-/-}$ mice show onset of severe illness later than M4In1Rev-infected mice, and fewer M4In1-infected mice die, again indicating that M4In1 is attenuated *in vivo*.
As before, the limited sample sizes for 129 mice infected at 6 weeks old does not allow for any firm conclusions to be drawn. While our initial results suggest that M4In1 is also attenuated in the lungs of these mice further studies are required to

demonstrate that the phenotype observed in the IFNγR$^{-/-}$ mice is also present in wild-type 129 mice.

The attenuated lung pathology at d13 coupled with earlier viral clearance from the lung in M4In1-infected mice would suggest the mutation could have altered an immune evasion/modulation gene. Owing to the proximity of the mutation to the known immune evasion gene M3, this gene would appear a likely candidate for potential upregulation. All previous studies investigating the role of M3 in the lung have determined that disruption of the gene does not affect viral replication (van Berkel *et al.*, 2002; Bridgeman *et al.*, 2001); however these studies have not investigated if lung pathology is altered. Therefore there is a possibility that alteration in M3 transcription may result in a change in lung pathology without affecting viral replication. Our results in the spleen do not support the suggestion that the M4In1 mutation is altering M3 transcription in any way; however we were unable to ascertain if this was the case in the lung. This leaves an alteration in M3 transcription in the lung a possible explanation for the M4In1 phenotype. There is evidence that viral transcription in the lung is regulated differently to transcription in the spleen at late time points post-infection (Roy *et al.*, 2000; Wakeling *et al.*, 2001). It is therefore possible that the M4In1 mutation is able to affect transcription in the lung at earlier time points without affecting it in the spleen, and we were not able to investigate viral transcription in the lung.

Another explanation for the altered lung pathology seen on infection of M4In1 relates to the existence of as-yet uncharacterised transcripts in the region of this mutation. There are two transcripts identified *in vitro* by Dutia *et al.* (2004) of 4.3 kb and 3.2 kb that span this region and are present in the mRNA fraction. Our attempts to isolate these transcripts from OMK cells infected with M4In1 or control viruses were unsuccessful; however it would be interesting to determine if either of the transcripts were disrupted by the presence of the M4In1 mutation. Results suggest that the mutation disrupts an immunomodulatory function of the virus, based on the alteration of lung pathology and the lack of any affect on viral replication. If either or both of these transcripts are shown to be disrupted or altered in the M4In1 virus, this would

suggest a potential function for them. However at present this is speculative as disruption to the transcripts has not been demonstrated in the M4In1 virus.

M4In1 is able to traffic normally to the spleen and establishes infection at equivalent levels to wild-type MHV-68. The latest time point studied was 40 days post-infection, and at this later time point the M4In1 mutation had no effect on viral load. Previous studies have not indicated that this mutation affects reactivation in the spleen in any way (B. Dutia, unpublished data), and spleen sections from d13–d40 show no differences in IFNγR$^{-/-}$ and 129 mice infected with M4In1, M4In1Rev or PHA4 (B. Gangadharan, unpublished data). It would therefore appear that the effects of the M4In1 mutation are limited to the acute infection of the lung.

Several naturally occurring deletion mutants of MHV-68 have been isolated, including MHV-72. This virus lacks genes M1, M2 and M3, and also the tRNA-like molecules. The development of tumours at late time points post-infection in mice infected with this virus may be attributed to the presence of a 2.5 kb region present in MHV-72 but absent in MHV-76 (Oda *et al.*, 2005). This 2.5 kb region includes the M4 gene and the upstream region including the area of the M4In1 mutation.

A study where the M4 gene was inserted into the left-hand end of the MHV-76 genome did not investigate the long-term effects of the addition M4 to the MHV-76 genome (Townsley *et al.*, 2004). Therefore it is not possible to determine at this point whether the tumorigenic phenotype observed following infection with MHV-72 is attributable to either M4 or the upstream sequences. Our studies using the M4In1 virus did not investigate tumorigenesis at late time points, although this may also have provided some insight into the role of the M3-M4 intergenic region in the development of tumours following viral infection.

In conclusion we have identified a region of the MHV-68 genome that contributes to pathology in the lung at early time points. This region may contain as yet uncharacterised transcripts that are altered by the mutation carried by the M4In1 virus. Further studies are required to determine if this is the case, or if the mutation in the M4In1 virus is altering viral pathogenesis in some other way.

Chapter 6: Conclusions

Developing a greater understanding of MHV-68 pathogenesis allows insights into the mechanisms used by other clinically important herpesviruses. In particular, MHV-68 persistence in the lung may be relevant to at least one human syndrome. Idiopathic pulmonary fibrosis (IPF) is characterised by progressive fibrosis in the lung in association with varying degrees of inflammation (Katzenstein *et al.*, 1998). A number of different drug regimes have been investigated as potential treatment for this syndrome, but at present there is no conclusive evidence that any of these methods are effective, and many of these treatments are associated with significant side effects. At present lung transplantation is the only therapy shown to increase long-term survival in IPF patients; however the availability of such transplants limits the number of patients that can receive this treatment (reviewed by Walter *et al.*, 2006).

The underlying cause of IPF is unknown. However several studies have demonstrated the presence of herpesvirus DNA in the lungs of a significant percentage of IPF patients (Stewart *et al.*, 1999b), with up to 97% of patients identified as having one or more herpesviruses in the lung in one study (Tang *et al.*, 2003). Most commonly associated with IPF are CMV, EBV, HHV-7 and HHV-8. Interestingly, a syndrome extremely similar to IPF can be reproduced in mouse lungs following infection with MHV-68. This syndrome is seen following infection of mice treated with bleomycin (Lok *et al.*, 2002), or following infection of IFNγR$^{-/-}$ mice (Mora *et al.*, 2005), but in not following infection of untreated or immunocompetent mice. This indicates that herpesvirus infection alone is not sufficient to drive the IPF-like syndrome observed following MHV-68 infection, but in association with injury to the lung tissue or immunosuppression lung fibrosis can develop.

As a potential factor in the development of IPF, investigation of herpesvirus infection of the lung is increasingly important. The murine IFNγR$^{-/-}$ model shows that MHV-68 infection can produce a syndrome with striking similarities to human IPF. Therefore study of MHV-68 in the lung may allow further understanding of disease onset and progression, particularly in the early stages of the disease where clinical symptoms may not yet be apparent. Our study has identified a number of viral factors that affect herpesvirus persistence in the lung, and may provide potentially targets for treatment

in the future. The viral thymidine kinase gene is common to all herpesviruses, and in the MHV-68 model the loss of this gene significantly reduces long-term viral load. The MHV-68 ORF73 gene has a similar effect on levels of viral persistence at late time points, and has a homologue in KSHV, a possible causative agent of IPF.

Our study also shows that reactivation from latency may be important for maintenance of viral load during long-term lung infection. Experiments involving the M11- and ORF72-deficient viruses need to be repeated with larger sample groups to improve statistical analysis. Reactivation from latency is enhanced in mice deficient in the type II interferon response (Steed *et al.*, 2006), and therefore may be an important factor in the development of the IPF-like disease in IFNγR$^{-/-}$ mice.

Despite the increasing evidence that the presence of a herpesvirus in the lung is associated with IPF, there does not appear to be any investigation into the effect of anti-viral treatment on IPF progression. This would be an interesting experiment to carry out in the IFNγR$^{-/-}$ mouse model of lung fibrosis, to determine if disease outcome is affected by this treatment. IFNγ-1b has been investigated as a treatment for IPF, as the downregulation of TGF-β by type II interferon may prevent TGF-β-driven fibroblast proliferation and collagen synthesis. While this treatment has shown some promise in clinical trials, the effects appear to be limited to individuals in the early stages of disease, and the small sample sizes available for trials do not allow easy analysis of the effectiveness of treatment. This is an experiment that could easily be repeated in the mouse model to overcome the problem of small sample sizes.

While HCMV has been suggested as a causative agent of IPF, this has not been investigated in the murine CMV model. As with the gamma-2-herpesvirus MHV-68, the lungs have been shown to be a major reservoir of MCMV (Balthesen *et al.*, 1993; Kurz *et al.*, 1997), but whether this virus is able to induce fibrosis in the lungs of IFNγR$^{-/-}$ mice is unknown. This experiment might provide further clues as to the potential involvement of CMV in development of IPF.

As well as identification of viral genes common to a number of herpesviruses that play a role during infection of the lung, we have also identified a factor in the unique

region of the MHV-68 genome involved in acute infection of the lung. The introduction of a mutation at genome co-ordinate 8409 in an apparently non-coding region of the genome surprisingly alters the viral phenotype in the lung around d13 post-infection. Introduction of 19 bp containing 3 in-frame stop codons in this region results in less severe pathology in the lungs of mice infected with this mutant virus, and reduced mortality in juvenile mice compared to infection with wild-type virus.

Initial investigations of neighbouring genes revealed no deficit in transcription *in vitro* or *in vivo* in the spleen. However the observed phenotype was in the lung and we were unable to determine if either M3 or M4 transcription were affected by the M4In1 mutation in this organ. As mentioned previously, there are several examples of MHV-68 genes that are regulated differently in the lung and the spleen.

The identification of two previously unidentified transcripts by Dutia *et al.* (2004) in the region of the mutation provides a possible explanation for the attenuated phenotype observed in the lungs of M4In1-infected mice. The position of these transcripts would suggest the possibility of overlapping genes, a feature observed in the genomes of other members of the herpesvirus family (e.g. HSV-1 $\gamma_1$34.5 and ORFs P and O) (Roizman & Pellet, 2001). While we were unable to demonstrate the presence of the transcripts, or their disruption as a result of the mutation in the M4In1 virus, this is still a possible explanation for the observed phenotype. Repetition of experiments to investigate the presence of these transcripts following *in vitro* infection with M4In1 should resolve this question. In the event that one or both of the transcripts are altered in the M4In1 virus, the next stage of investigation would involve more exact characterisation of these transcripts.

An alternative possibility is that the introduction of the mutation at 8409 bp is affecting the activity of genes outside the immediate region. At present there are no examples in the MHV-68 genome of promoter or enhancer regions acting at a significant distance to the target gene; however that does not mean this is not possible. Use of real-time PCR has allowed investigation of the neighbouring M3 and M4 genes, and the same technique could be applied to determine if the M4In1 mutation is affecting transcription of other MHV-68 genes. As the M4In1 phenotype is most

obvious in the lung, investigation of transcription in this organ would be more likely to highlight any differences between the M4In1 and wild-type viruses. Genes with a potential role in the lung include M1 (see chapter 4), M4 (Evans *et al.*, 2006; Townsley *et al.*, 2004) and K3 (Stevenson *et al.*, 2002). Given that the M4In1 phenotype appears to affect lung pathology without significant changes in viral replication, a gene or genes involved in modulation of the host immune response would appear most likely to produce the altered phenotype.

As well as apparently untranscribed regions involved in viral pathology, the left end of the MHV-68 genome also contains a number of defined ORFs whose function has not yet been fully defined. Of the four ORFs in this region the M1 gene is the least investigated, and elucidation of its role during infection may provide further insights into viral pathogenesis.

Despite early indications that the M1 gene was a homologue of the poxvirus serpin SPI-1, a gene with known anti-apoptotic properties, the functional regions of the serpin are absent in M1 (Virgin *et al.*, 1997; Bowden *et al.*, 1997). While the anti-apoptotic properties of M1 have not been investigated, it appears that despite a possible common origin to SPI-1, M1 has evolved an alternative function, or at least a function independent of the hinge domain and reactive site loop of the serpin gene.

Initial results indicate an important role for M1 during acute infection of the lung. In the absence of the M1 gene, viral titres are significantly elevated at all time points studied, and the virus is cleared more slowly. While a number of genes have been identified whose absence decreases viral replication during acute infection (including ORF54 [Song *et al.*, 2005], ORF21 [Coleman *et al.*, 2003] and ORF27 [May *et al.*, 2005a]), no other MHV-68 gene has been identified whose absence results in increased viral replication. This suggests a novel function for M1 in control of viral replication in the lung, acting to prevent excess replication in this organ. Reduction or inhibition of replication may result in fewer targets for the immune response and hence aid viral persistence and possible spread to other organs. Studies are ongoing in other laboratories to investigate levels of M1 transcription in the lung, but results are as yet unpublished.

M1 also appears to play a substantial role in the spleen. Loss of the gene results in a severe splenomegaly deficit in association with a failure to increase the number of splenocytes. During acute phase latency viral load is reduced, and yet *ex vivo* reactivation from latency is elevated. A reduction in viral load in the spleen during acute phase latency is a observed following disruption of the M4 gene (Evans *et al.*, 2006; Geere *et al.*, 2006), indicating that control of viral load in the spleen is attributable to more than one viral factor. The secreted glycoprotein M4 shares structural properties with the M1 protein, indicating a possible link between the properties of these two genes (Alexander *et al.*, 2002). However, the enhanced reactivation from latency has only been demonstrated in M1-deficient viruses (Clambey *et al.*, 2000), demonstrating that M1 and M4 are not functionally redundant. Our preliminary results confirm the findings by Clambey *et al.*, and indicate that the normal role of M1 in the spleen involves reduction or inhibition of reactivation. Whether this occurs by controlling the host cell environment to maintain the virus in a quiescent state, or by inhibiting viral factors that drive reactivation remains to be investigated. Ongoing studies in our laboratory to determine the crystal structure of M1 may provide further information as to the potential binding sites of this protein and hence determine its interactions with other proteins.

The inability of the M1Δ virus to drive splenomegaly may indicate a role for this gene in driving host cell proliferation. A number of viral genes are known homologues of host cell cycle proteins (e.g. v-cyclin) but no homology to host cell cycle proteins has been demonstrated for M1. This would suggest M1 may drive cell cycle progression by an as-yet undiscovered mechanism, or that M1 is able to activate other viral factors that are able to drive splenomegaly. Again, further studies into the structure of M1 may provide insight into M1 interactions with other proteins.

Previous structural and sequence analysis have demonstrated similarities between the M1 and M3 genes of MHV-68 (van Berkel *et al.*, 1999; Alexander *et al.*, 2002). The secreted M3 protein is a broad spectrum chemokine binding protein, and is able to disrupt *in vitro* chemotaxis of lymphocytes (Jensen *et al.*, 2003). However, despite apparent similarities between the two genes, M3 has no obvious role during acute infection in the lung, or in establishment of or reactivation from latency, properties

that are key features of the M1 gene. M1 also lacks residues important in mediating M3 interaction with chemokines, indicating that this aspect of the M3 protein is not also possessed by M1. Therefore it appears unlikely that M1 and M3 are in any way functionally redundant.

It is therefore clear that further studies are required to investigate the different areas of MHV-68 pathogenesis investigated in this thesis. While a number of genes involved in long term persistence in the lung have been identified, repetition of these experiments are necessary to confirm results. The left end of the MHV-68 genome is important in viral pathogenesis, but contains a number of regions whose function remains to be defined. These include both defined ORFs and apparently non-coding regions. Further investigation of this region will provide insights into MHV-68 pathogenesis.

References

Ackermann, M. (2006). "Pathogenesis of gammaherpesvirus infections." Vet Microbiol **113**(3-4): 211-22.

Adler, H., M. Messerle, *et al.*. (2001). "Virus reconstituted from infectious bacterial artificial chromosome (BAC)-cloned murine gammaherpesvirus 68 acquires wild-type properties in vivo only after excision of BAC vector sequences." J Virol **75**(12): 5692-6.

Adler, H., M. Messerle, *et al.*. (2000). "Cloning and mutagenesis of the murine gammaherpesvirus 68 genome as an infectious bacterial artificial chromosome." J Virol **74**(15): 6964-74.

Ahn, J. W., K. L. Powell, *et al.*. (2002). "Gammaherpesvirus lytic gene expression as characterized by DNA array." J Virol **76**(12): 6244-56.

Akula, S. M., F. Z. Wang, *et al.*. (2001). "Human herpesvirus 8 interaction with target cells involves heparan sulfate." Virology **282**(2): 245-55.

Albrecht, J. C., J. Nicholas, *et al.*. (1992). "Primary structure of the herpesvirus saimiri genome." J Virol **66**(8): 5047-58.

Alexander, J.M., C.A. Nelson, *et al.*. (2002). "Structural basis of chemokine sequestration by a herpesvirus decoy receptor." Cell **111**: 343-356

Allen, M. D., L. S. Young, *et al.*. (2005). "The Epstein-Barr virus-encoded LMP2A and LMP2B proteins promote epithelial cell spreading and motility." J Virol **79**(3): 1789-802.

Arrand, J. R., L. Rymo, *et al.*. (1981). "Molecular cloning of the complete Epstein-Barr virus genome as a set of overlapping restriction endonuclease fragments." Nucleic Acids Res **9**(13): 2999-3014.

Babcock, G. J., D. Hochberg, *et al.*. (2000). "The expression pattern of Epstein-Barr virus latent genes in vivo is dependent upon the differentiation stage of the infected B cell." Immunity **13**(4): 497-506.

Balthesen, M., M. Messerle, *et al.*. (1993). "Lungs are a major organ site of cytomegalovirus latency and recurrence." J Virol **67**(9): 5360-6.

Barton, E. S., M. L. Lutzke, *et al.*. (2005). "Alpha/beta interferons regulate murine gammaherpesvirus latent gene expression and reactivation from latency." J Virol **79**(22): 14149-60.

Belz, G. T., H. Liu, *et al.*. (2003). "Absence of a functional defect in CD8+ T cells during primary murine gammaherpesvirus-68 infection of I-A(b-/-) mice." J Gen Virol **84**(Pt 2): 337-41.

Ben-Ezra, J., D. A. Johnson, *et al.*. (1991). "Effect of fixation on the amplification of nucleic acids from paraffin-embedded material by the polymerase chain reaction." J Histochem Cytochem **39**(3): 351-4.

Blasdell, K., C. McCracken, *et al.*. (2003). "The wood mouse is a natural host for Murid herpesvirus 4." J Gen Virol **84**(Pt 1): 111-3.

Blaskovic, D., M. Stancekova, *et al.*. (1980). "Isolation of five strains of herpesviruses from two species of free living small rodents." Acta Virol **24**(6): 468.

Boname, J. M. and P. G. Stevenson (2001). "MHC class I ubiquitination by a viral PHD/LAP finger protein." Immunity **15**(4): 627-36.

Borah, S., S. C. Verma, *et al.*. (2004). "ORF73 of herpesvirus saimiri, a viral homolog of Kaposi's sarcoma-associated herpesvirus, modulates the two cellular tumor suppressor proteins p53 and pRb." J Virol **78**(19): 10336-47.

Bortz, E., J. P. Whitelegge, *et al.*. (2003). "Identification of proteins associated with murine gammaherpesvirus 68 virions." J Virol **77**(24): 13425-32.

Boshoff, C. and Y. Chang (2001). "Kaposi's sarcoma-associated herpesvirus: a new DNA tumor virus." Annu Rev Med **52**: 453-70.

Bowden, R. J., J. P. Simas, *et al.*. (1997). "Murine gammaherpesvirus 68 encodes tRNA-like sequences which are expressed during latency." J Gen Virol **78 (Pt 7)**: 1675-87.

Bridgeman, A., P. G. Stevenson, *et al.*. (2001). "A secreted chemokine binding protein encoded by murine gammaherpesvirus-68 is necessary for the establishment of a normal latent load." J Exp Med **194**(3): 301-12.

Brooks, M. A., A. N. Ali, *et al.*. (1995). "A rabbitpox virus serpin gene controls host range by inhibiting apoptosis in restrictive cells." J Virol **69**(12): 7688-98.

Brown, H. J., M. J. Song, *et al.*. (2003). "NF-kappaB inhibits gammaherpesvirus lytic replication." J Virol **77**(15): 8532-40.

Bustin, S. A. (2005). "Real-time, fluorescence-based quantitative PCR: a snapshot of current procedures and preferences." Expert Rev Mol Diagn **5**(4): 493-8.

Callan, M. F. (2004). "The immune response to Epstein-Barr virus." Microbes Infect **6**(10): 937-45.

Campadelli-Fiume, G., F. Cocchi, *et al.*. (2000). "The novel receptors that mediate the entry of herpes simplex viruses and animal alphaherpesviruses into cells." Rev Med Virol **10**(5): 305-19.

Cardin, R. D., J. W. Brooks, *et al.*. (1996). "Progressive loss of CD8+ T cell-mediated control of a gamma-herpesvirus in the absence of CD4+ T cells." J Exp Med **184**(3): 863-71.

Carroll, M. C. and M. B. Fischer (1997). "Complement and the immune response." Curr Opin Immunol **9**(1): 64-9.

Carroll, P. A., E. Brazeau, *et al.*. (2004). "Kaposi's sarcoma-associated herpesvirus infection of blood endothelial cells induces lymphatic differentiation." Virology **328**(1): 7-18.

Chang, Y., E. Cesarman, *et al.*. (1994). "Identification of herpesvirus-like DNA sequences in AIDS-associated Kaposi's sarcoma." Science **266**(5192): 1865-9.

Chesler, D. A. and C. S. Reiss (2002). "The role of IFN-gamma in immune responses to viral infections of the central nervous system." Cytokine Growth Factor Rev **13**(6): 441-54.

Ciampor, F., M. Stancekova, *et al.*. (1981). "Electron microscopy of rabbit embryo fibroblasts infected with herpesvirus isolates from Clethrionomys glareolus and Apodemus flavicollis." Acta Virol **25**(2): 101-7.

Clambey, E. T., H. W. t. Virgin, *et al.*. (2000). "Disruption of the murine gammaherpesvirus 68 M1 open reading frame leads to enhanced reactivation from latency." J Virol **74**(4): 1973-84.

Clambey, E. T., H. W. t. Virgin, *et al.*. (2002). "Characterization of a spontaneous 9.5-kilobase-deletion mutant of murine gammaherpesvirus 68 reveals tissue-specific genetic requirements for latency." J Virol **76**(13): 6532-44.

Cliffe, A. R. (2005). The biological role of viral tRNA-like molecules in a murine gammaherpesvirus infection. Laboratory for Clinical & Molecular Virology. Edinburgh, University of Edinburgh. **PhD**.

Coleman, H. M., B. de Lima, *et al.*. (2003). "Murine gammaherpesvirus 68 lacking thymidine kinase shows severe attenuation of lytic cycle replication in vivo but still establishes latency." J Virol **77**(4): 2410-7.

Coleman, H. M., S. Efstathiou, *et al.*. (2005). "Transcription of the murine gammaherpesvirus 68 ORF73 from promoters in the viral terminal repeats." J Gen Virol **86**(Pt 3): 561-74.

Coppola, M. A., E. Flano, *et al.*. (1999). "Apparent MHC-independent stimulation of CD8+ T cells in vivo during latent murine gammaherpesvirus infection." J Immunol **163**(3): 1481-9.

Coulter, L. J., H. Wright, *et al.*. (2001). "Molecular genomic characterization of the viruses of malignant catarrhal fever." J Comp Pathol **124**(1): 2-19.

Crawford, D. H. (2001). "Biology and disease associations of Epstein-Barr virus." Philos Trans R Soc Lond B Biol Sci **356**(1408): 461-73.

Dal Canto, A. J., H. W. t. Virgin, *et al.*. (2000). "Ongoing viral replication is required for gammaherpesvirus 68-induced vascular damage." J Virol **74**(23): 11304-10.

Damania, B. and R. C. Desrosiers (2001). "Simian homologues of human herpesvirus 8." Philos Trans R Soc Lond B Biol Sci **356**(1408): 535-43.

de Lima, B. D., J. S. May, *et al.*. (2005). "Murine gammaherpesvirus 68 bcl-2 homologue contributes to latency establishment in vivo." J Gen Virol **86**(Pt 1): 31-40.

de Lima, B. D., J. S. May, *et al.*. (2004). "Murine gammaherpesvirus 68 lacking gp150 shows defective virion release but establishes normal latency in vivo." J Virol **78**(10): 5103-12.

Desrosiers, R. C., V. G. Sasseville, *et al.*. (1997). "A herpesvirus of rhesus monkeys related to the human Kaposi's sarcoma-associated herpesvirus." J Virol **71**(12): 9764-9.

Dewals, B., L. Gillet, *et al.*. (2005). "Antibodies against bovine herpesvirus 4 are highly prevalent in wild African buffaloes throughout eastern and southern Africa." Vet Microbiol **110**(3-4): 209-20.

Dittmer, D., C. Stoddart, *et al.*. (1999). "Experimental transmission of Kaposi's sarcoma-associated herpesvirus (KSHV/HHV-8) to SCID-hu Thy/Liv mice." J Exp Med **190**(12): 1857-68.

Dittmer, D. P., C. M. Gonzalez, *et al.*. (2005). "Whole-genome transcription profiling of rhesus monkey rhadinovirus." J Virol **79**(13): 8637-50.

Dutia, B. M., D. J. Allen, *et al.*. (1999). "Type I interferons and IRF-1 play a critical role in the control of a gammaherpesvirus infection." Virology **261**(2): 173-9.

Dutia, B. M., D. J. Roy, *et al.*. (2004). "Identification of a region of the virus genome involved in murine gammaherpesvirus 68-induced splenic pathology." J Gen Virol **85**(Pt 6): 1393-400.

Dutia, B. M., J. P. Stewart, *et al.*. (1999). "Kinetic and phenotypic changes in murine lymphocytes infected with murine gammaherpesvirus-68 in vitro." J Gen Virol **80 (Pt 10)**: 2729-36.

Ebrahimi, B., B. M. Dutia, *et al.*. (2001). "Murine gammaherpesvirus-68 infection causes multi-organ fibrosis and alters leukocyte trafficking in interferon-gamma receptor knockout mice." Am J Pathol **158**(6): 2117-25.

Ebrahimi, B., B. M. Dutia, *et al.*. (2003). "Transcriptome profile of murine gammaherpesvirus-68 lytic infection." J Gen Virol **84**(Pt 1): 99-109.

Efstathiou, S., Y. M. Ho, *et al.*. (1990). "Cloning and molecular characterization of the murine herpesvirus 68 genome." J Gen Virol **71 (Pt 6)**: 1355-64.

Efstatiou, S., C.M.Preston (2005). "Towards an understanding of the molecular basis of herpes simplex virus latency,." Virus Research **111**: 108-119.

Ehtisham, S., N. P. Sunil-Chandra, *et al.*. (1993). "Pathogenesis of murine gammaherpesvirus infection in mice deficient in CD4 and CD8 T cells." J Virol **67**(9): 5247-52.

Emery, V. C., A. V. Cope, *et al.*. (1999). "The dynamics of human cytomegalovirus replication in vivo." J Exp Med **190**(2): 177-82.

Emini, E. A., J. Luka, *et al.*. (1986). "Establishment and characterization of a chronic infectious mononucleosislike syndrome in common marmosets." J Med Virol **18**(4): 369-79.

Ensser, A., R. Pflanz, *et al.*. (1997). "Primary structure of the alcelaphine herpesvirus 1 genome." J Virol **71**(9): 6517-25.

Epstein, M. A., B. G. Achong, *et al.*. (1964). "Virus Particles in Cultured Lymphoblasts from Burkitt's Lymphoma." Lancet **15**: 702-3.

Epstein, M. A., A. J. Morgan, *et al.*. (1985). "Protection of cottontop tamarins against Epstein-Barr virus-induced malignant lymphoma by a prototype subunit vaccine." Nature **318**(6043): 287-9.

Evans, A. G., N. J. Moorman, *et al.*. (2006). "The M4 gene of gammaHV68 encodes a secreted glycoprotein and is required for the efficient establishment of splenic latency." Virology **344**(2): 520-31.

Farrell, P. J., M. Hollyoake, *et al.*. (1997). "Direct demonstration of persistent Epstein-Barr virus gene expression in peripheral blood of infected common marmosets and analysis of virus-infected tissues in vivo." J Gen Virol **78 (Pt 6)**: 1417-24.

Feichtinger, H., E. E. Kaaya, *et al.*. (1992). "[Opportunistic malignant lymphomas in SIV infected primates--a model for Epstein-Barr virus associated lymphomas in AIDS]." Verh Dtsch Ges Pathol **76**: 189-93.

Fickenscher, H. and B. Fleckenstein (2001). "Herpesvirus saimiri." Philos Trans R Soc Lond B Biol Sci **356**(1408): 545-67.

Flano, E., S. M. Husain, *et al.*. (2000). "Latent murine gamma-herpesvirus infection is established in activated B cells, dendritic cells, and macrophages." J Immunol **165**(2): 1074-81.

Flano, E., I. J. Kim, *et al.*. (2003). "Differential gamma-herpesvirus distribution in distinct anatomical locations and cell subsets during persistent infection in mice." J Immunol **170**(7): 3828-34.

Flano, E., I. J. Kim, *et al.*. (2002). "Gamma-herpesvirus latency is preferentially maintained in splenic germinal center and memory B cells." J Exp Med **196**(10): 1363-72.

Flano, E., D. L. Woodland, *et al.*. (2001). "Analysis of virus-specific CD4(+) t cells during long-term gammaherpesvirus infection." J Virol **75**(16): 7744-8.

Fowler, P. and S. Efstathiou (2004). "Vaccine potential of a murine gammaherpesvirus-68 mutant deficient for ORF73." J Gen Virol **85**(Pt 3): 609-13.

Fowler, P., S. Marques, *et al.*. (2003). "ORF73 of murine herpesvirus-68 is critical for the establishment and maintenance of latency." J Gen Virol **84**(Pt 12): 3405-16.

Fruh, K., E. Bartee, *et al.*. (2002). "Immune evasion by a novel family of viral PHD/LAP-finger proteins of gamma-2 herpesviruses and poxviruses." Virus Res **88**(1-2): 55-69.

Furman, M. H. and H. L. Ploegh (2002). "Lessons from viral manipulation of protein disposal pathways." J Clin Invest **110**(7): 875-9.

Gangappa, S., L. F. van Dyk, *et al.*. (2002). "Identification of the in vivo role of a viral bcl-2." J Exp Med **195**(7): 931-40.

Garber, D. A., P. A. Schaffer, *et al.*. (1997). "A LAT-associated function reduces productive-cycle gene expression during acute infection of murine sensory neurons with herpes simplex virus type 1." J Virol **71**(8): 5885-93.

Gasper-Smith, N. and K. L. Bost (2004). "Initiation of the host response against murine gammaherpesvirus infection in immunocompetent mice." Viral Immunol **17**(4): 473-80.

Geere, H. M. (2004). Characterisation of the mutations within the coding region of the M4 gene in MHV-68. Laboratory for Clinical & Molecular Virology. Edinburgh, University of Edinburgh. **MSc**.

Geere, H. M., Y. Ligertwood, *et al.*. (2006). "The M4 gene of murine gammaherpesvirus 68 modulates latent infection." J Gen Virol **87**(Pt 4): 803-7.

Goodbourn, S., L. Didcock, *et al.*. (2000). "Interferons: cell signalling, immune modulation, antiviral response and virus countermeasures." J Gen Virol **81**(Pt 10): 2341-64.

Grandvaux, N., B. R. tenOever, *et al.*. (2002). "The interferon antiviral response: from viral invasion to evasion." Curr Opin Infect Dis **15**(3): 259-67.

Granzow, H., B. G. Klupp, *et al.*. (2001). "Egress of alphaherpesviruses: comparative ultrastructural study." J Virol **75**(8): 3675-84.

Greenspan, J. S., D. Greenspan, *et al.*. (1985). "Replication of Epstein-Barr virus within the epithelial cells of oral "hairy" leukoplakia, an AIDS-associated lesion." N Engl J Med **313**(25): 1564-71.

Gregory, C. D., M. Rowe, *et al.*. (1990). "Different Epstein-Barr virus-B cell interactions in phenotypically distinct clones of a Burkitt's lymphoma cell line." J Gen Virol **71 (Pt 7)**: 1481-95.

Guasparri, I., S. A. Keller, *et al.*. (2004). "KSHV vFLIP is essential for the survival of infected lymphoma cells." J Exp Med **199**(7): 993-1003.

Gupta, A., J. J. Gartner, *et al.*. (2006). "Anti-apoptotic function of a microRNA encoded by the HSV-1 latency-associated transcript." Nature **442**(7098): 82-5.

Haan, K. M. and R. Longnecker (2000). "Coreceptor restriction within the HLA-DQ locus for Epstein-Barr virus infection." Proc Natl Acad Sci U S A **97**(16): 9252-7.

Hengge, U. R., T. Ruzicka, *et al.*. (2002). "Update on Kaposi's sarcoma and other HHV8 associated diseases. Part 1: epidemiology, environmental predispositions, clinical manifestations, and therapy." Lancet Infect Dis **2**(5): 281-92.

Herold, B. C., D. WuDunn, *et al.*. (1991). "Glycoprotein C of herpes simplex virus type 1 plays a principal role in the adsorption of virus to cells and in infectivity." J Virol **65**(3): 1090-8.

Hewitt, E. W., L. Duncan, *et al.*. (2002). "Ubiquitylation of MHC class I by the K3 viral protein signals internalization and TSG101-dependent degradation." Embo J **21**(10): 2418-29.

Honess, R. W. and B. Roizman (1974). "Regulation of herpesvirus macromolecular synthesis. I. Cascade regulation of the synthesis of three groups of viral proteins." J Virol **14**(1): 8-19.

Huggett, J., K. Dheda, *et al.*. (2005). "Real-time RT-PCR normalisation; strategies and considerations." Genes Immun **6**(4): 279-84.

Humme, S., G. Reisbach, *et al.*. (2003). "The EBV nuclear antigen 1 (EBNA1) enhances B cell immortalization several thousandfold." Proc Natl Acad Sci U S A **100**(19): 10989-94.

Husain, S. M., E. J. Usherwood, *et al.*. (1999). "Murine gammaherpesvirus M2 gene is latency-associated and its protein a target for CD8(+) T lymphocytes." Proc Natl Acad Sci U S A **96**(13): 7508-13.

Jacoby, M. A., H. W. t. Virgin, *et al.*. (2002). "Disruption of the M2 gene of murine gammaherpesvirus 68 alters splenic latency following intranasal, but not intraperitoneal, inoculation." J Virol **76**(4): 1790-801.

Janz, A., M. Oezel, *et al.*. (2000). "Infectious Epstein-Barr virus lacking major glycoprotein BLLF1 (gp350/220) demonstrates the existence of additional viral ligands." J Virol **74**(21): 10142-52.

Jenner, R. G. and C. Boshoff (2002). "The molecular pathology of Kaposi's sarcoma-associated herpesvirus." Biochim Biophys Acta **1602**(1): 1-22.

Jensen, K. K., S. C. Chen, *et al.*. (2003). "Disruption of CCL21-induced chemotaxis in vitro and in vivo by M3, a chemokine-binding protein encoded by murine gammaherpesvirus 68." J Virol **77**(1): 624-30.

Jia, Q., V. Chernishof, *et al.*. (2005). "Murine gammaherpesvirus 68 open reading frame 45 plays an essential role during the immediate-early phase of viral replication." J Virol **79**(8): 5129-41.

Johannessen, I. and D. H. Crawford (1999). "In vivo models for Epstein-Barr virus (EBV)-associated B cell lymphoproliferative disease (BLPD)." Rev Med Virol **9**(4): 263-77.

Jung, J. U., J. K. Choi, *et al.*. (1999). "Herpesvirus saimiri as a model for gammaherpesvirus oncogenesis." Semin Cancer Biol **9**(3): 231-9.

Kanda, T., M. Otter, *et al.*. (2001). "Coupling of mitotic chromosome tethering and replication competence in epstein-barr virus-based plasmids." Mol Cell Biol **21**(10): 3576-88.

Kapadia, S. B., B. Levine, *et al.*. (2002). "Critical role of complement and viral evasion of complement in acute, persistent, and latent gamma-herpesvirus infection." Immunity **17**(2): 143-55.

Kapadia, S. B., H. Molina, *et al.*. (1999). "Murine gammaherpesvirus 68 encodes a functional regulator of complement activation." J Virol **73**(9): 7658-70.

Kari, B. and R. Gehrz (1993). "Structure, composition and heparin binding properties of a human cytomegalovirus glycoprotein complex designated gC-II." J Gen Virol **74 (Pt 2)**: 255-64.

Katzenstein, A. L. and J. L. Myers (1998). "Idiopathic pulmonary fibrosis: clinical relevance of pathologic classification." Am J Respir Crit Care Med **157**(4 Pt 1): 1301-15.

Kieff E, R. A. (2001). Epstein Barr virus and its Replication.

Kim, I. J., E. Flano, *et al.*. (2003). "Maintenance of long term gamma-herpesvirus B cell latency is dependent on CD40-mediated development of memory B cells." J Immunol **171**(2): 886-92.

Kruger, J. M., P. J. Venta, *et al.*. (2000). "Prevalence of bovine herpesvirus-4 infection in cats in Central Michigan." J Vet Intern Med **14**(6): 593-7.

Kurz, S. K., M. Rapp, *et al.*. (1999). "Focal transcriptional activity of murine cytomegalovirus during latency in the lungs." J Virol **73**(1): 482-94.

Lam, N. and B. Sugden (2003). "LMP1, a viral relative of the TNF receptor family, signals principally from intracellular compartments." Embo J **22**(12): 3027-38.

Laquerre, S., R. Argnani, *et al.*. (1998). "Heparan sulfate proteoglycan binding by herpes simplex virus type 1 glycoproteins B and C, which differ in their contributions to virus attachment, penetration, and cell-to-cell spread." J Virol **72**(7): 6119-30.

Leao, J. C., A. Caterino-De-Araujo, *et al.*. (2002). "Human herpesvirus 8 (HHV-8) and the etiopathogenesis of Kaposi's sarcoma." Rev Hosp Clin Fac Med Sao Paulo **57**(4): 175-86.

Lee, S. P., J. M. Brooks, *et al.*. (2004). "CD8 T cell recognition of endogenously expressed epstein-barr virus nuclear antigen 1." J Exp Med **199**(10): 1409-20.

Lehman, I. R. and P. E. Boehmer (1999). "Replication of herpes simplex virus DNA." J Biol Chem **274**(40): 28059-62.

Li, Q., M. K. Spriggs, *et al.*. (1997). "Epstein-Barr virus uses HLA class II as a cofactor for infection of B lymphocytes." J Virol **71**(6): 4657-62.

Lok, S. S., Y. Haider, *et al.*. (2002). "Murine gammaherpes virus as a cofactor in the development of pulmonary fibrosis in bleomycin resistant mice." Eur Respir J **20**(5): 1228-32.

Lomonte, P., M. Bublot, *et al.*. (1996). "Bovine herpesvirus 4: genomic organization and relationship with two other gammaherpesviruses, Epstein-Barr virus and herpesvirus saimiri." Vet Microbiol **53**(1-2): 79-89.

Lorenzo, M. E., J. U. Jung, *et al.*. (2002). "Kaposi's sarcoma-associated herpesvirus K3 utilizes the ubiquitin-proteasome system in routing class major histocompatibility complexes to late endocytic compartments." J Virol **76**(11): 5522-31.

Lybarger, L., X. Wang, *et al.*. (2003). "Virus subversion of the MHC class I peptide-loading complex." Immunity **18**(1): 121-30.

Macen, J. L., R. S. Garner, *et al.*. (1996). "Differential inhibition of the Fas- and granule-mediated cytolysis pathways by the orthopoxvirus cytokine response modifier A/SPI-2 and SPI-1 protein." Proc Natl Acad Sci U S A **93**(17): 9108-13.

Mackay, I. M., K. E. Arden, *et al.*. (2002). "Real-time PCR in virology." Nucleic Acids Res **30**(6): 1292-305.

Mackett, M., J. P. Stewart, *et al.*. (1997). "Genetic content and preliminary transcriptional analysis of a representative region of murine gammaherpesvirus 68." J Gen Virol **78 (Pt 6)**: 1425-33.

Macrae, A. I., B. M. Dutia, *et al.*. (2001). "Analysis of a novel strain of murine gammaherpesvirus reveals a genomic locus important for acute pathogenesis." J Virol **75**(11): 5315-27.

Macrae, A. I., E. J. Usherwood, *et al.*. (2003). "Murid herpesvirus 4 strain 68 M2 protein is a B-cell-associated antigen important for latency but not lymphocytosis." J Virol **77**(17): 9700-9.

Macsween, K. F. and D. H. Crawford (2003). "Epstein-Barr virus-recent advances." Lancet Infect Dis **3**(3): 131-40.

Magrath, I. (1990). "The pathogenesis of Burkitt's lymphoma." Adv Cancer Res **55**: 133-270.

Marques, S., S. Efstathiou, *et al.*. (2003). "Selective gene expression of latent murine gammaherpesvirus 68 in B lymphocytes." J Virol **77**(13): 7308-18.

Martinez-Guzman, D., T. Rickabaugh, *et al.*. (2003). "Transcription program of murine gammaherpesvirus 68." J Virol **77**(19): 10488-503.

Maul, G. G., A. M. Ishov, *et al.*. (1996). "Nuclear domain 10 as preexisting potential replication start sites of herpes simplex virus type-1." Virology **217**(1): 67-75.

May, J. S., H. M. Coleman, *et al.*. (2005a). "Murine gammaherpesvirus-68 ORF28 encodes a non-essential virion glycoprotein." J Gen Virol **86**(Pt 4): 919-28.

May, J. S., H. M. Coleman, *et al.*. (2004). "Forced lytic replication impairs host colonization by a latency-deficient mutant of murine gammaherpesvirus-68." J Gen Virol **85**(Pt 1): 137-46.

May, J. S., B. D. de Lima, *et al.*. (2005b). "Intercellular gamma-herpesvirus dissemination involves co-ordinated intracellular membrane protein transport." Traffic **6**(9): 780-93.

May, J. S., J. Walker, *et al.*. (2005c). "The murine gammaherpesvirus 68 ORF27 gene product contributes to intercellular viral spread." J Virol **79**(8): 5059-68.

McGeoch, D. J., F. J. Rixon, *et al.*. (2006). "Topics in herpesvirus genomics and evolution." Virus Res **117**(1): 90-104.

Medveczky, P., E. Szomolanyi, *et al.*. (1984). "Classification of herpesvirus saimiri into three groups based on extreme variation in a DNA region required for oncogenicity." J Virol **52**(3): 938-44.

Melendez, L. V., M. D. Daniel, *et al.*. (1968). "An apparently new herpesvirus from primary kidney cultures of the squirrel monkey (Saimiri sciureus)." Lab Anim Care **18**(3): 374-81.

Melendez, L. V., R. D. Hunt, *et al.*. (1972). "Herpesvirus ateles, a new lymphoma virus of monkeys." Nat New Biol **235**(58): 182-4.

Melroe, G. T., N. A. DeLuca, *et al.*. (2004). "Herpes simplex virus 1 has multiple mechanisms for blocking virus-induced interferon production." J Virol **78**(16): 8411-20.

Messerle, M., I. Crnkovic, *et al.*. (1997). "Cloning and mutagenesis of a herpesvirus genome as an infectious bacterial artificial chromosome." Proc Natl Acad Sci U S A **94**(26): 14759-63.

Mettenleiter, T. C. (2002a). "Brief overview on cellular virus receptors." Virus Res **82**(1-2): 3-8.

Mettenleiter, T. C. (2002b). "Herpesvirus assembly and egress." J Virol **76**(4): 1537-47.

Mettenleiter, T. C. (2004). "Budding events in herpesvirus morphogenesis." Virus Res **106**(2): 167-80.

Mistrikova, J., M. Mrmusova-Supolikova, *et al.*. (2004). "Leukemia-like syndrome in Balb/c mice infected with the lymphotropic gamma herpesvirus MHV-Sumava: an analogy to EBV infection." Neoplasma **51**(2): 71-6.

Mocarski ES, C. C. (2001). Cytomegalovirus and their replication, Lippincott Williams & Wilkins.

Moghaddam, A., J. Koch, *et al.*. (1998). "Infection of human B lymphocytes with lymphocryptoviruses related to Epstein-Barr virus." J Virol **72**(4): 3205-12.

Moghaddam, A., M. Rosenzweig, *et al.*. (1997). "An animal model for acute and persistent Epstein-Barr virus infection." Science **276**(5321): 2030-3.

Molesworth, S. J., C. M. Lake, *et al.*. (2000). "Epstein-Barr virus gH is essential for penetration of B cells but also plays a role in attachment of virus to epithelial cells." J Virol **74**(14): 6324-32.

Moon, K. B., P. C. Turner, *et al.*. (1999). "SPI-1-dependent host range of rabbitpox virus and complex formation with cathepsin G is associated with serpin motifs." J Virol **73**(11): 8999-9010.

Moore, P. S. and Y. Chang (2001). "Molecular virology of Kaposi's sarcoma-associated herpesvirus." Philos Trans R Soc Lond B Biol Sci **356**(1408): 499-516.

Moorman, N. J., C. Y. Lin, *et al.*. (2004). "Identification of candidate gammaherpesvirus 68 genes required for virus replication by signature-tagged transposon mutagenesis." J Virol **78**(19): 10282-90.

Moorman, N. J., H. W. t. Virgin, *et al.*. (2003b). "Disruption of the gene encoding the gammaHV68 v-GPCR leads to decreased efficiency of reactivation from latency." Virology **307**(2): 179-90.

Moorman, N. J., D. O. Willer, *et al.*. (2003a). "The gammaherpesvirus 68 latency-associated nuclear antigen homolog is critical for the establishment of splenic latency." J Virol **77**(19): 10295-303.

Mora, A. L., C. R. Woods, *et al.*. (2005). "Lung infection with gamma-herpesvirus induces progressive pulmonary fibrosis in Th2-biased mice." Am J Physiol Lung Cell Mol Physiol **289**(5): L711-21.

Moser, J. M., M. L. Farrell, *et al.*. (2006). "A gammaherpesvirus 68 gene 50 null mutant establishes long-term latency in the lung but fails to vaccinate against a wild-type virus challenge." J Virol **80**(3): 1592-8.

Moss, D. J., S. R. Burrows, *et al.*. (2001). "The immunology of Epstein-Barr virus infection." Philos Trans R Soc Lond B Biol Sci **356**(1408): 475-88.

Mossman, K. L. and A. A. Ashkar (2005). "Herpesviruses and the innate immune response." Viral Immunol **18**(2): 267-81.

Mukherjee, S., P. Trivedi, *et al.*. (1998). "Murine cytotoxic T lymphocytes recognize an epitope in an EBNA-1 fragment, but fail to lyse EBNA-1-expressing mouse cells." J Exp Med **187**(3): 445-50.

Muller, U., U. Steinhoff, *et al.*. (1994). "Functional role of type I and type II interferons in antiviral defense." Science **264**(5167): 1918-21.

Nanbo, A., K. Inoue, *et al.*. (2002). "Epstein-Barr virus RNA confers resistance to interferon-alpha-induced apoptosis in Burkitt's lymphoma." Embo J **21**(5): 954-65.

Nash, A. A., B. M. Dutia, *et al.*. (2001). "Natural history of murine gamma-herpesvirus infection." Philos Trans R Soc Lond B Biol Sci **356**(1408): 569-79.

Nash, A. A. and N. P. Sunil-Chandra (1994). "Interactions of the murine gammaherpesvirus with the immune system." Curr Opin Immunol **6**(4): 560-3.

Niesters, H. G. (2001). "Quantitation of viral load using real-time amplification techniques." Methods **25**(4): 419-29.

Nordengrahn, A., M. Merza, *et al.*. (2002). "Prevalence of equine herpesvirus types 2 and 5 in horse populations by using type-specific PCR assays." Vet Res **33**(3): 251-9.

Nordengrahn, A., M. Rusvai, *et al.*. (1996). "Equine herpesvirus type 2 (EHV-2) as a predisposing factor for Rhodococcus equi pneumonia in foals: prevention of the bifactorial disease with EHV-2 immunostimulating complexes." Vet Microbiol **51**(1-2): 55-68.

Obar, J. J., D. C. Donovan, *et al.*. (2004). "T-cell responses to the M3 immune evasion protein of murid gammaherpesvirus 68 are partially protective and induced with lytic antigen kinetics." J Virol **78**(19): 10829-32.

Ochsenbein, A. F., D. D. Pinschewer, *et al.*. (1999). "Protective T cell-independent antiviral antibody responses are dependent on complement." J Exp Med **190**(8): 1165-74.

O'Connor, M., M. Peifer, *et al.*. (1989). "Construction of large DNA segments in Escherichia coli." Science **244**(4910): 1307-12.

Oda, W., J. Mistrikova, *et al.*. (2005). "Analysis of genomic homology of murine gammaherpesvirus (MHV)-72 to MHV-68 and impact of MHV-72 on the survival and tumorigenesis in the MHV-72-infected CB17 scid/scid and CB17+/+ mice." Pathol Int **55**(9): 558-68.

Oksenhendler, E., G. Carcelain, *et al.*. (2000). "High levels of human herpesvirus 8 viral load, human interleukin-6, interleukin-10, and C reactive protein correlate with exacerbation of multicentric castleman disease in HIV-infected patients." Blood **96**(6): 2069-73.

O'Leary, J. J., G. Browne, *et al.*. (1994). "The importance of fixation procedures on DNA template and its suitability for solution-phase polymerase chain reaction and PCR in situ hybridization." Histochem J **26**(4): 337-46.

Osorio, F. A., D. E. Reed, *et al.*. (1982). "Experimental infection of rabbits with bovine herpesvirus-4: acute and persistent infection." Vet Microbiol **7**(6): 503-13.

Pappova, M., M. Stancekova, *et al.*. (2004). "Pathogenetical characterization of isolate MHV-60 of mouse herpesvirus strain 68." Acta Virol **48**(2): 91-6.

Parry, C. M., J. P. Simas, *et al.*. (2000). "A broad spectrum secreted chemokine binding protein encoded by a herpesvirus." J Exp Med **191**(3): 573-8.

Peacock, J. W. and K. L. Bost (2000). "Infection of intestinal epithelial cells and development of systemic disease following gastric instillation of murine gammaherpesvirus-68." J Gen Virol **81**(Pt 2): 421-9.

Pegtel, D. M., J. Middeldorp, *et al.*. (2004). "Epstein-Barr virus infection in ex vivo tonsil epithelial cell cultures of asymptomatic carriers." J Virol **78**(22): 12613-24.

Pepper, S. D., J. P. Stewart, *et al.*. (1996). "Murine gammaherpesvirus-68 encodes homologues of thymidine kinase and glycoprotein H: sequence, expression, and characterization of pyrimidine kinase activity." Virology **219**(2): 475-9.

Perng, G. C., C. Jones, *et al.*. (2000). "Virus-induced neuronal apoptosis blocked by the herpes simplex virus latency-associated transcript." Science **287**(5457): 1500-3.

Pfeffer, S., A. Sewer, *et al.*. (2005). "Identification of microRNAs of the herpesvirus family." Nat Methods **2**(4): 269-76.

Pfeffer, S., M. Zavolan, *et al.*. (2004). "Identification of virus-encoded microRNAs." Science **304**(5671): 734-6.

Potempa, J., E. Korzus, *et al.*. (1994). "The serpin superfamily of proteinase inhibitors: structure, function, and regulation." J Biol Chem **269**(23): 15957-60.

Prota, A. E., D. R. Sage, *et al.*. (2002). "The crystal structure of human CD21: Implications for Epstein-Barr virus and C3d binding." Proc Natl Acad Sci U S A **99**(16): 10641-6.

Purewal, A. S., A. V. Smallwood, *et al.*. (1992). "Identification and control of the cis-acting elements of the immediate early gene of equid herpesvirus type 1." J Gen Virol **73 (Pt 3)**: 513-9.

Rajcani, J., D. Blaskovic, *et al.*. (1985). "Pathogenesis of acute and persistent murine herpesvirus infection in mice." Acta Virol **29**(1): 51-60.

Raslova, H., M. Berebbi, *et al.*. (2001). "Susceptibility of mouse mammary glands to murine gammaherpesvirus 72 (MHV-72) infection: evidence of MHV-72 transmission via breast milk." Microb Pathog **31**(2): 47-58.

Ray, C. A., R. A. Black, *et al.*. (1992). "Viral inhibition of inflammation: cowpox virus encodes an inhibitor of the interleukin-1 beta converting enzyme." Cell **69**(4): 597-604.

Reddehase, M. J., J. Podlech, *et al.*. (2002). "Mouse models of cytomegalovirus latency: overview." J Clin Virol **25 Suppl 2**: S23-36.

Rickabaugh, T. M., H. J. Brown, *et al.*. (2004). "Generation of a latency-deficient gammaherpesvirus that is protective against secondary infection." J Virol **78**(17): 9215-23.

Roizman B, K. D. (2001). Herpes Simplex Viruses and their Replication.

Roizman B, P. E. (2001). The Family Herpesviridae: A Brief Introduction, Lippincott Williams & Wilkins.

Rosbottom, J. (2003). The molecular pathogenesis of ovine herpesvirus-2. Laboratory for Clinical & Molecular Virology. Edinburgh, University of Edinburgh. **PhD**.

Rosbottom, J., R. G. Dalziel, *et al.*. (2002). "Ovine herpesvirus 2 lytic cycle replication and capsid production." J Gen Virol **83**(Pt 12): 2999-3002.

Roy, D. J., B. C. Ebrahimi, *et al.*. (2000). "Murine gammaherpesvirus M11 gene product inhibits apoptosis and is expressed during virus persistence." Arch Virol **145**(11): 2411-20.

Sakisaka, T., T. Taniguchi, *et al.*. (2001). "Requirement of interaction of nectin-1alpha/HveC with afadin for efficient cell-cell spread of herpes simplex virus type 1." J Virol **75**(10): 4734-43.

Santoni, F., I. Lindner, *et al.*. (2006). "Molecular interactions between porcine and human gammaherpesviruses: implications for xenografts?" Xenotransplantation **13**(4): 308-17.

Sarawar, S. R., B. J. Lee, *et al.*. (2002). "Chemokine induction and leukocyte trafficking to the lungs during murine gammaherpesvirus 68 (MHV-68) infection." Virology **293**(1): 54-62.

Sarid, R., O. Flore, *et al.*. (1998). "Transcription mapping of the Kaposi's sarcoma-associated herpesvirus (human herpesvirus 8) genome in a body cavity-based lymphoma cell line (BC-1)." J Virol **72**(2): 1005-12.

Schaefer, B. C., J. L. Strominger, *et al.*. (1997). "Host-cell-determined methylation of specific Epstein-Barr virus promoters regulates the choice between distinct viral latency programs." Mol Cell Biol **17**(1): 364-77.

Schulz, T. F. (1998). "Kaposi's sarcoma-associated herpesvirus (human herpesvirus-8)." J Gen Virol **79 (Pt 7)**: 1573-91.

Schulz, T. F. (2000). "Kaposi's sarcoma-associated herpesvirus (human herpesvirus 8): epidemiology and pathogenesis." J Antimicrob Chemother **45 Suppl T3**: 15-27.

Selverajah, S. (2001). Early events following murine gammaherpesvirus (MHV-68) infection. Department of Veterinary Pathology. Edinburgh, University of Edinburgh. **PhD**.

Shope, T., D. Dechairo, *et al.*. (1973). "Malignant lymphoma in cottontop marmosets after inoculation with Epstein-Barr virus." Proc Natl Acad Sci U S A **70**(9): 2487-91.

Simas, J. P., R. J. Bowden, *et al.*. (1998). "Four tRNA-like sequences and a serpin homologue encoded by murine gammaherpesvirus 68 are dispensable for lytic replication in vitro and latency in vivo." J Gen Virol **79 (Pt 1)**: 149-53.

Simas, J. P. and S. Efstathiou (1998). "Murine gammaherpesvirus 68: a model for the study of gammaherpesvirus pathogenesis." Trends Microbiol **6**(7): 276-82.

Simas, J. P., S. Marques, *et al.*. (2004). "The M2 gene product of murine gammaherpesvirus 68 is required for efficient colonization of splenic follicles but is not necessary for expansion of latently infected germinal centre B cells." J Gen Virol **85**(Pt 10): 2789-97.

Simas, J. P., D. Swann, *et al.*. (1999). "Analysis of murine gammaherpesvirus-68 transcription during lytic and latent infection." J Gen Virol **80 (Pt 1)**: 75-82.

Skepper, J. N., A. Whiteley, *et al.*. (2001). "Herpes simplex virus nucleocapsids mature to progeny virions by an envelopment --> deenvelopment --> reenvelopment pathway." J Virol **75**(12): 5697-702.

Slobedman, B., S. Efstathiou, *et al.*. (1994). "Quantitative analysis of herpes simplex virus DNA and transcriptional activity in ganglia of mice latently infected with wild-type and thymidine kinase-deficient viral strains." J Gen Virol **75 (Pt 9)**: 2469-74.

Song, M. J., S. Hwang, *et al.*. (2005). "Identification of viral genes essential for replication of murine gamma-herpesvirus 68 using signature-tagged mutagenesis." Proc Natl Acad Sci U S A **102**(10): 3805-10.

Spear, P. G. (2004). "Herpes simplex virus: receptors and ligands for cell entry." Cell Microbiol **6**(5): 401-10.

Spear, P. G., S. Manoj, *et al.*. (2006). "Different receptors binding to distinct interfaces on herpes simplex virus gD can trigger events leading to cell fusion and viral entry." Virology **344**(1): 17-24.

Steed, A. L., E. S. Barton, *et al.*. (2006). "Gamma interferon blocks gammaherpesvirus reactivation from latency." J Virol **80**(1): 192-200.

Stevenson, P. G. and S. Efstathiou (2005). "Immune mechanisms in murine gammaherpesvirus-68 infection." Viral Immunol **18**(3): 445-56.

Stevenson, P. G., S. Efstathiou, *et al.*. (2000). "Inhibition of MHC class I-restricted antigen presentation by gamma 2-herpesviruses." Proc Natl Acad Sci U S A **97**(15): 8455-60.

Stevenson, P. G., J. S. May, *et al.*. (2002). "K3-mediated evasion of CD8(+) T cells aids amplification of a latent gamma-herpesvirus." Nat Immunol **3**(8): 733-40.

Stewart, J. P., J. J. Egan, *et al.*. (1999b). "The detection of Epstein-Barr virus DNA in lung tissue from patients with idiopathic pulmonary fibrosis." Am J Respir Crit Care Med **159**(4 Pt 1): 1336-41.

Stewart, J. P., N. J. Janjua, *et al.*. (1996). "Identification and characterization of murine gammaherpesvirus 68 gp150: a virion membrane glycoprotein." J Virol **70**(6): 3528-35.

Stewart, J. P., N. Micali, *et al* . (1999). "Murine gamma-herpesvirus 68 glycoprotein 150 protects against virus-induced mononucleosis: a model system for gamma-herpesvirus vaccination." Vaccine **17**(2): 152-7.

Stewart, J. P., O. J. Silvia, *et al.*. (2004). "In vivo function of a gammaherpesvirus virion glycoprotein: influence on B-cell infection and mononucleosis." J Virol **78**(19): 10449-59.

Stewart, J. P., E. J. Usherwood, *et al.*. (1998). "Lung epithelial cells are a major site of murine gammaherpesvirus persistence." J Exp Med **187**(12): 1941-51.

Sunil-Chandra, N. P., J. Arno, *et al.*. (1994). "Lymphoproliferative disease in mice infected with murine gammaherpesvirus 68." Am J Pathol **145**(4): 818-26.

Sunil-Chandra, N. P., S. Efstathiou, *et al.*. (1992a). "Virological and pathological features of mice infected with murine gamma-herpesvirus 68." J Gen Virol **73 (Pt 9)**: 2347-56.

Sunil-Chandra, N. P., S. Efstathiou, *et al.*. (1992b). "Murine gammaherpesvirus 68 establishes a latent infection in mouse B lymphocytes in vivo." J Gen Virol **73 (Pt 12)**: 3275-9.

Sunil-Chandra, N. P., S. Efstathiou, *et al.*. (1993). "Interactions of murine gammaherpesvirus 68 with B and T cell lines." Virology **193**(2): 825-33.

Suzuki, T., P. J. Higgins, *et al.*. (2000). "Control selection for RNA quantitation." Biotechniques **29**(2): 332-7.

Svobodova, J., D. Blaskovic, *et al.*. (1982). "Growth characteristics of herpesviruses isolated from free living small rodents." Acta Virol **26**(4): 256-63.

Tang, Y. W., J. E. Johnson, *et al.*. (2003). "Herpesvirus DNA is consistently detected in lungs of patients with idiopathic pulmonary fibrosis." J Clin Microbiol **41**(6): 2633-40.

Tarakanova, V. L., F. Suarez, *et al.*. (2005). "Murine gammaherpesvirus 68 infection is associated with lymphoproliferative disease and lymphoma in BALB beta2 microglobulin-deficient mice." J Virol **79**(23): 14668-79.

Telford, E. A., M. J. Studdert, *et al.*. (1993). "Equine herpesviruses 2 and 5 are gamma-herpesviruses." Virology **195**(2): 492-9.

Telford, E. A., M. S. Watson, *et al.*. (1995). "The DNA sequence of equine herpesvirus 2." J Mol Biol **249**(3): 520-8.

Tellam, J., G. Connolly, *et al.*. (2004). "Endogenous presentation of CD8+ T cell epitopes from Epstein-Barr virus-encoded nuclear antigen 1." J Exp Med **199**(10): 1421-31.

Thellin, O., W. Zorzi, *et al.*. (1999). "Housekeeping genes as internal standards: use and limits." J Biotechnol **75**(2-3): 291-5.

Thompson, M. P. and R. Kurzrock (2004). "Epstein-Barr virus and cancer." Clin Cancer Res **10**(3): 803-21.

Thompson, R. L. and N. M. Sawtell (2000). "Replication of herpes simplex virus type 1 within trigeminal ganglia is required for high frequency but not high viral genome copy number latency." J Virol **74**(2): 965-74.

Thorley-Lawson, D. A. (2001). "Epstein-Barr virus: exploiting the immune system." Nat Rev Immunol **1**(1): 75-82.

Thorley-Lawson, D. A. and A. Gross (2004). "Persistence of the Epstein-Barr virus and the origins of associated lymphomas." N Engl J Med **350**(13): 1328-37.

Tibbetts, S. A., J. Loh, *et al.*. (2003). "Establishment and maintenance of gammaherpesvirus latency are independent of infective dose and route of infection." J Virol **77**(13): 7696-701.

Tibbetts, S. A., F. Suarez, *et al.*. (2006). "A gamma-herpesvirus deficient in replication establishes chronic infection in vivo and is impervious to restriction by adaptive immune cells." Virology.

Tibbetts, S. A., L. F. van Dyk, *et al.*. (2002). "Immune control of the number and reactivation phenotype of cells latently infected with a gammaherpesvirus." J Virol **76**(14): 7125-32.

Tierney, R. J., N. Steven, *et al.*. (1994). "Epstein-Barr virus latency in blood mononuclear cells: analysis of viral gene transcription during primary infection and in the carrier state." J Virol **68**(11): 7374-85.

Townsley, A. C., B. M. Dutia, *et al.*. (2004). "The m4 gene of murine gammaherpesvirus modulates productive and latent infection in vivo." J Virol **78**(2): 758-67.

Tripp, R. A., A. M. Hamilton-Easton, *et al.*. (1997). "Pathogenesis of an infectious mononucleosis-like disease induced by a murine gamma-herpesvirus: role for a viral superantigen?" J Exp Med **185**(9): 1641-50.

Tsurumi, T. and A. Kudoh (2005). "[Replication of Epstein-Barr virus and host cell response]." Seikagaku **77**(9): 1180-4.

Tsygankov, A. Y. (2005). "Cell transformation by Herpesvirus saimiri." J Cell Physiol **203**(2): 305-18.

Uprichard, S. L. and D. M. Knipe (1997). "Assembly of herpes simplex virus replication proteins at two distinct intranuclear sites." Virology **229**(1): 113-25.

Upton, J. W., L. F. van Dyk, *et al.*. (2005). "Characterization of murine gammaherpesvirus 68 v-cyclin interactions with cellular cdks." Virology **341**(2): 271-83.

Usherwood, E. J., A. J. Ross, *et al.*. (1996a). "Murine gammaherpesvirus-induced splenomegaly: a critical role for CD4 T cells." J Gen Virol **77 (Pt 4)**: 627-30.

Usherwood, E. J., J. P. Stewart, *et al.*. (1996c). "Characterization of tumor cell lines derived from murine gammaherpesvirus-68-infected mice." J Virol **70**(9): 6516-8.

Usherwood, E. J., J. P. Stewart, *et al.*. (1996). "Absence of splenic latency in murine gammaherpesvirus 68-infected B cell-deficient mice." J Gen Virol **77 (Pt 11)**: 2819-25.

van Berkel, V., B. Levine, *et al.*. (2002). "Critical role for a high-affinity chemokine-binding protein in gamma-herpesvirus-induced lethal meningitis." J Clin Invest **109**(7): 905-14.

van Dyk, L. F., J. L. Hess, *et al.*. (1999). "The murine gammaherpesvirus 68 v-cyclin gene is an oncogene that promotes cell cycle progression in primary lymphocytes." J Virol **73**(6): 5110-22.

van Dyk, L. F., H. W. t. Virgin, *et al.*. (2000). "The murine gammaherpesvirus 68 v-cyclin is a critical regulator of reactivation from latency." J Virol **74**(16): 7451-61.

van Dyk, L. F., H. W. t. Virgin, *et al.*. (2003). "Maintenance of gammaherpesvirus latency requires viral cyclin in the absence of B lymphocytes." J Virol **77**(9): 5118-26.

Vanderplasschen, A., M. Bublot, *et al.*. (1993). "Attachment of the gammaherpesvirus bovine herpesvirus 4 is mediated by the interaction of gp8 glycoprotein with heparinlike moieties on the cell surface." Virology **196**(1): 232-40.

Vandesompele, J., K. De Preter, *et al.*. (2002). "Accurate normalization of real-time quantitative RT-PCR data by geometric averaging of multiple internal control genes." Genome Biol **3**(7): RESEARCH0034.

Viejo-Borbolla, A. and T. F. Schulz (2003). "Kaposi's sarcoma-associated herpesvirus (KSHV/HHV8): key aspects of epidemiology and pathogenesis." AIDS Rev **5**(4): 222-9.

Virgin, H. W. t., P. Latreille, *et al.*. (1997). "Complete sequence and genomic analysis of murine gammaherpesvirus 68." J Virol **71**(8): 5894-904.

Virgin, H. W. t., R. M. Presti, *et al.*. (1999). "Three distinct regions of the murine gammaherpesvirus 68 genome are transcriptionally active in latently infected mice." J Virol **73**(3): 2321-32.

Virgin, H. W. t., R. M. Presti, *et al.*. (1999). "Three distinct regions of the murine gammaherpesvirus 68 genome are transcriptionally active in latently infected mice." J Virol **73**(3): 2321-32.

Wagner, M. and U. H. Koszinowski (2004). "Mutagenesis of viral BACs with linear PCR fragments (ET recombination)." Methods Mol Biol **256**: 257-68.

Wakeling, M. N., D. J. Roy, *et al.*. (2001). "Characterization of the murine gammaherpesvirus 68 ORF74 product: a novel oncogenic G protein-coupled receptor." J Gen Virol **82**(Pt 5): 1187-97.

Walter, N., H. R. Collard, *et al.*. (2006). "Current perspectives on the treatment of idiopathic pulmonary fibrosis." Proc Am Thorac Soc **3**(4): 330-8.

Wang, F., P. Rivailler, *et al.*. (2001). "Simian homologues of Epstein-Barr virus." Philos Trans R Soc Lond B Biol Sci **356**(1408): 489-97.

Wang, G. H., T. L. Garvey, *et al.*. (1999). "The murine gammaherpesvirus-68 M11 protein inhibits Fas- and TNF-induced apoptosis." J Gen Virol **80 (Pt 10)**: 2737-40.

Weck, K. E., M. L. Barkon, *et al.*. (1996). "Mature B cells are required for acute splenic infection, but not for establishment of latency, by murine gammaherpesvirus 68." J Virol **70**(10): 6775-80.

Weck, K. E., A. J. Dal Canto, *et al.*. (1997). "Murine gamma-herpesvirus 68 causes severe large-vessel arteritis in mice lacking interferon-gamma responsiveness: a new model for virus-induced vascular disease." Nat Med **3**(12): 1346-53.

Weck, K. E., S. S. Kim, *et al.*. (1999a). "Macrophages are the major reservoir of latent murine gammaherpesvirus 68 in peritoneal cells." J Virol **73**(4): 3273-83.

Weck, K. E., S. S. Kim, *et al.*. (1999b). "B cells regulate murine gammaherpesvirus 68 latency." J Virol **73**(6): 4651-61.

Wedderburn, N., J. M. Edwards, *et al.*. (1984). "Infectious mononucleosis-like response in common marmosets infected with Epstein-Barr virus." J Infect Dis **150**(6): 878-82.

Weinberg, J. B., M. L. Lutzke, *et al.*. (2004). "Mouse strain differences in the chemokine response to acute lung infection with a murine gammaherpesvirus." Viral Immunol **17**(1): 69-77.

Weinberg, J. B., M. L. Lutzke, *et al.*. (2002). "Elevated chemokine responses are maintained in lungs after clearance of viral infection." J Virol **76**(20): 10518-23.

Welch, H. M., C. G. Bridges, *et al.*. (1992). "Latent equid herpesviruses 1 and 4: detection and distinction using the polymerase chain reaction and co-cultivation from lymphoid tissues." J Gen Virol **73 (Pt 2)**: 261-8.

Whitby, D., A. Stossel, *et al.*. (2003). "Novel Kaposi's sarcoma-associated herpesvirus homolog in baboons." J Virol **77**(14): 8159-65.

Wolfstein, A., C. H. Nagel, *et al.*. (2006). "The inner tegument promotes herpes simplex virus capsid motility along microtubules in vitro." Traffic **7**(2): 227-37.

Woodland, D. L., E. J. Usherwood, *et al.*. (2001). "Vaccination against murine gamma-herpesvirus infection." Viral Immunol **14**(3): 217-26.

Wu, T. T., E. J. Usherwood, *et al.*. (2000). "Rta of murine gammaherpesvirus 68 reactivates the complete lytic cycle from latency." J Virol **74**(8): 3659-67.

Young, L. S. and A. B. Rickinson (2004). "Epstein-Barr virus: 40 years on." Nat Rev Cancer **4**(10): 757-68.

Yu, Y. Y., M. R. Harris, *et al.*. (2002). "Physical association of the K3 protein of gamma-2 herpesvirus 68 with major histocompatibility complex class I molecules with impaired peptide and beta(2)-microglobulin assembly." J Virol **76**(6): 2796-803.